New concepts of UV/H₂O₂ oxidation

WATER RESEARCH FOUNDATION℠
ADVANCING THE SCIENCE OF WATER®

GREATER CINCINNATI WATER WORKS

PHILIPS

dunea DUIN & WATER

KWR
Watercycle Research Institute

BTO

New concepts of UV/H₂O₂ oxidation

BTO 2011.046
June 2011

Colofon

Title
New concepts of UV/H$_2$O$_2$ oxidation

Project number
B111.604

Research Program
Water treatment

Project manager
E.F. Beerendonk

Client
BTO, Water Research Foundation

Quality Assurance
M. Nederlof

Editor
C.H.M. Hofman-Caris, E.F. Beerendonk

Sent to
This report has been distributed among BTO-participants and by the Water Research Foundation, and is publicly available.

Preface

This report describes a project on new concepts of UV/H_2O_2 oxidation. This research project is a cooperation between KWR Watercycle Research Institute (KWR), Dunea, Greater Cincinnati Water Works (GCWW) and Philips Lighting. The project has been made possible through partnership funding from Joint Research Programme of the Dutch water utilities (BTO), Water Research Foundation (WaterRF) and Ministry of Economic Affairs in the Netherlands (through Agentschap NL, formerly known as SenterNovem).

Several persons from these companies and institutes have contributed to this work. We would like to thank Debbie Metz, Maria Meyer from GCWW, Jaak Geboers and Fred van Lierop from Philips Lighting, Ton Knol and Karin Lekkerkerker from Dunea and Danny Harmsen and Minne Heringa from KWR, who are the authors of the contributions in this report. Obviously, many persons from these companies were involved, who are mentioned in the acknowledgements in the separate chapters of this report. Furthermore, we would like to thank Alice Fulmer and Rick Karlin of WaterRF for their contributions to this project and this report.

KWR gratefully acknowledges that the WaterRF is the joint owner of the technical information upon which this report is based. KWR thanks WaterRF for its financial, technical, and administrative assistance in funding the project through which this information was discovered. Mention of trade names or commercial products does not constitute WaterRF endorsement or recommendations for use. Similarly, omission of products or trade names indicates nothing concerning WaterRF's position regarding product effectiveness or applicability.

Summary

Water quality may be threatened by the presence of new contaminants, increasing concentrations of contaminants, and seasonal or diurnal variations in water sources. Advanced oxidation processes are important barriers against organic micropollutants in drinking water treatment. Application of UV combined with hydrogen peroxide oxidation, followed by filtration over granular activated carbon (GAC), is a solid and flexible barrier against a broad range of organic micropollutants

The use of UV light for disinfection of water has been known for several decades. Since the mid nineties the combination of UV light and hydrogen peroxide has been studied as a barrier for organic micropollutants. Medium or low pressure UV lamps are used. These, mercury containing, lamps emit either a broad UV spectrum between 200-400 nm (MP lamps), or a specific wavelength (253.7 nm for LP lamps). Hydrogen peroxide is dosed to the water before it enters the UV reactor. By means of UV irradiation the hydrogen peroxide is converted into hydroxyl radicals, which non-selectively react with all kinds of organic compounds. Apart from this oxidation process, some compounds will be converted by direct photolysis from the UV irradiation, or possibly by both processes.

In principle, UV/hydrogen peroxide oxidation may result in mineralization of the organic compounds present in the water, but in general the aim is not to achieve total mineralization. In many cases it appears to be sufficient to degrade the pollutants, in order to render them better biodegradable, resulting in lower required doses of UV and H_2O_2. This, however, may result in the formation of byproducts, the effects of which still have not been fully studied. Although total mineralization is not the goal of UV/hydrogen peroxide oxidation processes, still their major disadvantage is their relatively high energy demand. At the start of the project, state of the art UV/H_2O_2 technology in general used medium pressure (MP) UV lamps.

The aim of this project was to lower the energy demand, the total costs and the formation of byproducts of the UV/H_2O_2 technology for drinking water production, keeping the conversion level of the pollutants at least at the same level. Therefore, three different types of lamps were studied: medium pressure (MP), low pressure (LP) and a new type of lamp: the dielectric barrier discharge (DBD) lamp, which was being developed by Philips Lighting.

The project was divided into ten work packages:

1. Proof of principle: LP lamps can be at least as effectively for hydroxyl radical generation as MP lamps (KWR)
2. Investigation into a new Dielectric Barrier Discharge (DBD) lamp and its electrical power system (Philips Lighting)
3. Development of mercury (Hg)-free lamps and ballasts in UV/H_2O_2
4. Research into LP-Hg in UV/H_2O_2 (Philips Lighting)
5. Development of LP-Hg in UV/H_2O_2 (Philips Lighting)
6. Design and development of a pilot plant (KWR)
7. Pilot plant research at GCWW applying LP and MP lamps
8. Pilot plant research at Dunea applying LP, MP and DBD lamps
9. Testing of analytical methods for genotoxicity research
10. Design of a combined full scale oxidation and filtration unit (KWR)

In this report, the results of all 10 work packages are included. Every chapter deals with a certain work package or combination of work packages, and was written by the project partner who carried out the work. In chapter 11 the general discussion and conclusions regarding all work packages are given.

The general flow sheet of a UV/H_2O_2 pilot system is shown in Figure 1-1. It consists of a stirred tank for the test water, a H_2O_2 dosing unit, a mixer, the UV reactor with its electrical equipment, another mixer after the reactor, and some sample points. Furthermore, there are dosing units for dosing micropollutants or bacteriophages to the test water.
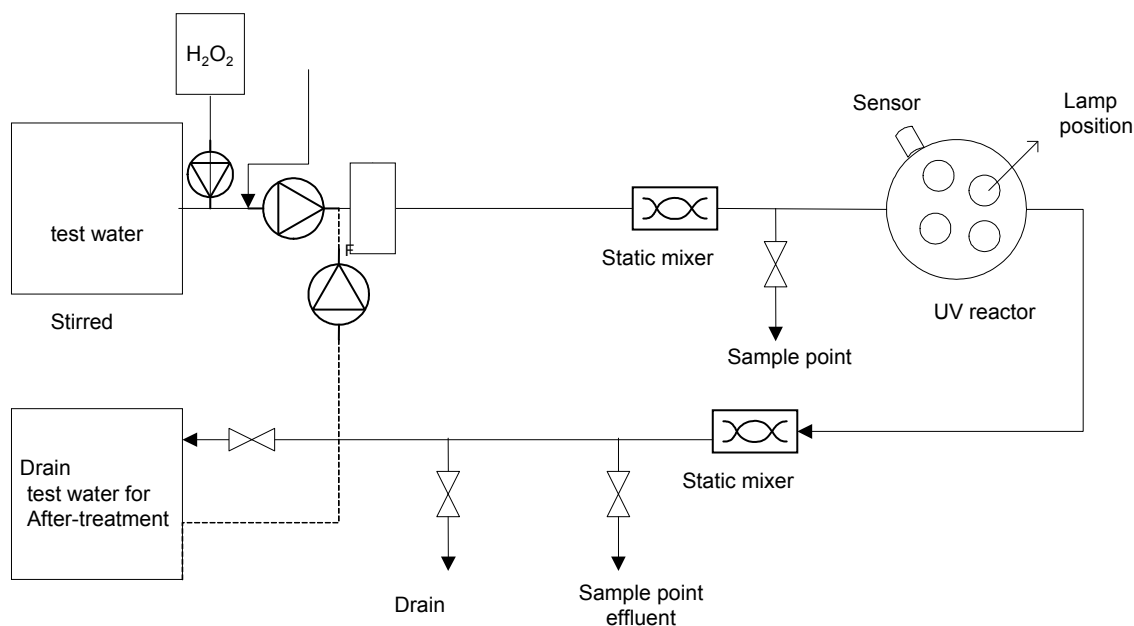
Figure 1-1: General flow sheet of a UV/H₂O₂ pilot plant

Depending on the circumstances, this flow sheet can be adapted at the actual site. In every chapter the exact flow sheet applied for that particular work package is shown.

In chapter 3 the results of Work package 1 are shown. On laboratory and pilot scale it was demonstrated that Low Pressure UV lamps can be more efficient for UV/H₂O₂ processes than Medium Pressure lamps. DBD lamps were shown to give a performance in between MP and LP UV lamps for several kinds of organic micropollutants, tested in pretreated water from both Dunea (Meuse water) and GCWW (Ohio River). The better the water quality (e.g. regarding UV transmission) the more effective the process will be. In general, the formation of nitrite and AOC is the lowest with LP UV lamps. As with all three types of lamps an inactivation of 8 log was obtained with MS 2 phages, it can be concluded that disinfection probably will not be a problem in the UV/H₂O₂ system. Thus, both LP and BDB lamps can be a good alternative for MP lamps. Which lamp will be the best option will depend on the circumstances (e.g. water quality), requirements and possibilities in each individual case.

In order to remove the excess of H₂O₂ and the byproducts that may have been formed, it is recommended to apply GAC filtration after the UV/H₂O₂ process.

In chapter 4 work packages 2-5, carried out at Philips Lighting, are described. Two new types of lamps were developed: the High Output Low Pressure amalgam lamp (HO-LP UV lamp) and the Dielectric Barrier Discharge Lamp (DBD lamp). The first one by now has been successfully taken into production and is commercially available. Although the DBD lamp showed good results, both in the pilot of KWR as well as in the pilot of Dunea, this lamp will not be further developed as long as there is no reasonable return of investment. On the other hand, no full scale treatment plants will be developed, as long as this DBD lamp will not have been fully developed.

Chapter 5 (WP 6) deals with the design and building of pilot plants. Two pilot plants were built: one at GCWW and one at Dunea.
The results obtained in WP 7 with the GCWW pilot plant, using either LP or MP UV lamps, are described in chapter 6. A good conversion was obtained for all contaminants tested. When the water was first treated with GAC, the water quality improved, resulting in a lower energy demand and higher

conversion efficiency of the process. Seasonal variations also affect the energy demand of the process. A significant advantage was observed in using UV combined with H_2O_2 versus only photolysis by UV irradiation for the degradation of several compounds. The process, however, results in an increase in the total AOC concentration.

In chapter 7 (WP 8) the results obtained with the Dunea pilot plant are shown. These results in general are in good accordance with the results obtained at GCWW. Here too, seasonal variations were observed to affect the process efficiency. The performance of the DBD lamp was in between the performance of MP and LP lamps. The use of MP lamps results in a relatively high amount of AOC formation, whereas LP lamps, for similar degradation performance, give the lowest AOC formation.

The average Electrical Energy per Order (E_{EO} = the amount of energy required to convert a certain compound in a certain reactor) for the pilot reactors applied in this research is shown in Table 1.

Table 1: Average E_{EO} (kWh/m^3-order) for the pilot plants used in this investigation

Pilot Plant	MP	LP	DBD
KWR	~ 0.7	~ 0.4	~ 0.4
Dunea	~ 1.4	~ 0.4	0.3 – 2
GCWW autumn	0.4-1.8	~ 0.3-1.0	
GCWW winter	~0.2-1.2	~ 0.2-0.6	
GCWW spring	~0.2-1.2	~ 0.1-0.5	
GCWW summer	0.4-1.5	~ 0.1-0.3	

Care has to be taken in comparing the results for the different pilot plants shown in table 1. The pilot reactors of Dunea and GCWW had been partly optimized for the lamps they had been equipped with. The KWR pilot reactor had not been optimized for a special type of lamp, but can be operated with all three types of lamps.

In chapter 8 a model is presented that has been developed at KWR to predict the performance of UV/H_2O_2 reactors. It is based on the combination of a kinetic model, describing both photolysis and oxidation processes, and Computational Fluid Dynamics, modeling the flow through the reactor vessel. Good results were obtained with all pilot plants at the three locations (KWR, Dunea and GCWW).

Formation of genotoxic by-products could be demonstrated in some situations with the Ames II test. This research, carried out in WP 9, is described in chapter 9.

Finally, in chapter 10 (WP 10) some suggestions are given for the design of a UV/H_2O_2 reactor, combined with a GAC contactor in the same unit.

The general conclusions of this research are, that all three types of lamps can be used to effectively degrade organic micropollutants and to obtain disinfection. The LP lamps seem to be the most efficient, although the DBD lamps may be a good alternative. Unfortunately, their development will not be continued at the moment. Applying a GAC contactor after the UV/H_2O_2 process not only removes the excess of H_2O_2, but also any (genotoxic) byproducts that may have been formed during the process.

A more detailed general overview and more comprehensive conclusions of the research carried out in the framework of this project and its results can be found in chapter 11. Which factors have to be taken into account when it is considered to build a UV/H_2O_2 process, or to implement this technology into an existing water treatment plant is described in chapter 12. Finally, in chapter 13, suggestions for future research are given. In this chapter also those projects are mentioned, which were already started and can be considered as a sequel to the work described in this report.

Contents

12 Practical implementation of UV/H₂O₂ technology in water treatment plants 195

When it is considered to apply UV/H₂O₂ technology at a full plant scale, several tools now are available to establish whether in this particular case this would be a suitable technology, and, if so, how it should be implemented. 197

1 Abbreviations and Conversions

Table 1-1 Abbreviations

ADK	Adenylate kinase
AOC	Assimilable Organic Carbon
ATP	Adenosine-5′-triphosphate
ATZ	Atrazine
CFD	computational fluid dynamics
CONV	Conventional
DBD	dielectric barrier discharge
DI	De ionized
EBCT	Empty bed contact time
EDC	Endocrine disrupting compounds
EE2	17-α-Ethynylestradiol
E_{EO}	Electrical energy per order
GAC	Granular activated carbon
GCWW	Greater Cincinnati Water Works
HPC	heterotrophic plate count
Ibu	Ibuprofen
LC	liquid chromatography
LP	low pressure
MCC	Maximum contaminant level
MDL	Minimum detection limit
MP	medium pressure
MIB	Methyl iso-borneol
MS2	Bacteriophage
NDMA	N-nitrosodimethylamine
NOM	natural organic matter
NOX	Nitrogen oxide
OMP	Organic micropollutant
pCBA	Para chloro benzoic acid
polyP	Poly phosphate
PPK	Poly phosphate kinase
RMTP	Richard Miller Treatment Plant (GCWW)
RO	Reverse osmosis
SPE	Solid Phase Extraction
SUVA	Specific UV absorbance (= UV/DOC)
THMs	Trihalomethane compounds
UV-C	UV irradiation 100-280 nm

Table 1-2 Conversion factors

TYPE		MULTIPLY BY …	TO OBTAIN …
Density	g/cm^3	62.43	lbs/ft^3
Electrical Energy per Order (E_{EO})	kWh/m^3-order	0.264	kWh/1000 gal
Flow	m^3/h	4.403	Gpm
	ML/d	0.264	Mgd
Length	m	3.281	Ft
	cm	0.394	In
Pressure	bar	14.50	psi (lbf/in^2)
Velocity	m/s	3.281	ft/s
Volume	L	0.624	Gal

2 Introduction

Solid barriers against (organic) micropollutants in drinking water are becoming more and more important, as there is an increasing variation in pollutants in ground and surface water, and a continuous improvement in the analytical techniques. Organic micropollutants are compounds which, because of their properties, emissions and/or concentrations in the environment, may represent a more than negligible risk for man or environment. In general, they can be characterized as persistent, bio accumulative, ecotoxic or harmful for human health (e.g. carcinogenic, reprotoxic, mutagenic or hormone disruptant). For some compounds an actual hazard to human health has not been established, but even in that case, the possible effects of a cocktail of several compounds on human health or environment are unknown yet.

Application of UV/H_2O_2 oxidation followed by granular activated carbon (GAC) adsorption represents a solid and flexible barrier against a broad range of organic micropollutants. The state-of-the-art UV/H_2O_2 technology at the start of this project (2006) was equipped with MP lamps, which rendered it possible to design a compact installation with a small footprint.

This study consisted of ten "work packages" (as shown in Table 2-1), carried out by four participants: KWR Watercycle Research Institute, Dunea, Greater Cincinnati Water Works and Philips Lighting. Each chapter of this report deals with one or more work packages, described by the participant involved.

Table 2-1: Workpackages in the total project

Workpackage	Titel
1	Proof of efficacy of lamp types (KWR)
2-5	Research and development on new lamps and ballasts for UV/H_2O_2 oxidative treatment (Philips Lighting)
6	Design and build $UV/H_2O_2/GAC$ pilot plant
7	Pilot plant research I (GCWW)
8	Pilot plant research II (Dunea)
9	Formation and removal of genotoxicity during UV/H_2O_2-GAC treatment (KWR)
10	Design combined full scale oxidation unit (KWR)

In chapter 3 the proof of efficacy of lamp types is described by KWR. Apart from medium pressure (MP) lamps, there also are low pressure (LP) UV lamps, which have a smaller electrical power, and thus represent a larger footprint. However, their energy consumption is lower, their energy efficiency higher (25-30% for LP lamps and only 15 % for MP lamps) and their expected life span is at least twice as long as for MP UV lamps. In this study both types of lamps have been compared. Especially the energy requirement of both lamps is a very important factor, as the costs of energy form a substantial part of the operational costs of a UV/H_2O_2 installation.

In chapter 4 the results of work packages 2, 3, 4 and 5, carried out by Philips Lighting are described. Philips Lighting is developing new types of lamps. One of them is a low pressure amalgam lamp with high power. Another innovation is the development of a mercury free type of UV lamp, which combines the advantages of LP and MP lamps, without their disadvantages. This lamp too was tested in the KWR pilot reactor and in a specially designed pilot plant at Dunea.

Chapter 5 deals with the design and building of UV/H_2O_2 GAC pilot plants by KWR.

The UV/H_2O_2 process combines two processes: direct photolysis of organic compounds by absorption of UV light, and oxidation of compounds by means of •OH radicals, formed by absorption of UV light by H_2O_2. First the effectiveness of the latter process was tested with various lamps. Subsequently, the conversion of organic micropollutants, hormones and pesticides with different types of lamps was studied in the KWR pilot reactor (chapter 3) and in pilot reactors both at GCWW and at Dunea. The

process effectiveness for these compounds and disinfection were measured. Chapter 6 shows the results obtained in the pilot plant research at GCWW, whereas chapter 7 shows the results of the pilot plant at Dunea (work packages 7 and 8 respectively). In chapter 8 modeling of the UV/H_2O_2 process by KWR is described. The possible formation of genotoxic compounds during UV irradiation is the topic dealt with in chapter 9 by KWR (work package 9: formation and removal of genotoxicity during UV/H_2O_2-GAC treatment). Chapter 10 deals with the feasibility of a combined full scale oxidation unit together with GAC contactors at KWR (work package 10).

Proof of efficacy of lamp types

Work package 1; KWR

Authors: C.H.M. Hofman-Caris, E.F. Beerendonk, D.J.H. Harmsen

3 Work Package 1: Proof of efficacy of lamp types (KWR)

3.1 Introduction

During the past few years analytical techniques to detect organic micropollutants have been much improved. That is part of the reason more and more micropollutants are being detected in ground and surface water. The other reason is that the amount and types of micropollutants are continuously increasing, for example because medication consumption is increasing. UV has been used for some decades now in order to obtain disinfection of drinking water. UV irradiation can also be applied to convert organic compounds by means of photolysis. However, not all compounds are sensitive toward photolysis, and if they are, it strongly depends on the UV wavelength. So, it is not possible to use UV irradiation to obtain sufficient conversion of all micropollutants. If H_2O_2 is also added to the water, part of the UV irradiation will be absorbed by the H_2O_2, resulting in the formation of hydroxyl radicals ($\bullet$OH). These radicals are very reactive, and react nonselectively with most (organic) compounds. In principle organic micropollutants can be converted into CO_2 and H_2O. However, in practice this goal hardly ever is reached. Most compounds are converted into smaller, often better biodegradable compounds. In order to remove the excess of H_2O_2 and the remaining organic compounds from the water, the water is subsequently filtered over granular activated carbon (GAC). Thus, a very solid and flexible barrier against organic micropollutants can be obtained.

Currently, there are two types of UV lamps commercially available: Low Pressure (LP) and Medium Pressure (MP) lamps, both containing mercury. When this study was started, in Dutch water treatment using UV irradiation, mostly MP lamps were used (Martijn 2006). The suitability of other types of lamps for UV/H_2O_2 processes was investigated, and the effects on disinfection and on conversion of organic micropollutants (hormones and pesticides) were considered as well. Furthermore, Philips lighting has been developing a mercury free type of UV lamp: the dielectric barrier discharge lamp, which is described in chapter 4. The effectiveness of the radical formation process for LP, MP and BDB lamps also was studied.

3.1.1 Back ground information (theory)

UV/H_2O_2

Research aimed at the application of the UV/H_2O_2 oxidation process for drinking water treatment was started in the 1990's. The practical application of the process for drinking water purification is relatively new. It became possible partly as a result of the development of small, powerful Medium Pressure (MP) UV lamps, which emit light over the total UV-C range (200 – 285 nm). MP-lamps can be produced with a power up to 15 kW, resulting in compact installations. In the Netherlands, Advanced Oxidation Processes (AOP) for the production of drinking water are always followed by granular activated carbon (GAC) adsorption to remove the excess H_2O_2 and the assimilable organic carbon (AOC).

To activate the UV/H_2O_2 oxidation process, hydrogen peroxide (H_2O_2) is added to the water prior to the UV-reactor. The effect of the process is based on two principles: direct conversion by UV (photolysis) and conversion by hydroxyl radicals. These hydroxyl radicals are formed by absorption of UV by H_2O_2.

H_2O_2 is split in two hydroxyl radicals by absorption of UV light (hv):

$H_2O_2 \Rightarrow 2 \bullet OH$
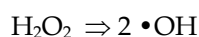
Conversion of unwanted compounds can take place by absorption of UV light (photolysis) or oxidation (reaction with $\bullet$OH):

$$\text{compound} \quad \overset{\cdot OH}{\underset{h\nu}{\Rightarrow}} \quad \text{degradation compound(s)} + CO_2 + H_2O.$$
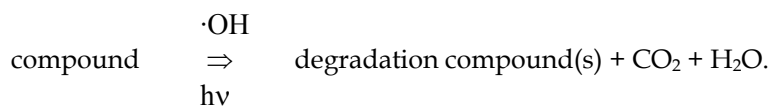
The •OH radicals react within milliseconds with target compounds like pesticides. Degradation products will be formed, and some compounds may even be mineralized towards CO_2 and H_2O. Furthermore, the target compounds may be converted by direct absorption of the UV irradiation (photolysis). According to the first law of photochemistry, photolysis can only take place if the compound really absorbed UV photons.

The relation between the end concentration C and the UV dose is expressed by the following mathematical formula (Bolton et al., 2001):

$$-\ln \frac{C}{C_0} = k * \text{UV-dose}$$

With:
C_0 = initial concentration of target compound
C = concentration of target compound at a certain UV-dose

As the hydroxyl radicals also react with other, naturally occurring compounds in the water, like humic acids and inorganic ions (including (bi) carbonate HCO_3^-/CO_3^{2-}) a relatively high amound of radicals has to be produced to obtain sufficient conversion of the target compounds.

Furthermore, these side reactions may result in the formation of by -products like assimilable organic carbon. [Kruithof en Kamp, 2000; IJpelaar *et al.*, 2005; IJpelaar *et al.*, 2006]. The amount of disturbance by compounds present in the water and the formation of byproducts during the oxidation process depend on the type of lamp used.

At the moment both low pressure and medium pressure UV lamps are used internationally in drinking water treatment (e.g., for water disinfection).

In conventional mercury containing lamps, the UV-light is produced by ionizing the mercury by means of electrical discharge. Thus the mercury atoms are brought into an excited state. When they return to the ground state photons are released. The energy of these photons, and thus the wavelength of the light emitted, depends on the pressure of the gas in the UV lamp. At a low pressure (1 – 10 millibar) UV-light at a wavelength of 253.7 nm is emitted. At a higher pressure (1 – 3 bar) a broad spectrum of wavelengths between <200 and 800 nm is emitted (see Figure 3-1). This is the essential difference between a LP and a MP UV lamp [Van der Pol and Krijnen, 2005]. For oxidation purposes mainly MP lamps are used.

Determination of UV dose

The UV dose is a very important parameter in the experiments described. Which dose a compound receives does not only depend on the output of the lamps, but also on e.g. flow conditions and residence time in the reactor. There are several ways the dose can be determined.
- Generally, commercial reactors have been equipped with sensors that give a reading, which can be used. This type of dose determination was used in the research carried out at GCWW and Dunea.
- In a collimated beam set-up the dose can be calculated very accurately, as flow conditions do not really play a role. The dose depends on the output of the lamp, and on some factors, like the petri-factor. It can be determined using an actinometer (a compound for which the relation between dose and conversion is very clear) in pure water (milli Q). Several actinometers have been described in literature (Bolton, 2003; Jin 2006).

- Biodosimetry is a method, where first a dose-reponse relation is established between inactivation of a certain microorganism in a water matrix, and the dose applied, using a collimated beam set-up. Subsequently, the inactivation of this microorganism is determined in a flow-through reactor, and related to the UV dose the organism has received according to the dose-response relation.
- "Chemidosimetry" is a procedure similar to biodosimetry, using a model micropollutant in stead of a microorganism. Workpackage 1 this procedure has been applied, using atrazine as the model compound.
- Finally, CFD calculations can be used to determine the average dose in a reactor. The dose thus calculated was used in modeling procedures, and in comparing modeling results of UVPerox I and II with experimental results obtained.

Medium pressure UV/H_2O_2 oxidation

An advantage of the use of MP lamps is the broad range of wavelengths emitted. In case the wavelength emitted equals the wavelength that can be absorbed by a target compound, this compound can be degraded. Formation of •OH radicals also depends on absorption of certain wavelengths by the hydrogen peroxide. In general, it can be expected that as more UV light is absorbed, more radicals will be formed, resulting in a better conversion of target compounds.

MP UV/H_2O_2 oxidation forms a broad barrier against organic micropollutants. The following characteristics can be attributed to UV/H_2O_2 oxidation systems, equipped with MP lamps:

- The conversion of electrical energy to UV-C is 12 – 15%. Part of the energy is emitted in wavelengths that do not contribute to photolysis nor to the formation of hydroxyl radicals (up to 25% is visible light).
- A significant part of the UV-C radiation is absorbed by organic matter and nitrate (background absorption between 200 and 240 nm). As a result more energy is required in order to convert the target compounds, compensating for this loss of energy.
- As a result of the absorption of UV radiation by dissolved organic carbon and nitrate, assimilable organic carbon and nitrite are formed respectively.
  Nitrite is formed by absorption of UV light with a wavelength < 240 nm by nitrate. Nitrite can effectively be removed by filtration on active carbon with a sufficient contact time [Kamp et al., 2007].
- The guaranteed lifespan of the MP lamps is relatively short: 3,000 – 4,000 hours (< ½ year at discontinuous use according to the manufacturer);
- Maximum of 15 kW.

Figure 3-1 shows the emission spectrum of a common MP lamp and the wavelength depending absorption of H_2O_2.
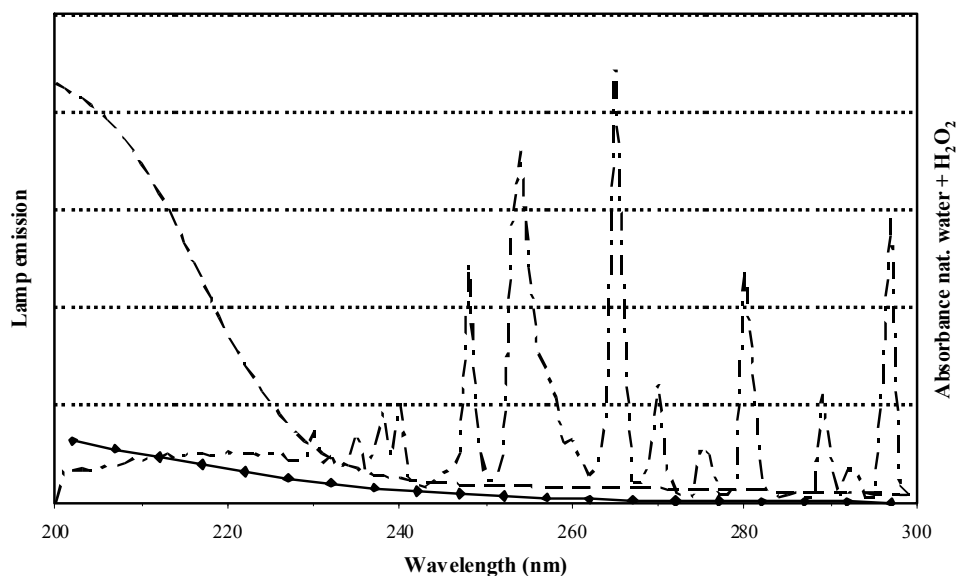
Figure 3-1Emission spectrum of a MP-lamp (———) and the absorptions of a common pretreated natural water (– – –) and of a 10 mg/L H_2O_2 solution (according to the Lambert-Beer law) (♦). Composition of natural water: DOC-content: 3.6 mg/L C; [NO3-]: 11.2 mg/L.

Low pressure UV/H_2O_2 oxidation

The characteristics of the MP lamps, as described above, are partly disadvantageous (low energy efficiency, short lifespan). These disadvantages can be reduced by using lamps emitting another range of wavelengths. A low pressure (LP) UV lamp emits light of mainly one wavelength: 253.7 nm. LP lamps have the following characteristics, possibly resulting in a lower energy demand, smaller chance of byproduct formation and lower costs:

- about 30% of the electrical energy is converted into UV-light;
- less energy loss by:
  - heat (lamp temperature ~ 45 ∘C);
  - unusable wavelengths (> 95% of the light emitted is 253,7 nm UV-C light);
  - absorption by natural compounds (DOC, nitrate);
- smaller chance of byproduct formation (and thus probably lower concentration of by -products) as a result of the lower absorption of natural water at 253.7 nm;
- LP lamps have an expected lifespan of 9,000 – 10,000 hours, as a result of which they can be used longer than one year under continuous operation (according to the manufacturer)

However, the power of the present generation of LP lamps is less than 1 kW, which is notably lower than that of MP lamps (15 kW). As a result, the footprint of a UV/H_2O_2 installation equiped with LP-lamps will be larger than for an installation with MP-lamps, as more LP lamps are required to obtain the same total UV power as with MP lamps, as was done in this research for comparison purposes. Although for plant processes probably not the same total UV power will be required for both types of lamps, still the footprint for installations equipped with LP lamps will be larger.
As only one wavelength is emitted, the contribution of photolysis to the conversion of organic micropollutants is small. To obtain a sufficient barrier against organic micropollutants, a relatively larger contribution by oxidation processes is required.

Figure 3-2 shows the emission spectrum of a LP-lamp and the wavelength depending absorption by H_2O_2.
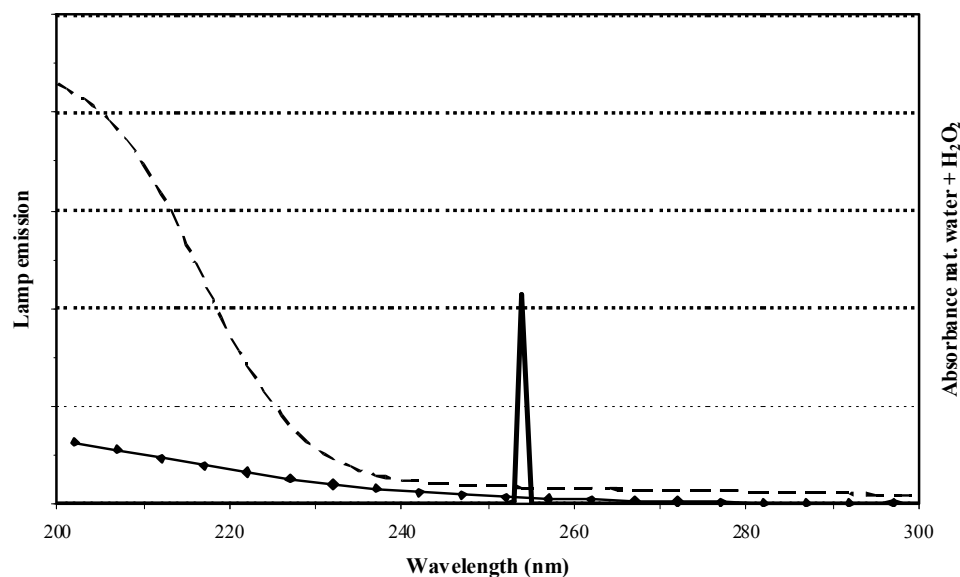
Figure 3-2 Emission spectrum of a LP-lamp (——) and the absorptions of a common pretreated natural water(– – –) and of a 10 mg/L H_2O_2-solution (according to the Lambert-Beer law) (♦). Composition of the natural water: DOC-content: 3.6 mg/L C; [NO_3^-]: 11.2 mg/L

In Table 3-1 the main differences between both types of UV lamps are summarized.

Table 3-1 Main differences between LP and MP mercury UV lamps

LP mercury lamp	MP mercury lamp
Low power: <1 kiloWatt	High power: ≤30 kiloWatt
Emission: 253,7 nm	Emission: 200 – 800 nm
High energy efficiency: ~ 30%	Low energy efficiency: ~ 15%
Relatively long lifespan: ~ 9,000 hours*	Relatively short lifespan: 4,000 – 6,000 hours*

* average expected lifespan according to the lamp manufacturer.

Dielectric Barrier Discharge (DBD)- UV/H_2O_2 oxidation

Both MP as well as LP lamps contain mercury. These mercury based lamps show some disadvantages, like:
- Presence of mercury (environmental disadvantage)
- Quartz sleeves required;
- Lamp should burn inside a quartz sleeve, to obtain the required lamp temperature
- Temperature dependence of "Low Pressure-High Output" (LP-HO) lamps;
- Slow start up.

Philips Lighting is developing a lamp without mercury, the Dielectric Barrier Discharge (DBD) lamp that would combine the advantages of LP and MP lamps, without their drawbacks. Dielectric barrier discharge is the electrical discharge between two electrodes separated by an insulating dielectric barrier. The lamps use an excimer gas. An eximer ("excited dimer") is a short-lived dimeric or heterodimeric molecule, formed from two species, at least one of which is in an electronic excited state. When this compound returns to its ground state UV photons can be emitted.

The 300 W DBD lamp which has been used in this investigation is a mercury free UV-lamp, emitting UV-light with a peak between a wavelength of 240 and 245 nm. For the lamps that are being developed, it is expected that the energy efficiency will be 24%, with a possible power up to 2000 W.

3.2 Hydroxyl radical formation

The efficiency of hydroxyl radical formation depends on the UV wavelength emitted. The H_2O_2 extinction decreases with increasing wavelength between 200 and about 280 nm (Figure 3-1 and Figure 3-2). MP-lamps cover this range. However, in the range where H_2O_2 absorption is strongest (200 – 235 nm), the emittance of the MP lamps is rather weak (Figure 3-1). Furthermore, natural compounds like DOC and nitrate show a strong absorbance in this wavelength range (200 – 235 nm). Both aspects result in a low hydroxyl radical formation in this wavelength range.
Although the extinction of H_2O_2 at 253.7 nm is low, the radical formation by LP lamps may be rather efficient, as a result of the very low absorption of UV irradiation by DOC and nitrate at 253.7 nm. This resulted in the following hypothesis.

Hypothesis
As a result of the low absorption by the water matrix at a wavelength of 253.7 nm (which is specific for LP lamps) the radical production at this wavelength may be higher than at wavelengths below 254 nm, even though at 253.7 nm the absorption by H_2O_2 is notably lower than at a lower wavelengths.

This hypothesis was verified by means of calculations of the fraction of UV light absorbed by H_2O_2 (Bolton, 2001). According to this calculation, H_2O_2 absorbs 21.4% of the UV-light (total 'photon flow') from a LP lamp, compared to 15.5 % from an MP-lamp. The theoretical data were experimentally verified using a compound that is known to effectively react with hydroxyl radicals [Rosenfeldt *et al.*, 2004]. To determine the amount of hydroxyl radicals formed, a "hydroxylprobe" can be used. A well known hydroxyl probe is *para*-chlorobenzoic acid (pCBA) [Elovitz and von Gunten, 1999]. Results of these tests will be described elsewhere in this report.

3.3 Set-up work package 1 "proof of principle"

In the literature (Bolton 2001), calculations have been performed for both MP and LP UV lamps, based on a range of wavelengths of 200 to 800 nm for MP lamps and 253.7 nm for LP lamps. It is known that H_2O_2 will absorb more UV light at a lower wavelength than at 253.7 nm. However, the absorption by the water matrix at lower wavelengths will be higher too. Thus, it was calculated that H_2O_2 may absorb the light from a LP lamp up to 30% more efficiently than the light from an MP lamp. An example of such calculations is given in appendix XIX.
Based on these calculations, the hypothesis was formulated, that, as a result of the low UV absorption of the water matrix at a wavelength of 253.7 nm, the production of radicals from H_2O_2 will be higher than at lower wavelengths, although the absorption by H_2O_2 will be lower at a wavelength of 253.7 nm. This hypothesis was tested.

3.4 Materials and methods

In work package 1 tests were carried out using the collimated beam set up of KWR and a small pilot plant (pilot reactor), which had been built especially for this project. This pilot reactor can be equipped with all types of UV lamps. During the investigation, the performance of a LP UV-lamp and of a new, mercury free UV-lamp (DBD) developed by Philips Lighting were compared with the performance of a MP UV-lamp, which is already applied in practice. Furthermore, experiments were carried out at various water qualities and different peroxide concentrations.

3.4.1 UV lamps

All lamps used in this project were made available by Philips Lighting BV in Roosendaal, the Netherlands.

Collimated beam
MP lamp: Philips HOK 20/100; 2 kW medium pressure lamp

LP lamp: Philips TUV PL-L95/4P; 95 W HO low pressure lamp. This lamp has been developed by Philips Lighting, and is described in section 4.3 of this report.

DBD lamp: 300W DBD lamp, producing UV irradiation with a peak emittance at a wavelength between 240 en 245 nm . This lamp is a prototype of a new type of UV lamp, which is being developed by Philips Lighting (see section 4.1).

Pilot plant
MP lamp: HOK, lamp code 586/3. During the experiments the lamp is dimmed to about 10% of the Total power, in order to obtain a UV-output which is comparable with the other lamp types.

LP lamp: prototype 2KW LP lamp length 210 cm

DBD lamp: 300W DBD lamp, emitting UV-light with a peak emittance of 240 to 245 nm

3.4.2 Collimated beam installation

The UV dose is defined as the energy (or the amount of photons) absorbed by an irradiated object during a certain period per area or volume. In UV installations for water treatment, water flows along the lamps (or quartz sleeves). The UV dose then is determined by the lamp intensity and the residence time of a particle or microorganism in the reactor. This residence time in turn depends on the flow profile and the reactor geometry, which is difficult to characterize. Because of this reason often a collimated beam set up is used in laboratories, as it can be operated under standard conditions.

A collimated beam set up offers the possibility to determine the effect of the UV dose on the inactivation of micro organisms and the conversion of chemical compounds under controlled and ideal conditions at a laboratory scale. In the KWR installation dose-effect relations can be measured. The set up can be equipped with various types of UV lamps, like LP and MP mercury lamps. In this way the dose-effect relation of a specific lamp can be determined [Harmsen, 2004]. The collimated beam set up is schematically shown in Figure 3-3.
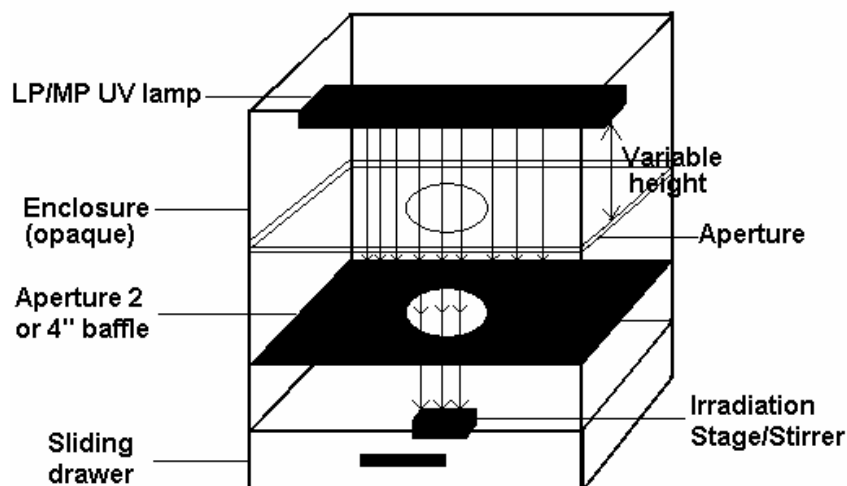
Figure 3-3 Schematic picture of a collimated beam installation

The lamp ('beamer' in Figure 3-3) is placed in a box made of stainless steel. The irradiation enters a wooden box through a hole. By means of a collimator, formed by adjustable plates, a parallel UV bundle hits the water sample. As the plates are removed or adjusted, the bundle can be adjusted, obtaining an optimal uniform irradiation of the sample surface. Furthermore, the sample is stirred during the irradiation.

By means of an automatic shutter, the UV irradiation is interrupted after a certain irradiation time. The required irradiation time is calculated based on specific conditions (like UV_{254nm} (LP-lamp) or $UV_{200-300nm}$ (DBD- or MP-lamp), the UV-intensity of the lamp, sample volume, petri factor) [Bolton en Linden, 2003] using the spreadsheet of Bolton. If disinfection tests are carried out, a correction is made for the (DNA) absorption curve in the calculation of the irradiation time. During UV/H_2O_2 tests, such a correction is not made.

The UV dose (mJ/cm^2) has been defined as the product of the irradiation time (t in seconds) and the irradiation intensity (wavelength dependent UV output of the lamp) in mW/cm^2. A detailed description of the calculation of UV doses can be found in report BTO 04.014 *Protocol Collimated Beam UV* [Harmsen, 2004] and in the article "Standardization of Methods for Fluence (UV Dose) Determination in Bench-scale UV Experiments" [Bolton and Linden, 2003].

The lamp intensity (= irradiation intensity) is determined using an IL 1700 Research Radiometer and a SED sensor. This sensor detects UV-light between 185 and 310 nm. This equals the wavelength range that is applied for disinfection and conversion of organic micropollutants (in this range also the irradiation can be found which causes inactivation of micro organisms and conversion of organic micropollutants). Besides, the sensor has been equipped with a filter (the "wide-eye diffuser" (W)). This diffuser ensures that the light, entering the sensor under various corners, attributes equally to the total intensity measured.

3.4.3 UV-pilot installation

Using the KWR UV pilot installation experiments can be carried out on a small scale (up to 5 m^3/h). The effect of the UV dose on the inactivation of micro organisms and the conversion of chemical compounds can be determined. During the experiments water quality, the type of UV lamp, the water flowrate through the reactor and the H_2O_2-concentration can be varied. By varying the water flow, the UV dose is varied equally: the higher the flow, the lower the UV dose applied.

Before starting experiments with the pilot installation, first the relation between flow and UV dose had to be established. This can be done in several ways:
- Calculation by means of Computational Fluid Dynamics (CFD) modeling,
- Determinatin by means of a biodosimeter (desinfection),
- Determination by means of a chemidosimeter (UV/H_2O_2).

A biodosimeter consists of a suspension of bacterial spores (in this project MS2 phages were used), for which the UV sensitivity is calibrated at a laboratory scale. The biodosimeter test is used to test UV systems, in which a (series of) reactor(s) is certified based on measurements using one prototype. Furthermore, the biodosimeter test can be applied to determine the effectiveness of UV systems under practical conditions, establishing the effect of process parameters (flow, UV intensity) and local water quality. In this test, micro organisms (MS2 phages) are injected into the water before UV irradiation. The inactivation of these micro organisms by means of UV has been determined under well known circumstances using a collimated beam set-up. Subsequently, the inactivation of these micro organisms in the pilot plant is measured, and the UV dose is determined as the dose corresponding to an equal inactivation obtained in the collimated beam set up.

To determine the UV dose in a UV/H_2O_2 process, a chemidosimeter is used. This procedure is similar to the procedure for a biodosimeter, with the difference that instead of the suspension of bacterial spores, a solution of a certain chemical compound is used. In our case atrazine was used as the chemidosimeter, because it can easily be converted by means of UV, is easy to analyze, and gives reliable results.

During validation, only photolysis is considered (so no H_2O_2 is added). In this way the effect of UV in the UV reactor can be determined. In case H_2O_2 would have been added, two simultaneous processes, photolysis and UV oxidation, would have been studied.
During the validation, first the dose response curve of atrazine in the water which should be tested, was determined, using the collimated beam set-up. Subsequently, the conversion of atrazine in the pilot reactor was determined at various water flows. Based on the results obtained, the desired water flow (i.e., UV dose) could be established. This validation with atrazine should be repeated every time conditions (lamp type, water quality) are changed. The validation procedure has been extensively described in appendix VIII.

Apart from the validation of the pilot reactor with atrazine, the reactor had been modeled using Computational Fluid Dynamics (CFD) [Lanzhu Shao, 2007, Hofman, 2008]. CFD had been applied to obtain a better idea of the flow profile through the reactor. The reactor is shown in Figure 3-4. In appendix I a picture of the reactor, including the LP lamps) is shown.
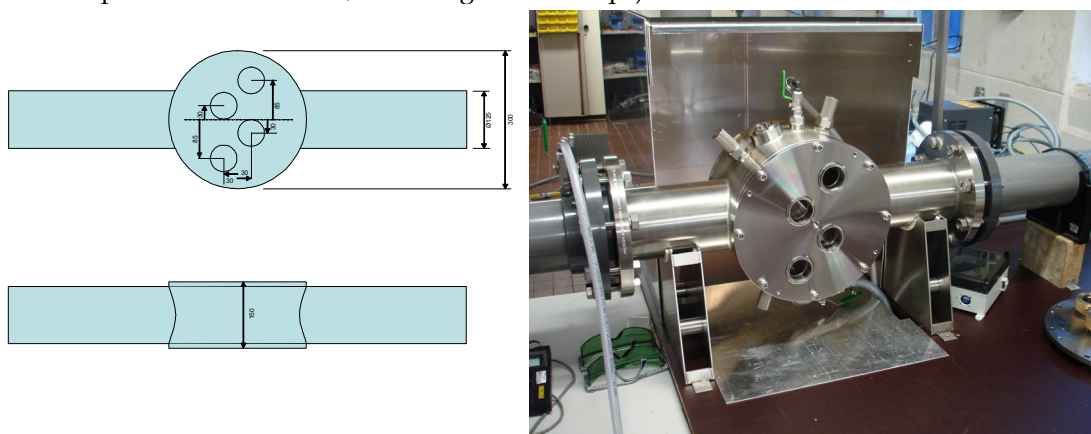
Figure 3-4 picture of the UV pilot reactor at KWR watercycle research institute

In Figure 3-5 the flow diagram of the pilot reactor with equipment is shown. The water to be tested is kept in stainless steel tanks with a volume of about 700 L. The water is pumped through the reactor. The dosing point of hydrogen peroxide is situated before the pump. The water flow is adjusted by means of a valve and a flow meter, with a maximum flow of 5 m³/hour. A static mixer is located after the flow

meter to ensure optimum mixing of the solution (water and peroxide). The influent sample point is located after this static mixer.

The reactor can be equipped with four lamps. In this set-up either LP-, MP-, or DBD-lamps can be used, depending on the flanges used. Pictures of the reactor vessel with and without lamps are shown in appendix I. Using a UV sensor (MUV2.4WR UV referenzradiometer with a 'SUV20.2A2Y1R/150/UVD6 (RO001' sensor, sensitivity up to 360 nm) the UV intensity of one lamp is measured. Furthermore at the side of the reactor there is a window, enabling the experimentator to watch the operation of the lamps.

After the reactor a static mixer is placed, followed by the sampling point for the effluent samples. Depending on the solution used, the water is discharged into the sewer, or collected in a vessel for treatment, to prevent an irresponsible amount of organic micropollutants entering the sewer. During this treatment, the solution passes the UV reactor several times, before it is discharged into the sewer.
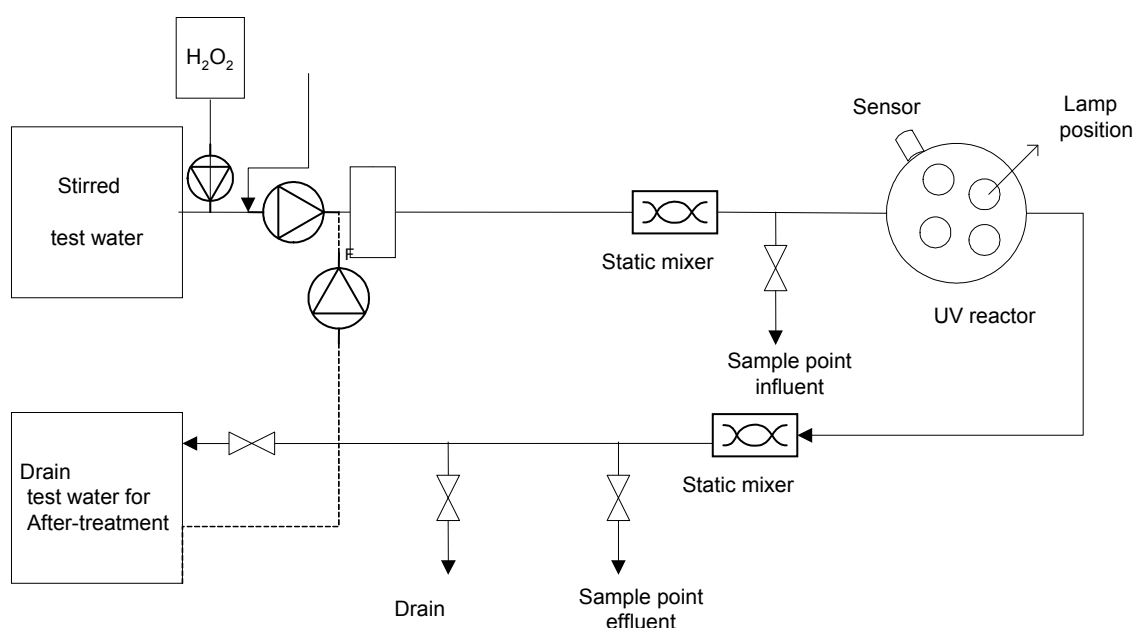
Figure 3-5 Flow diagram of the UV pilot reactor with equipment

3.4.4 Chemicals

Hydrogen peroxide 30% (H$_2$O$_2$); JT Baker, casnr. 7722-84-1.
H$_2$O$_2$ from a stock solution is diluted with milliQ until the required concentration is reached.

Sodiumsulfite (Na$_2$SO$_3$); JT Baker, casnr. 7757-83-7.
To neutralize the H$_2$O$_2$ 1 g of sodium sulfite is added to 1L solution.

Radical formation

4-chlorobenzoid acid 99% (pCBA): SAF Sigma, casnr. 74-11-3.
A 40 mg pCBA/L stock solution is prepared (according to receipe LOA-007). Using this stock solution the desired pCBA concentrations for the collimated beam experiments is prepared.

Conversion of organic micropollutants and desinfection capacity

The starting concentration of the organic micropollutants in the stock solution was selected in such a way, that a conversion of at least 95% by UV/H$_2$O$_2$ can be determined.

Collimated Beam tests
Stock solution of atrazines 200 μg/L
Atrazine; Dr. Ehrenstorfer GmbH, casnr. 1912-24-9.
Simazine; Dr. Ehrenstorfer GmbH casnr. 12234-9.

Cyanazine; Dr. Ehrenstorfer GmbH, casnr. 21725-46-2.
Desethylatrazine; Dr. Ehrenstorfer GmbH, casnr. 6190-65-4.
Desisopropylatrazine: Dr. Ehrenstorfer GmbH, casnr. 1007-28-9.

For every compound 200 μg was weighed and dissolved in milli Q water. Subsequently the solution was diluted to 1 L.

Stock solution of hormones, 4 μg/L
Estrone : Riedel-de Haën, casnr. 53-16-7.
Estradiol : Riedel-de Haën, casnr. 50-27-1.
17-beta-estradiol : Riedel-de Haën, casnr. 50-28-2.
17alpha-estradiol : Sigma Aldrich Chemie BV, casnr. 57-91-0.
17alpha-ethinylestradiol; Riedel-de Haën, , casnr. 57-63-6.

For every compound 4 μg was weighed and dissolved in milli Q water. Subsequently the solution was diluted to 1 L.

UV pilot tests
Stock solution of organic micropollutants 1 mg/L
The following medicines have been dosed:

B-blockers
Sotalol: EDQM, casnr. 3930-20-9.
Metoprolol: Sigma Aldrich Chemie BV, casnr. 37350-58-6.

Antibiotics
Lincomycine: Riedel-de Haën, , casnr. 7179-49-9.
Sulfamethoxazole: EDQM, casnr. 723-46-6.
Erythromycine: Sigma Aldrich Chemie BV, casnr.114-07-8.

Analgetics (e.g. pain killers)
Fenazone (antipyrin): Fluka'casnr. 60-80-0.
Ibuprofen: Sigma Aldrich Chemie BV, casnr. 15687-27-1.
Diclofenac: Sigma Aldrich Chemie BV, casnr. 15307-79-6.

Anti epileptic
Carbamazepine: Sigma Aldrich Chemie BV, casnr. 298-46-4.

Cholesterol lowering medicines
Bezafibrate Sigma Aldrich Chemie BV, casnr. 41859-67-0.

The following pesticides were dosed:
Alachlor: Dr. Ehrenstorfer GmbH, casnr. 15972-60-8.
Atrazine: Dr. Ehrenstorfer GmbH, casnr. 1912-24-9.
Cyanazine: Dr. Ehrenstorfer GmbH, casnr. 21725-46-2.
Metazachlor: Dr. Ehrenstorfer GmbH, casnr. 67129-08-2.

The following volatile compound was dosed:
MTBE: Fluka, casnr. 1634-04-4. MTBE is used as a fuel additive.

For every compound, except ibuprofen, 1 mg was weighed and subsequently dissolved in milli Q water. For ibuprofen 5 mg were dissolved. The solutions were diluted to 1L.

Stock solution and desinfection capacity
MS2 phages (F-specific RNA phages) were cultivated from the American Type Culture Collection (ATCC#15597B1) of GAP Enviro Microbial Services.

Test water
All experiments in work package 1 were carried out using pretreated surface water of Dunea and GCWW. The sample points and the complete treatment schematics are shown in Appendix II.

Dunea
Water from the River "Andelse Maas" (side branch of the Meuse), was treated by Dunea in Bergambacht, the Netherlands, by means of coagulation, sedimentation-micro sieves, rapid sand filtration.

GCWW
Surface water from the Ohio River was treated by the Richard Miller plant GCWW (SF GCWW) by means of coagulation, flocculation, sedimentation (2x) and rapid sand filtration.

Set-up of hydroxyl radical formation experiments

In the first part of work package 1 the hydroxyl radical formation for the various types of lamps was determined. Experiments were carried out using the Collimated Beam set-up of KWR.

pCBA was used to determine the hydroxyl radical formation. From literature (Pereira 2007; Yuan 2009) it is known that pCBA hardly can be converted by means of photolysis by UV iradiation. However, it can effectively be degraded by means of •OH radicals). First the analytical method for pCBA was validated, and the effect of the matrix was established. These results are shown in appendix IV. Subsequently, experiments were carried out using two types of water and three different lamps to determine and compare the hydroxyl radical formation for LP-, MP- and DBD-UV lamps. Experiments were carried out using pretreated water from Dunea in Bergambacht (NL) and from GCWW (USA). pCBA and H_2O_2 were added. To be able to correct the results for photolysis, a dosage of 0 mg H_2O_2 was included. During all experiments, 60 mL of sample was irradiated in the collimated beam set-up. All samples, except the samples for H_2O_2 analyses, were quenched immediately after irradiation with 100 mg sodium sulfite and subsequently analyzed for pCBA and H_2O_2. Sulfite was added to prevent a possible continuation of reactions of compounds with H_2O_2 in the samples. 100 mg of sulfite is a large excess of sulfite, which ensures that all H_2O_2 will be removed. Additionally, the water composition (pH, HCO_3^-, nitrate and non-purgable organic carbon (NPOC), UV-absorption spectrum) was analyzed.

Set-up and experimental procedures are described in more detail in Appendix V. In Table 3-2 all process conditions during the collimated beam tests are shown.

Table 3-2 Process conditions of collimated beam experiments to determine hydroxyl radical formation

phase	Lamp	Water type	additions		UV-Dose
			pCBA (µg/L)	H_2O_2 (mg/L)	(mJ/cm^2)
1a	MP	Dunea	400	0	0-300-450-600-750
				10	0-300-450-600-750
1b	MP	Dunea	400	5	0-300-450-600-750
		GCWW	400	0	0-450-600
				5 - 10	0-300-450-600-750
	LP	Dunea	400	0	0-450-600
				5 - 10	0-300-450-600-750
		GCWW	400	0	0-450-600
				5 - 10	0-300-450-600-750
	DBD	Dunea	400	0	0-450-600
				5 - 10	0-300-450-600-750
		GCWW	400	0	0-450-600
				5 - 10	0-300-450-600-750

Set-up of collimated beam experiments for conversion of organic micropollutants

After the radical formation of the different types of lamps had been measured, experiments were carried out to determine the conversion of organic micropollutants and the disinfection capacity of these lamps. First, collimated beam experiments were carried out, applying three different UV doses and a selection of hormones and triazines to obtain an idea on the degree of conversion.

These experiments were also carried out using pretreated water from Dunea in Bergambacht and from GCWW. Hormones, triazines and H_2O_2 were added to the water, and 100 mL samples were irradiated. Afterwards, all samples, except for the samples for H_2O_2 analysis, were immediately quenched with 100 mg of sodium sulfite, and analyzed for hormones, triazines and H_2O_2. Additionally, the water composition (pH, HCO_3^-, nitrate and NPOC, UV-absorption spectrum) was analyzed.

Set-up and experimental procedures is described in more detail in Appendix VI. In Table 3-3 all process conditions during the collimated beam tests are shown.

Table 3-3 Process conditions during collimated beam tests to determine the conversion of organic micropollutants (1 ng/L = 1.60 ng/gal)

lamp	Water type	additions			UV-Dose
		Hormones[*] (ng/L)	Triazines[*] (µg/L)	H_2O_2 (mg/L)	(mJ/cm^2)
MP	Dunea	40	2	10	0-300-600
	GCWW	40	2	10	0-300-600
LP	Dunea	40	2	10	0-300-600
	GCWW	40	2	10	0-300-600
DBD	Dunea	40	2	10	0-300-600
	GCWW	40	2	10	0-300-600

[*] Specifications of the hormones and triazines are given above

Set-up of pilot experiments for conversion of organic micropollutants and disinfection capacity

First the pilot reactor was validated, by determining which flow is required to obtain a certain UV dose. Validation has to be carried out for each combination of lamp type and type of water separately, as the UV dose depends on the water composition (e.g. UV transmission, Total Organic Carbon (TOC) and nitrate content) and the UV spectrum. Atrazine (without H_2O_2 addition) was used as a chemidosimeter. Set-up and validation have been extensively described in Appendix VIII.

Subsequently, the conversion of organic micropollutants with or without H_2O_2 was measured for the three types of lamps. Also the disinfection capacity and the formation of byproducts were investigated.

Experiments were carried out using pretreated river Meuse water from Dunea, Bergambacht. This water was transported in 700 L stainless steel tanks. For every test, except for the disinfection experiments with MP- or LP-lamps, a new solution of organic micropollutants and MS-2 phages was prepared (composition see section 3.5.3). During the experiments the solution was stirred, ensuring a homogeneous solution.

Before the experiments samples were taken from the tank, for analysis of the influent concentrations. An excess of sulfite (1g/L) was added, in order to obtain the same matrix as for samples taken after irradiation. To these latter samples, sulfite is added to ensure that all H_2O_2 is converted in order to prevent any further reactions of the organic micropollutants in the samples. No sulfite was added to samples for determination of H_2O_2 concentration or (in) organic macro parameters.

Samples for H_2O_2 analysis in the UV/H_2O_2 influent were taken at the influent sampling point before the UV reaction vessel. The samples for analysis of organic micropollutants after UV/H_2O_2 were taken from the effluent sampling point positioned after the static mixer. To all effluent samples 1 g/L sulfite was added. Samples were taken after a residence time of at least three times the reactor volume. Furthermore, before and after UV/H_2O_2 treatment samples were taken for analysis of natural organic matter (NOM) (Liquid Chromatography – Organic Carbon Detection; LC-OCD). Nitrite and AOC were measured in order to determine the byproduct formation during UV/H_2O_2. To samples for AOC analysis 1 g/L Na_2SO_3 was added. This was not done for LC-OCD and nitrite analysis, as it would have disturbed the analysis. Besides, nitrite is formed by photolysis of nitrate, and will not be affected by the presence of H_2O_2 in the sample.

For determination of the disinfection capacity, 100 mg/L Na_2SO_3 was added to the influent samples as well as to the effluent samples. It had been established that this addition does not affect the F-specific RNA phages (MS2 phages).

During the pilot experiments, process conditions (flow, signal of the UV sensor, effluent temperature) were measured. A detailed description of the pilot experiments can be found in appendix VII. In Table 3-4 the process conditions during these experiments are shown.

Table 3-4 Process conditions during pilot UV experiments using pretreated water from Dunea in Bergambacht

Lamp	additions			UV-Dose
	Org. micropollutants[*],[**] (µg/L)	MS-2 phages (pve/L)	H_2O_2 (mg/L)	(mJ/cm^2)
MP	2		0-10	0-300-450
		$5*10^9$	10	0-450
LP	2		0-10	0-300-450
		$5*10^9$	10	0-450
DBD	2		0-10	0-300-450
		$5*10^9$	10	0-450

[*] Specification of the organic micropollutants can be found above.
[**] For ibuprofen 10µg/L was addeddosed.

3.5   Results: Formation of radicals

3.5.1 Water quality

In July 2006 collimated beam experiments were carried out to determine the formation of hydroxyl radicals by various types of UV-lamps. The conversion of pCBA by UV/H_2O_2 was studied in both pretreated water of Dunea (Bergambacht) and of GCWW (for details on the pretreatment, see chapters 6 and 7). Based on the results obtained, the respective contributions of photolysis and oxidation processes (UV/H_2O_2) can be calculated.

The water quality was determined and a UV-scan was measured, the results of which are shown in appendix XI. An overview is shown Table 3-5.

Table 3-5 Overview of water quality during collimated beam experiments to determine the hydroxyl radical formation

Water type	Nitrate	pH	HCO_3	NPOC	UV-T$_{254nm}$
	mg/L NO_3		mg/L HCO_3	mg/L C	%
Dunea Bergambacht	6,6 - 8,9	8,01 – 8,20	135 – 136	3,5 - 3,7	79-81
GCWW	4,0 – 5,3	7,80 – 8,06	70 – 89	1,5 - 2,4	86-87

For both locations pretreated water was used, that was obtained from the point in the purification process where UV/H_2O_2 treatment may be implemented in future.
Based on the data in Table 3-5 it is to be expected that UV processes will be more efficient at GCWW than at Dunea, as the UV transmittance at GCWW is higher.

3.5.2 Results obtained with pretreated water from Dunea Bergambacht

Experiments were carried out using pretreated water from Dunea Bergambacht, various peroxide concentrations (0, 5 and 10 mg H_2O_2/L), and MP-, LP- and DBD- UV lamps. The results are shown in *Table 3-6*.

Table 3-6 Results on Hydroxyl radical formation in collimated beam experiments with water from Dunea

Test	Dose	MP		LP		DBD	
		H_2O_2	pCBA	H_2O_2	pCBA	H_2O_2	pCBA
	mJ/cm²	mg/L	µg/L	mg/L	µg/L	mg/L	µg/L
1	0	0,38*	404	0,14	402	0,41	405
	450		242		371		311
	600		210		366		293
2	0	5,1	393	4,9	406	5,4	400
	300		265		290		204
	450	5,1	225	5,1	241	5,5	147
	600		184		203		106
	750	5,0	173	5,0	173	5,4	78
3	0	10,1	398	10,6	403	10,9	404
	300		179		219		125
	450	10,0	127	10,6	159	10,6	70
	600		96		120		39
	750	10,1	73	10,6	91	10,6	23

* blank signal, not corrected for during measurements.

From the H_2O_2 analyses it can be concluded that in all cases the desired amount of peroxide has been added. The results show a clear decrease in pCBA concentration at higher UV dose and/or higher peroxide concentration. Calculations of pCBA conversion (%) and log $[pCBA]/[pCBA]_0$ are shown in appendix XII.

In Figure 3-6 the conversion of pCBA is shown as a function of UV dose during photolysis (0 mg H_2O_2/L) and during the combination of photolysis and oxidation (10 mg H_2O_2/L), for all three types of lamps.
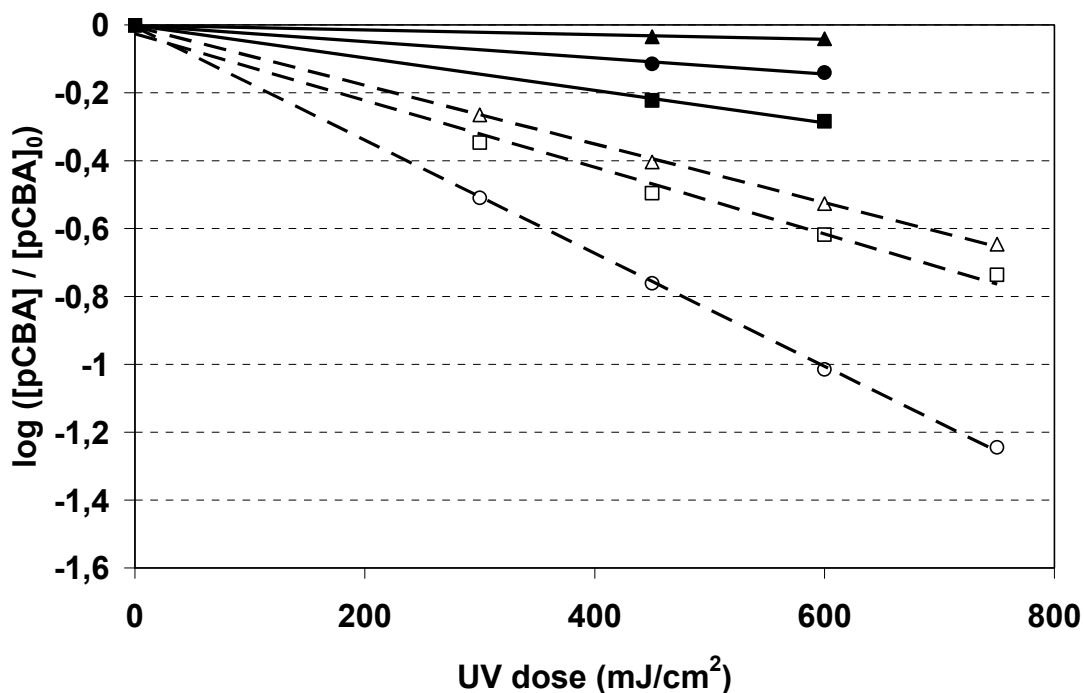
Figure 3-6 log [pCBA]/[pCBA]$_0$ versus UVdose (Dunea, Bergambacht) without H$_2$O$_2$; (■) MP; (▲) LP; (●) DBD and with 10 mg/L H$_2$O$_2$; (- □-) MP; (-Δ-) LP; (- ○ –) DBD.

The highest photolytic conversion (0 mg H$_2$O$_2$) of pCBA is obtained with the MP lamp, followed by the DBD-lamp. The LP-lamp hardly caused any photolysis of pCBA. This was expected based on the absorption spectrum of pCBA (appendix XI, Figure XI.1) which absorbs irradiation at a wavelength between 200 and 260 nm, with a peak absorbance between 220 and 250 nm (tailing to 260 nm). The MP lamp emits UV-light with a wavelength between 200 and 800 nm, covering the absorption range of pCBA. The DBD lamp has a smaller range of wavelengths (230-280 nm), rendering this lamp less effective for pCBA photolysis than the MP lamp. The LP lamp only emits at 253.7 nm, which renders photolysis of pCBA rather unlikely.

Correcting the results for the contribution of photolysis in the presence of 10 mg/L H$_2$O$_2$ shows that at a UV dose of 600 mJ/cm^2 the contribution of hydroxyl radicals to the conversion of pCBA is highest for the DBD lamp (0.9 log) and the LP lamp (0.5 log), whereas the contribution with the MP lamp is much lower (0.3 log). These results confirm the hypothesis given in 3.2.

3.5.3 Results obtained with pretreated water from GCWW

Experiments were carried out using pretreated water from GCWW, various peroxide concentrations (0, 5 and 10 mg H_2O_2/L), and MP-, LP- and DBD- UV lamps. The results are shown in Table 3-7.

Table 3-7 Results on Hydroxyl radical formation in collimated beam experiments with water from GCWW

Test	Dose	MP		LP		DBD	
		H_2O_2	pCBA	H_2O_2	pCBA	H_2O_2	pCBA
	mJ/cm²	mg/L	µg/L	mg/L	µg/L	mg/L	µg/L
1	0	0,16*	395	0,08*	405	0,11*	405
	450		223		371		318
	600		271		364		297
2	0	5,1	312	5,0	408	5,2	401
	300		284		258		176
	450	5,1	187	5,2	209	5,3	120
	600		124		176		82
	750	5,1	119	5,0	140	5,2	24
3	0	10,1	396	10,1	405	10,5	399
	300		160		184		93
	450	10,1	130	10,2	127	10,4	47
	600		145		88		23
	750	10,1	53	10,1	60	10,4	13

* blank signal, not corrected for during measurements.

From the H_2O_2 analyses it can be concluded that in all cases the desired amount of peroxide has been added. Some of the results obtained with the MP lamp cannot be explained yet: the pCBA conversion seems to be higher at a lower UV dose, in the absence of H_2O_2. Possibly some samples have been switched, although this does not seem to be likely. Furthermore, the starting concentration of pCBA at 5 mg H_2O_2/L seemed to be 312 µg/L, whereas 400 µg/L had been added, resulting in a lower conversion of pCBA. This could not have been caused by uncertainties in the analysis method, as the inaccuracy is <5%. As there seemed to be enough reliable data to draw conclusions on, it was decided not to repeat these experiments.

During the experiment with 10 mg H_2O_2/L surprisingly more pCBA was retrieved after application of a dose of 600 mJ/cm² (145 µg/L) than after a UV-dose of 450 mJ/cm² (130 µg/L). The result obtained at 600 mJ/cm² and a H_2O_2 concentration of 10 mg/L is shown in the graph (figure 7, red marked point), but has not been taken into account during further calculations.

Calculations of pCBA conversion (%) and log [pCBA]/[pCBA]$_0$ for all experiments are shown in appendix XII. In Figure 3-7 the conversion of pCBA is shown as a function of UV dose during photolysis (0 mg H_2O_2/L) and during the combination of photolysis and oxidation (10 mg H_2O_2/L), for all three types of lamps.
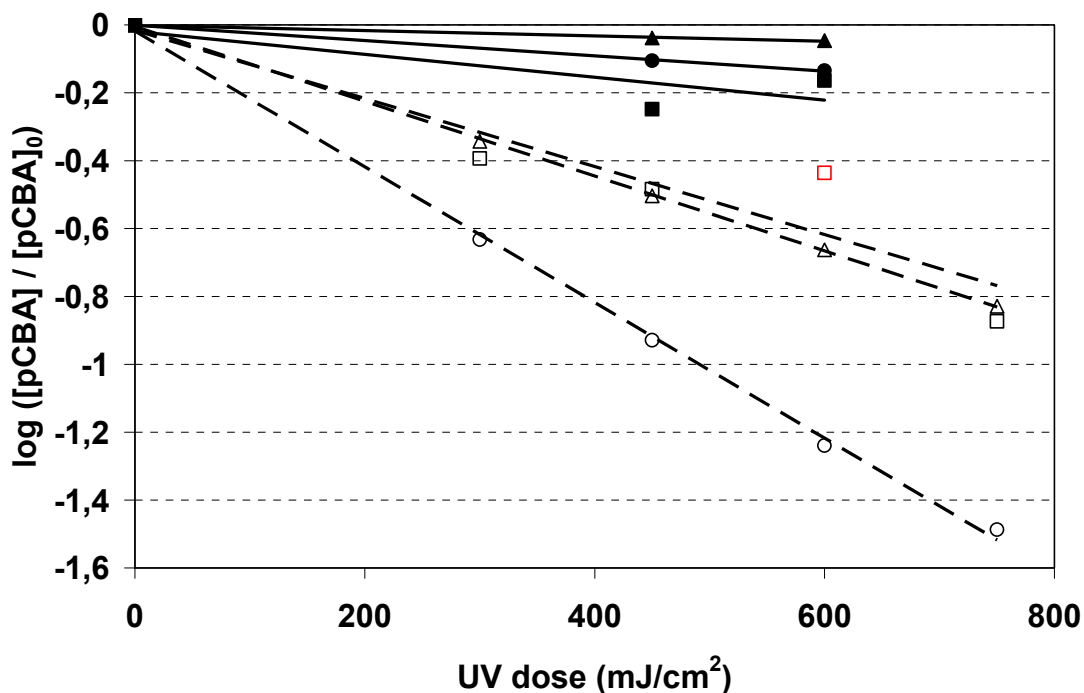
Figure 3-7 log [pCBA]/[pCBA]$_0$ versus UV dose preteated water of GCWW without H$_2$O$_2$; (■) MP; (▲) LP; (●) DBD and with 10 mg/L H$_2$O$_2$; (-□-) MP; (-Δ-) LP; (-○-) DBD.

Just like in case of the Dunea water, the conversion of pCBA through photolysis is most important with the MP UV-lamp, followed by the DBD lamp and finally the LP lamp.

After correction for the contribution of photolysis at 10 mg H$_2$O$_2$/L, the results obtained with GCWW water are similar to the results obtained with Dunea water. The largest conversion of pCBA as a result of hydroxyl radical formation, at a UV dose of 600 mJ/cm2 is observed with the DBD lamp (1.0 log) and the LP lamp (0.6 log). The contribution of hydroxyl radical formation in case of an MP lamp is lower (0.3log). Thus, tests with GCWW water confirm the hypothesis, that as a result of the low UV absorption of the water matrix at a wavelength of 253.7 nm (which is specific for an LP lamp) the hydroxyl radical formation of this type of lamp will be higher than at lower wavelengths, despite the fact that at this wavelength the radical production from H$_2$O$_2$ is lower too.

3.5.4 Comparison of Hydroxyl radical formation in water from Dunea Bergambacht versus GCWW

Comparing the results obtained with Dunea water and with GCWW water, it can be concluded that the conversion of pCBA is higher in GCWW water, which can mainly be attributed to hydroxyl radical formation. This can be explained by the better water quality of GCWW's water compared to Dunea's water (see Table 3-5), as a result of which the Dunea water matrix can absorb more UV irradiation (appendix XI).

Conclusions:
During application of UV/H$_2$O$_2$ (10 mg/L H$_2$O$_2$):
- Total conversion of pCBA:
  DBD > MP > LP UV-lamp.

- Contribution of photolysis in total conversion of pCBA:
  MP > DBD > LP UV-lamp.

- Hydroxyl radical formation based on conversion of pCBA:
  DBD > LP > MP UV-lamp.

- The hypothesis, that as a result of the lower UV absorption by the water matrix at a wavelength of 253.7 nm (which is specific for LP lamps) the hydroxyl radical formation at this wavelength is higher than at lower wavelengths, despite the fact that at this wavelength the UV absorption by H_2O_2 is lower, has been verified. It was concluded, that this hypothesis is valid.

3.6 Results for the conversion of organic micropollutants and disinfection capacity

3.6.1 Results of collimated beam experiments for the conversion of organic micropollutants

In order to determine the conversion of (a selection of) organic micropollutants for various types of lamps, collimated beam experiments were carried out at UV doses of 300 and 600 mJ/cm^2 and hydrogen peroxide concentration of 10 mg/L. Pretreated water from both Dunea in Bergambacht and from GCWW (Ohio River) was used. The experiments were carried out in the period of July 20th – 26th 2006.

Furthermore, the water quality was determined, and a UV scan was made of the water. The results are shown in appendix XI. The range of these parameters is shown in Table 3-8.

Table 3-8 Range of several water quality parameters during collimated beam experiments

Water sample	Nitrate mg/L NO_3	pH	HCO_3 mg/L HCO_3	NPOC mg/L C
Dunea	6.6	7.92 – 8.20	133-136	2.5
GCWW	4.0	7.80 – 8.04	70 – 73	2.0

Conversion of organic micropollutants

During the collimated beam experiments the conversion of hormones and triazines was determined. The analytical results and the conversion calculations are shown in appendix XIII.

Hormones
In Figure 3-8 and Figure 3-9 the results for the conversions of hormones is shown for the three types of lamps.

Figure 3-8 Conversion of hormones in Dunea water with 10 mg H_2O_2/L at a UV dose of 300 en 600 mJ/cm²; **(∎)** *MP;* **(∎)** *LP;* **(∎)** *DBD*

Figure 3-9 Conversion of hormones in GCWW water with 10 mg H_2O_2/L at a UV dose of 300 en 600 mJ/cm²; **(∎)** *MP;* **(∎)** *LP;* **(∎)** *DBD*

For experiments carried out with MP lamps, in all cases maximum conversion was obtained. It can be concluded that an MP lamp is very suitable to convert hormones at a UV dose of 300 mJ/cm². There is one exception: 17α-estradiol in GCWW water (Figure 3-9), showed a conversion of 80% at a UV dose of 600 mJ/cm². This may be due to an experimental or analytical error, as in Dunea water, which has a lower UV transmission than the GCWW water, the maximum conversion was measured. Therefore, it seems logical that the actual conversion of 17α-estradiol has been higher too. In some cases the conversion observed at Dunea seemed to be higher than at GCWW. This was caused by the almost complete conversion obtained, as a result of which the effluent concentrations were below the detection limits.

Under similar experimental conditions, the DBD lamp gave more or less the same results as the MP lamp. At a dose of 300 mJ/cm² GCWW water showed a conversion of at least 86%, and Dunea water of 92%. At a dose of 600 mJ/cm² the DBD lamp gave complete conversion of all hormones in all cases.

As was expected, the LP lamp resulted in a lower conversion of hormones than the MP and DBD lamp. At a dose of 300 mJ/cm² in Dunea water 68-78% of the hormones was converted, whereas at a dose of 600 mJ/cm² 83% of estriol and 86% of estrone conversion was obtained. At the latter dose all other hormones tested were converted up to 90%.

With GCWW pretreated water, at a dose of 300 mJ/cm², 65% of the estriol and 70% of the estrone was converted. In all other cases over 80% conversion was obtained. At 600 mJ/cm² more than 95% of all hormones appeared to be converted, with the exception of estriol (88%). Thus, it can be concluded that also the LP lamp can be applied to obtain a high conversion of hormones.

The results obtained confirm previous results, showing high conversion of hormones by applying UV/H_2O_2 with either LP or MP lamps [Rosenfeld and Linden, 2004]. During that investigation the conversion of 17α-ethynylestradiol and 17B-estradiol by means of photolysis as well as UV/H_2O_2 (1,000 mJ/cm², 15 mg/L H_2O_2) was studied. Application of only photolysis (without H_2O_2) hardly gave any hormone conversion. Using a LP lamp less than 5% of 17α-ethynylestradiol and 17B-estradiol was converted, whereas using a MP lamp resulted in a conversion of 22% for 17α- ethynylestradiol and 18% for 17B-estradiol. Addition of 15 mg/L H_2O_2 resulted in a conversion exceeding 95%, independent of the type of lamp used. 15 mg/L is an unrealistic concentration for applicaton purposes, and was only applied for checking whether complete conversion can be obtained by increasing the hydroxyl radical concentration.

The lower conversion of hormones by means of processes with LP lamp can be explained from the fact that with LP lamps the main process is oxidation by hydroxyl radicals, whereas with MP and DBD lamps the contribution of photolysis is larger. It is expected, that this effect is most important for MP lamps. At a dose of 600 mJ/cm² under otherwise identical circumstances, the use of a LP lamps results in a conversion that is 5-10% lower than for MP or DBD lamps.

In general hormones appear to be converted rather well by means of UV/H_2O_2. In many cases the hormone concentration after UV was found to be below the lower detection limit. In those cases the conversion was assumed to be about half the value of the lower detection limit.

Triazines
In Figure 3-10 and Figure 3-11 the results obtained with mixtures of triazines and all three types of lamps are shown. When the results for triazines are compared with the results obtained with hormones as described above, it can be concluded that the conversion for triazines is less than for hormones. This confirms the rather difficult splitting of the triazine ring [Watanabe *et al.*], which requires a higher UV-dose to obtain the same conversion as with hormones.
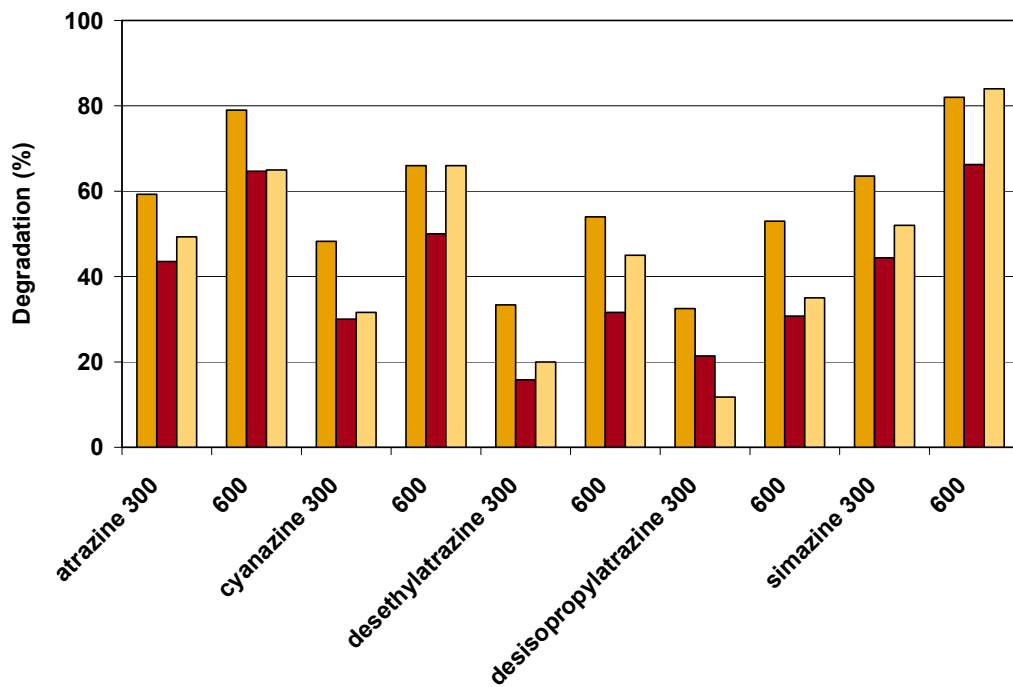
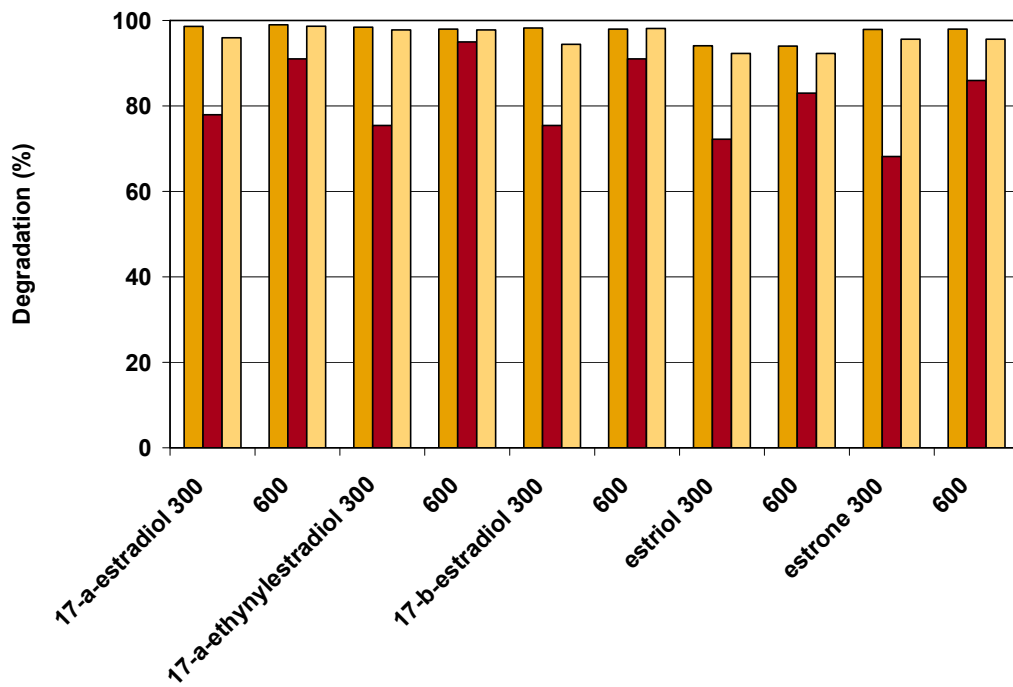*Figure 3-10 Conversion of triazines in Dunea water with 10 mg H₂O₂/L at a UV dose of 300 en 600 mJ/cm²;*
(■) MP; (■) LP; (■) DBD

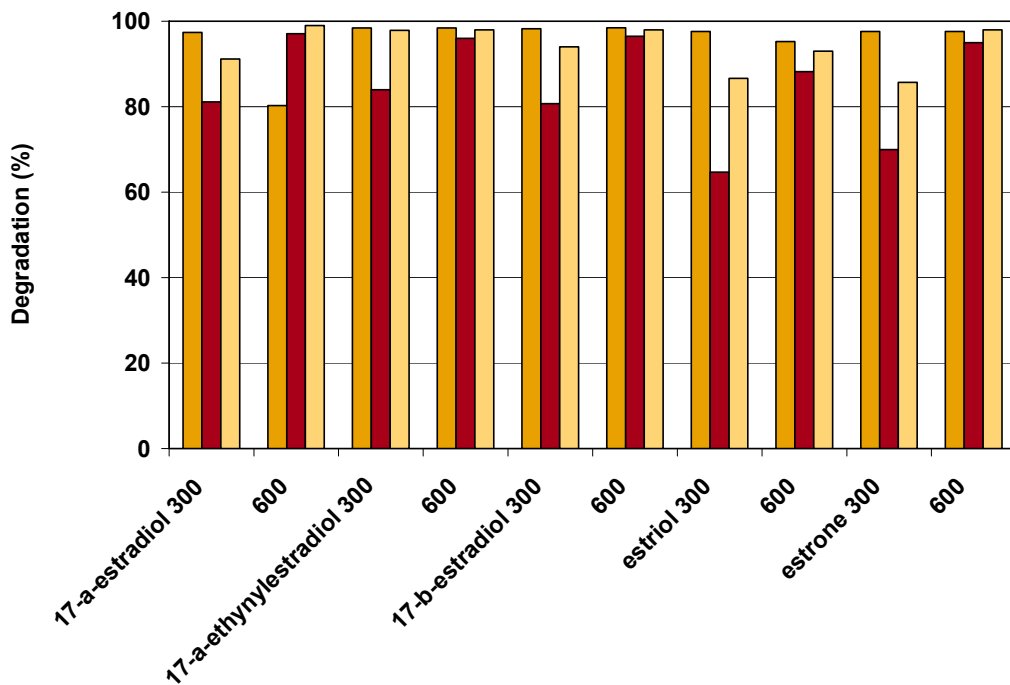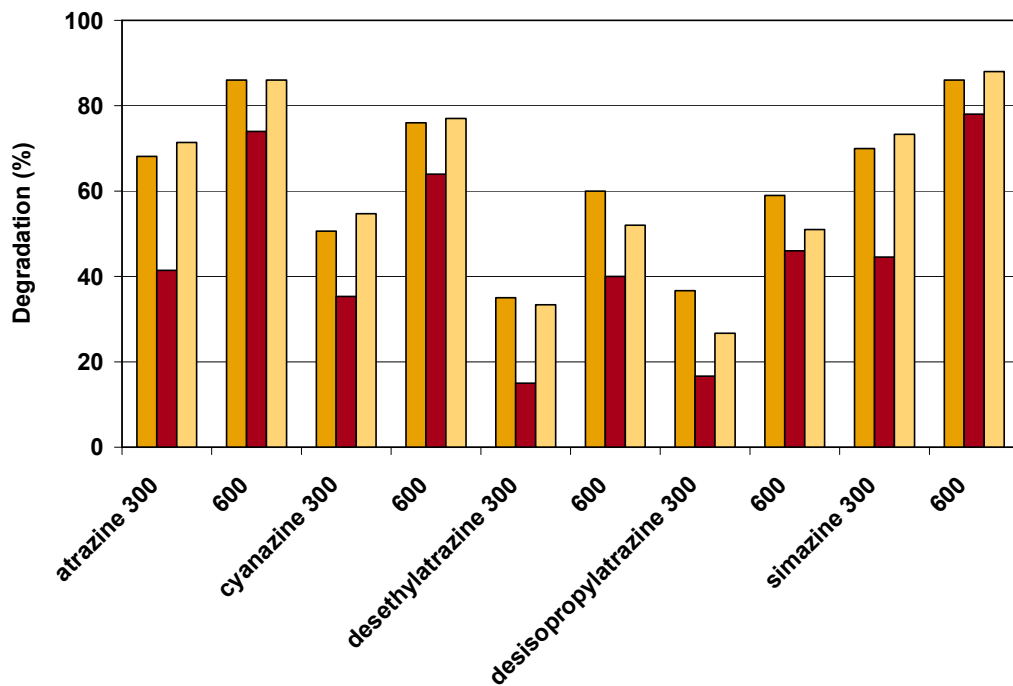*Figure 3-11 Conversion of triazines in GCWW water with 10 mg H₂O₂/L at a UV dose of 300 en 600 mJ/cm²;*
(■) MP; (■) LP; (■) DBD

Like in the case of hormones, the highest conversion of triazines in the UV/H$_2$O$_2$ process is obtained with the MP lamp. In the Dunea water, the DBD lamp gives a lower conversion of triazines than the MP lamp, with the exception of cyanazine and simazine. In the GCWW water, the DBD lamp appears to give nearly the same conversion of triazines as the MP lamp, with small differences. The LP lamp gives a lower conversion than the MP and the DBD lamp, as a result of the fact that a LP lamp only emits UV light with a wavelength of 253.7 nm, whereas the MP and DBD lamp emit a broader range of wavelengths.

Regardless of the type of lamp applied, atrazine, cyanazine and simazine always show the highest conversion, compared to Desethylatrazine (DEA) and disiopropylatrazine (DIA). The highest conversion can be obtained when a MP or DBD lamp is used. At a dose of 600 mJ/cm^2 65-88% of the compounds are converted. With a LP lamp a conversion of 50 – 78% can be obtained for atrazine, cyanazine and simazine.
For DEA and DIA the conversion seems to be lower. These compounds show the highest conversion when treated with a MP lamp (54-60%), followed by the DBD-lamp (35 – 52%) and finally the LP- lamp (31-46%) at a dose of 600 mJ/cm^2.

Using a LP lamp at a dose of 600 mJ/cm^2 under otherwise identical conditions results in a 10-15% lower conversion of triazines than can be obtained by using a MP or DBD lamp. The very low conversion obtained for DEA and DIA can be explained by the fact that these compounds can be considered as the first degradation products that will be formed by oxidation of atrazine by means of hydroxyl radicals [Arnold *et al.*1995]. Thus, these products will be less sensitive to further oxidation.
Experiments with pCBA (3.5) showed that in case a LP lamp is applied, the major part of conversion is realized by means of oxidation by •OH radicals, whereas in case of DBD or MP lamps also photolysis will be important. As a result, it is to be expected that the difference between LP and MP lamps for DEA and DIA will be larger than for the other triazines, which have not yet been oxidized.

Differences in the water quality affect the conversion of compounds dosed. It was observed that a higher conversion was obtained in pretreated water from GCWW than in water from Dunea. For most compounds a difference of about 10% was observed at a dose of 600 mJ/cm^2. For collimated beam experiments a correction is made for UV absorption in the wavelength range of 200 -300 nm [Bolton en Linden, 2003]. Thus, the difference in UV transmission should not cause a difference in conversion. However, bicarbonate (HCO$_3^-$) and carbonate (CO$_3^{2-}$) ions are known radical scavengers [Weeks and Rabani, 1966]. The reaction constants for the reaction between hydroxyl radicals and HCO$_3^-$ and CO$_3^{2-}$ are $1,5 \cdot 10^7$ M^{-1}s^{-1} and $4,2 \cdot 10^8$ M^{-1}s^{-1}, respectively [Tuhkanen, 2004]. The target compounds have reaction constants of about 10^9 M^{-1}s^{-1} [Stefan et al., 2005]. As the HCO$_3^-$ concentration is much higher than the concentration of target compounds, it is to be expected that the HCO$_3^-$ ions affect the •OH to a large extend. Studies however showed that the hydroxyl radical formation largely depends on the presence of the chloride ion [Liao *et al.*,2001]. At a concentration of less than 250 mM Cl$^-$ a minimum effect of HCO$_3^-$ ions can be observed. This is explained from the formation of carbonate radicals as a second oxidizing medium [Von Gunten and Hoigné, 1994; Beltrán et al., 1996b]. These carbonate radicals are formed from a reaction between hydroxyl radicals, bicarbonate and carbonate ions. At this moment it still is not yet clear whether differences in chloride and bicarbonate concencentrations in the pretreated water of Dunea and GCWW account for the small difference in conversion of hormones and triazines. For hormones the oxidation is so effective that the water quality does not play an important role.

Conclusions:

The following conclusions only are valid for the hormones and triazines that have been studied in this investigation, under the experimental conditions applied (collimated beam).
- Conversion of hormones and triazines under otherwise equal conditions:
  MP > DBD > LP

- Applying a UV/H$_2$O$_2$ process with a MP-lamp results in a conversion of hormones > 93% at a dose of 300 mJ/cm^2.

- Applying a UV/H$_2$O$_2$ process with a LP-lamp results in a conversion of hormones > 82% at a dose of 600 mJ/cm^2.

- Application of a LP-lamp under otherwise equal conditions at a UV dose of 600 mJ/cm^2 results in a conversion of hormones that is 5-10% lower than can be obtained by means of a MP or DBD lamp .

- Applying a UV/H$_2$O$_2$ process with a MP-lamp at a dose of 600 mJ/cm^2 results in a triazine conversion of 54 - 86%.

- Applying a UV/H$_2$O$_2$ process with a LP-lamp at a dose of 600 mJ/cm^2 results in a triazine conversion of 31 - 78%.

The conversion of hormones and triazines seems to be about 5-20%% lower in pretreated water from Dunea than in water from GCWW. This can be attributed to the differences in water quality between Dunea and GCWW (Dunea water having a higher concentration of nitrate and NPOC, and a lower UV-T).

3.6.2 Results of conversion of organic micropollutants in the UV pilot reactor

Conversion of organic micropollutants

UV reactors for disinfection purposes can be validated by means of biodosimetry: their performance is related to the inactivation of a known microorganism. A similar procedure can be applied to validate a UV/H$_2$O$_2$ reactor, by relating its performance to the conversion of a wellknown compound like e.g. atrazine. The pilot reactors in this report have been validated at a conversion of 80% for atrazine. After the pilot reactor had been validated, experiments were carried out to determine the conversion of organic micropollutants by means of photolysis and UV/H$_2$O$_2$ oxidation. The process conditions of the experiments are shown in appendix XIV. The water quality data and UV scans of the water tested are shown in appendix XV. The results of the analyses and calculations of the conversion of organic micropollutants are described in appendix XV. By comparing the UV scans and the water quality parameters, it can be concluded that the circumstances were similar during all experiments. In all cases the desired amount of hydrogen peroxide had been added.

An additional experiment had been carried out, in order to determine the influence of hydrogen peroxide, without UV irradiation, on the concentration of organic micropollutants. For this experiment, a sample was taken of the influent of Dunea water, containing 10 mg/L H$_2$O$_2$ and organic micropollutants, during the experiments carried out with the DBD lamp. After 0 minutes and after 30 minutes (the same time frame in which the experiments normally take place) the concentration of all organic micropollutants was analyzed. It was found that the concentrations of the organic micropollutants did not change during this period (see appendix XVI).

In Figure 3-12, Figure 3-13, and Figure 3-14 the results for the conversion of organic micropollutants for all three types of lamps are shown. The UV dose was calculated using the dose response curve determined for atrazine (see appendix VIII). In all cases the same trend can be observed: higher conversion of organic micropollutants can be achieved by increasing the UV dose and/or the addition of H$_2$O$_2$. This is in accordance with the results obtained from the collimated beam experiments (3.6.1).
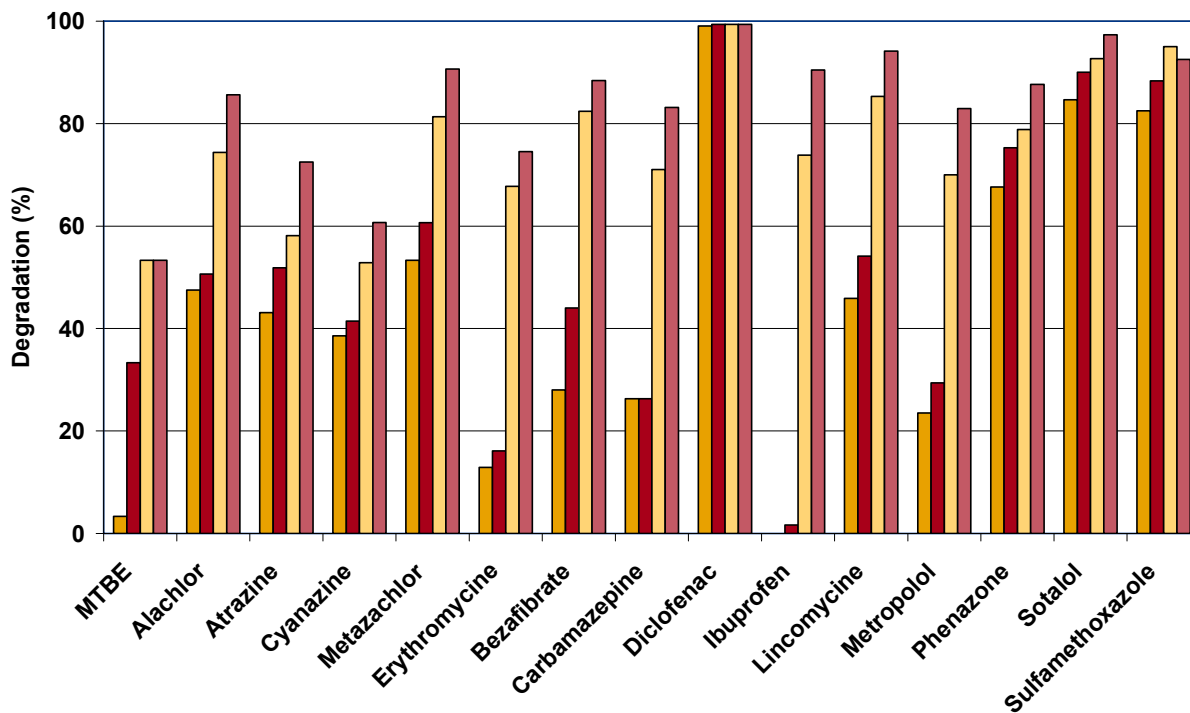
Figure 3-12 Conversion of organic micropollutants during UV-pilot testing. Pretreated Dunea water with the MP-lamp; (■) without H_2O_2, dose 300 mJ/cm²; (■) without H_2O_2, dose 450 mJ/cm²; (■) 10 mg/L H_2O_2, dose 300 mJ/cm²; (■) 10 mg/L H_2O_2, dose 450 mJ/cm².

From Figure 3-12 it can be concluded that in many cases by applying a UV/H_2O_2 process, using an MP lamp at a dose of 450 mJ/cm² and with addition of 10 mg/L H_2O_2 in Dunea water, more than 80% of a compound is converted (only in 4 of the 15 examples this conversion was not reached). Sotalol and diclofenac appeared to be converted for over 95%, for atrazine and erythromycine a conversion of about 75% was obtained, and for cyanazine 61%. The lowest conversion, 53%, was found for MTBE.

Photolysis (no H_2O_2 addition) at 450 mJ/cm² results in a conversion of 90% for sulfamethoxazole and sotalol, and for diclofenac even 99% was measured. In all other cases, except for phenazone and ibuprofen, 25-60% of the compounds are converted by means of photolysis only. For phenazone a conversion of 75% was obtained. Ibuprofen appears to be hardly converted by means of photolysis, although addition of H_2O_2 results in a conversion of 90%. In most cases H_2O_2 is required to obtain a significant conversion of the compounds.
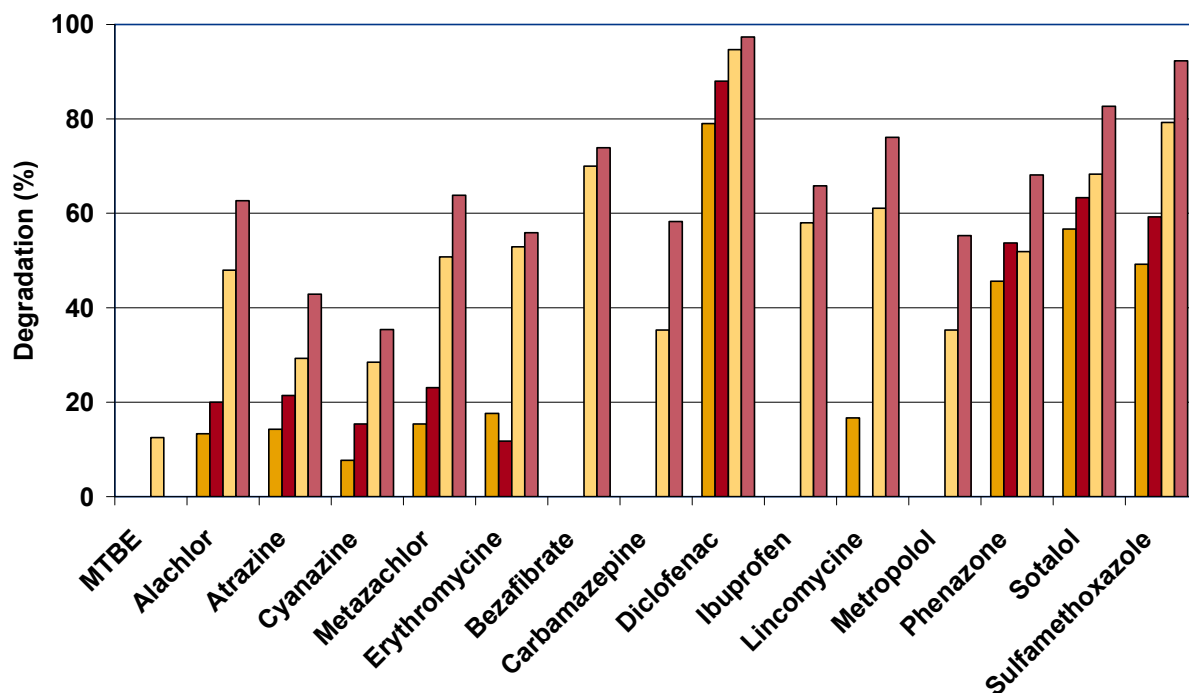
Figure 3-13 Conversion of organic micropollutants during UV-pilot testing. Pretreated Dunea water with the LP-lamp; (■) without H_2O_2, dose 300 mJ/cm²; (■) without H_2O_2, dose 450 mJ/cm²; (■) 10 mg/L H_2O_2, dose 300 mJ/cm²; (■) 10 mg/L H_2O_2, dose 450 mJ/cm².

UV/H_2O_2 with an LP lamp at a dose of 450 mJ/cm² and in the presence of 10 mg/L H_2O_2 for Dunea water results in a conversion of over 80% for sulfamethoxalzole, sotalol and diclofenac. Diclofenac is converted 97% with the LP lamp. Most compounds are converted for 60 – 80%. As like it is the case with MP lamps, cyanazine, atrazine and erythromycine are converted to a lesser degree (35, 43, en 56% respectively). MTBE is hardly converted. It is striking that in the influent more or less the same MTBE concentration is found as after UV/H_2O_2 treatment. This probably is caused by the fact that the conversion is so low, that the differences are within the experimental uncertainty, and thus the MTBE conversion by means of LP lamps cannot be determined.

Diclofenac is converted for 88% by photolysis at 450 mJ/cm². The conversion of phenazone, sotalol and sulfamethoxalzole by photolysis is between 50 – 65%. Alachlor, atrazine, cyanazine, metazachlor and erythromycine show a conversion of 10 -25%. MTBE, bezafibrate, carbamazinepine, ibuprofen, lincomycine and metropolol cannot be converted by photolysis using a LP lamp.
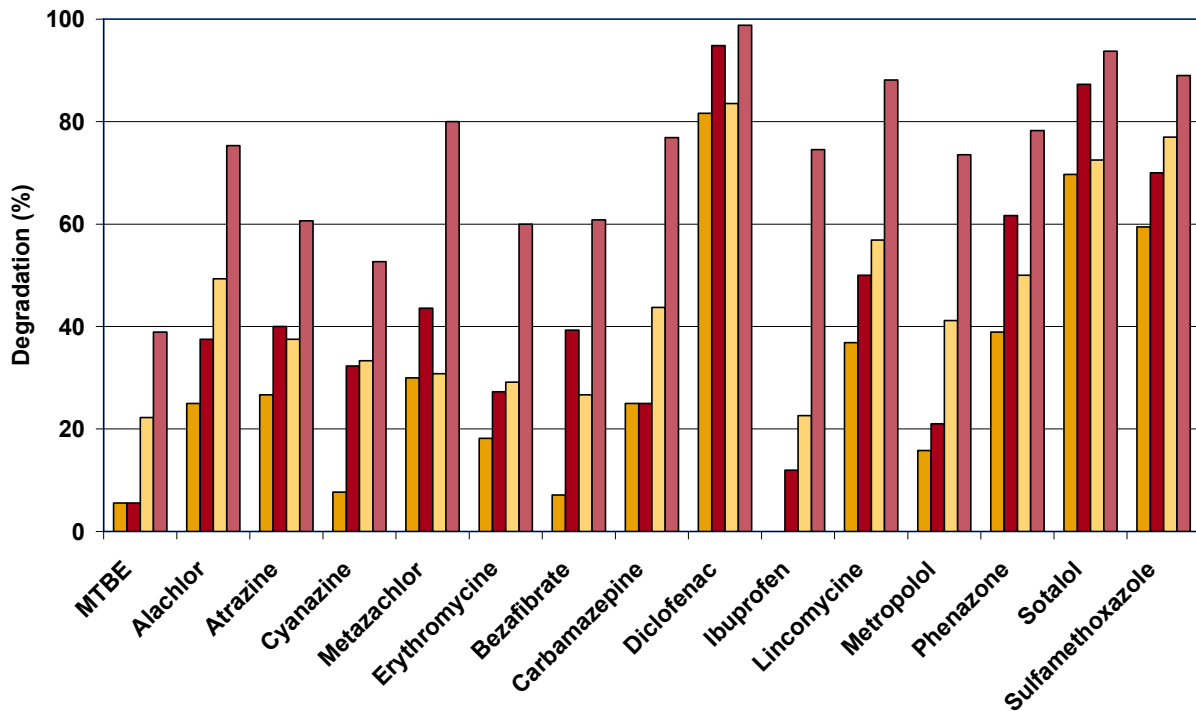
Figure 3-14 Conversion of organic micropollutants during UV-pilot testing. Pretreated Dunea water with the DBD-lamp; (■) without H_2O_2, dose 300 mJ/cm²; (■) without H_2O_2, dose 450 mJ/cm²; (■) 10 mg/L H_2O_2, dose 300 mJ/cm²; (■) 10 mg/L H_2O_2, dose 450 mJ/cm².

The UV/H_2O_2 process by means of a DBD lamp in Dunea water, at a dose of 450 mJ/cm² and a H_2O_2 concentration of 10 mg/L results in over 80% conversion of lincomycine, sulfamethoxalzole, sotalol and diclofenac. Diclofenac is even converted up to 99% by means of the DBD-lamp. The other compounds, with the exception of MTBE and cyanazine, are converted for 60 – 80%. For cyanazine a conversion of 53% was obtained. For MTBE the conversion did not exceed 39%.

Through photolysis at a dose of 450 mJ/cm², diclofenac and sotalol are effectively converted (95 and 87% respectively). For lincomycine, phenazone and sulfamethoxalzole, a photolytic conversion of 50 – 70% is obtained. In all other cases, except for MTBE and ibuprofen, 20 -45% conversion can be obtained by photolysis. MTBE and ibuprofen appeared to hardly be converted through photolysis if a DBD lamp is used.
Similar to the situation with the MP lamp, ibuprofen hardly can be converted by photolysis (12%), although addition of H_2O_2 results in an increase in conversion up to 75%.

Table 3-9 gives an overview of the conversion of organic micropollutants per type of lamp as a result of photolysis and of photolysis combined with oxidation.

Table 3-9 Conversion of organic micropollutants using various types of lamps in the UV pilot reactor at a chemidosimeter (atrazine) dose of 450 mJ/cm²

	UV (Photolysis)			UV/H_2O_2 (oxidation)		
	conversion (%)			conversion(%)		
	0 -60	>60	>80	0 -60	>60	>80
MP	MTBE carbamazepine alachlor atrazine cyanazine erythromycine bezafibrate ibuprofen lincomycine metropolol	Metazachlor phenazone	Diclofenac sotalol sulfa-methoxazole	MTBE	Alachlor atrazine cyanazine erythromycine	Carbamazepine alachlor metazachlor bezafibrate diclofenac ibuprofen lincomycine metropolol phenazone sotalol sulfa-methoxazole
LP	Carbamazepine MTBE, alachlor atrazine cyanazine metazachlor erythromycine bezafibrate ibuprofen lincomycine metropolol phenazone sulfa-methoxazole	sotalol	Diclofenac	MTBE atrazine cyanazine erythromycine Carbamazepine metropolol	alachlor cyanazine metazachlor bezafibrate ibuprofen lincomycine phenazone	Diclofenac sotalol sulfa-methoxazole
DBD	Carbamazepine MTBE, alachlor atrazine cyanazine metazachlor erythromycine bezafibrate ibuprofen lincomycine metropolol phenazone sulfa-methoxazole	sotalol	diclofenac	MTBE cyanazine erythromycine	carbamazepine alachlor atrazine metazachlor bezafibrate ibuprofen metropolol phenazone	Diclofenac lincomycine sotalol sulfa-methoxazole

Comparison of the results shows that conversion of organic micropollutants, applying the same UV dose, is most effective using an MP lamp, followed by a DBD lamp. As was expected, the LP lamp showed the lowest conversion. These results are in good accordance with the results obtained during the collimated beam experiments, although in the pilot experiments, apart from atrazine and cyanazine, other compounds were used. For atrazine and cyanazine similar results were obtained in the pilot reactor and in the collimated beam set-up.

The difference in conversion found for the various types of lamps mainly is caused by the contribution of photolysis during the conversion process. As a result, the conversion of compounds by UV irradiation for LP lamps both with and without addition of H_2O_2 addition is 20-30% lower than for a MP lamp. For a DBD lamp this conversion is about 10% lower than for a MP lamp.

N.B. These conclusions were based on experiments carried out with only one type of water (pretreated water of Dunea, Bergambacht) and one UV dose, which had been based on the dose response curve of atrazine. As a result, these data cannot be compared with data generated in other investigations, based on another way of UV dose calculations (e.g. by means of Computational Flow Dynamics modeling).

Conclusions:

- Conversion of organic micropollutants with UV/H_2O_2 under otherwise similar conditions: MP > DBD > LP

- The difference in conversion for the various types of lamps mainly is caused by the contribution of photolysis during the process.

- Applying a UV/H_2O_2 process equiped with a MP lamp at a calculated dose of 450 mJ/cm^2 results in a conversion of most organic micropollutants over 80%, and of MTBE of 53%.

- Photolysis of diclofenac is very effective for every type of lamp. Using a LP lamp at a dose of 450 mJ/cm^2 results in a conversion of 88%.

- Ibuprofen can hardly be converted by means of photolysis, independent of the type of lamp. However, addition of H_2O_2 results in a high conversion. In case a LP lamp at a dose of 450 mJ/cm^2 is applied, a conversion of 66% can be obtained.

3.7   Formation of byproducts

During the UV/H_2O_2 treatment of water byproducts may be formed, like e.g. nitrite and AOC [Harmsen *et al*, 2005]. Absorption of UV irradiation may convert nitrate and DOC in nitrite and AOC respectively (section 3.7). UV-Absorption by nitrate and DOC mainly occurs in the wavelength range of 200-240 nm. According to Figure 3-1 and Figure 3-2, the emission spectrum of the MP lamp shows the largest overlap with the absorption spectra of nitrate and DOC. The DBD lamp (225-240 nm) shows a smaller overlap, whereas the emission spectrum of the LP lamp in principle shows no overlap with the absorption spectra. As a result the possibility to form nitrite and AOC is expected to be MP > DBD > LP.

Samples were analyzed for nitrite and AOC during the experiments in the pilot reactor with 10 mg H_2O_2/L. The results and their standard deviation are shown in Table 3-10 and Figure 3-15 and Figure 3-16.

Table 3-10 Results of analyzes of nitrite and AOC formation at various types of UV-lamps (µg/L=1.60 µg/gal)

Lamp	Dose mJ/cm^2	P-17 µg/L C	RSD	NOX µg/L C	RSD	AOC µg/L C	RSD	Nitrite µg/L NO$_2^-$
MP	300	28	1	41	6	70	6	457
	450	43	1	65	10	104	24	562
LP	300	7	1	19	1	26	9	0,9
	450	21	16	38	12	58	17	15
DBD	300	14	15	33	6	47	16	79
	450	87	59	81	35	164	39	112

P-17 and NOX are bacterial strains (van der Kooij et al., 1982)
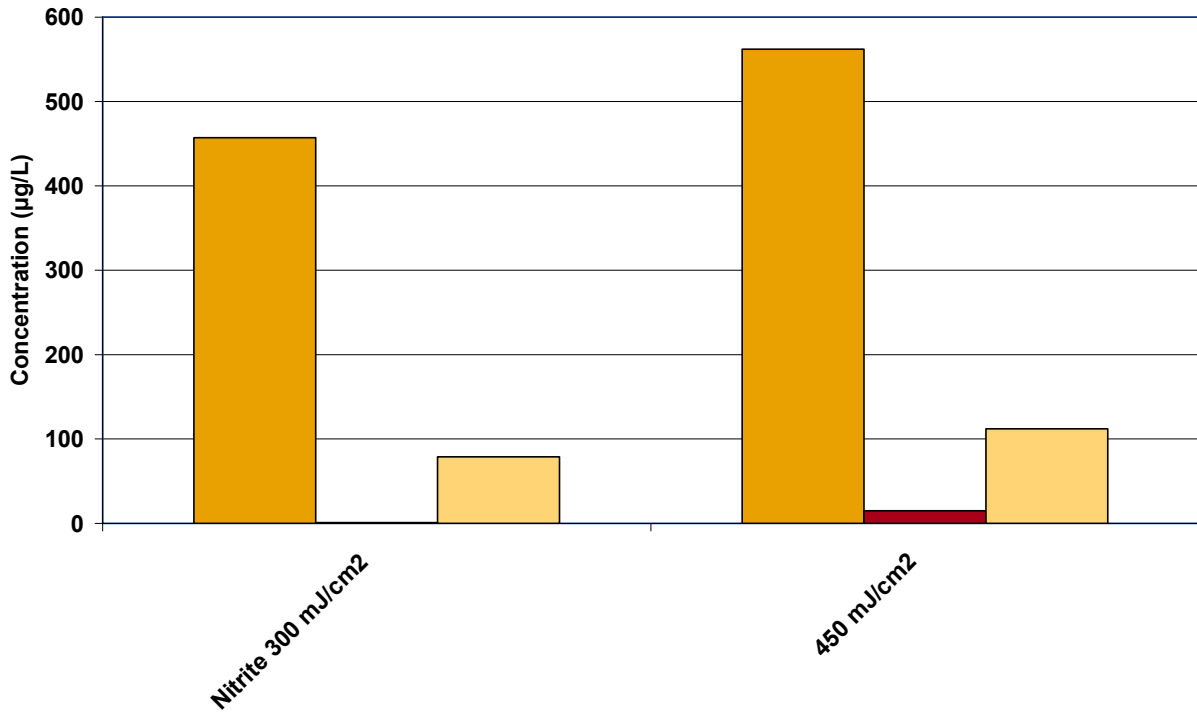
Figure 3-15 Formation of nitrite (NO₃) in UV pilot experiments; Dunea water, UV dose 300 and 400 mJ/cm²; (■)MP-lamp; (■) LP-lamp; (■) DBD-lamp (µg/L=1.60 µg/gal)
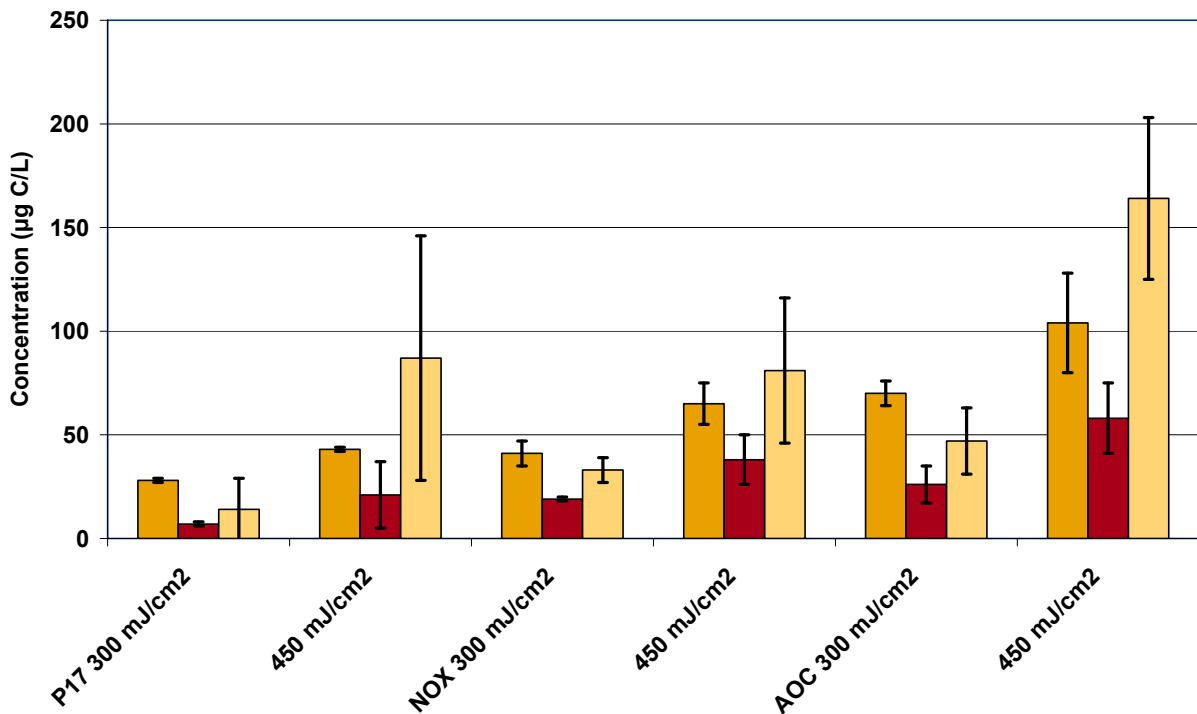
Figure 3-16 Formation of AOC (P-17 and NOX))in UV pilot experiments; Dunea water, UV dose 300 and 400 mJ/cm²; (■)MP-lamp; (■)LP-lamp; (■) DBD-lamp (µg/L=1.60 µg/gal)

Most nitrite obviously is formed using the MP UV-lamp, followed by the DBD lamp. At a dose of 450 mJ/cm² 562 µg NO₂⁻/L is formed, using the MP-lamp. For the DBD lamp the nitrite concentration is a factor five less, which is about the standard for drinking water (100 µg NO₂⁻/L) [Staatsblad van het Koninkrijk der Nederlanden; 2001]. Applying the LP-lamp resulted in the formation of only 15 µg NO₂⁻/L. According to the UV spectrum of the LP lamp, no nitrite formation had been expected, as the conversion of nitrate into nitrite takes place in the wavelength range < 240 nm, and > 300 nm, with a minimum around 254 nm. It still is unclear whether the nitrite observed was formed by reaction of nitrate with •OH radicals, or that this is an experimental uncertainty. Previous investigations [Mark *et al.*, 1996; Sharpless en Linden, 2001] have shown that nitrite formation by means of hydroxyl radicals is possible, but only to a limited extend.

For AOC, two strains were determined: P-17 and NOX. Most AOC was observed using the MP and the DBD lamp. It should be noticed that at a dose of 300 mJ/cm² more AOC is formed applying a MP lamp than using a DBD lamp, whereas at a dose of 450 mJ/cm² exactly the opposite was observed. Application of the DBD lamp results in the formation of AOC. Based on the UV emission spectra of the lamps, it had been expected that for the MP lamp more UV irradiation would be absorbed by DOC than for the DBD lamp. At the moment there is not yet an explanation for the higher AOC concentrations observed at a dose of 450 mJ/cm² for the DBD-lamp. However, the standard deviation of the measurements is relatively large. Especially the measurements for P-17 seem to have a very large relative standard deviation (RSD) of 87 ± 59 µg/L C, as a result of which the results obtained for the MP- and the DBD-lamp overlap.

N.B. The results shown above have been based on one single experiment. In order to be able to give an unambiguous statement on the formation of AOC using an MP or DBD lamp, more data will be required. However, the formation of byproducts is the subject of work packages 7 and 8, which will be extensively described in a next chapter.

The results obtained agree quite well with results of previous investigation [Kruithof and Kamp., 2000; IJpelaar *et al.*, 2005; IJpelaar *et al.*, 2006; Harmsen *et al., 2005*].
Although nitrite may be formed by the UV/H₂O₂ process, in practice this will not be a problem for application of the technique in drinking water purification. In practice the UV/H₂O₂ process always is followed by GAC adsorption to quench excess of H₂O₂. During this process step, nitrite will also be removed. [Kruithof en Kamp, 2000].

Conclusions:

- During application of a UV/H₂O₂ process, under otherwise similar conditons, most nitrite is formed in this order:
  MP > DBD > LP

- During application of a UV/H₂O₂ process, under otherwise similar conditons, most AOC is formed in this order:
  MP ≈ DBD > LP

3.8   Inactivation of MS2-phages

Apart from experiments to determine the conversion of organic micropollutants by a UV/H₂O₂ process, the pilot reactor also was used for experiments to establish the disinfection capacity of this process. The inactivation of MS2 phages, at a dose of 450 mJ/cm² and a H₂O₂ concentration of 10 mg/L with the three different lamp types was studied. MS2 phages were selected, as these are known as a good biodosimeter (easy analysis, good conversion by means of UV irradiation, reliable measurement method to determine the biocide dose). Besides, MS2 phases are relatively insensitive towards UV irradiation, compared with most pathogens. In order to obtain a 3 log reduction for MS 2 phages, a dose of 54 mJ/cm² is required, whereas for cryptosporidium and giardia 12 mJ/cm², and for legionella pneumophila 23 mJ/cm² is sufficient [Hijnen *et al.*, 2006]. As a result of this relatively low sensitivity of MS2 phages towards UV

irradiation, they are very suitable to obtain information on the inactivation of pathogenic micro organisms in a UV/H$_2$O$_2$ process.

The log reduction of MS2 phages is calculated using the following formula to determine the disinfection capacity:

$$\text{Log reduction} = \text{Log}\left(\frac{N_s}{N_0}\right) \qquad (4)$$

With:
N_0 = average concentration of not irradiated samples at a dose of 0 mJcm^2;
N_s = average concentration of irradiated samples at each UV dose.

The results and calculations are described in appendix XVII. The log reduction for the various lamp types is shown in Figure 3-17. For every type of lamp this log reduction was measured three times (3 independent samples, taken shortly after each other) under otherwise similar conditions.
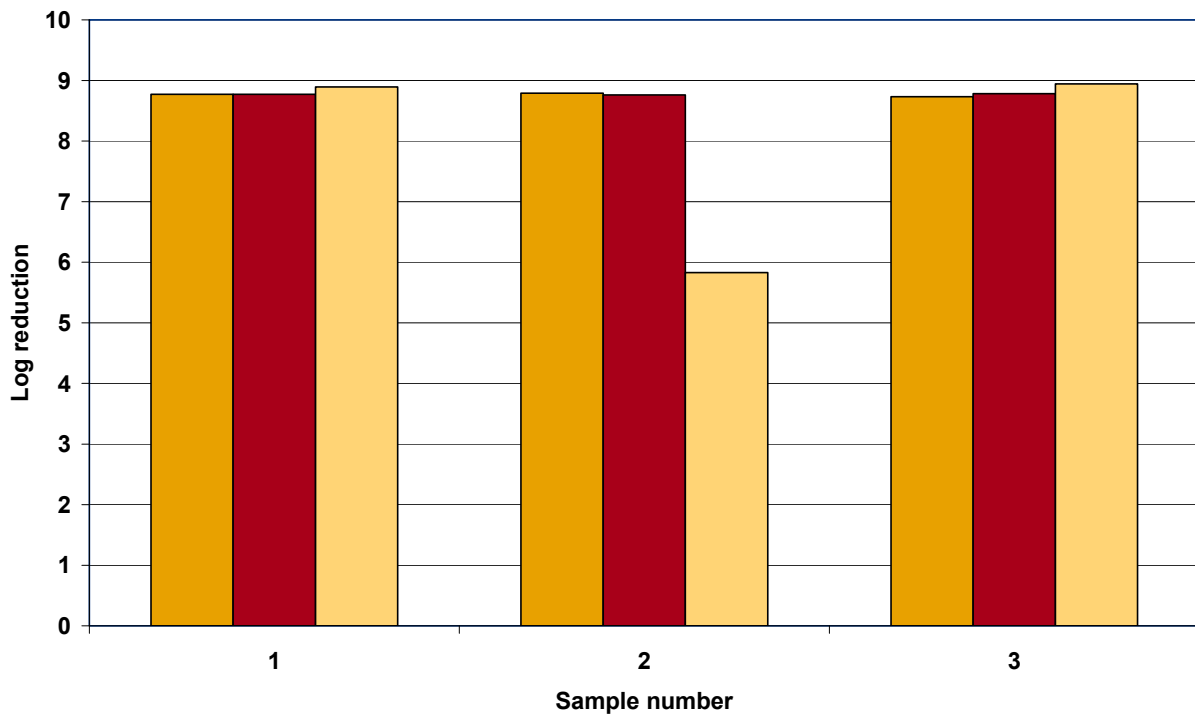
Figure 3-17 Log reduction of MS2 phages during UV-bench experiments with Dunea water at a dose of 450 mJ/cm^2 and 10 mg/L H$_2$O$_2$; (■)MP-lamp; (■)LP-lamp; (■) DBD-lamp.

A decline in the reduction of MS2 phages by the UV/H$_2$O$_2$ process was observed in sample 2 with the DBD-lamps . There is no clear explanation for this result. It may be possible this was caused by an external MS2 contamination. In all other cases no MS2 phages could be observed after the UV/H$_2$O$_2$ process. This had been expected, as in general a UV dose of 40-80 mJ.cm2 is used for inactivation of the MS2, and in this case an almost tenfold dose was applied. However, as disinfection is a very important issue in water treatment, it had to be verified.
It can be concluded that by application of UV/H$_2$O$_2$ at a UV dose of 450 mJ/cm^2 (according to the conditions applied in the UV pilot reactor and the atrazine chemidosimeter results) at least an 8 log reduction can be obtained, independent of the type of UV lamp applied. Thus, under the circumstances applied, it is expected that most pathogenic micro organisms (like e.g. cryptosporidium, giardia en

legionella pneumophila) will be inactivated to a sufficient extent. However, this naturally has to be confirmed in experiments using pathogens.

Conclusions:

- Application of a UV/H_2O_2 process with MP-, LP- or DBD-lamps and a UVdose of 450 mJ/cm^2 (and 10 mg/L H_2O_2) was shown to result in an 8 log reduction for MS2 phages.

3.9   Discussion

For all experiments in the UV pilot reactor UV doses for each lamp were calculated based on the dose response curve of atrazine as a chemidosimeter. In this way the conversion of organic micropollutants can be compared at a certain UV dose.

Another way to compare the various lamps (in the same reactor) is to use the "Electrical Energy per Order (E_{EO}) [Bolton *et al.*, 2001]. The E_{EO} shows how much energy (kWh/m^3) is required to convert 90% (C_0/C_t = 10, or log (C_0/C_t) = 1)of a certain compound in a certain reactor. The following formula is used to calculate this E_{EO}:

$$E_{EO} = \frac{P}{F * \log(C_0/C_t)} \qquad (5)$$

With:

P:	electric lamp power (Total power of lamp and power supply) (kW)
F:	water flow (m^3/h)
C_0:	starting concentration C
C_t:	end concentration C

The E_{EO} is specific for a compound and a reactor (design) and can largely differ from one reactor to another. This is caused by differences in design and dimensions of the various reaction vessels and the flow profile through the reactors. Therefore, the E_{EO} 's calculated here only are valid for the conversion of compounds in the pilot reactor of KWR Watercycle Research Institute, and can be higher or lower in other reactors under similar conditions.

The E_{EO} shown here has been calculated for conversion of organic micropollutants in Dunea water at a dose of 450 mJ/cm^2 in the presence of 10 mg/L H_2O_2. These calculations are shown in appendix XVIII. In Figure 3-18 the E_{EO} for some organic micropollutants tested in this study is shown.
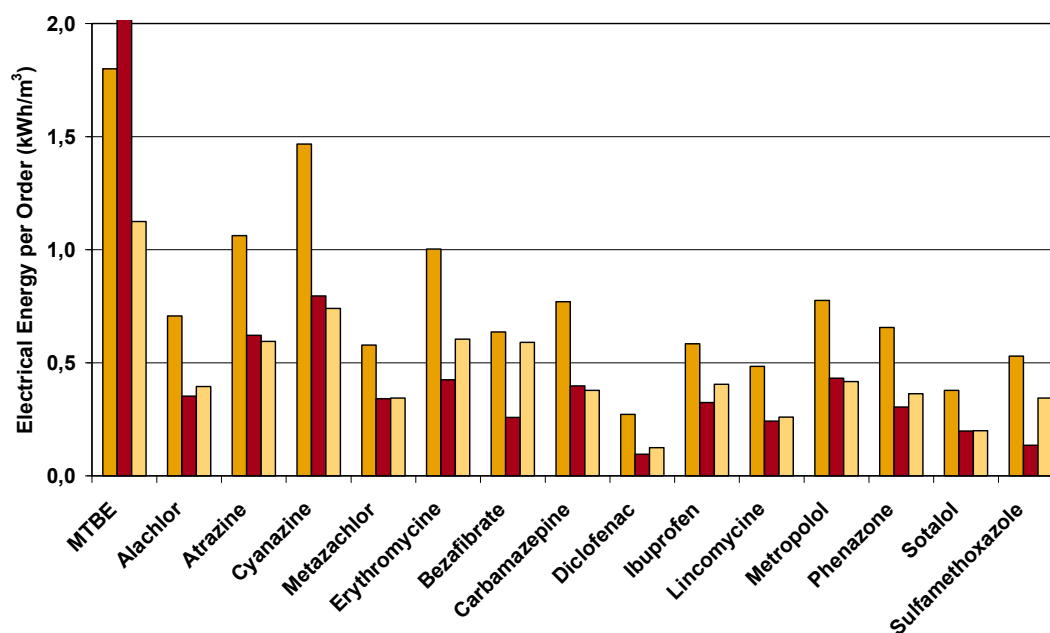
Figure 3-18 conversion of organic micropollutants by means of UV/H₂O₂ in Dunea water at a dose of 450 mJ/cm²
*and 10 mg/L H₂O₂ (■) MP lamp; (■) **LP** lamp; (☐) DBD lamp (1kWh/m³ = 0.624 kWh/kgal).*

The E_{EO} for MTBE in a UV/H₂O₂ process with LP UV-lamps is above the range as shown at the vertical axis in Figure 3-18, and has a value of between 11 and 55 kWh/m³.

The E_{EO}'s for UV/H₂O₂ reactors equipped with LP UV lamps show the lowest values (except for MTBE). Most E_{EO} values are lower than 0.5 kWh/m³; however, for atrazine an E_{EO} of 0.62 kWh/m³ and for cyanazine a value of 0.80 kWh/m³ was found. The E_{EO} values for the MP lamp appear to be about twice as high as for the LP lamp. With the exception of bezafibrate and sulfamethoxazole, the E_{EO}'s for the DBD lamp are similar to those for the LP lamp.

The lower E_{EO} values for organic micropollutants in a reactor equipped with an LP lamp compared with a reactor equipped with an MP lamp can be explained from the fact that the lamp efficiency for LP lamps is higher than for MP lamps (30% for a LP lamp versus 15% for a MP lamp). As a result of this higher efficiency, in theory the UV dose required for conversion of organic micropollutants may be up to twice as high for an LP lamp than for an MP lamp. However, as experiments have shown that such a high dose is not necessary in order to realize the same conversion with LP lamps as with MP lamps, the actual E_{EO} for conversion of organic micropollutants with LP lamps will be lower than the E_{EO} for MP lamps.

For the DBD lamp it can be seen that the conversion of organic micropollutants as well as the lamp energy and efficiency (with the present assumption of 24%, based on data of Philips) are in between the values characteristic for LP and MP lamps. As a result, the E_{EO} values for the DBD lamp are more or less equal to those observed for the LP lamp.

A higher E_{EO} value does not necessarily mean that fewer lamps will be required. As a result of the high electric power of the MP lamp (up to about 30 kW), in comparison with the LP lamp (up to about 300 W), less MP lamps will be required to treat the same water volume by means of UV irradiation. The DBD lamp from Philips has an electric power comparable to the power of the MP lamp. As the E_{EO} values for the DBD lamp in most cases seem to be lower than for the MP lamps, this may result in a reduction in the number of lamps.

From the collimated beam experiments with pCBA it can be concluded that with the LP lamps all conversion is caused by •OH radicals, whereas with MP and DBD lamps the conversion is partly realized by means of photolysis. Experiments with organic micropollutants carried out subsequently with the collimated beam setup and the pilot reactor confirm the results of the pCBA tests. For all organic micropollutants tested, the conversion, based on a UV dose according to the atrazine chemidosimeter, is highest for the MP lamp, followed by the DBD lamp and finally the LP lamp. The difference in conversion is mainly caused by the contribution of photolysis during the process. Notwithstanding the fact that by application of the MP lamp the most efficient photolysis process can be obtained, H_2O_2 will have to be added in order to obtain the required conversion of organic micropollutants under acceptable process conditions.

Comparison of the E_{EO} values and the conversion data (based on a UV dose according to the atrazine chemidosimeter) leads to the conclusion that, by application of the UV/H_2O_2 process with Dunea water for all three types of lamps, diclofenac is most effectively converted, followed by sulfamethoxalzole, sotalol and lincomycine. The conversion of atrazine, cyanazine and erythromycine seems to be lower than the conversion of the other organic micropollutants tested. In all cases the conversion of MTBE is found to be lower than the conversion of the other organic micropollutants. For LP lamps the E_{EO} of MTBE seems to be unlikely high, which is caused by the extremely low conversion. As this was only measured once, we cannot draw any conclusions from this result. Furthermore, from the collimated beam experiments it can be concluded that hormones can be converted very well by means of the UV/H_2O_2 process, independent of the type of lamp applied.

Apart from the conversion of organic micropollutants by means of UV/H_2O_2, also the formation of byproducts and the disinfection capacity of the process with various lamp types has been studied. From experiments with MS2 phages it was concluded that a high inactivation of MS2 phages can be obtained. With Dunea water, a UV dose of 450 mJ/cm² (according to the atrazine chemidosimeter) and a concentration of 10 mg H_2O_2/L an 8-log reduction of the MS2 phages was obtained, independent of the type of lamp. Because of this result, and the fact that a relatively high UV dose is applied in UV/H_2O_2 processes, it can be assumed that the inactivation of pathogenic microorganisms in this process under these conditions will be guaranteed.

With regard to the formation of byproducts, it was observed that MP lamps result in the highest formation of nitrite and AOC. Under the circumstances applied (Dunea water, a UV dose of 450 mJ/cm² (according to the atrazine chemidosimeter) and a concentration of 10 mg H_2O_2/L) nitrite concentrations higher than the official Dutch standard of 100 µg/L were found with the MP lamps. For DBD lamps the values observed were more or less equal to this standard. By applying biological activated carbon filtration (BACF) the nitrite as well as the excess H_2O_2 will be removed, and the AOC concentration will be decreased [Kruithof en Kamp,2000; Kamp *et al.*, 2007]. An investigation into the formation of possibly genotoxic compounds will be described in chapter 7.

From the results obtained with water from GCWW and from Dunea (Bergambacht) it can be concluded that a better water quality results in an improved conversion of organic micropollutants. This implies that the UV/H_2O_2 process can be optimized by improving the water quality, resulting in lower costs and a decreased footprint of the process. Water quality parameters that can be improved are the UV transmission (a higher transmission will result in a higher process yield for the UV), and the hydrogen carbonate concentration (removal of this radical scavenger will improve the yield of the oxidation process). Similarly, removal of other radical scavengers, such as nitrate, will result in a more effective UV/H_2O_2 process. However, the costs of such pretreatment should not be higher than the cost reductions obtained in the advanced oxidation process.

One of the goals of work package 1 was to compare the UV/H_2O_2 process with LP lamps and with the new DBD lamps (which still are in the development phase) with the state-of-the-art UV/H_2O_2 process with MP lamps. All three lamps have advantages and disadvantages. At the moment, it is not yet possible to give a general advice to which type of lamps is the best: that depends on the demands of the user, the local circumstances (water quality, space availability, etc.) and the technical developments with regard to the DBD lamp. More information on this DBD lamp is found in chapter 4.

Although the DBD lamp is still in the development phase at Philips Lighting, it may be a good alternative to LP or MP UV lamps. For the experiments in this project a prototype DBD lamp was used, and some assumptions with regard to lamp efficiency were made. Finally, further developments of this DBD lamp will determine whether or not this lamp can be applied for practical UV/H_2O_2 processes. At the moment, MP lamps will be preferred in those cases, where little space is available to build a UV/H_2O_2 reactor. However, in case the footprint of the installation is not a problem, a reactor equipped with LP lamps may be a good alternative, especially as these lamps cause less byproduct formation (AOC and nitrite) than MP or DBD lamps, and as their E_{EO} for the conversion of organic micropollutants is lower.

3.10 Conclusions and recommendations

Conclusions

In work package 1 "Conversion of organic micropollutants by means of UV/H_2O_2 oxidation" the performance of low pressure UV lamps and of a new Dielectric Barrier Discharge -UV-lamp, developed by Philips Lighting was compared with the state of the art medium pressure UV lamps, which already are used at full plant scale treatment processes.

In the first part of work package 1, experiments were carried out using pretreated water from the GCWW plant in Cincinnati or Dunea in Bergambacht (The Netherlands). The formation of hydroxyl radicals in a collimated beam set-up was studied, leading to the following conclusions:

-   During the UV/H_2O_2 process the contribution of photolysis to the total conversion is in the order:
    MP > DBD > LP UV-lamp.
-   During the UV/H_2O_2 process the contribution of hydroxyl radicals is in the order of:
    DBD > LP > MP UV-lamp.
-   If the UV/H_2O_2 process is applied to water with a better "quality" (UV transmission, bicarbonate, carbonate and chloride content), the contribution of photolysis to the total process stays equal, whereas the contribution by oxidation by means of hydroxyl radicals increases.
-   The hypothesis, that as a result of the low UV absorption of the water matrix at a wavelength of 253.7 nm (which is specific for the LP lamp) the production of hydroxyl radicals is higher than at lower wavelengths, although at 253.7 nm the UV absorption of H_2O_2 is typically lower, was found to be correct.

In the second part of work package 1 the effect of different types of UV lamps on the conversion of organic micropollutants was studied. Experiments were carried out in the collimated beam set-up using pretreated water of GCWW or Dunea, and in the KWR pilot reactor, using Dunea water. This leads to the following conclusions:

-   For all organic micropollutants tested, best results were obtained for the MP lamp, followed by the DBD lamp and finally the LP lamp. This difference can be explained by contribution of photolysis to the conversion process. In all cases the dose was set based on atrazine conversion as a chemidosimeter.
-   The "electrical energy per order" shows how much energy (kWh/m^3) is required to convert 90% of a compound. In our pilot reactor it was found that:
    LP = DBD < MP
    Bezafibrate and sulfamethoxazole appear to be the exception to this rule, showing an order of LP < DBD < MP
-   In spite of the higher electrical energy per order, less MP lamps will be required than LP lamps, in order to obtain an equal conversion. This is caused by the higher electrical power of the MP lamps compared with LP lamps.

Taking into account the electrical energy per order and the conversion based on a UV dose according to the atrazine chemidosimeter, it can be concluded that application of the UV/H_2O_2 process on pretreated Dunea water gives the best conversion of diclofenac, followed by lincomycine, sulfamethoxalzole, and sotalol, independent of the type of UV lamp used. The conversion of atrazine, cyanazine and erythromycine seems to be lower than of the other compounds under similar conditions. Under all circumstances the conversion of MTBE is lowest.

Furthermore, from collimated beam experiments, it can be concluded that the conversion of hormones (Estrone, Estradiol, 17-beta-esradiol, 17alfa-estradiol en 17alfa-ethinyloestradiol) by means of UV/H_2O_2 is good, independent of the type of lamp used.

The pilot reactor also was used to investigate the formation of byproducts and the disinfection capacity during the UV/H_2O_2 process. Experiments were carried out using pretreated Dunea water at a dose of and with a concentration of 450 mJ/cm^2 and 10 H_2O_2 mg/L. This gave the following results:

- Under otherwise similar conditions, for the formation of nitrite the order is:
  MP > DBD > LP
- Under otherwise similar conditions, for the formation of AOC the order is:
  MP = DBD > LP
- For application of the UV/H_2O_2 process the formation of ("high" concentrations of) nitrite will not be a problem as the UV/H_2O_2 process will always be followed by activated carbon adsorption, which removes excess H_2O_2. In this way, also nitrite and AOC will be effectively removed from the water, resulting in acceptable concentrations.
- Application of the UV/H_2O_2 process with MP-, LP- or DBD-lamps at a dose of 450 mJ/cm^2 and a concentration of 10 mg H_2O_2/L was shown to result in an inactivation of 8 log for MS2 phages.

N.B.: These conclusions were drawn for the organic micropollutants tested under the experimental conditions applied, and cannot automatically be extended to other circumstances or compounds.

Based on the results obtained in work package 1, it can be concluded that LP-lamps and DBD-lamps (which are still in the development phase) may be a good alternative for the present state-of-the-art UV/H_2O_2 process with MP-lamps.

Recommendations

The study was carried out using pretreated water from GCWW and Dunea, in order to confirm the hypothesis proposed, and to obtain information on the conversion of organic micropollutants by means of the UV/H_2O_2 process. It was investigated whether LP lamps or DBD lamps, which are being developed, can be an alternative for the present state-of-the-art UV/H_2O_2 process with MP-lamps. Both the LP- and DBD lamp can be an alternative, but it is not possible to give a clear statement which lamp will be the best option. Every lamp has its advantages and disadvantages, and which lamp will be best for a certain application will depend on the circumstances, requirements and possibilities in each individual case. Other chapters (for the results of work packages 7 and 8) describe the results obtained with pilot plants both at Dunea in Bergambacht and at GCWW in Cincinnati. In Cincinnati the LP and MP lamp were compared, whereas in Bergambacht the DBD lamp was also taken into account.

Furthermore, it should be decided which organic micropollutants will be "leading" to determine the process conditions required. This is based on a combination of highest E_{EO} and conversion required during the UV/H_2O_2 process. For these target compounds the conversion kinetics have to be determined by means of collimated beam experiments using various lamps. These results can be used to develop a model, which can be combined with CFD modeling. In this way reactors can be optimized. Besides, the model can be used to predict the conversion of "new organic micropollutants", and to determine whether an actual reactor can be optimized.

To obtain a better idea on the formation of byproducts and the influence of water quality changes during the year, it was recommended to repeat the experiments with Dunea water in especially designed pilot plants equipped with LP-, MP- and DBD-lamps. It was strongly recommended to study the formation of

AOC, because, based on the results of work package 1, it had not yet become clear which type of lamp yields the highest AOC formation. More experimental data were required in order to obtain a clear picture on this topic.

Additionally, it was recommended to investigate the use of activated carbon after the UV/H_2O_2 process to remove excess H_2O_2. In this way it will be possible to directly determine whether, and to which extent, the byproducts formed can be removed, and whether the results obtained are in accordance with data from literature. Various H_2O_2 concentrations would have to should be tested to determine the optimum correlation between the UV/H_2O_2 process and the conversion of organic micropollutants.

To study the formation of hydroxyl radicals, applying another •OH radical probe, like 4-chlorobenzoic acid, was considered. This •OH-probe should have the same properties with regard to hydroxyl radicals as pCBA, but should be less dependent on UV photolysis.

With regard to the validation of the UV pilot plant, it was recommended to reconsider atrazine as a chemidosimeter, because it did not function optimally. The atrazine chemidosimeter can be possibly optimized, or otherwise another chemidosimeter that can be applied in a UV reactor should be considered to improve the validation of the UV reactor.

Research and development on new lamps and ballasts for UV/H$_2$O$_2$ oxidative treatment

Work packages 2-5; Philips Lighting

Authors: J. Geboers, F. v. Lierop

4 Work package 2-5: Research and development on new lamps and ballasts for UV/H$_2$O$_2$ oxidative treatment (Philips Lighting)

4.1 Contents work packages 2-5

At the start of this project, the state of the art UV lamps were either Low Pressure (LP) or Medium Pressure (MP) lamps. LP UV-lamps have a higher efficiency than MP lamps. However, their main disadvantage is their relatively low output, as a result of which a large amount of lamps will be required for a water treatment plant, and the process will show a large footprint. Modifying the principle of LP lamps in such a way, that their output increases (so called "High Output-Low Pressure lamps") would overcome this disadvantage. The development of such a HO-LP lamp was part of the work carried out by Philips Lighting within the framework of this project.

By developing a HO-LP UV-lamp one problem still remains: both MP as well as LP lamps contain mercury, which, from an ecological point of view, is a disadvantage. This problem may be solved by applying a totally different mechanism to obtain UV irradiation: dielectric barrier discharge. The development of DBD lamps was part of this project too.

Four work packages were carried out by Philips Lighting. Their contents are shown below (section 4.1.1 - 4.1.4):

4.1.1 WP2: Research Hg free lamps and ballasts in UV/H$_2$O$_2$

In this work package, the discharge principles for emission of the optimal wavelength were identified. The most promising candidates were selected, and prototypes were built. Then a test facility for lamp evaluation was built, and the performance of the research samples was measured and evaluated. Based on the results, a decision was taken on the final concept for the development phase. Finally, a statement was made on the feasibility of Hg free lamps in UV/H$_2$O$_2$ systems.

4.1.2 WP3: Develop Hg free lamps and ballasts in UV/H$_2$O$_2$

In this work package, a development HG free lamp and ballast samples were built, and tested in a pilot reactor for their performance in UV/H$_2$O$_2$. The system performance was evaluated and improved, and the critical production parameters and material specifications were determined. The final lamp and ballast design were validated. Finally, Hg free lamps in UV/H$_2$O$_2$ systems were validated.

4.1.3 WP4: Research into LP-Hg in UV/H$_2$O$_2$

The limits in current low pressure lamps in UV/H$_2$O$_2$ applications were determined, and directions for extension of the current platform were selected. Test lamps and ballasts were built, and the performance of research samples in UV/H$_2$O$_2$ were measured and evaluated. Then, a decision was made on the final concept for the development phase, and a statement on the feasibility of LP-HG lamps in UV/H$_2$O$_2$ systems was made.

4.1.4 WP5: Development of LP-Hg in UV/H$_2$O$_2$

In this work package, a development LP-Hg lamp and ballast samples were built, and tested in a pilot reactor for their performance in UV/H$_2$O$_2$. The system performance was evaluated and improved, and

the critical production parameters and material specifications were determined. The final lamp and ballast design were validated. Finally, Hg free lamps in UV/H_2O_2 systems were validated.

4.2   Research new type of +UV- lamps (DBD lamps)

(lead: Philips Lighting, partner KWR Watercycle Research Institute)

4.2.1 Introduction

Philips Lighting started research work on a new mercury free UV lamp as early as 2002.
A Dielectric Barrier Discharge (DBD) source generates UV output from excimer molecules with very high electrical efficiency using high-voltage AC excitation. In a DBD configuration one electrode (or both) is separated from the plasma by an insulating dielectric layer, and the discharge consists of a series of short-lived narrow filamentary channels or micro-discharges that occur stochastically in time.

The main advantages of this new lamp technology are:
- Instant-on UV power
- Totally temperature independent also when dimmed.
- Works in direct contact with the water: no UV power losses through the sleeve
- Low environmental impact

Philips Research invented the possibility to change the UV spectrum by the use of special phosphors. This opens possibilities to optimize the spectrum for advanced oxidation in water used to remove organic contaminants in water, allowing reduction of the power consumption.
Philips decided in 2005 to start a feasibility project to investigate the feasibility of a high power UV system. The technical targets of the project were:
- 2000 W electrical lamp power
- 1.3 W/cm^2 electrical lamp power density (input power divided by outer lamp surface)
- 26 % UV lamp efficiency not GAC corrected (wavelength range: 200 nm …400 nm)
- > 90 % driver efficiency
- Lamp replacement 80 % @ 10,000 hrs

To achieve these goals, the following working areas and subtasks were defined:
- Increase power density and lamp efficiency
  - Build-up better understanding of electrical lamp behavior and lamp-driver interaction
  - Adaptation of lamp design to high power operation.
  - Build-up of a high power lab-driver to achieve a lamp power density of 1.3 W/cm^2
  - Optimization of UVC phosphor
  - Improve light out-coupling via reflective coating.
- Build-up of a 2kW prototype system
  - Development of 2000 W driver prototype
  - Build-up of a test reactor including internal and external lamp cooling and side-on UVC measurement
- Improvement of lamp maintenance
  - Investigation of degradation effects
  - Protective phosphor coating

4.2.2 Results and discussion

By the end of 2006 a working 2 kW prototype system with 26% lamp efficiency could be demonstrated.

Figure 4-1 Test reactor with measurement adaptor
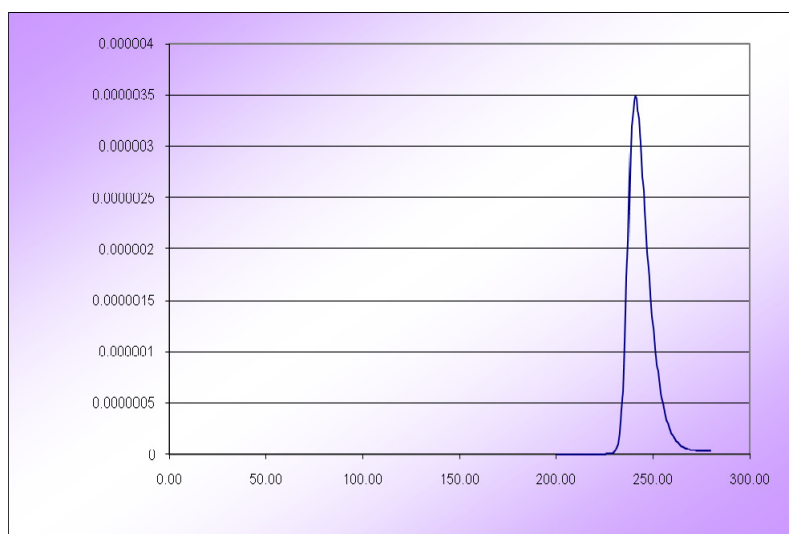
Figure 4-2 Lamp spectrum (positioned at the middle window)

Also several lower wattage prototypes have been built for use in the KWR pilot reactor. (see Figure 4-3)
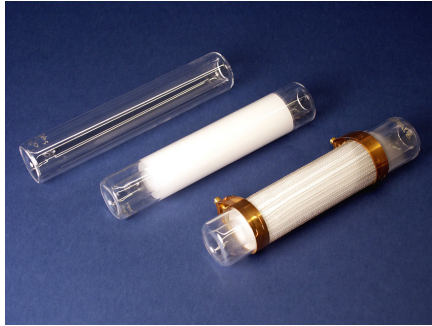
Figure 4-3 Several prototypes of het new LP UV-lamp

UV measurements in the KWR pilot reactor have been made to be able to calculate the treatment efficiency. Based on the outcome of the KWR reactor test, improvements could be made to the new Dunea reactor. In this Dunea system the lamp efficiency could be increased by use of a lamp driver based on the 2 kW prototype.

4.2.3 Application of new type of lamp in pilot plant experiments

The "dielectric barrier discharge" or DBD lamp, described above, has been used in tests on a pilot scale. Experiments were carried out with the pilot reactor of KWR, and in the pilot plant of Dunea. The results of these experiments are described in chapters 3, 5, and 7.

4.2.4 Conclusions

It was proven that it is possible to develop a DBD lamp, which can be used for water purification at at least a pilot scale. During the KWR experiments lamps with an electric efficiency of 7% were used, by the time the Dunea pilot experiments were run, this had been improved towards about 12%. The final goal will be 26%. If this goal is reached, the lamp performance for UV/H_2O_2 reactions (expressed as E_EO) has been calculated to be in between the performance of an LP and an MP lamp.
Unfortunately, economic considerations interfere with the further development of this lamp. As long as the lamp has not been fully developed (showing an efficiency of over 20%), water companies are not likely to develop full scale plants based on these lamps. On the other hand, as long as there is no obvious market (water companies developing full scale reactors with DBD lamps), Philips will not likely invest more in the development of these lamps. As a result, DBD lamps for large scale applications, although promising, probably will not become available in the near future. As water treatment should become more and more based on sustainable technology, this is very unfortunate, for the DBD lamp might not only solve the problem of the presence of mercury in UV-lamps, but also result in a lower energy demand of the purification process.
At the moment Philips is further developing the DBD lamps for point of use applications.

4.3   Development high power amalgam lamp (HO-LP UV lamp)
(lead: Philips Lighting, partner KWR Watercycle Research Institute)

4.3.1 Introduction:

Low pressure mercury lamps and medium pressure mercury lamps are well known UV lamp types. Both types are used in UV water disinfection, each with their specific advantages. Medium pressure UV lamp types combine a very high lamp power (typically from 2,000 W up to 15,000 W or higher) with reasonable energy efficiency around 13% (UV output power versus electric lamp input power). In the

last 10 years the power of low pressure UV lamp has steadily increased especially with the development of amalgam low pressure lamps types reaching lamp powers up to 325W with energy efficiency up to 30%.

For the UV advanced oxidation process a very high UV power is needed (more than 10 times higher than for UV disinfection). For that reason mainly medium pressure lamps are used.

Within this project the efficiency of low pressure and medium pressure lamps to remove contaminants in drinking water with UV/H$_2$O$_2$ advanced oxidation was studied (WP1, 7 and 8). Other work packages (WP4 and 5) concerned the research/development of low pressure amalgam lamps with a substantially increased lamp power. If successful this will allow the use of energy efficient amalgam lamps in the advanced oxidation process without the disadvantage of a very large footprint for their installation.

4.3.2 Research results:

Philips has worked on the development of the amalgam UV platform since 2003.

The main advantages of the new high power lamp concept are:
- Highest lamp power in amalgam technology (less lamps per unit; smaller footprint of pilot or treatment plant)
- Optimized lamp – driver interaction (developed as a system)
- Controlled amalgam operating temperature (beneficial during dimming)

Currently this is the highest lamp power available in the amalgam field (see Figure 4-4 and Figure 4-5). The technical targets that have been realized are:
- High lamp input power (800W)
- High UV output (min. 230W UVC @100 hrs)
- Good efficiency (30%)
- Lamp replacement in line with amalgam portfolio (80% @ end of life)
- Stable lamp operating characteristics during dimming
- Long usefull life (12,000 hrs)
- Industry lowest mercury dose for this lamp technology

To achieve these goals, the following working areas and subtasks have been completed:
- Increase lamp power while maintaining lamp efficiency
  - Develop and test design criteria (outside original power window)
  - Investigate higher current electrode design (8A)
  - Investigation of degradation effects
- Build a prototype system
  - Development of 800 W lamp and driver
    - Investigate driver requirements (pre-heat, starting, dimming)
  - Test system in application
    - Horizontal and vertical operation
    - Water temperature (5 – 30C)
    - Nominal lamp power and dimmed conditions
- Adapt production processes
  - Modify manufacturing equipment to handle bigger diameter, longer length and bigger electrodes (8A)
  - Develop manufacturing process for amalgam fixation in the pinch

Figure 4-4 Lamp sample (800 W)
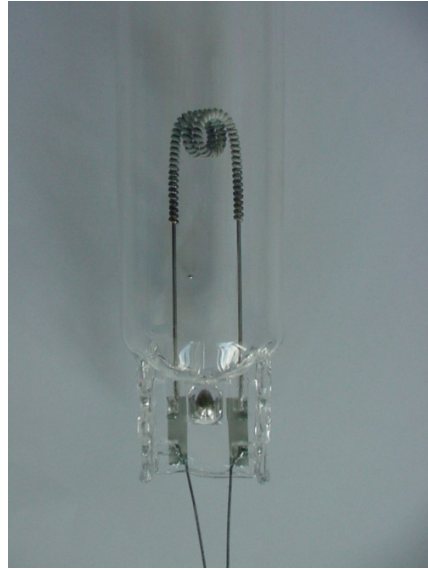
Figure 4-5 Amalgam in the pinch

In Figure 4-6 the maintenance of 3 groups of lamps has been tracked to the specified life span of 12,000 hours (100-hour output normalized as 100%). Lamps have been tested under normal laboratory conditions in horizontal burning positions. It can be seen that the specified minimum output targets at end of life have been met.
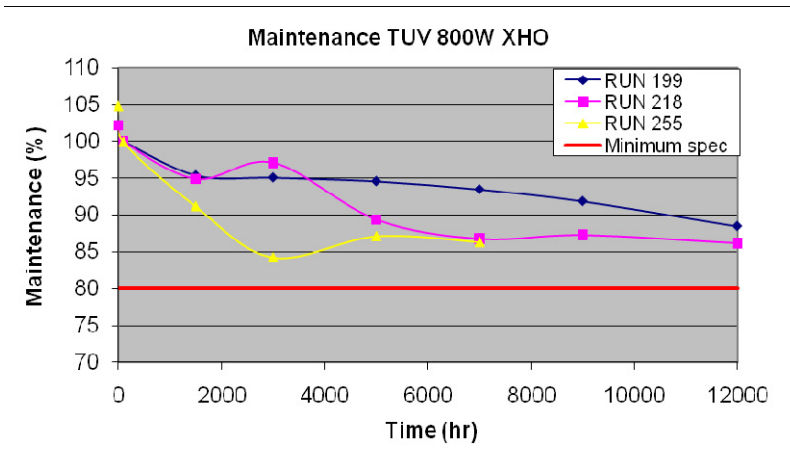
Figure 4-6 Achieved maintenance results for 800 W

In Figure 4-7 below, the lamp power of a typical LP-HO lamp is given as function of the water temperature in a test installation (burning horizontal). The UVC output is also given for the same temperature range, and it can be seen that the lamp output is stable for the entire temperature range
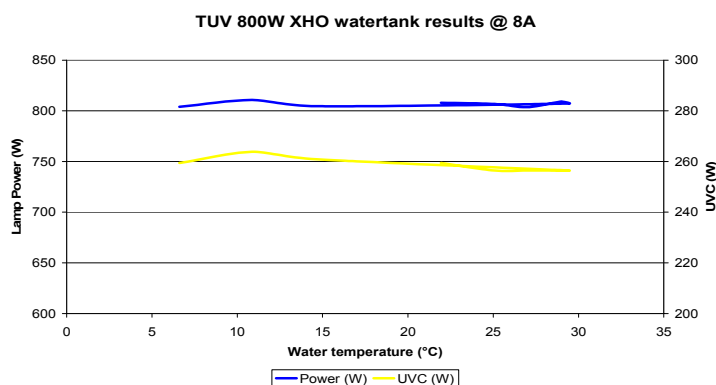
Figure 4-7 Power, output as function of water temperature

Figure 4-8 Test tank for 800 W amalgam lamps

4.3.3 Application of the new LP UV-lamp in pilot plant experiments

The new type of LP UV-lamp described above has successfully been used in experiments carried out at KWR (see chapter 3) in the pilot reactor. In the Dunea pilot plant conventional LP lamps were applied.

4.3.4 Conclusion:

With this new lamp the power gap between medium pressure lamps and amalgam lamps has been drastically reduced. The 800-W amalgam lamp system is completely in line with the existing amalgam portfolio. The new system combines a considerable increase in lamp power with a stable lamp performance during dimming. All originally specified life span characteristics have been reached.
The results from pilot testing show that low pressure amalgam lamps have the best E_{EO} and with this new high power amalgam lamps it becomes possible to build advanced oxidation systems with a footprint 3 times smaller than with the common LP lamps.
The High Output amalgam lamp has been successfully taken into production and is commercially available as a system.

Design and build UV/H$_2$O$_2$/GAC pilot plant

Work Package 6; KWR

Authors: E.F. Beerendonk, D.J.H. Harmsen, C.H.M. Hofman-Caris

5 Work package 6: Design and build UV/H$_2$O$_2$/GAC pilot plant

Both GCWW as well as Dunea were planning to build a pilot plant, to investigate whether UV/H$_2$O$_2$ technology would be a suitable technology for application in their treatment plants. The results of these investigations are described in chapters 6 and 7 (WP7 and 8 respectively). In WP6, guidelines and requirements for the pilot plants for WP7 and WP8 were collected. GCWW and Dunea used these guidelines and requirements to build their pilot plants and to order UV-reactors for either LP, MP or DBD UV-lamps. The pilot plants were build at the Richard Miller Treatment Plant of GCWW in Cincinnati and pumping station Bergambacht of Dunea.

5.1 Goals for pilot testing

To reach the goals of WP7 and 8, different pilot units with different types of lamps were compared. In WP7 at GCWW, LP and MP lamps were compared, in WP8 LP, MP and DBD lamps were compared at Dunea. The goals of the tests in WP7 and 8 were:
1. To test the different UV lamps in combination with hydrogen peroxide (H$_2$O$_2$) under different oxidation conditions as a barrier for organic micropollutants with varying properties, e.g. pharmaceuticals, pesticides, EDCs, individual chemicals like MTBE, NDMA.
2. Test the combination of UV/H$_2$O$_2$ and GAC adsorption as a barrier for organic micropollutants and removal of byproducts and escess H$_2$O$_2$. Thus, the operational requirements for a treatment plant can be determined.
3. Establish the formation potential of byproducts (nitrite, AOC, genotoxicity) under the oxidation conditions as established at point 2.
4. Establish whether NDMA is formed in water prior to and after GAC adsorption under the oxidation conditions as described under item 1 (important for GCWW due to additional chlorination, as NDMA can be formed via chlorination or chloramination of organic nitrogen containing water)
5. Establish the energy consumption of UV/H$_2$O$_2$ with different types of UV-lamps under the conditions established at point 2.
6. Test the removal of H$_2$O$_2$ by GAC following the UV-reactors with different lamp types.
7. Translate the data to the application of UV/H$_2$O$_2$ on a practical scale and calculate the capital and O&M costs.

Originally, another goal was to determine the disinfection potential of the pilot reactors by measuring inactivation of pathogens with MS2 phages as surrogate. After the research in WP1 and information from literature the project group concluded that the disinfection potential of UV/H$_2$O$_2$-oxidation is very high (for disinfection) due to the relatively high UV-dose applied. As a result of that, no disinfection tests were conducted in the pilot research in WP7 and WP8.

5.2 Set-up of the pilot plants

5.2.1 Flow sheets

A simplified flow sheet of a pilot system with 2 reactors is shown in Figure 5-1.
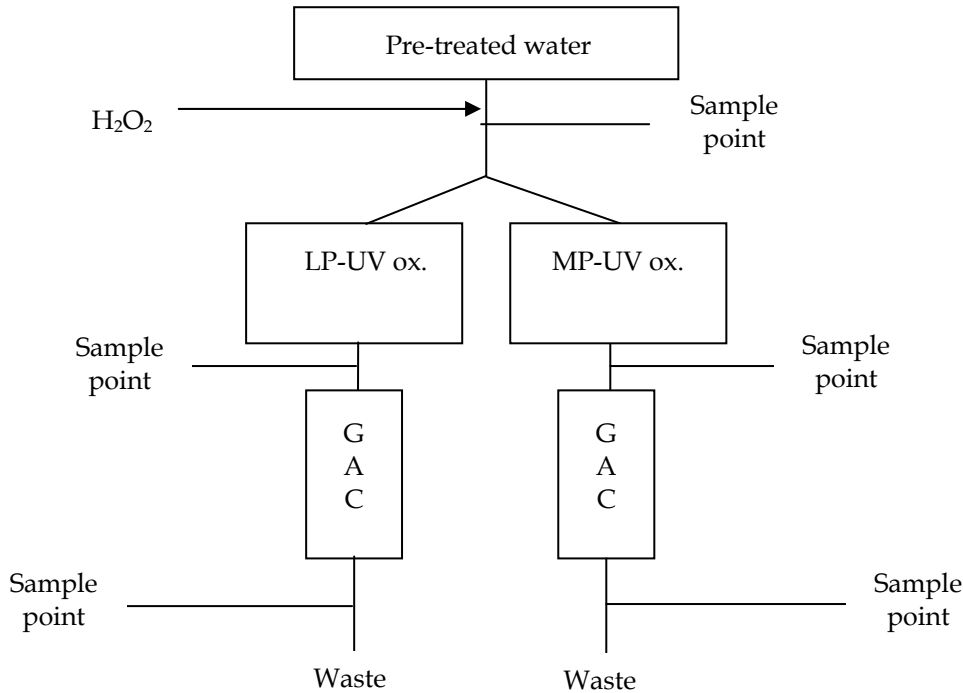
Figure 5-1 Set-up of the pilot plant with LP- UV/H_2O_2 and MP-UV/H_2O_2 units connected parallel and followed by GAC filtration.

In the pilot systems, the treated water is collected in an equalization tank after which the feed water is directed to the pilot reactors. H_2O_2 is dosed and mixed by a static mixer before the water enters the UV reactor. A sample point to analyze the reactor influent is available between the static mixer and the reactor.A static mixer after the UV-reactor ensures that samples taken post- reactor are homogeneous and representative. The presence of insufficiently degraded micropollutants, the formation of degraded products and byproducts (nitrite, AOC), and the required quenching of unreacted H_2O_2 after UV/H_2O_2 necessitated GAC adsorption in the last step of the pilot plant process (see Figure 5-1). After the GAC contactor, the water is fed to the drinking water treatment plant or discharged to the sanitary sewer depending on the water quality of the GAC-effluent. During the spiking tests, the post-UV/H_2O_2 water and post-GAC water were considered waste because of the uncertainty of the complete degradation or adsorption of some of the injected micro-pollutants.

A more detailed flow sheet for a pilot system with one reactor is shown in Figure 5-2.
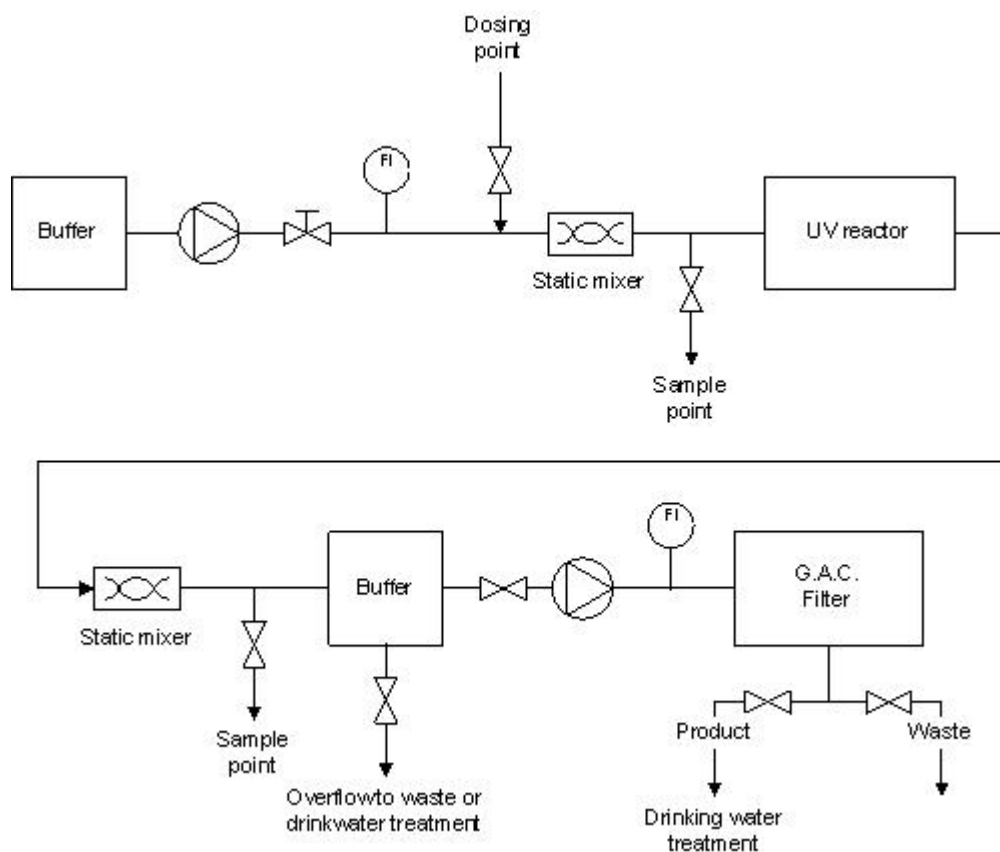
Figure 5-2 Detailed flow diagram of the pilot plant.

5.2.2 Operating conditions pilot plants

The results of the collimated beam tests and the pilot tests performed by Kiwa WR in WP1 were used to establish the operating conditions with respect to UV dose and H_2O_2 dose in the pilot research. Atrazin was used as a target organic micropollutant because it is a contaminant historically detected at low levels in some seasons in the source water of GCWW and Dunea. The operating conditions of the pilot plants should lead to e.g. 80% degradation of atrazine. Another reason to select atrazin as a target compound is that it is relatively recalcitrant towards degradation with UV/H_2O_2.

It is important that the pilot plants should be operated at a capacity that reflects the operational conditions of the drinking water treatment plant in practice and that the UV units in the pilot research should have a minimal volume to avoid scale-up issues. For example, the reactor would be too small if the distance between the lamps and the reactor wall affected the flow and light profiles and the travel depth of the UV light. It would be ideal to have a pilot unit with a capacity of 25 m^3/h , but this would imply relatively high costs for installation and operation (required amount of chemicals, water loss etc.). Therefore, in most cases, distances of 10 cm with capacities of approximately 5 m^3/h were used. It was established that with such pilot plants the goals mentioned in paragraph 5.1 could be reached.

The GAC-columns, after the UV/H_2O_2-process, are expected to remove excess H_2O_2, the degradation products of organic micropollutants and other possible byproducts (AOC, nitrite, possibly genotoxic compounds, etc.). For the degradation of micropollutants and removal of AOC, an empty bed contact time (EBCT) of 10 minutes or more is recommended. The type of carbon to be used is determined by GCWW and Dunea. GCWW used the type of carbon that is used in the full scale RMTP. Dunea used Chemviron TL839.

5.2.3 Influent water quality

To prevent fouling of the quartz tubes and UV reactors, surface water needs to be pretreated before entering the pilot plant. For instance coagulation and filtration can lead to a water quality that is acceptable for the application of UV/H_2O_2. Such pretreatment can also increase UV-transmission, which will lead to lower use of energy to achieve a certain UV-dose in the UV-reactors. However, it should be kept in mind, that the process should be economically feasible too: the total process should not become more expensive by implementing the pretreatment step. GAC can also increase UV transmission of the pretreated water, but removal of the degradation products, byproducts and excess H_2O_2 by GAC after UV/H_2O_2 required that GAC adsorption took place at the end of the process, and therefore GAC was not used in the pretreatment step (it would not be feasible to have GAC before as well as after the UV/H_2O_2 process).

5.3   Requirements pilot reactors

During the project it was decided to perform tests in WP7 and WP8 with:
-    Commercially available reactors. Except for the reactor with the DBD lamps since this reactor will not be commercially available. Dunea, Philips and KWR designed the reactor for tests with the DBD lamp.
-    Conventional LP lamps, not Philips improved LP-HO lamps.

In the process of ordering pilot reactors for the LP- and MP-lamps, several requirements were used:
-    Capacity of the reactor(s), 2 – 10 m^3/h.
-    UV-dose of the reactor(s), 450 – 900 mJ/cm^2.
-    H_2O_2 dose, 5 – 10 mg/L.
-    Manual or automatic regulation of the UV and H_2O_2 dose depending on water flow.
-    Automatic regulation of the UV dose based on UV sensor that includes UV transmission of the water, output of the UV lamps and fouling of the quartz tubes. Only change dosages manually during experiments with micropollutants or longer periods of other settings.
-    Preferably one UV sensor for each lamp.
-    Results of CFD modeling for UV dose distribution and residence time (distribution) of water in the reactor.
-    Reactors should be mounted in horizontal position for mercury LP and MP lamps.
-    A wiping system is needed, either manual or automatic.
-    Available space for reactor and equipment.
-    Costs for the reactor, equipment, service, spare parts (lamps, quartz tubes, etc.) and maintenance.
-    Average use of energy and operating costs, given by the suppliers.
-    Costs for installing the reactor, start up, instruction and support by the supplier.
-    Quartz panes in the reactor to check burning lamps visually.
-    Guidelines for use of the reactor, including indication of UV dose based on UV intensity, residence time in reactor, flow and UV transmission.
-    Full specification of the reactor, including technical drawings.
-    Net volume of the reactor.
-    Information about the method to calculate UV intensity of the lamps and UV dose.
-    Lamp specs: effectiveness for UV/C, required power and decrease in output as a function of burning hours.
-    Specs of the UV sensors, stability, transmission curve and the method to interpret sensor signals.
-    Security and system information.
-    Electrical drawings.
-    Guarantee conditions.

Both the MP as well as the LP pilot reactor at GCWW was purchased from Aquionics.
The LP pilot reactor at Dunea was obtained from ITT Wedeco, and designed with a flow of 5 m^3/h. The MP pilot reactor was obtained from Berson UV Technology.

The pilot reactor for the DBD lamps was designed by KWR and LIT Technology (a Russian UV supplier, who was asked by Philips to help in the design). The design was based on the pilot reactor of KWR that was used in WP1. Since the flanges for mounting the DBD lamps were specially made and expensive, these flanges were reused in the pilot reactor for WP8.

The reactor for the DBD lamps was designed by using Computational Fluid Dynamics (CFD) calculations. CFD calculations led to insights into the dose distribution through the reactor. Besides the average UV dose (D_{mean})can be calculated by means of CFD. In the dose distribution, the low dose range is of major importance for the performance of UV reactors (especially in case of disinfection) and is well represented by the D_{10} (the 10th percentile of the dose). The dose distribution is therefore characterized by the ratio between D_{10} and the average UV dose D_{mean}, calculated as the factor D_{10}/D_{mean}. When D_{10}/D_{mean} equals 1, the system resembles a perfect plug flow with no variations in doses. If D_{10}/D_{mean} is smaller than 1, the hydraulics of the system are suboptimal. After CFD-calculations with several designs of the reactor, using the flanges as mentioned above, the design with the best D_{10}/D_{mean} was selected for the pilot reactor in WP8. After designing the reactor (see chapter 8), Melamo (a construction company in The Netherlands) built the reactor. Details on CFD modeling and calculations are given in chapter 8.

Pilot plant research I

Work Package 7; GCWW

Authors: D.H. Metz, M. Meyer

6 Work package 7: Pilot plant research I (GCWW)

6.1 Introduction

Greater Cincinnati Water Works (GCWW) is designing a 908,500-m^3/d (240-MGD) ultraviolet (UV) disinfection facility for a drinking water plant that treats Ohio River water. GCWW additionally wished to determine the efficacy of UV/H_2O_2 for reducing pharmaceuticals and other organic contaminants. Therefore, GCWW joined a Dutch/U.S. collaboration to determine if low pressure (LP) and medium pressure (MP) UV/H_2O_2 and direct UV photolysis processes could effectively degrade micro-pollutants in conventionally treated (see section 6.3.1 for further details) and granular activated carbon (GAC) treated process streams. GAC has long been considered an excellent technology for removing a broad spectrum of organic contaminants, particularly hydrophobic compounds, and in many cases it still is an excellent technology. However, breakthrough occurs as the GAC becomes exhausted, and hydrophilic compounds break through the GAC more quickly than hydrophobic compounds. A year-long UV/H_2O_2 study was conducted that examined a variety of seasonal and GAC breakthrough conditions. Additionally, operational requirements and organic and inorganic byproduct formation were studied. Because hydroxyl radicals react non-selectively with organic compounds, unintended byproduct formation was expected to occur. Assimilable organic carbon and biofilm formation were investigated.

The following hypotheses/assumptions were initially developed:

1) Based on pilot studies performed at KWR, it was assumed that reaction with hydroxyl radicals would be the predominant mechanism in the UV/H_2O_2 destruction of most introduced contaminants when using both the low pressure and medium pressure lamp technologies (some compounds, like e.g. NDMA, react very quickly by means of photolysis, when the right wavelength is applied). Therefore, the contaminant destruction of most introduced contaminants should be similar when medium pressure and low pressure technologies are normalized for atrazine destruction.

2) However, the medium pressure technology would likely require greater energy to achieve equal destruction because of the wavelengths that are not used for hydroxyl radical production (with LP lamps most UV irradiation can be used for hydroxyl radical formation). It was assumed that destruction by direct photolysis would be less efficient than either UV/H_2O_2 technology.

3) It was conjectured that the natural organic matter would be chemically altered by the UV/H_2O_2 process, increasing the microbiologically assimilable organic compounds and thus the biofilm formation potential.

4) It was assumed that granular activated carbon (GAC) adsorption would effectively adsorb larger, hydrophobic natural organic carbon molecules. Thus, when GAC effluent water was used as pilot influent, less microbiologically assimilable organic compounds would be formed than when the pilot influent was conventionally treated Ohio River water.

5) Following the UV/H_2O_2 process with GAC would reduce the biofilm potential, particularly when the GAC was most biologically active. The UV/H_2O_2 process would create smaller, more microbiologically assimilable compounds, enhancing the bioactivity of the GAC. Thus, the biologically active GAC would reduce smaller assimilable compounds, including hydrophilic materials.

6) MP and LP technologies could be compared for byproduct formation because the pilot was normalized for 80% atrazine destruction.

The scope of this research included the following:

- Exploring the applicability of two modes of contaminant destruction by UV, i.e., UV/H_2O_2 and photolysis.
- Comparing two plant sources with varying natural organic composition and concentration as influent to UV/H_2O_2 process
- Determining the effect of seasonal variations in water quality on UV/H_2O_2 and photolysis processes.
- Comparing medium pressure and low pressure lamp performance for both UV/H_2O_2 and photolysis processes.
- Evaluating the Electrical Energy per Order (E_{EO}) and compare the efficiency of MP to LP technology for both UV/H_2O_2 and photolysis processes.
- Determining GAC adsorption of EDCs without UV/H_2O_2 or photolysis processes and following UV/H_2O_2 process.
- Evaluating enhanced removal of EDCs with UV/H_2O_2 and biologically active GAC.
- Determining biofilm potential:
    - Increases with UV/H_2O_2 process.
    - Reduction through GAC following UV/H_2O_2 process.
    - Enhanced reduction through biologically active GAC.

6.2   Back ground information (theory)

6.2.1 Endocrine Disrupting Compounds (EDCs), Pharmaceuticals and Personal Care Products (PPCPs)

The presence of endocrine disrupting compounds (EDCs) in the US water bodies has been known and investigated since the 1960s (Stumm-Zollinger, 1965, and Tabak and Bunch, 1970). Initial research findings indicated that several natural and synthetic compounds were able to interfere with the hormonal systems in animals. These chemicals were identified as EDCs and included a variety of compounds which could mimic or block the natural estrogen (estrogenic), testosterone (androgenic), and thyroidal hormones in animals, resulting in deformities and reproductive problems in many aquatic wildlife species. Examples of such compounds with well documented endocrine disruptive activity are DDT, atrazine, and 17-α- ethynyl estradiol, while broader groups include steroid hormones, alkylphenols, phthalates and phytoestrogens (Snyder *et al.*, 2008).

Another group of environmental contaminants are the pharmaceuticals and personal care products (PPCPs), which include a variety of compounds such as antibiotics, anticeptics, surfactants, heart medications etc., which enter the environment through waste water discharges, animal feeding operations, agricultural runoff, and groundwater contamination. Advances in analytical technology in the last couple of decades have made the detection of many groups of compounds possible at trace levels.

The range of concentrations of these micropollutants in U.S. waters varies with the chemical and location between non-dectectable and up to 20 µg/L as reported for atrazine with the many being in the ng/L range (Snyder *et al.*, 2007). Traces of these contaminants also have been found in municipal drinking water systems, indicating that they may not be removed effectively by some treatment processes.

6.2.2 UV/H₂O₂ and Direct Photolysis

A promising technology for the destruction of EDCs and PPCPs is UV/H_2O_2 advanced oxidation, which combines the effects of direct and indirect UV photolysis (Pereira *et al.*, 2007). Direct photolysis takes place when a compound absorbs photons of certain energy capable of breaking down bonds (Hovorka *et al.*, 2001). Medium pressure lamps are more energy-intensive and emit a broad-spectrum of UV wavelengths, thus achieving direct UV photolysis at multiple wavelengths. Low pressure reactors primarily emit UV at 253.7 nm, and only achieve direct UV photolysis at this wavelength (Rosenfeldt, 2004). Light absorption behavior and direct UV photolysis of organic contaminants is also a function of

radiation wavelength. So, different wavelengths could influence the type, selectivity and yields of byproducts formed.

Indirect UV photolysis with hydrogen peroxide (H_2O_2) results in the cleavage of the HO-OH bond, causing the formation of hydroxyl radicals (·OH). Although the UV absorption coefficient of H_2O_2 is a function of UV wavelength, both LP and MP UV lamps emit wavelengths that can cause photolysis of H_2O_2 to generate hydroxyl radicals. UV photolysis of H_2O_2 is a rapid process and the produced hydroxyl radicals react non-selectively with organic compounds yielding carbon-centered radicals. They target mainly unsaturated bonds or abstract hydrogen from C-H bonds (Buxton, 1988) especially those in "α-position to π-systems, amines, ethers, thioethers, and carbonyls" (Hovorka *et al.*, 2001). These carbon-centered radicals in turn rapidly react with dissolved oxygen to form peroxyl-radicals, followed by the break down of peroxyl radicals to form oxyl-radicals, and the breakdown of oxyl-radicals to other radicals and stable reaction intermediates (Hovorka *et al.*, 2001). In UV/H_2O_2 systems many radical-based reactions take place (i.e., generation, propagation, termination).

The efficiency of the process is dependent upon the rate of formation of hydroxyl radicals, the presence and concentrations of hydroxyl radical scavengers and other parameters (i.e., UV absorbance of the process water, type and concentration of other organic impurities in water such as natural organic matter, type and concentration of target organic contaminants, water temperature). The most prominent scavengers are the dissolved organic compounds (DOC), and alkalinity (HCO_3^-, CO_3^{2-}), however H_2O_2 will also react with hydroxyl radicals (Pereira *et al.*, 2007). A byproduct of a UV system operating with MP lamps is the formation of nitrite (NO_2^-) resulting from the photolysis of background nitrate (NO_3^-) by the shorter emitted wavelengths (less than 240 nm) (Sharpless *et al.*, 2001).

The UV/H_2O_2 process is a very energy intensive process, and this energy consumption should be considered when lamp technologies are compared. A fundamental measurement of the energy efficiency of a UV advanced oxidation system is the Electrical Energy per Order (E_{EO}). It is defined as "the number of kilowatt-hours of electrical energy required to reduce the concentration of a contaminant by one order of magnitude in a specified volume of water", i.e., 1,000 gal (Sharpless *et al.*, 2005) or m^3. The formula used for the calculation of the E_{EO} in this pilot study is:

$$E_{EO}\left(\frac{kWh}{m^3 \cdot order}\right) = \frac{UV \ reactor \ draw \ (kW)}{flow \ (m^3/h) \times log\left(\frac{C_{inf}}{C_{eff}}\right)}$$

6.2.3 GAC Adsorption of EDCs

Historically, granular activated carbon (GAC) has been used for the adsorption of organic compounds in drinking water. Initially it was used primarily for taste and odor control, later for the removal of specific organic contaminants and most recently for disinfection byproduct control. GAC is an effective adsorbent primarily due to its porous nature. Activated carbon pores have been divided into three size classifications: micropores (pore radius <1 nm), mesopores (pore radius > 1 nm and < 25 nm) and macropores (pore radius >25 nm). The various pore sizes serve different roles in adsorption. In the GACs most frequently used in water treatment, micropores comprise most of the surface area and are largely responsible for the removal of smaller organic compounds such as benzene and trichloroethene. The mesopores are important for the adsorption of natural organic matter (NOM). Macropores comprise very little of the GAC surface area but play a major role in the transport of compounds to adsorption sites and may harbor microbes (often > 1,000 nm) that are very important to the biodegradation of undesirable constituents that occur in GAC (Sontheimer *et al.*, 1988). Organic adsorption onto GAC is known to be influenced by several variables including pore size distribution, internal surface area, GAC surface functional groups, electrostatic interactions, acidity, ash content, the size shapes and properties of the organic compounds and the pH, dissolved oxygen and ions in solution (Moore *et al.*, 2004). Adsorption is the mechanism for organics removal by GAC. An important aspect of GAC are the chemical properties of the pore surfaces. Oxygen containing compounds dominate the functional groups and display both acidic and basic characteristics. In general, less soluble organic compounds (hydrophobic) are better adsorbed than soluble compounds (hydrophylic). Therefore, polar compounds

which tend to be hydrophilic are less well-adsorbed than non-polar compounds. Halogenated methanes and ethylenes are not as well adsorbed as substituted phenols or polycyclic aromatic hydrocarbons (James M. Montgomery, Consulting Engineers, Inc., 1985). Westerhoff *et al.* (2005 b) found a correlation between log K_{ow} (measure of hydrophobicity) and the removal of 22 pharmaceutical and personal care products. The logK_{ow} values of the compounds introduced into the GCWW pilot plant can be found on Table 6-3.

Natural organic acids such as humics are fairly well-adsorbed by GAC especially at low pHs (James M. Montgomery, Consulting Engineers, Inc., 1985). Humic substances are likely to be present in natural waters all year round, while industrial micropollutants, pesticides, taste and odor compounds and algal toxins are more sporadically present. The surface charge of the GAC greatly affects adsorption of humic and fulvic acids (the major dissolved constituents of NOM) and other charged contaminants in water. The adsorption of these highly charged compounds will alter the adsorptive properties of GAC for other compounds (Sontheimer *et al.*, 1988 and Morris and Newcombe, 1993). Morris and Newcombe (1993) additionally found that the adsorption of humic matter from a raw source altered the surface properties of GAC. The adsorbed material caused the net charge of the GAC to be more negative.

Smaller pores are recognized as being most beneficial in adsorption because each wall of the pore exerts an attractive force, and in a small pore, adsorbed materials benefit from attractive forces from both walls in an overlapping manner (Moore *et al.*, 2004). Therefore, it logically follows that smaller organic contaminants would easily fit into the micropores and be held in place by the overlapping attractive forces. This supports the conventional historical knowledge mentioned previously. Newcombe *et al.* (1998) demonstrated that NOM with nominal molecular weights below 3,000 mainly loaded into micropores and somewhat less into mesopores, but that pore volume attributable to micropores and mesopores was lost almost equally through the adsorption cycle. This is likely due to the fact that new micropores are created as the mesopores partially fill with NOM (Newcombe *et al.*, 1998).

Because of the surface area created by pores, GAC provides an excellent substrate for biological activity. GAC pores provide protection from shear forces and the functional groups of the adsorbed organic material provides a mechanism for chemical binding. (Carvalho, *et al.*, 2001). Also, biofilms on a fixed media are less affected by organic loading changes than are suspended growth systems. Studies have shown that biologically active carbon can continue to be effective even when contaminant levels were low (Shi, *et al.*, 1995).

6.2.4 Peroxide Quenching

In order to obtain a hydroxyl radical concentration that is high enough for conversion of micropollutants, even if the UV absorption of H_2O_2 in the system will not be very high (see Figure 3-1 and Figure 3-2), a relatively high concentration of H_2O_2 is applied. During the UV/H_2O_2 process, not all the H_2O_2 will be converted to hydroxyl radicals, and at the end of the process residual hydrogen peroxide will be present in the water. Hydrogen peroxide may be quenched by chemicals such as chlorine or sodium hypochlorite, sodium thiosulfate, and sodium sulfite. Liu *et al.* (2003) showed that quenching hydrogen peroxide with the above inorganic compounds does not affect the formation of the U.S. regulated trihalomethanes and haloacetic acids. However, these tests did not include any UV exposure of the tested water prior to quenching. Alternatively, GAC may be used as means of residual hydrogen peroxide quenching. It has been proposed that hydrogen peroxide is catalytically decomposed on the surface of activated carbon initiated by a reaction with a surface hydroxyl group (Khalil *et al.*, 2001). Intermediates from the surface reaction, which could be hydroxyl radicals or superoxide radical anions (O_2^-), may react further with the surface producing oxygen and water or they may react with other organic chemicals (Miller and Valentine, 1995). It has also been proposed that the surface reaction and not the mass transfer would control the reaction rate of the decomposition of hydrogen peroxide on the activated carbon (Huang *et al.*, 2003). Hydrogen peroxide may also affect the oxygen functional groups of GAC, and it has been shown that under certain conditions it may increase the surface OH groups (Gomez-Serano *et al.*, 1994), and it may affect the adsorption capacity of GAC for phenol (Zeid *et al.*, 1995).

6.2.5 Biodegradable portion of natural organic matter (NOM)

Drinking water sources contain various levels of natural organic matter (NOM). While the composition of the NOM varies from location to location, there are some similarities in the structure. Humic substances comprise up to 75 % percent of the NOM (Volk, 1997). Organic matter originating from soils is derived from plant matter, which has a high lignin content. Lignin has a predominant aromatic fraction. NOM also provides reduced carbon that provides energy and carbon for bacterial metabolism (Kaplan, *et al.*, 2004). Kaplan and Gremm (1995) determined 54% of the most biodegradable material in the waters sampled was humic in nature. Butterfield, *et al.* (1997) additionally found that humic substances in the distribution system were the primary carbon source supporting distribution biofilm. However, while the formation of biofilms in the distribution system is believed to be ubiquitous, the degree of colonization varies from site to site.

6.2.6 What Causes Regrowth

Microbial growth in the distribution system is caused by various factors. Generally, four water quality parameters control microbial regrowth: temperature, assimilable organic carbon (AOC), availability of nutrients and residual disinfectant presence[*)] (Reasoner, *et al.*, 1991). However, LeChevallier, *et al.* (1996), investigated coliform regrowth in 31 drinking water systems. Their conclusion was that there was a complex interaction of physical, chemical operational and engineering factors involved in bacterial regrowth. Temperature, particulate protection of microorganisms, types of organisms colonizing the distribution system (e.g., resistance of microbes to disinfection) and nutrient concentrations are factors controlling the type and amount of biofilm (Baribeau, 2005). Kaplan, *et al.* (2004) determined that source waters possess NOM and biodegradable organic matter of widely different quantity and quality. These differences influence the community of heterotrophic bacteria that use the NOM as a source of carbon.

*) The Dutch situation differs from the US situation in that in the Netherlands the water is not chlorinated for desinfection purposes.

6.2.7 Molecular weight vs. AOC

Research to determine the chemical composition of biodegradable organic matter is on-going. It is known that lower molecular weight compounds are more easily transported across cell membranes enabling enzymatic reactions to proceed. Shi-hu *et al.* (2008) found that the AOC/TOC ratio increased with decreasing apparent MW. Hem and Efraimsen (2001) found 50-70% of the AOC fraction were <1,000 Daltons molecular weight. Other researchers observed good correlation between apparent molecular weight distribution (AMWD) and UV absorbance (at 254 nm) to TOC ratio and biodegradability of raw waters (Goel, *et al.* 1995). The AOC fraction is generally less than 1,000 MW (Hem and Efraim, 2001), and can include sugars, fatty acids, amino acids and peptides (Haddix, *et al.*, 2003). These results would confirm the simpler lower MW fractions would be the most assimilable by biodegrading micro-organisms.

6.2.8 OH radicals yielding more biologically labile compounds

The UV/H_2O_2 process forms hydroxl radicals that will attack organic compounds to form organic free radicals. Organic free radicals then can form aldehydes, ketones, alcohols, and carboxylic acids that can be used in microbial metabolism (Speitel *et al.*, 1999). Wu (1991) studied the biodegradation of commercial humic acid after UV/H_2O_2 treatment. Wu was able to increase biodegradability by 17%. Biodegradable dissolved organic carbon (BDOC) increased from 0.1 to 1.3 mg/L in Lake Austin Water in continuous flow experiments and 0.52 to 0.87 mg/L in Lake Houston Water. Acetic and oxalic acids are often found as intermediates of the NOM oxidation process, and these acids biodegrade readily (Speitel *et al.*, 1999).

6.2.9 Why Biofilms are a Problem

Biofilm formation can be a serious problem in the distribution system. Weinrich *et al*. (2009) states that
"In distributed water, bacterial regrowth is perhaps the most significant mechanism for water quality
deterioration between the treatment plant and the end user." Coliform bacteria and pathogenic
organisms can grow and be shielded in the biofilm and be difficult to eliminate. Biofilms can be
responsible for disinfectant depletion and problems with taste and odor. In chloraminated systems
nitrification may also occur. Even corrosion rate can be increased by the presence of biofilm under
certain conditions (Geesey, 1989 Water Science and Technology). Van der Kooij et al. (1992) have
recommended that unchlorinated systems maintain AOC values below 10 μg/L (Lechevallier, *et al*., 1990,
1996) however, provided some evidence that chlorinated systems may limit regrowth and coliform
occurrence by maintaining AOC less than 50 to 100 μg/L.

AOC Method

Two laboratory tools have been developed to assess the potential of drinking water to support
microbiological growth: the AOC method developed by van der Kooij in 1982 and biodegradable
dissolved organic carbon (BDOC) developed by Servais (1989). Huck (1990) suggests that the parameter
most appropriate for biofilm potential assessment depends upon the given situation and the objective of
the measurement. He recommends that BDOC be used for determining the ability to biodegrade organic
matter within a specific plant. AOC makes use of two specific strains of organisms that allow for
universal comparison of biofilm potential among diverse utilities. Pseudomonas fluorescens strain P-17
is able to utilize various compounds such as proteins, amino acids, carboxylic acids, carbohydrates,
alcohols and aromatic acids. It has great nutritional variability. Spirillium strain NOX is more selective
in its growth substrates. Only carboxylic acids and a few amino acids promoted growth of NOX. In
situations such as ozonation where compounds not utilized by P-17 are present, Spirillium strain NOX is
used. Also, in cases of low AOC this organism tends to grow better than P-17. Therefore, this method
can be used to obtain information about the chemical composition of the AOC (AwwaRF and KIWA,
1988) AOC results are considered to be a biofilm potential indicator, while BDOC is more of a direct
biodegradability test using indigenous organisms and nutrient sources.

For the AOC method, organic–free glassware is used to collect samples. Water sample is heated to kill
indigenous bacterial population and inoculated with two organisms. The sample is incubated and the
growth of the organisms monitored. When the growth of the organism reaches the stationary phase, the
carbon nutrient is considered to be exhausted. Cell yields are measured and carbon equivalents are
calculated to determine yield coefficients for the substrate (Van der Kooij, 1982). The AOC test has been
found to be a useful tool for predicting bacterial growth in the distribution system. However, it should
be noted that carbon is not always the limiting nutrient (LeChevallier, 1987and 1991).

Annular Reactor Method

The annular reactor methodology for biofilm formation was developed by Sharp, et. al (2001), to assess
the adherence and growth of bacterial populations on pipe surfaces in the distribution system[*]. To make
this assessment, it is important to simulate pipe materials, pipe velocities and make use of indigenous
organisms and natural nutrient levels, i.e. ratio of organic carbon to nitrogen to phosphorous. Pipe
velocities greatly affect the ability of microbes to attach to pipe interiors. High pipe velocities can cause
shearing of the biofilm. Donlan and Pipes (1988) concluded that water velocity had an inverse
relationship with biofilm counts. LeChevallier, *et al*. (1998) reported that the type of pipe material also
was a key factor in biofilm growth. Servais (1989) elucidated the importance of using indigenous
microorganisms to give a realistic representation of actual plant conditions. Additionally, a method was
needed that could consider seasonal variations. The annular reactor is able to measure the biofilm
regrowth potential of continuous plant and distribution streams utilizing actual distribution conditions.
It contains coupons as surfaces for biofilm growth. These coupons can be made of various pipe
materials, and the unit can be set to simulate a range of pipe velocities.

[*] In the Dutch situation a biofilm monitor is used instead of an annular reactor.

Bioluminescence Method

In order to quantify the biofilm on the annular reactor coupons, the material must be removed and processed by methods such as traditional heterotrophic plate count or by the detection of adenosine -5'-triphosphate (ATP) in metabolically active cells by a bioluminescence protocol. The bioluminescence methodology is based on detection of ATP in metabolically active cells. ATP is involved in all aspects of metabolism, and, therefore, can be used to determine the viability of microbial cells. ATP disappears within two hrs of living matter death (Driebel, 2008).

The firefly luciferase-based (bioluminescence) assay for detecting ATP was established by Bautista *et al.* (1994) as a way to rapidly monitor microorganisms on surfaces. Satoh, *et al.* (2004) developed an additional method to increase the sensitivity of the bioluminescence assay. They developed the polyphosphate-ATP amplification reaction. This amplification reaction employs adenylate kinase (ADK), to convert adenosine monophosphate (AMP) and ATP to two molecules of adenosine diphosphate (ADP); and polyphosphate (polyP) kinase (PPK), which converts two molecules of ADP back to two molecules of ATP. Using these reactions, ATP is amplified exponentially, resulting in high levels of bioluminescence in the firefly luciferase reaction (Asami *et al.*, 2006).

$$ATP + D\text{-}Luciferin + O_2 \rightarrow Oxyluciferin + AMP + PPi + CO_2 + Light\ (560nm)$$

(Driebel, 2008)

If ATP in microorganisms or cells is to be measured, it must be extracted efficiently without allowing it to degrade. A wide variety of ATP-extracting reagents have been described (Karl, 1980, and Stanley, 1986). Generally, the best solvent for extraction is trichloroacetic acid (TCA). TCA efficiently releases ATP from microorganisms and cells while inactivating enzymes that might quickly degrade the ATP before measurement. Because TCA inhibits the bioluminescence reaction, the lowest concentration of TCA needed for extraction should be used (Karl, 1980, and Stanley, 1986).

A luminometer is used to quantify the ATP bioluminescence. It gives a direct measurement of the light intensity and therefore a direct quantification of ATP. The light is quantified as relative light units (RLU), and the intensity of the emission is proportional to the concentration of ATP.

6.3   Experimental set-up

6.3.1 Facilities

The source water for the UV/H_2O_2 pilot influent was drawn from two locations within Greater Cincinnati Water Works' (GCWW) Ohio River treatment plant. The first location was after coagulation, settling and filtration, i.e, conventional treatment (CONV). The second location was from the GAC adsorber effluent (Post-GAC). A schematic of the full-scale process train, indicating these locations, is shown in Figure 6-1.
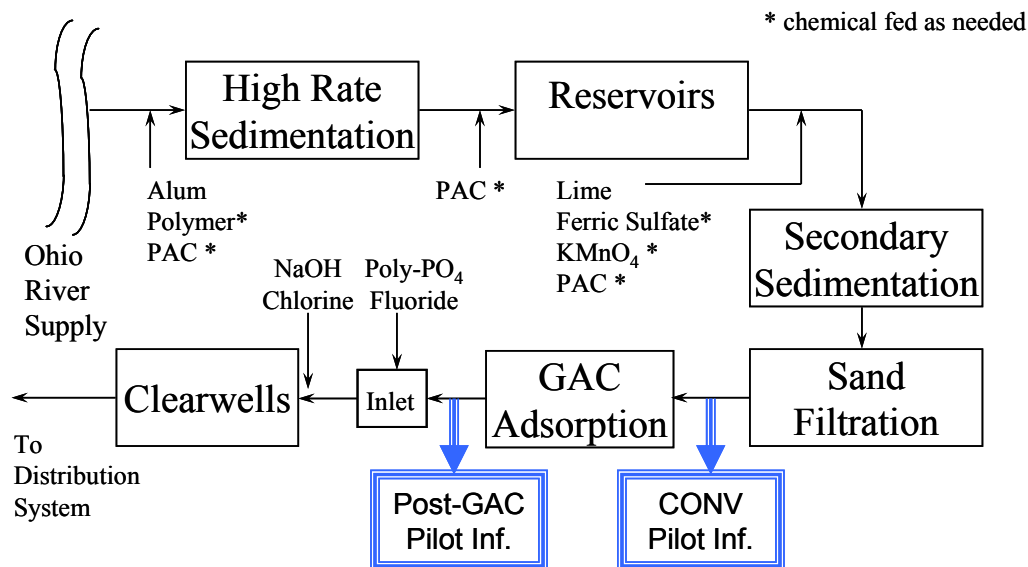
Figure 6-1 Schematic of the Richard Miller Treatment Plant

This surface water plant drew water from the Ohio River at mile point 462.8. An average of 12.7 mg/L alum was added to the water prior to primary settling. A cationic polymer was added at an average of 1.2 mg/L to improve sedimentation and filtration. The water was then flocculated and settled in lamella plate-pack settlers with a design detention time of 36 minutes. This process removed approximately 80 to 90 percent of the turbidity. The water then passed through two settling and storage reservoirs of 1,423,000 m^3 (376 MG) combined capacity. These structures were originally the primary settling facilities, but now polish sedimentation and provide storage, which is especially useful during a spill event. Spills occur frequently on this industrially impacted river, and these structures provide enough storage capacity to by-pass the raw intake for 2 to 3 days. Water leaving these structures has an average turbidity of 2 NTU. Iron sulfate (averaging 1.3 mg/L) was added intermittently. The water for this study was then filtered at a rate of 946 m^3/h (6 MGD) through rapid sand filters containing 61-76.2 cm (24 - 30 in.) of sand at a rate of 7.3 m/h (3.0 gpm/ft^2). This water was drawn as one of the two pilot influent process streams (CONV process stream).

Water exiting the filters was sent to the granular activated carbon (GAC) facility. The GAC contactors were filled with 3.5 m (11.4 ft) of carbon and were operated in a down-flow, gravity mode. Carbon contact time is 15 minutes at design flow, but typically averaged about 20 minutes during the study. The GAC removes a broad spectrum of organic compounds generally occurring on the industrial Ohio River. Water entering the GAC facility has a TOC averaging 1.86 mg/L; water exiting the facility has a relatively low TOC averaging 0.89 mg/L. The GAC facility also served to significantly reduce disinfection byproduct precursors and biodegradable activated carbon. Turbidity was further reduced through the GAC. Turbidity in the finished product averaged 0.06 NTU with a maximum of 0.10 NTU.

After becoming exhausted (average combine effluent of 150 days, maximum 200) the GAC is thermally reactivated in the presence of steam and very low oxygen. The reactivation is accomplished on site in one of two multiple hearth furnaces. GAC losses during reactivation were approximately 7.5 percent. Make-up GAC was added to achieve the 3.5 m (11.4 ft) GAC bed. This carbon treated water was drawn as the second of the two pilot influent process streams (Post-GAC process stream).

After GAC adsorption, the water was chlorinated for disinfection (Ave. 1.6 mg/L), pH adjusted by the addition of sodium hydroxide (Ave. 7.8 mg/L), fluoridated (Ave. 0.7 mg/L) and sodium hexametaphosphate (Ave. 0.35 mg/L) was added to reduce deposition. It then flows into a baffled clearwell which gives ample detention time to achieve microbiological inactivation.

Table 6-1 presents the pertinent water quality data for the two pilot influent streams. The CONV pilot influent stream is more variable than the Post-GAC pilot influent stream. Temperature, alkalinity and anions do not change through the GAC adsorption process.

Table 6-1 Water quality of CONV and Post-GAC water at RMTP

Water Quality Parameter	September 2007 - August 2008					
	CONV			Post-GAC		
	Average	Minimum	Maximum	Average	Minimum	Maximum
pH	7.8	7.2	8.8	7.7	7.3	8.3
TOC (mg/L)	1.86	1.22	2.64	0.89	0.37	1.35
UV254	0.046	0.024	0.086	0.016	0.01	0.035
Total Alkalinity (mg/L as CaCO$_3$)	64.3	49	82			
Total Dissolved Solids (mg/L)	245.3	138	404			
Sodium (mg/L)	25.2	14.6	42.8	25.9	14.9	42.9
Chloride (mg/L)				27.3	22.1	32.4
Fluoride (mg/L)				0.18	0.11	0.3
Nitrate (mg/L)				0.92	0.82	1.01
Sulfate (mg/L)				58.7	58.4	59
Temperature	16.3	4.5	28.4			

6.3.2 Pilot plant design

GCWW's pilot plant consisted of a constant head tank, the peroxide and contaminant feed systems, the UV reactors, the GAC column skids, and the annular reactors. Figure 6-2 shows the layout of the pilot including the location of the chemical injection and sampling points.

CONV or Post GAC water was pumped by 1.5 HP iron-cast centrifugal pumps into the 600 L (160 gal) polyethylene constant head tank. The constant head tank was located about 6 m (20 ft) above the UV reactors to provide sufficient head for the water flow through the unit. The total water flow was measured by a magnetic flow meter located in the main line before the first injection point. At the end of the main line the water flow split into two lines and after a flow control valve and a magnetic flow meter, it entered each of the UV reactors.

The contaminant solution and the 8% hydrogen peroxide solution were injected into two PVC online injection mixers located 0.9 m (3 ft) apart in the main line to ensure complete mixing. The contaminant solution was pumped from a polypropylene 19 or 115 L (5 gal or 30 gal) tank through a diaphragm pump into the online mixer. The hydrogen peroxide was purchased at 35% (FMC Oxypure) in 210 L (55 gal) drums, and it was diluted down to 8% on a regular basis into 115 and 230 L (30 and 60 gal) day tanks. It was fed constantly in the second mixer through a positive displacement pump. A 2 μg/L atrazine concentration and a 10 mg/L H$_2$O$_2$ concentration were targeted.

The medium pressure (MP) reactor was purchased from Aquionics (Hanovia model Photon II TOC reduction range; Figure 6-3a), and consisted of one MP lamp oriented parallel to the flow, and could be operated at 4 power levels ranging from 75 to 100% of the power. The reactor's internal diameter was about 15 cm and its chamber length was approximately 97 cm. The 3.5 kW MP lamp and sleeve were Super TOC models from Aquionics with an expected lifetime for the lamp of 8,000 hours. The reactor also included an immersed pre-calibrated UV monitor (Hanovia) sensitive to UVC wavelengths, and a manual rubber wiper. A digital display on the power supply box indicated the UV intensity, UV dose, run hours, and temperature, and allowed for flow and UVT input for the computation of the UV dose. The flow range through the reactor could vary between 1.8 to 10 m³/h (8 and 44 gpm).

The low pressure (LP) reactor was also purchased from Aquionics (Hanovia model ALT320 TOC reduction range; Figure 6-3 b), and consisted of eight LP lamps oriented parallel to the central axis and placed equidistantly at about a 11 cm radius from that axis. The reactor's diameter was about 31 cm and its chamber length was approximately 97 cm. The 80 W LP lamps and sleeves were standard disinfection models from Aquionics with an expected lifetime for the lamps of 12,000 hours. The reactor also included an immersed pre-calibrated UV monitor (Hanovia) sensitive to UVC wavelengths, and no wipers. A display on the power supply box indicated the UV intensity, run hours, and on/off lamps. The flow range through the reactor could vary between 1.8 to 10 m^3/hr (8 and 44 gpm).

The effluent from both UV reactors, as well as pilot influent water before the hydrogen peroxide injection point were pumped to four GAC pilot columns. The two GAC columns fed by the influent water before the addition of peroxide, and after the injection of contaminants, were the control columns. Each of the remaining two columns received the effluent of the MP reactor or the effluent of the LP reactor. The GAC in the later two columns and one of the control columns was reactivated GAC acquired directly from the reactivation facility at Richard Miller Treatment Plant (RMTP). The second control column included GAC produced by an alternative regeneration process. The GAC was bituminous coal, US mesh size 12x40 with 0.55-0.75 mm effective size, and apparent density of 0.48 g/cm^3 (30 lbs/ft^3) The GAC bed depth in the 10.2 cm (4 inch) diameter columns was about 173 cm (68 inches), and the empty bed contact time (EBCT) was set to 15 minutes to simulate RMTP full-scale GAC contactor operation. The GAC column skids also included clearwells and a backwash system.

The last pieces of equipment in the pilot process line were four annular reactors (Biosurface Technologies, model 1120 LS; Figure 6-4), which were connected to the effluent lines of the GAC columns, Figure 6-2. The annular reactors were chosen to simulate a velocity of a typical water distribution main and are described further in the analytical methodologies section.
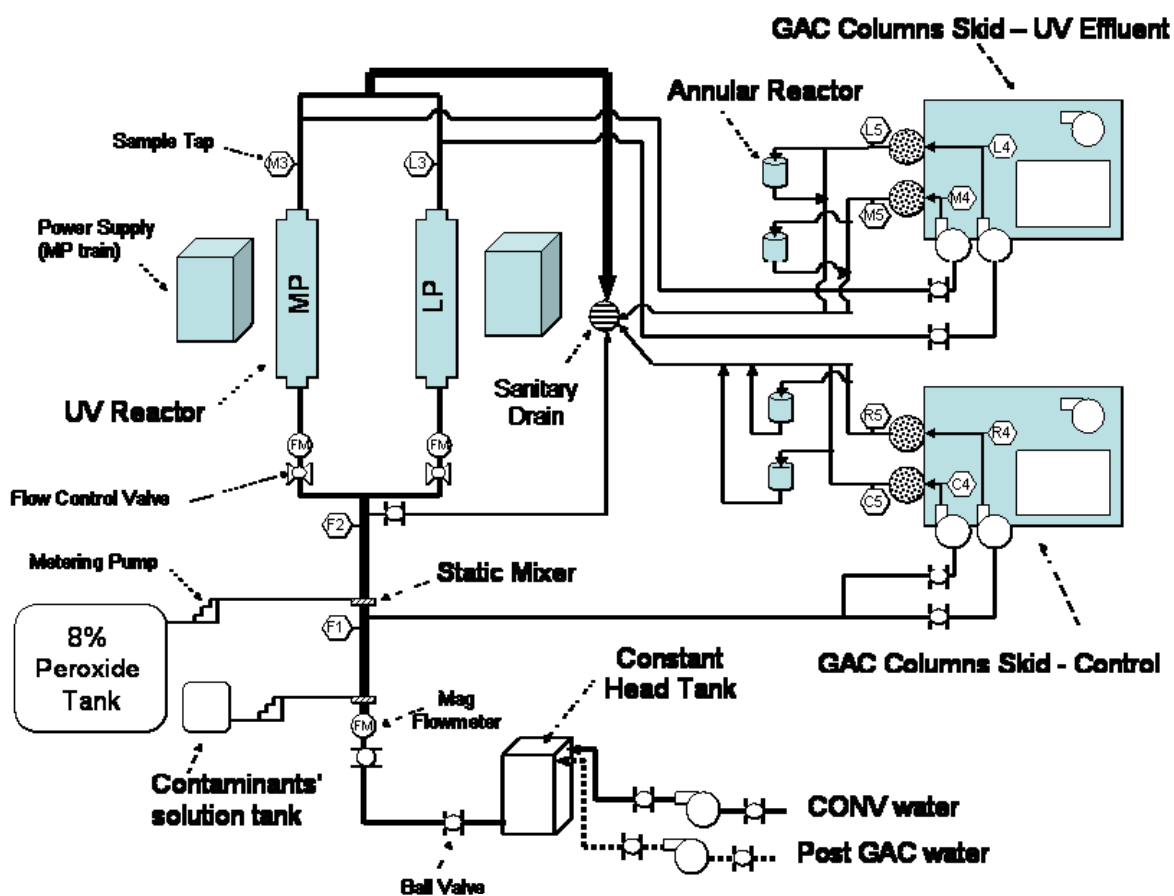
Figure 6-2 Pilot plant schematic at GCWW

(a)

(b)

(c)
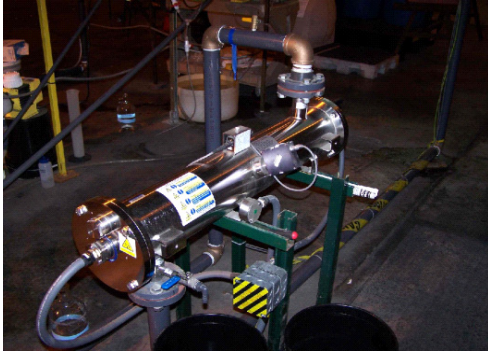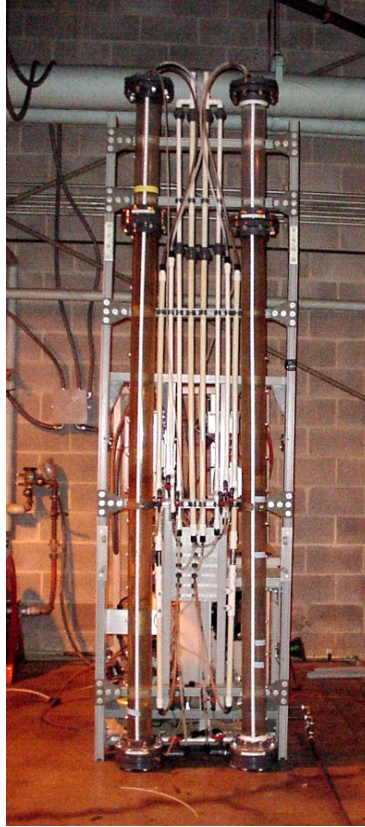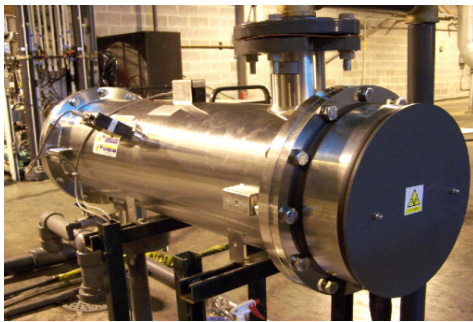
Figure 6-3 UV pilot equipment at GCWW (a) MP Reactor, (b) LP reactor, (c) GAC pilot contactors

Figure 6-4 Annular reactor for biofilm tests

6.3.3 Pilot plant operation

The pilot study was structured in a way that would address the multiple research objectives within a period of 12 months. In order to capture the seasonal variations of the influent water quality, the selected contaminants were spiked quarterly, and the same parameters were consistently monitored. The pilot unit was constructed in the summer of 2007 and the tests began in the fall of 2007. Figure 6-5 shows the process schematic of the pilot unit with the sampling points.

The pilot unit was operated continuously for twelve consecutive months. During each quarter there were three phases of testing: (a) UV advanced oxidation with CONV influent water, (b) UV advanced oxidation with Post-GAC influent water, and (c) UV photolysis with Post-GAC influent water. For both UV advanced oxidation phases the operation of the system was based on performance. The goal was to operate the advanced oxidation system so that atrazine would degrade by 80% through both the MP and LP reactor trains. The hydrogen peroxide concentration was maintained at 10 mg/L at all times (except during the UV photolysis testing) and the UV dose was adjusted by changing the flow through the reactors, and for the MP reactor by adjusting the power levels. Since the UVT_{254} and TOC concentration of the water varied seasonally, tests were performed at the beginning of each phase using atrazine to determine the operational conditions of the UV reactors. An 80% atrazine degradation (or analogous MTBE degradation) was targeted for the UV/H_2O_2 phases to determine the operational conditions of the UV reactors. MTBE was also used during those tests until the relationship between the degradation of atrazine and MTBE was established[*], and then MTBE was used as a surrogate since its analysis was much easier and faster than atrazine's. Once the flow and power level were determined for both reactors, the solution of contaminants was spiked into the pilot influent to determine the degradation of all the contaminants at those conditions. The above method was followed with both CONV and Post-GAC pilot influent. Following the Post GAC advanced oxidation phase, the hydrogen peroxide feed was discontinued, the UV dose at the reactors was set at the lowest level and the contaminant spiking was repeated. When the three phases were completed, the pilot influent was switched to CONV water and the reactors and flows were set at the 80% atrazine degradation conditions until the next quarter began.

[*] It was found that the about 60-65% of MTBE is converted under conditions that will result in about 80% atrazine conversion.

Every time that the water in the pilot was switched, the cast iron pump for either the CONV or Post-GAC water was primed to avoid potential fouling of the sleeves. The sleeve in the MP reactor was wiped on a daily basis with the manual rubber wiper. At the beginning of each quarter the pilot was shut down to have the sleeves of both reactors cleaned. The reactors were drained and the sleeves were removed and cleaned with 0,1N HCl solution and finally rinsed. Before the sleeves were placed back, the inside of the reactors was wiped and the UV sensors were removed and wiped with isopropyl alcohol. The GAC columns were backwashed on a regular basis, about once per week, except during the spring season where they required more frequent backwashing due to air-binding.

During the 12 month study several water quality, operational and performance parameters were monitored at the pilot, as shown in Table 6-2. The pilot was monitored on a daily basis for flows, UV reactor intensity and applied UV dose. The UVT of the pilot influent was monitored and the hydrogen peroxide concentration was determined before and after the reactors and after the GAC contactors. Additionally several other water quality parameters, such as TOC, alkalinity, nitrate and nitrite were tested at various frequencies across the pilot. The analytical methods for these tests are also shown in Table 6-2.
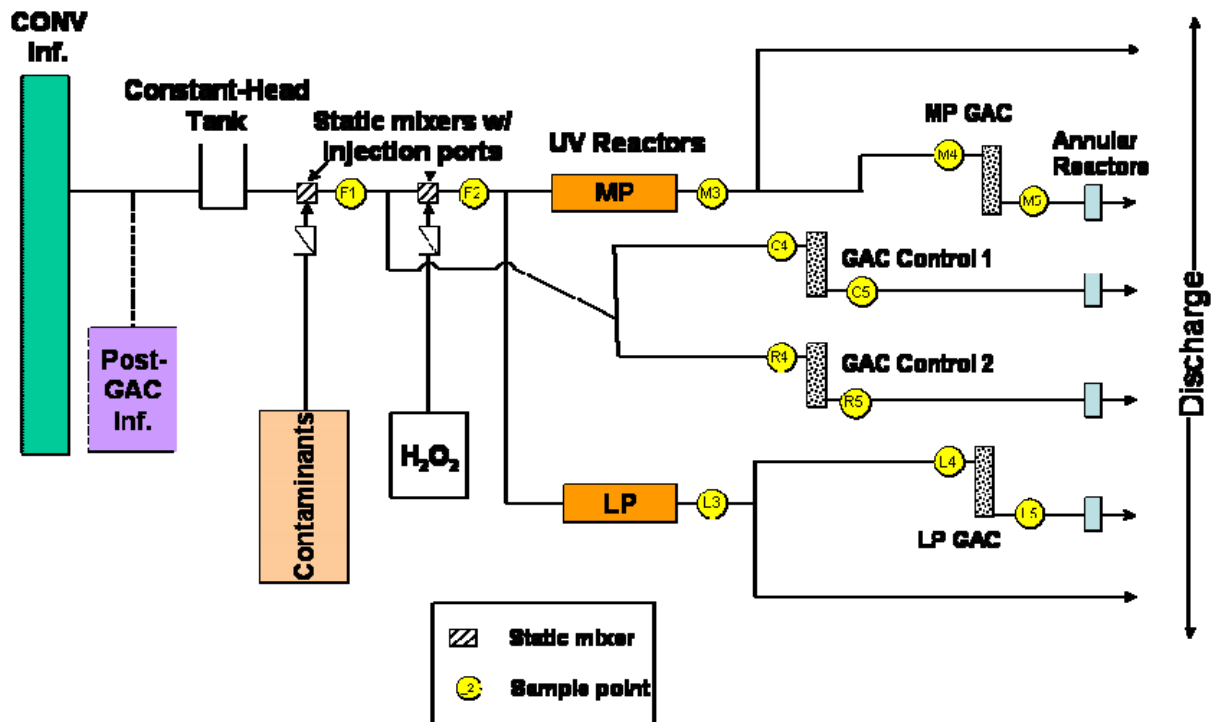
Figure 6-5 Pilot plant process schematic at GCWW

Table 6-2 Water quality sampling protocol and pilot performance monitoring

Parameter	Sampling/monitoring frequency	Method
Operational/Performance		
Hydrogen peroxide[2]	Once per day	
Flows	Three times per day	
Reactor UV intensity	Three times per day	
UV dose (MP)	Three times per day	
Lamps on/off & run hours	Three times per day	
Water Quality		
UVT	Once per day	St. M.[1] 5910
pH/Temperature	Once per day	St. M. 4500-H
TOC	Twice per week	St. M. 5310C
Alkalinity	Once per week	St. M. 2320
UV scan 200-300nm	Once per week	St. M. 5910
Nitrate	Once per week	USEPA 300
Nitrite	Once per week	USEPA 300
Iron	Once per week	Hach 8008
AOC	Three times per quarter	St. M. 9217B

1. AWWA *Standard Methods for Examination of Water and Wastewater*.
2. The methods for hydrogen peroxide measurement are described in the Materials and Analytical Methodologies section.

6.3.4 Materials and analytical methodologies

Several contaminants of interest were reviewed by GCWW to be used in this study, and the factors considered for their selection were:

- Past detection in RMTP's source water (Ohio River) and removal by existing treatment processes.
- Representation of most major emerging contaminant groups.
- The chemical formulas, bonds and structure of the compounds.
- The degree of degradation by UV advanced oxidation based on the results from the collimated beam tests performed by KWR.
- The potential for destruction by photolysis.
- Analytical capability by GCWW and KWR.
- Cost and availability of the compounds.

The contaminants selected for spiking were atrazine, metolachlor, methyl-tetra-butylether (MTBE), methylisoborneol (MIB), ibuprofen, gemfibrozil, and 17-α-ethynylestradiol. Their structures and constants related to advanced oxidation and adsorption are shown in Table 6-3. The constant k_{OH} is the second order reaction rate constant between the compound and hydroxyl radicals, while K_{ow} is the octanol-water partition coefficient. K_{ow} is defined as the ratio of the concentration of a chemical in octanol and in water, and it has been correlated to the water solubility of the chemical.

Table 6-3 Selected contaminants for pilot spiking at GCWW

Compound	Structure	Major Groups	k_{OH} $(M^{-1}s^{-1})$	$\log K_{ow}$
Atrazine		Triazine ring, secondary amines	$2.6 \cdot 10^9$ (1)	2.61 (2)
Metolachlor		Aromatic ring, amide, methoxy, chlorine	$6.9 \cdot 10^9$ (3)	3.13 (4)
MTBE		Ether	$1.6 \cdot 10^9$ (5)	1.20 (6)
MIB		alcohol	$8.2 \cdot 10^9$ (7)	3.1 (8)
Ibuprofen		Aromatic ring, carboxylic acid		3.97 (9)
Gemfibrozil		Aromatic ring, carboxylic acid, ether	$10 \cdot 10^9$ (10)	4.77 (11)
17-α-ethynylestradiol		Phenol, ethynyl, aliphatic rings, alcohol	$1.08 \cdot 10^{10}$ (12)	3.67 (13)

(1) Haag, 1992
(2) (4) (9) (11) (13) Snyder *et al.*, 2007
(3) Changlong *et al.*, 2007
(5) (6) Kavanaugh *et al.*, 2003
(7) Glaze at al, 1990
(8) Westerhoff *et al.*, 2005 a
(10) Razavi *et al.*, 2009
(12) Rosenfeldt and Linden, 2004

The contaminants were purchased in pure form with the exception of MIB which was purchased dissolved in DI water. The contaminant stock solution was made by initially hydrating the powder contaminants with RO water, adding metolachlor and MTBE, followed by 24 hour mixing in RO water in dark. The solution was then vacuum filtered using 0.45 μm membrane, and finally the MIB solution was added and mixed in the stock solution. The stock solutions were prepared right before the spiking events

to avoid degradation of the contaminants. Table 6-4 shows the spiking level of each contaminant at the pilot unit and the analytical methods used for their detection.

Table 6-4 Origin and spiking level of contaminants at GCWW's pilot unit.

Compound	Manufacturer	Purchased form	Spiking level	Analytical method	MDL
Atrazine	Supelco	Powder 98% pure	2 µg/L	USEPA 525.2	0.1 µg/L
Metolachlor	Supelco	Liquid 99.5% pure	2 µg/L	USEPA 525.2	0.1 µg/L
MTBE	Supelco	1000mg ampule	4 µg/L	USEPA 524.2	0.2 µg/L
MIB	Arizona State University	DI Solution 40mg/L	40 ng/L	AWWA 6040D	2 ng/L
Ibuprofen	Sigma Aldrich	Powder 98% pure	10 µg/L	KWR LOA-602	0.5 µg/L
Gemfibrozil	Sigma Aldrich	Powder 99% pure	2 µg/L	KWR LOA-602	0.1 µg/L
17-α-ethynylestradiol	Sigma Aldrich	Powder 98% pure	100 ng/L	KWR LOA-539	5 ng/L

The contaminant samples were collected in triplicates in either glass or polypropylene bottles and vials using 0.4 g sodium sulfite to quench the residual hydrogen peroxide. Atrazine, metolachlor, MTBE and MIB were analyzed at the RMTP plant, while the samples with ibuprofen, gemfibrozil, and 17-α-ethynylestradiol were frozen and sent to KWR in the Netherlands for analyses.

The hydrogen peroxide used at the pilot unit was 35% Oxypure Grade from FMC. It was diluted to 8% with RO water in day tanks, and its exact concentration was measured by permanganate titration. According to this method about 10 mL of the 8% hydrogen peroxide was weighted and then washed into a 250 mL volumetric flask with RO water and mixed thoroughly. Twenty-five milliliters were transferred in a 400 mL beaker containing 250 mL RO water and 10 mL sulfuric acid, and it was titrated to a permanent pink color with 0.3N potassium permanganate.

Hydrogen peroxide was dosed at 10 mg/L at the pilot influent and samples from all pilot locations were measured daily. The method used initially was iodometric titration with a hydrogen peroxide test kit (model HYP-1) by Hach, and it was replaced during the second quarter of testing with a spectophotometric analysis provided by KWR method LAM-048. According to this method either 5 or 10 mL of the water sample (depending on expected H_2O_2 concentration) was transferred to 100 mL flask, followed by 8 mL of 1.8 M sulfuric acid and 2 mL of Potassium bis(oxalate)oxotitanate(IV) dehydrate ($K_2[TiO(C_2O_4)_2]\cdot2H_2O$), and then the flask was filled with RO water and mixed. After 15 minutes the sample was transferred to a 5 cm cell and analyzed using a spectrophotometer at 400 nm. The measurement was converted to H_2O_2 concentration based on a calibration curve.

6.3.5 Biofilm Methodologies

Annular reactors were used to assess biofilm potential after GAC adsorption in unchlorinated process streams. Four model 1320LS Laboratory Annular Reactors from BioSurface Technologies Corp. received flow from the effluent of the four GAC columns. The experiment ran during one month (from September 4, 2008 to October 2, 2008), which corresponded to run-day 300 to 328 of the GAC. Before being placed in service, the reactors were disassembled and thoroughly cleaned, and then the polycarbonate coupons were inserted into the designated slots in the carousels. The annular reactors were reassembled without the motors and placed in plastic bags suitable for autoclaving. A second autoclave resistant bag was used to hold the plastic tubing for autoclaving. The components were

moistened with deionized water, the bags sealed and autoclaved for 15 minutes at 1.034 bars (15 psi) at a temperature of 120°C. The sterilized units were reassembled on site with motors and controllers and set to a flow rate of 8 mL/minute and a carousel rotational speed of 90 revolutions per minute. These conditions simulated a pipe velocity of 0.30 m/sec (1 foot/second). A stop watch was used to time the revolutions, and the rotational speed was adjusted accordingly. The flow was similarly monitored and adjusted. The units were covered with tall cardboard boxes and dark tubing was utilized to minimize algal growth. The flows and rotational speed were checked bi-weekly.

The biofilm was quantified by heterotrophic plate count and ATP bioluminescence analysis. At the end of the annular reactor run, before removing the coupons, the working surfaces and annular reactor sampling port were disinfected. A hemostat was disinfected by soaking in alcohol and inserting it into the 815°C commercially available infrared heating device (Bacti-Cinerator II). An unused sterile coupon was then placed in a sterile test tube using the hemostat. The lid was left off of the tube for about a minute before capping tightly. This coupon served as the blank. Next, the hemostat was again sterilized and used to extract a sample coupon from the annular reactor. This coupon was placed in a sterile test tube and the test tube capped. This process was repeated for all the coupons in the reactor. The working surfaces were cleaned and disinfected and the process repeated for the remaining three annular reactors. A final blank coupon was then collected in the same fashion as the initial blank coupon.

The biofilm from six coupons per reactor were analyzed by heterotrophic plate count (HPC) analysis. A sterile, disposable cell scraper with a flexible blade was used to remove biofilm from the polycarbonate coupons. The blade was as wide as the coupon, so a single pass with either side of the blade was made. The blade portion of the scraper was removed next and added to a sterile centrifuge tube. The coupon was then rinsed with 1 mL of sterile phosphate buffered water, collected in the centrifuge tube with the scraper. The centrifuge tubes were all initially vortex mixed for 60 seconds and sonicated for 5 minutes to break up and homogenize the biofilm. Another 30 second mixing was performed just prior to removing a 0,1 mL aliquot of the solution. This aliquot was used to make dilutions of 0.01, 0.001, and 0.0001 mL for heterotrophic plate count analysis. All dilutions were plated out using a 0.1 mL sample dilution volume and the pour plate technique, in the hopes of finding one countable plate per coupon. (Standard Methods 9215 B).

The biofilm was removed from 12 coupons per reactor - 48 coupons total for the bioluminescence procedure. The blank coupon was processed first. The sterilized hemostat was used to raise and secure the coupon, leaving only the bottom 1 centimeter of the coupon still within the tube for support. The cap of the Utrasnap bioluminescence pen was removed and the swab withdrawn using sterile technique. The exposed surface of the coupon was wiped in thirds from left to right, top to bottom using three firm and consistent strokes. The swab was rotated to an unused section after each stroke. The swab was then returned to the bioluminescence tube and recapped, and the tube labeled. The hemostat was again sterilized and the process repeated for each coupon.

Bioluminescence was measured using a Hygiena System SURE Plus luminometer. Luminometer performance was monitored by analysis of two standard rods with known assigned values. Analysis of these standard rods occurred at the beginning and end of the luminometer analysis. Three readings were taken of each standard. The readings had to be within 20% of each other, and the average value had to be within 20% of the assigned value of the rods, for acceptable QC. Coupon samples were processed by removing the swab from the pen, carefully wiping the entire upper surface of each coupon as described above, then returning the swab into the pen. The pen was later activated by breaking the internal snap valve in the top bulb, and bending the pen bulb back and forth, squeezing twice. The swab tip was bathed in the expelled reagent by gently shaking the test pen for five seconds. The test pen was wiped with a laboratory tissue and inserted into the luminometer and the top was closed. Triplicate readings were taken after a 15 second stabilization period, and an average reading calculated. The process was repeated with each sample, with all samples being analyzed within one minute of activation.

6.4 Results and discussion

6.4.1 Background Water /Operational

The pilot unit was in continuous operation from October of 2007 until October 2008. During that period the pilot influent water showed seasonal variations or changes in water quality due to natural surface water fluctuations and the upstream treatment processes. The influent water quality parameters potentially affecting the performance of the UV advanced oxidation process were UVT, TOC concentration, alkalinity and iron concentration. Influent UVT and TOC concentration were expected to fluctuate during the year especially for the CONV pilot influent water, which was used most of the time during the pilot study.

The changes in UVT for the CONV and the Post GAC water can be seen in Figure 6-6. The CONV water UVT ranged between 84 and 95%/cm, with its lowest points being in December 2007 and the summer of 2008. The UVT of the Post-GAC water was more stable and fluctuated only between 95-98%/cm. The variation in UVT greatly affected the operation of the UV reactors and changes in flow and power level were required in order to achieve the required 80% atrazine degradation.
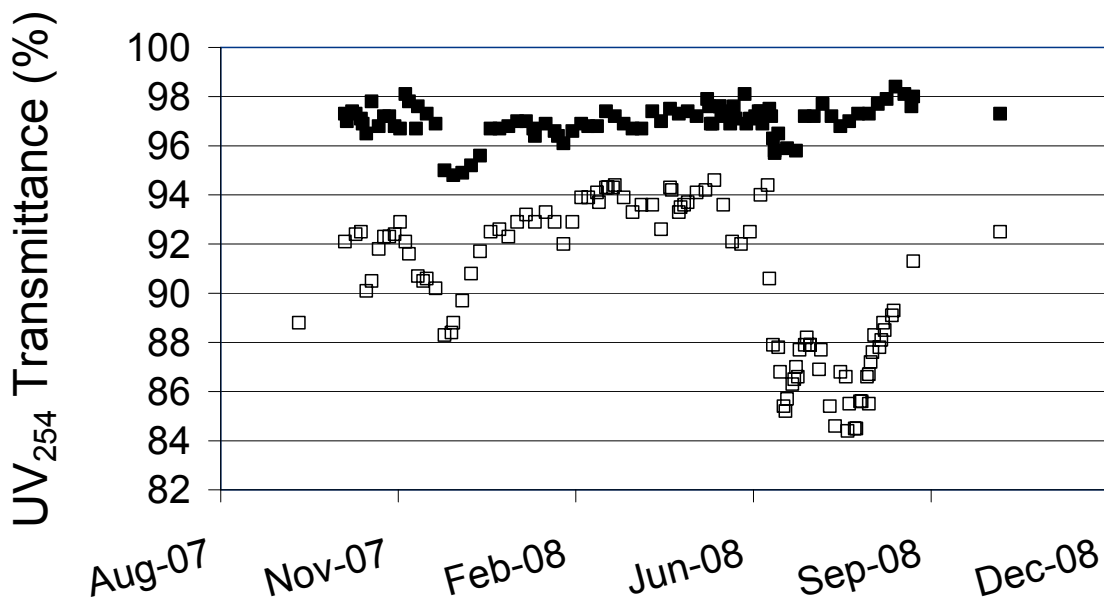
Figure 6-6 UV Transmittance of CONV and Post GAC water during pilot study. (■) Post-GAC Pilot Influent, (□) CONV Pilot Influent

The TOC concentration of the pilot influent water also changed during the 12 month study, fluctuating between 1.2-2.6 mg/L for the CONV water and 0.6-1.0 mg/L for the Post-GAC water. Figure 6-7 and Figure 6-8 show the influent TOC concentration of the pilot versus the TOC values at the effluent of each reactor. On average a slight 2-3% decrease in TOC concentration was observed through both reactors when CONV was the pilot influent water, while when Post-GAC influent water was used the decrease in TOC concentration through the reactors was on average 4-7%. This consistent small decrease of TOC through the UV reactors can be explained by the mineralization of natural organic matter (NOM) by the hydroxyl radicals formed in the reactors. Due to their redox potential of 2.8V, hydroxyl radicals have the potential of completely oxidizing organic molecules to carbon dioxide (Carr and Baird, 2000). Research has shown that under advanced oxidation conditions similar to the ones applied in this study, NOM was not mineralized but partially oxidized resulting in a shift of the NOM's molecular weight distribution towards smaller organic molecules. However, when prior treatment processes remove higher molecular

weight fractions of NOM as indicated by the drop in SUVA values, then UV/H_2O_2 at similar conditions used in this study may cause mineralization of NOM (Sarathy and Mohseni, 2007 and 2009). The CONV pilot influent water had already been processed by coagulation, flocculation and filtration which removed part of the TOC found in the river water, while the Post GAC had an additional removal of TOC due to adsorption. The reduction in SUVA values between the river, CONV, and Post-GAC water is very likely the reason that some mineralization of TOC was observed through the UV reactors during the UV/H_2O_2 process.
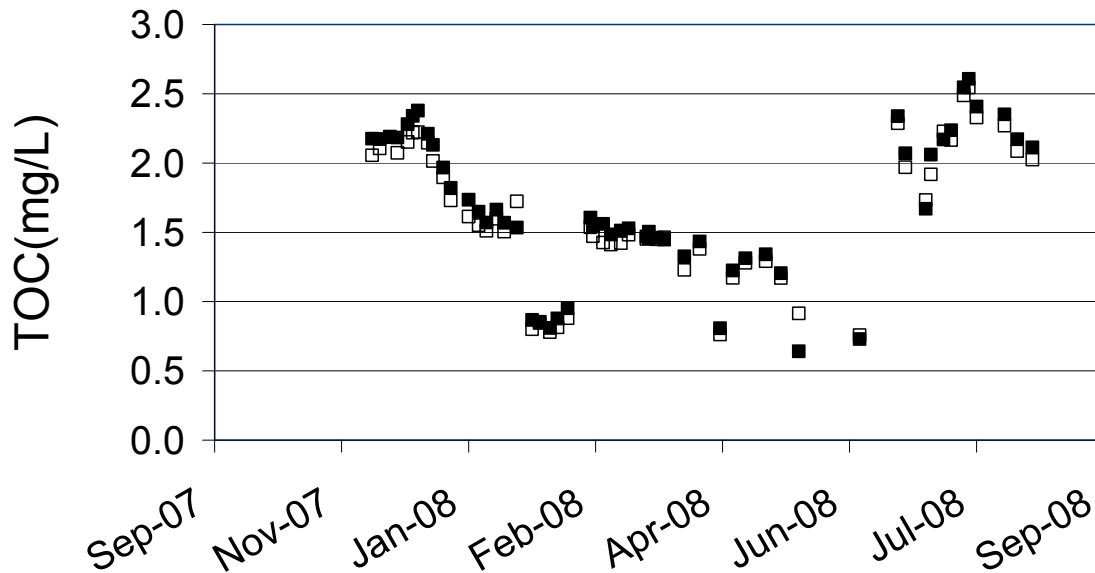
Figure 6-7 TOC through the MP Reactor. (■) TOC Influent, (□) TOC Effluent
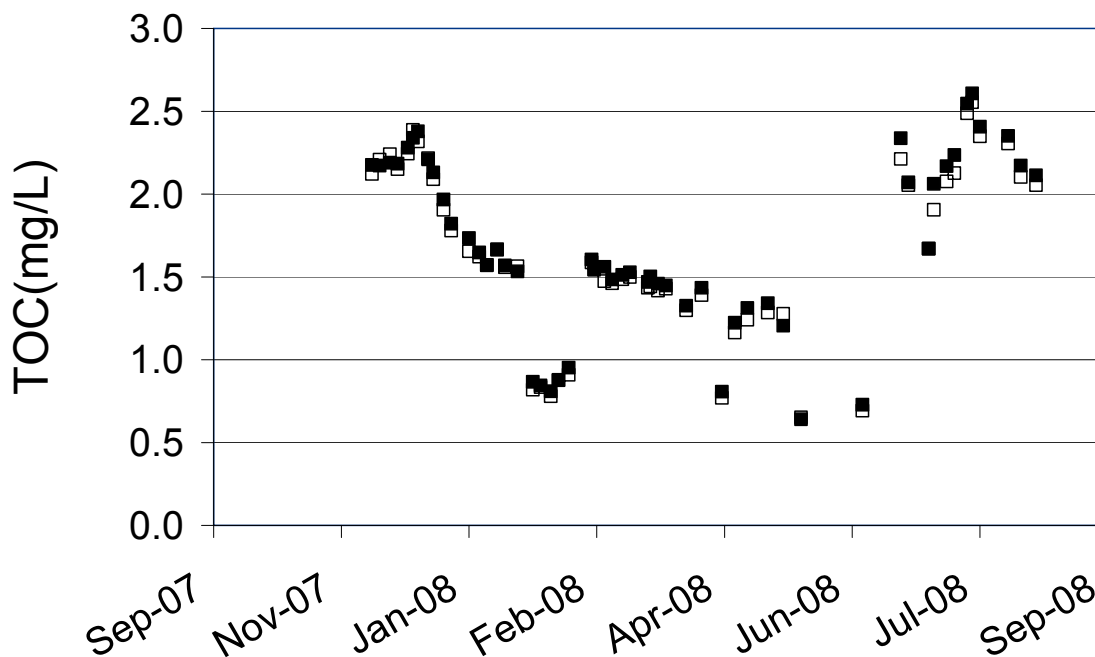
Figure 6-8 TOC through the LP Reactor. (■) TOC Influent, (□) TOC Effluent

Figure 6-9 represents TOC concentration through the pilot plant, including the effluent of the GAC pilot columns when CONV water was used as the pilot influent. The top three curves depict CONV influent TOC concentration and the two UV/H₂O₂ reactor effluent TOC values. The bottom four curves represent TOC concentrations for the GAC column effluent streams from the LP and MP reactor process trains and the two control GAC columns. Typical breakthrough curves were observed for all four GAC pilot column effluent streams. TOC concentration in the GAC effluent streams ranged from 0.2 to 1.6 mg/L over the study period. At the beginning of the GAC pilot column runs, there was excellent TOC removal, and over the first 140 to 150 days as the GAC became loaded with organics, the effluent TOC concentration exhibited a rising trend, even though the influent TOC concentration was declining. Steady-state was reached between 140 to 160 days. After this point, the GAC effluent TOC concentrations reflect the increases and decreases of the TOC concentration in the GAC influent. However, some removal was observed through all GAC columns during the study period. By run day 220 there was a clear separation in the TOC concentrations of the GAC effluent streams that had received UV/H₂O₂ pretreatment and those that had not (Figure 6-10). Overall, the GAC effluent following the UV/H₂O₂ reactors resulted in 8% less TOC concentration than the control GAC effluent streams. After GAC run day 220, the GAC effluent following the UV/H₂O₂ reactors averaged 16% less TOC concentration than the GAC effluent of the control process streams. It should be noted that after GAC run day 220 the water temperature was the warmest (26 to 29°C), reflecting summer conditions (June 18, 2008 to August 27, 2008). It is therefore likely that enhanced TOC concentration removal was attributable to more bioactivity caused by the warmer temperatures and more assimilable materials loaded onto the GAC after UV/H₂O₂ treatment. When UV/H₂O₂ is employed, changes to the molecular structure of dissolved organic matter occur. Larger molecules are fragmented into smaller molecular weight compounds and a decrease in aromaticity results. Additionally, the ratio of hydrophilic to hydrophobic compounds increases (Sarathy, *et al.*, 2007 and 2009). Smaller molecules of a hydrophilic nature tend to be more assimilable by microorganisms and thus more biodegradable.
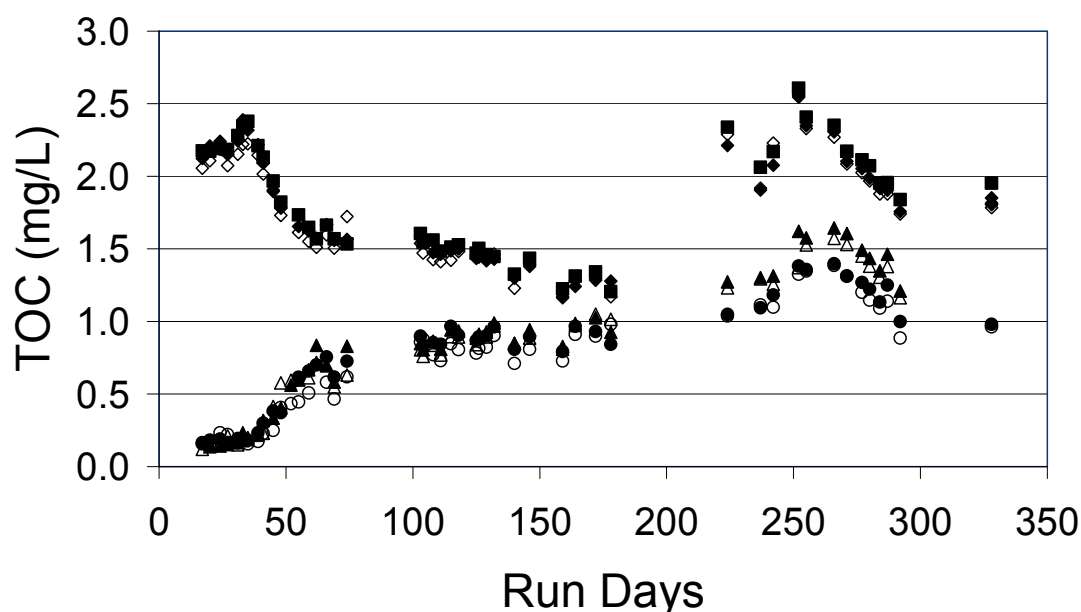
Figure 6-9 TOC through pilot-CONV Influent, (■) CONV Influent, (♦) Low-pressure reactor effluent, (◊) Medium-pressure reactor effluent, (▲) Control #1 GAC effluent , (△) Control #2 GAC effluent, (●) Low-pressure GAC effluent, (○) Medium-pressure GAC effluent
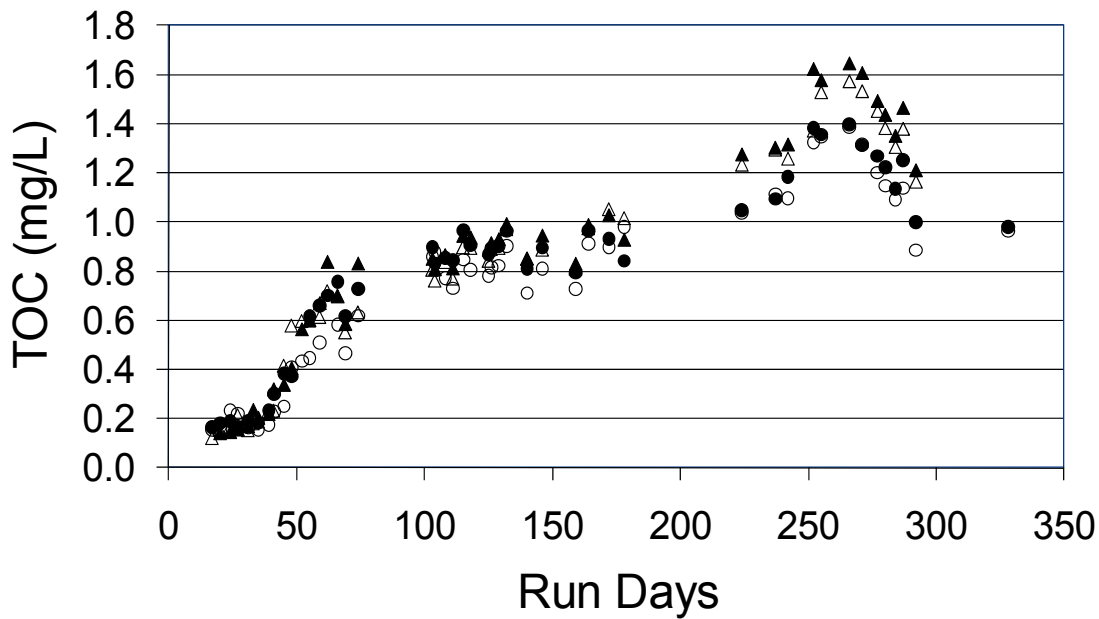
Figure 6-10 TOC breakthrough-GAC pilot columns, (▲) Control #1 GAC effluent, (Δ) Control #2 GAC effluent, (●) Low-pressure GAC effluent, (○) Medium-pressure GAC effluent

Alkalinity also exhibited seasonal variations as shown in Figure 6-11, and it varied between 49-82 mg/L for both CONV and Post-GAC water. Since alkalinity is also a scavenger of hydroxyl radicals, it was monitored for the influent and effluent of the UV reactors, but no significant or consistent changes were observed through the UV/H_2O_2 process. Iron was below the detection limit (20 µg/L) for the duration of the study.
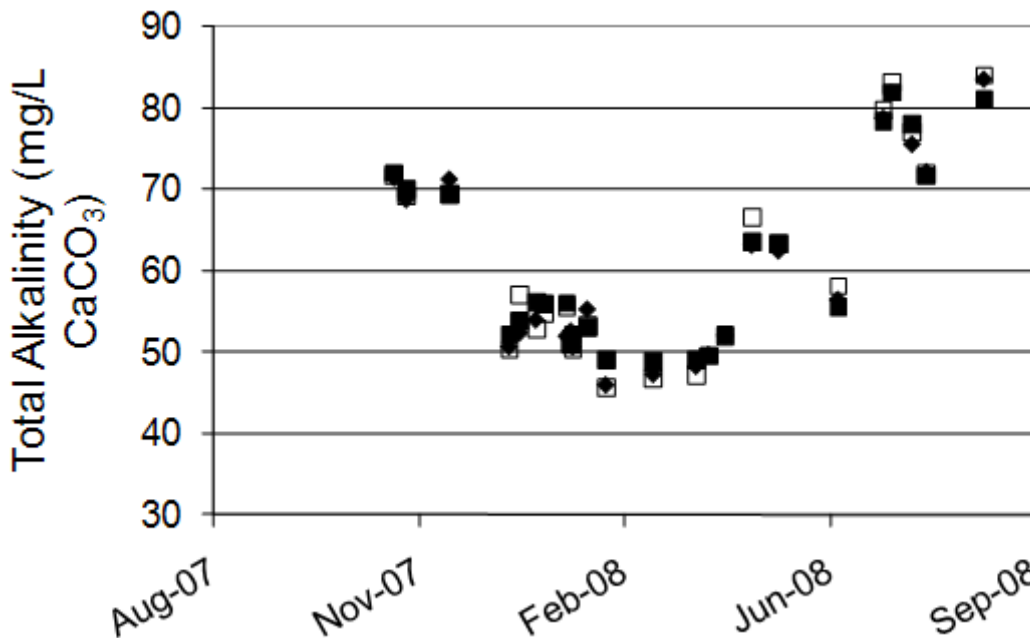
Figure 6-11 Alkalinity through UV Reactors. (■) Pilot Influent, (□) MP Effluent and (♦) LP

The pilot influent water contained low concentrations of nitrate, which varied seasonally between 0.5-1.3 mg/L (as nitrogen), and nitrite was below the limit of detection, as shown in Figure 6-12. About 10-

20% of the nitrate was converted to nitrite through the MP reactor, under the operating conditions of the system, as the lamp sleeves were not doped to eliminate this transformation. However, the nitrite concentrations were much lower than the U.S. regulated Maximum Contaminant Level (MCL) of 1 mg/L. Depending on influent nitrate concentration and the local regulations, unchlorinated systems may wish to use doped sleeves to reduce nitrate reduction. The sum of the nitrate and nitrite effluent concentrations exiting the MP reactor matched the reactor influent concentration of nitrate relatively well. This total nitrate-nitrite concentration also was below the U.S. regulated MCL of 10 mg/L as N. As expected there were no changes in the nitrate through the LP reactor and no formation of nitrite was observed as depicted in Figure 6-13.
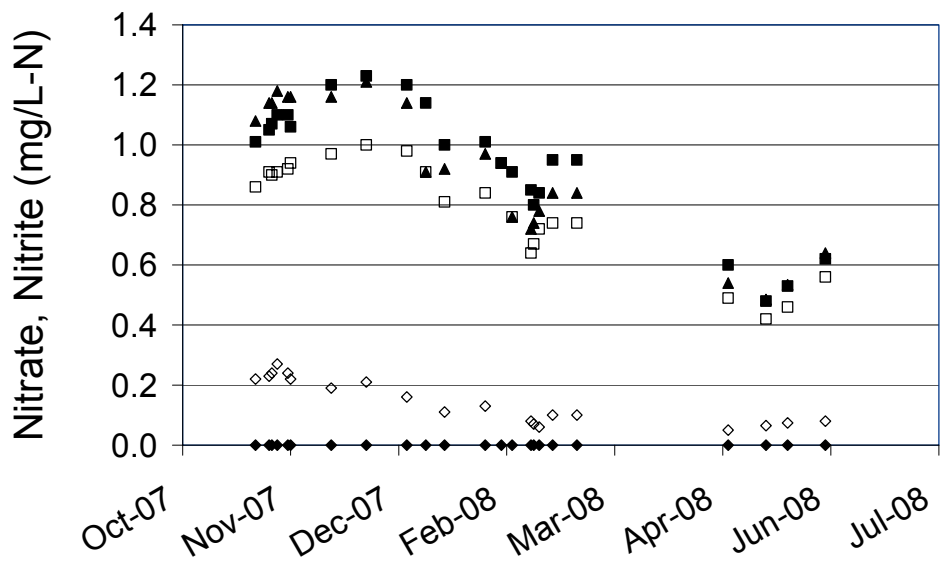
Figure 6-12 Nitrate-Nitrite Medium Pressure Reactor. (■) Nitrate Influent, (□) Nitrate Effluent, (♦) Nitrite Influent, (◊) Nitrite Effluent, (▲) Nitrate+Nitrite Effluent
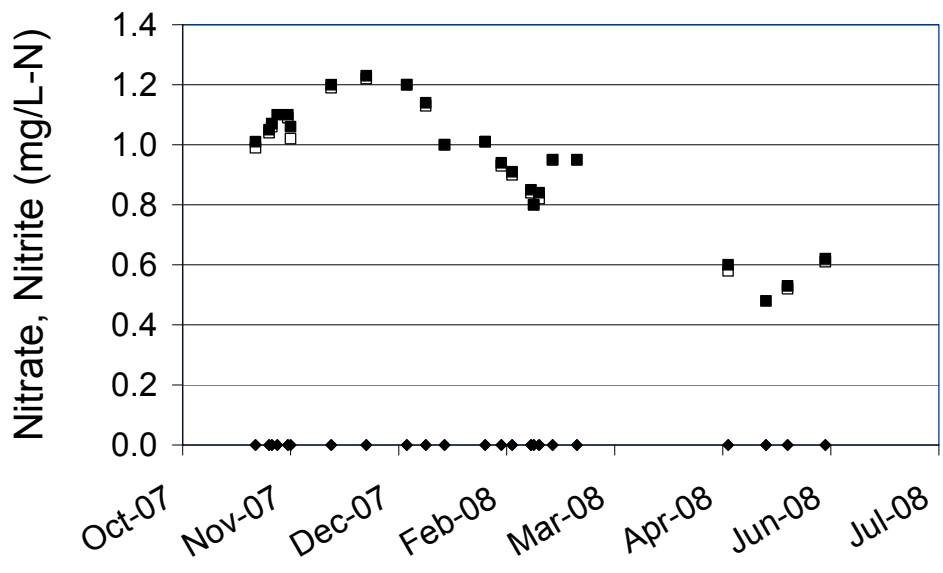
Figure 6-13 Nitrate-Nitrite Low Pressure Reactor. (■) Nitrate Influent, (□) Nitrate Effluent, (♦) Nitrite Influent, (◊) Nitrite Effluent

The influent and effluent hydrogen peroxide concentration of the UV reactors and GAC contactors was measured on a daily basis. The pilot influent peroxide averaged 10 mg/L (St.D. 0.5 mg/L), while the MP effluent had an average of 8.9 mg/L (STD = 0.5 mg/L), and the LP effluent 9.2 mg/L (STD = 0.6 mg/L).

Therefore, the hydrogen peroxide consumption was higher through the MP reactor than the LP reactor in order to achieve the same percentage of atrazine degradation. Hydrogen peroxide was never detected at the effluent of the GAC contactors, indicating that it was completely adsorbed/decomposed through the existing GAC beds. A side effect of the peroxide decomposition was the slow formation of gas in the GAC beds receiving the effluent of the UV reactors, which was more intense and visible during the spring months when the temperature of the influent water was rising, and the ambient temperature in the facility was higher.

The initial method used to analyze hydrogen peroxide through the pilot was an iodometric method, which gave accurate results for all sample points except for the effluent of the MP reactor and the effluent of the consecutive GAC contactor. The results of the MP effluent were 2-3 mg/L higher than the influent hydrogen peroxide, and the effluent of the GAC contactor showed a similar 3 mg/L breakthrough of hydrogen peroxide when this method was used. The analysts were not able to determine the cause of these anomalies, thus an alternative spectrophotometric method was developed (KWR, LAM-048). The spectrophotometric method was not subject to these errors and no new interferences were found.

6.4.2 Contaminant Degradation

UV/H$_2$O$_2$ with CONV pilot influent water

A primary operational goal of the pilot study was to consistently set the UV reactors at the proper UV dose that would achieve the benchmark 80% atrazine degradation. This became particularly challenging when CONV influent water was used, since the UVT of the water fluctuated significantly throughout the year, and different UV doses were required to keep the atrazine degradation constant. To achieve these conditions throughout the study, UV doses between 200-500 mJ/cm^2 were required for the MP reactor and doses between 1200-2000 mJ/cm^2 were required for the LP reactor (based on the manufacturer's UV dose tables). As shown in Figure 6-14, atrazine reduction was between 75-85% for most of the study quarters, with the only exception being the first quarter of the study when it was measured at 62% for the LP reactor. The reason for the low value the first quarter was likely iron fouling of the LP reactor sleeves because of an improperly primed pump. After the sleeves were cleaned the LP reactor could provide sufficient UV dose to reach the benchmark.
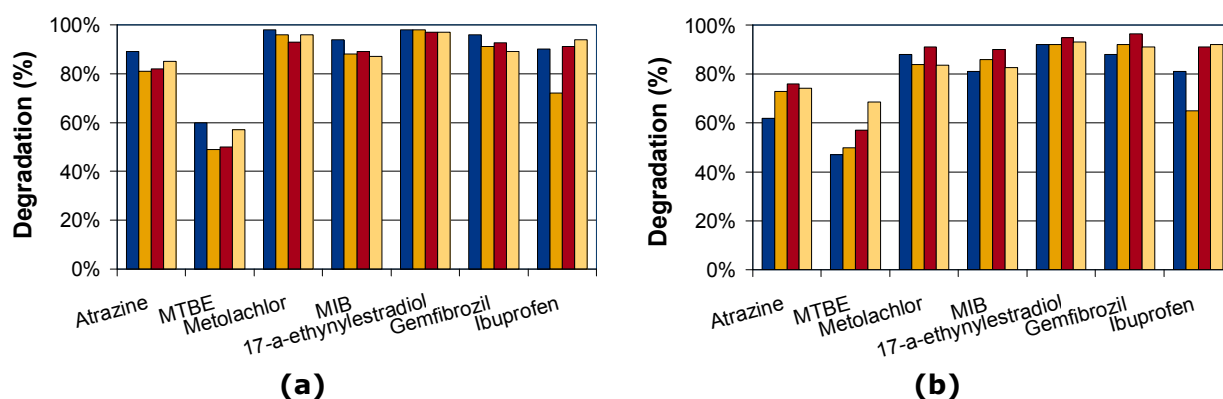
Figure 6-14 Contaminant degradation by UV/H$_2$O$_2$ in CONV water (a) MP Reactor, (b) LP reactor. (■) Fall 2007, (■) Winter 2008, (■) Spring 2008, (■) Summer 2008

With the exception of MTBE, the remaining six contaminants showed higher reduction rates than atrazine for most quarters. Their average destruction in the CONV water is presented in Figure 6-14, with 17-α-Ethynylestradiol (EE2) having the highest percent destruction at 98% and MTBE the lowest at 54%. The overall order of degradation was:
MTBE<Atrazine<Ibuprofen<MIB<Metolachlor=Gemfibrozil< 17-α-Ethynylestradiol

There were no significant differences in contaminant destruction between the MP and the LP reactors at the 80% atrazine level, which could be an indication that the primary mechanism of destruction is the reaction with hydroxyl radicals, with photolysis probably playing a less significant role. Rosenfeldt and Linden (2004) drew a similar conclusion when comparing the destruction of EDCs by photolysis and advanced oxidation with MP and LP lamps. The fact that at KWR in contrast with GCWW a difference between LP and MP lamps was found, can be attributed to the reactor design, which was the same for both LP and MP lamps at KWR (also see section 11.1). Additionally, the aforementioned order of degradation is similar to the order of the reaction rate constants with hydroxyl radicals (k_{OH}) for these contaminants, with MTBE having the lowest reported value at $1.6 \cdot 10^9$ and 17-α-Ethynylestradiol having the highest reported value of $1.08 \cdot 10^{10}$. Therefore, it would be expected for MTBE to present the lowest destruction among the other contaminants.

Table 6-5 Average degradation of contaminants (%) by the UV reactors with CONV influent water

	Atrazine	MTBE	Metolachlor	MIB	EE2	Gemfibrozil	Ibuprofen
MP	84	54	96	90	98	92	87
LP	74	56	87	85	93	92	82

UV/H_2O_2 with Post-GAC pilot influent water

When the higher UVT Post-GAC water was used as influent to the pilot reactors, adjustments to their flow and power level were made to reach the 80% atrazine degradation conditions. As shown in Figure 6-15 these conditions were met closely for both reactor types for almost all study quarters. Again, all the other contaminants except MTBE exhibited higher overall percent destruction than atrazine, and as shown in Figure 6-15 the average destruction results are similar for both MP and LP reactors.
By comparing the average values in Figure 6-14 and Figure 6-15 it seems that for most of the contaminants the average degradation levels were very similar for the CONV and Post-GAC water. Therefore, the difference in UVT and TOC content of the influent water did not affect the degree of contaminant degradation when the reactors were benchmarked based on performance.

(a)   **(b)**
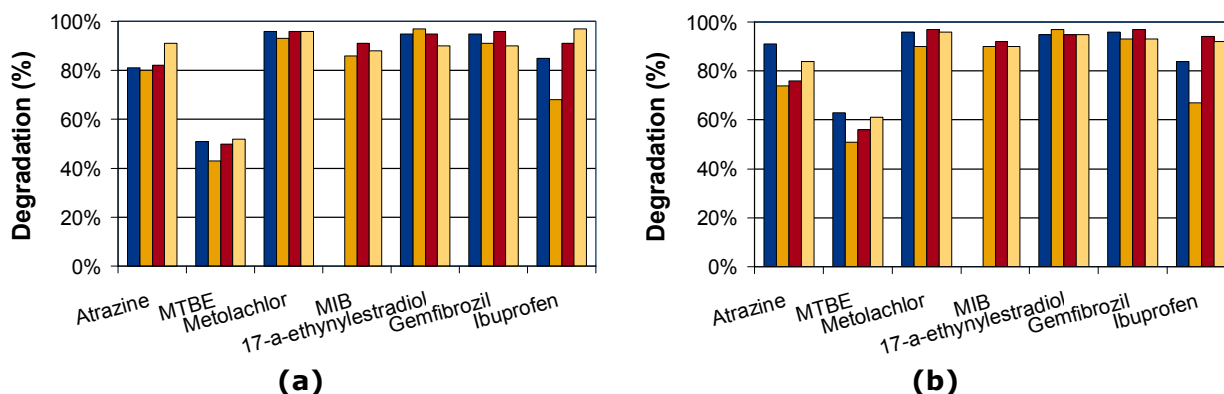
Figure 6-15 Contaminant degradation by UV/H_2O_2 in Post-GAC water (a) MP Reactor, (b) LP reactor. (■) Fall 2007, (■) Winter 2008, (■) Spring 2008, (■) Summer 2008

Table 6-6 Average degradation of contaminants (%) by the UV reactors with Post-GAC influent water

	Atrazine	MTBE	Metolachlor	MIB	EE2	Gemfibrozil	Ibuprofen
MP	84	51	95	88	94	93	85
LP	81	58	95	91	96	95	84

UV photolysis with Post-GAC pilot influent water

In addition to the UV/H_2O_2 experiments, tests were performed to examine the degradation of contaminants by photolysis using Post-GAC as pilot influent. Since the two reactor types could provide significantly different UV dose ranges, the photolysis tests were performed at the low end of UV doses for each reactor, which were around 280 mJ/cm² for the MP reactor and 800 mJ/cm² for the LP reactor (as estimated by the supplier's UV dose tables). Figure 6-16 shows the results for the MP and LP reactors, where the contaminant degradation by the MP reactor was significantly higher than that of the LP reactor even if the UV dose was almost a third of the LP dose. That demonstrates the advantage of the MP reactor during a photolysis process due to the effect of the wide UV spectrum on the destruction of various types of bonds. Additionally, atrazine, metolachlor, and 17-α-ethynylestradiol underwent significant degradation by photolysis through the MP reactor, not appreciably less than their UV/H_2O_2 destruction levels. These excellent results are in part due to the very high UVT of the Post-GAC pilot influent water. The remaining contaminants exhibited less than 50% removal by photolysis through the MP reactor compared to UV/H_2O_2. However, part of the degradation may be attributed to the formation of hydroxyl radicals by the UV photolysis of the background dissolved organic carbon (Pereira *et al.*, 2007).
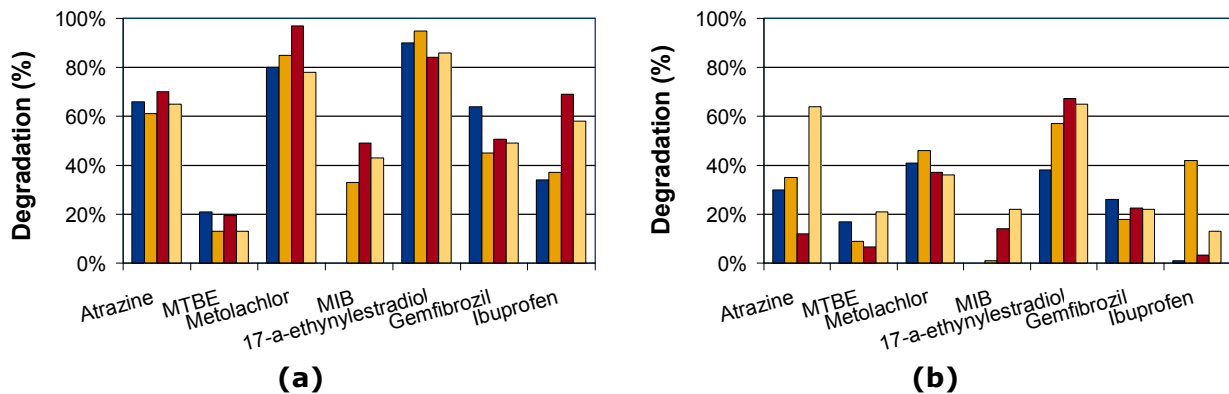
Figure 6-16 Contaminant degradation by UV photolysis in Post-GAC water (a) MP Reactor, (b) LP reactor. (■) Fall 2007, (■) Winter 2008, (■) Spring 2008, (■) Summer 2008

6.4.3 Electrical energy per order

UV/H_2O_2 MP reactor

The electrical energy per order E_{EO} for the degradation of each contaminant was calculated based on the rated energy of the reactor's lamp(s), the flow through the reactor and the influent and effluent concentration of the contaminant. Figure 6-17 shows the calculated E_{EO} values for the MP reactor for UV/H_2O_2 with CONV and Post-GAC pilot influent water. Overall, the values for CONV influent water were higher than the ones for the Post-GAC, as also was demonstrated by the averages per contaminant in Table 6-7. This was an expected outcome since the CONV water had lower UVT at all times compared to the Post-GAC water, thereby requiring more energy to produce hydroxyl radicals and achieve the same degree of degradation per contaminant than the Post-GAC pilot influent. Bolton and Stefan (2002) also demonstrated the decrease of E_{EO} (increase of efficiency) with the increase in UV transmittance for a UV batch reactor. They also presented the effect of the UV light's path length on the E_{EO} values,

observing that the E_{EO} increased sharply at small distances between the quartz sleeve and the reactor wall. This may explain the difference in the E_{EO} values calculated in this pilot study compared to the literature since the path length in the reactors was 5 cm (2 in) for the MP and 5-25 cm (2-10 in) for the LP reactor (due to the off-center configuration of the eight lamps in the LP reactor).

Among the contaminants, MTBE had the highest E_{EO} value for both pilot influent water scenarios, while metolachlor and 17-α-ethynyl estradiol had the lowest E_{EO} values. This was consistent with the order of degradation of the contaminants during the benchmark tests. Although there were differences between the E_{EO} values of the various contaminants, the E_{EO} ratio of the CONV to the Post-GAC water varied between 1.2 and 1.6 (Table 6-7). This is an indication that the contaminant degradation was affected in a similar way when the UVT of the water changed.

(a)   **(b)**
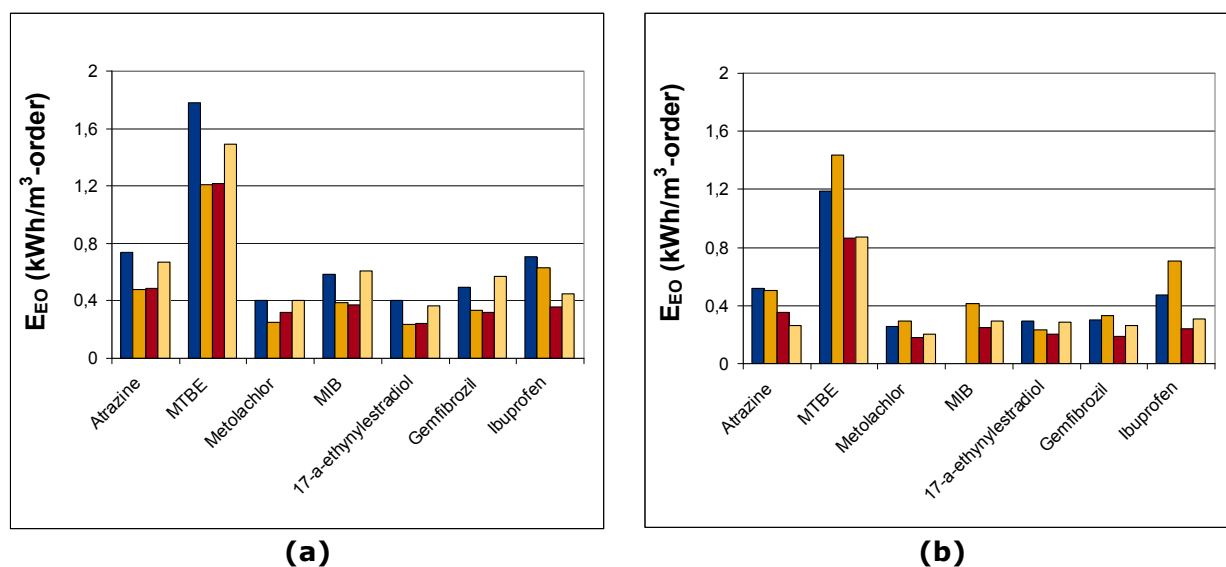
Figure 6-17 Contaminants E_{EO} by UV/H$_2$O$_2$ for MP reactor in (a) CONV water, (b) Post-GAC water. (■) Fall 2007, (■) Winter 2008, (■) Spring 2008, (■) Summer 2008(1 kWh/m^3-order = 0.634 kWh/kgal-order)

Table 6-7 Average E_{EO} (kWh/m^3-order) of contaminants for MP reactor under CONV and Post-GAC water (1 kWh/m^3-order = 0.634 kWh/kgal-order)

	Atrazine	MTBE	Metolachlor	MIB	EE2	Gemfibrozil	Ibuprofen
CONV	0.59	1.42	0.35	0.49	0.31	0.43	0.54
Post-GAC	0.41	0.90	0.23	0.32	0.25	0.27	0.43
E_{EO} Ratio CONV/Post-GAC	1.4	1.6	1.5	1.5	1.3	1.6	1.2

As mentioned previously, the TOC concentration and alkalinity of the CONV water fluctuated, ranging between 1.2-2.6 mg/L and 49-82 mg/L, respectively during the study period. Since TOC and alkalinity are hydroxyl radical scavengers, they were expected to interfere with the UV/H$_2$O$_2$ process. By plotting the E_{EO} of atrazine for the MP reactor against TOC concentration and alkalinity (Figure 6-18), it becomes obvious that at the beginning and the end of the study when TOC concentration and alkalinity were relatively high, the E_{EO} values were also at their highest levels. In the middle of the study these parameters and the E_{EO} values were much lower. The same pattern was observed for almost all

contaminants treated by the MP reactor, as evidenced for MTBE (Figure 6-19). Although this study produced an insufficient amount of data to completely evaluate the effect of TOC concentration on the E_{EO} values, a linear regression analysis between the two parameters (Figure 6-20) indicates that for the available data set there is a linear relationship between E_{EO} and TOC concentration for CONV influent range of TOC values. A linear relationship was established for both atrazine and MTBE. The E_{EO} of both contaminants increased with the increase of the TOC concentration, with MTBE being more sensitive to the changes in TOC concentration than atrazine.

Due to insufficient TOC concentration data a similar relationship could not be established when Post-GAC water was used as pilot influent.
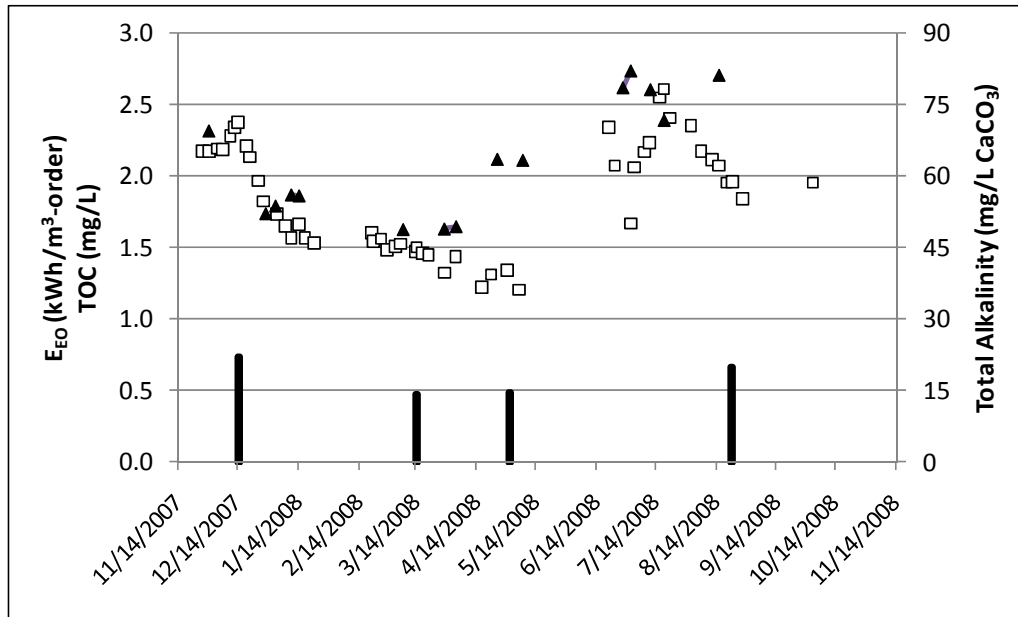
Figure 6-18 Atrazine E_{EO} for MP reactor in CONV water versus TOC concentration and Alkalinity. E_{EO} (bar), (□) TOC, (▲) Total Alkalinity (1 kWh/m³-order = 0.634 kWh/kgal-order)
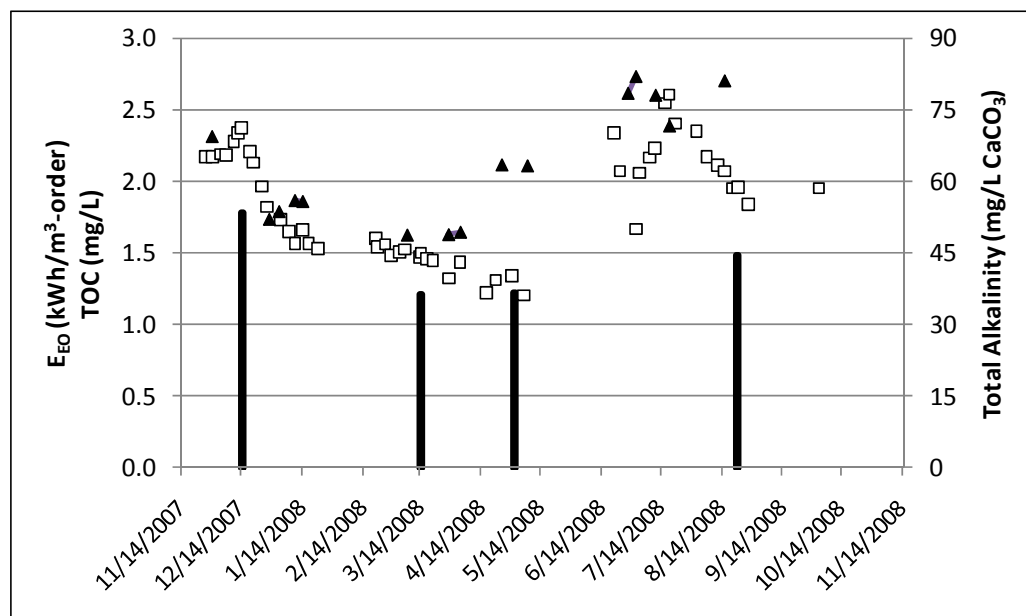
Figure 6-19 MTBE E_{EO} for MP reactor in CONV water versus TOC concentration and Alkalinity. E_{EO} (bar), (□) TOC concentration, (▲) Total Alkalinity (1 kWh/m³-order = 0.634 kWh/kgal-order)
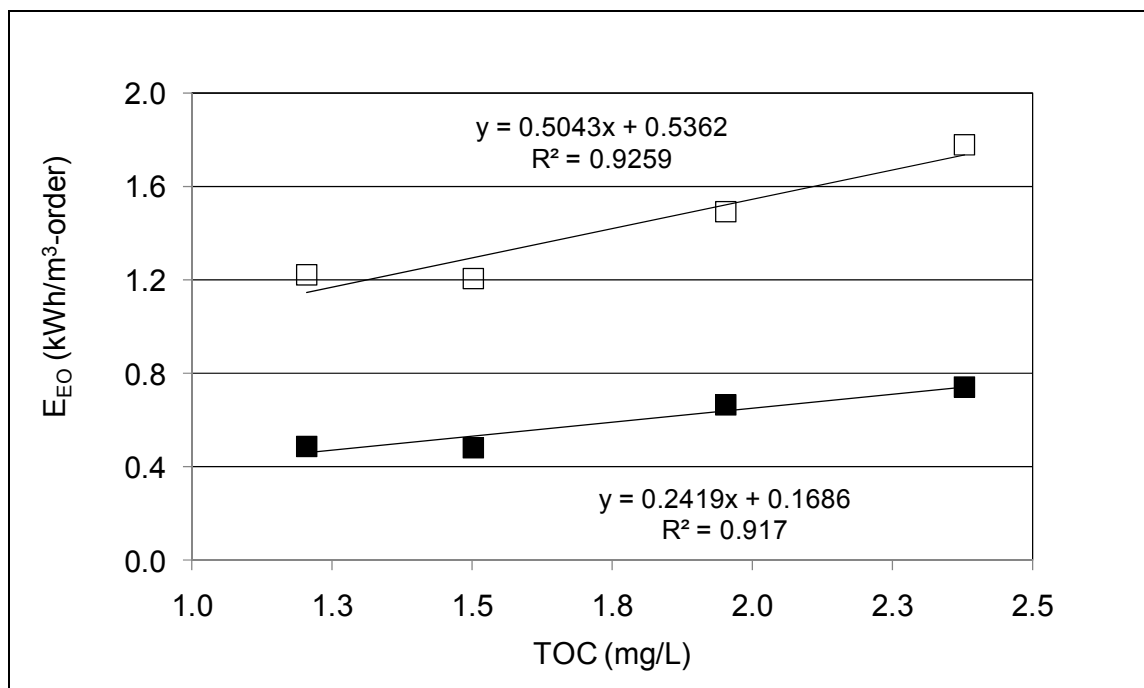
Figure 6-20 E_{EO} versus TOC concentration for MP reactor in CONV water. (■) Atrazine, (□) MTBE (1 kWh/m³-order = 0.634 kWh/kgal-order)

UV/H₂O₂ LP reactor

The E_{EO} values of the contaminants processed through the LP reactor are shown in Figure 6-21 for both the CONV and Post-GAC water. Similar to the results obtained by the MP reactor, the E_{EO} values with CONV water are higher than the ones required for Post-GAC water for a log removal of each contaminant (Table 6-8). This result can be explained by the lower UVT and higher TOC values of the CONV water compared to the Post-GAC water. The relationship between E_{EO} and TOC concentration could not be established for the LP reactor for either water source, mainly due to the lack of control of the sleeve fouling during each test season. Among the contaminants, MTBE had the highest energy requirements for one log degradation compared to the others, since it was the most difficult to degrade by UV/H₂O₂.

During the first quarter of testing with the CONV pilot inluent, the E_{EO} values of most contaminants were much higher than the other quarters. This was attributed to sleeve fouling in the LP reactor due to an improperly primed influent water pump. By eliminating that one E_{EO} value, the E_{EO} ratios between the CONV and Post-GAC water range for the most part between 1.5 and 2.0, slightly higher than the ratios observed with the MP reactor. Since the water quality parameters were the same for both reactors during these tests, the higher E_{EO} ratios with the LP reactor could be an indication of higher sensitivity to parameters such as UVT and TOC concentration, the primary water quality differences between CONV and Post-GAC water. However, the actual E_{EO} values between the pilot MP and LP reactor were not directly comparable, since the reactors had different designs and they had not been optimized for UV/H₂O₂ use. Generally though, it is known that LP systems are more efficient than MP systems and the LP E_{EO}S are much lower than the MP equivalent E_{EO}S, which was also demonstrated in this study.

(a)   **(b)**
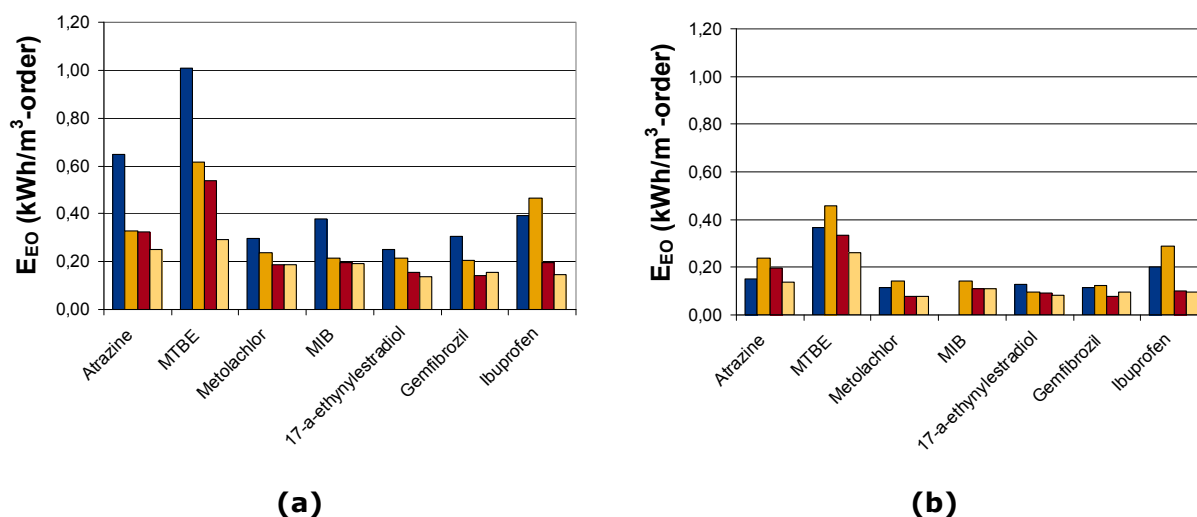
Figure 6-21 Contaminants E_{EO} by UV/H_2O_2 for LP reactor in (a) CONV water, (b) Post-GAC water. (■) Fall 2007, (■) Winter 2008, (■) Spring 2008, (■) Summer 2008 (1 kWh/m^3-order = 0.634 kWh/kgal-order)

The E_{EO} values found here differ from the values obtained at KWR, as shown in chapter 3.9. This can be explained from the fact that the KWR reactor had not been optimized or designed for a particular type of lamp. At KWR the same reactor was used for both LP as well as MP lamps (also see section 11.1). The E_{EO} stronly depends on the reactor design, as a result of which these values cannot always be compared.

Table 6-8 Average E_{EO} (kWh/m^3-order) of contaminants for LP reactor under CONV and Post-GAC water (1 kWh/m^3-order = 0.634 kWh/kgal-order)

	Atrazine	MTBE	Metolachlor	MIB	EE2	Gemfibrozil	Ibuprofen
CONV	0.30	0.48	0.20	0.20	0.17	0.17	0.27
Post-GAC	0.18	0.31	0.10	0.12	0.10	0.10	0.17
E_{EO} Ratio CONV/Post-GAC	1.7	1.6	2.0	1.7	1.7	1.6	1.5

UV photolysis with Post-GAC pilot influent water

All of the contaminants showed degradation under UV/H_2O_2 and photolysis conditions for both MP and LP reactors. However, the energy required for a log removal of each contaminant under the two processes varies significantly with the reactor type and contaminant. Figure 6-22 and Figure 6-23 show the estimated E_{EO} values for UV/H_2O_2 and UV photolysis for the MP and LP reactor respectively, and they have been plotted in the same scale to illustrate their differences. For all of the tested contaminants UV/H_2O_2 required the least amount of energy for a log removal compared to photolysis (Table 6-9 and Table 6-10) regardless of the type of UV lamp. 17-α-ethynylestradiol had the lowest E_{EO} for photolysis, which is only 1.5-2 times higher than its UV/H_2O_2 E_{EO} with either the MP or LP reactor, while MTBE had the highest photolysis E_{EO} being 4-5 times higher than the equivalent E_{EO} with UV/H_2O_2. This indicates that 17-α-ethynylestradiol is much more susceptible to photolysis than MTBE, and it may be economically feasible to use only photolysis for its removal, while for MTBE UV/H_2O_2 may be the best treatment choice since it requires far less energy compared to photolysis. Finally, for most of the contaminants, the E_{EO} ratio between UV photolysis and UV/H_2O_2 is lower for the MP reactor than the LP reactor, indicating that photolysis was more effective for the MP than the LP reactor, potentially due to the wider UV spectrum, which could photolyse different types of bonds. Specifically, atrazine has a high UV absorption rate at wavelengths less than 250 nm and also has a high photolysis quantum yield at this range, consequently UV photolysis by MP lamps is more efficient than photolysis by LP lamps

(Sharpless and Linden, 2005). Similarly, MIB has very low UV molar absorption at 254 nm, and much higher absorption at lower wavelengths, thus presenting greater degradation by photolysis and lower E_{EO} with the MP lamps versus the LP lamps (Rosenfeldt *et al.*, 2005). A similar effect can be observed for gemfibrozil.
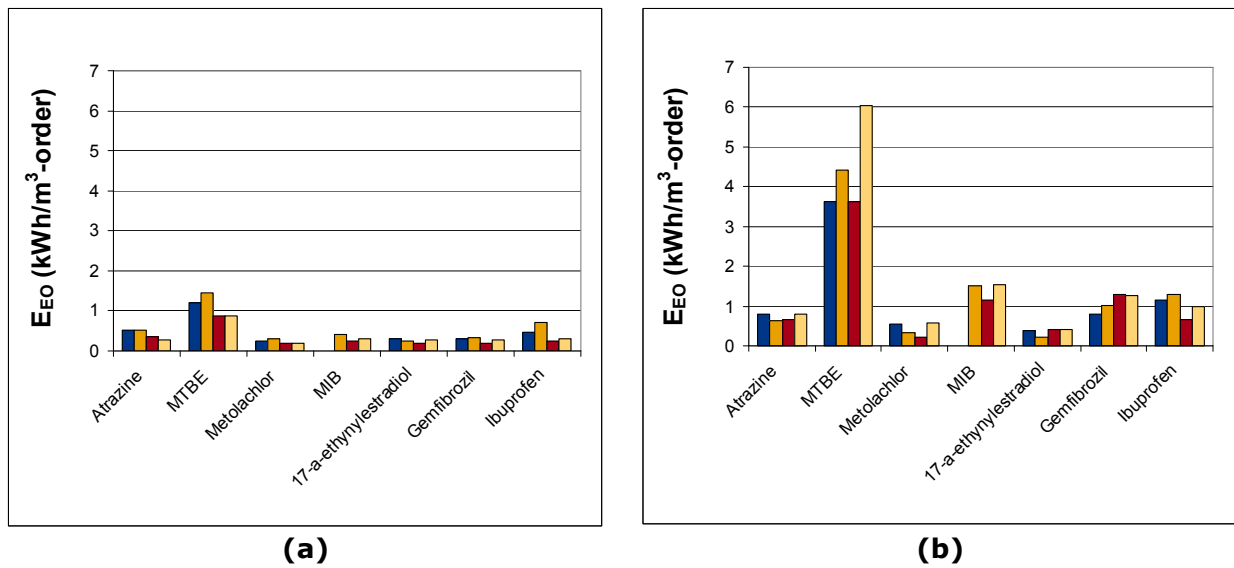
Figure 6-22 Contaminants E_{EO} for MP reactor in Post-GAC water by (a) UV/H_2O_2, (b) UV photolysis. (■) Fall 2007, (■) Winter 2008, (■) Spring 2008, (■) Summer 2008 (1 kWh/m^3-order = 0.634 kWh/kgal-order)

Table 6-9 Average E_{EO} (kWh/m^3-order) of contaminants for MP reactor under UV/H_2O_2 and UV photolysis (1 kWh/m^3-order = 0.634 kWh/kgal-order)

	Atrazine	MTBE	Metolachlor	MIB	EE2	Gemfibrozil	Ibuprofen
UV/H_2O_2	0.41	0.90	0.23	0.32	0.25	0.27	0.43
UV photolysis	0.72	4.42	0.42	1.40	0.36	1.09	1.02
E_{EO} Ratio UV photolysis / UV/H_2O_2	1.8	4.9	1.8	4.4	1.4	4.0	2.4
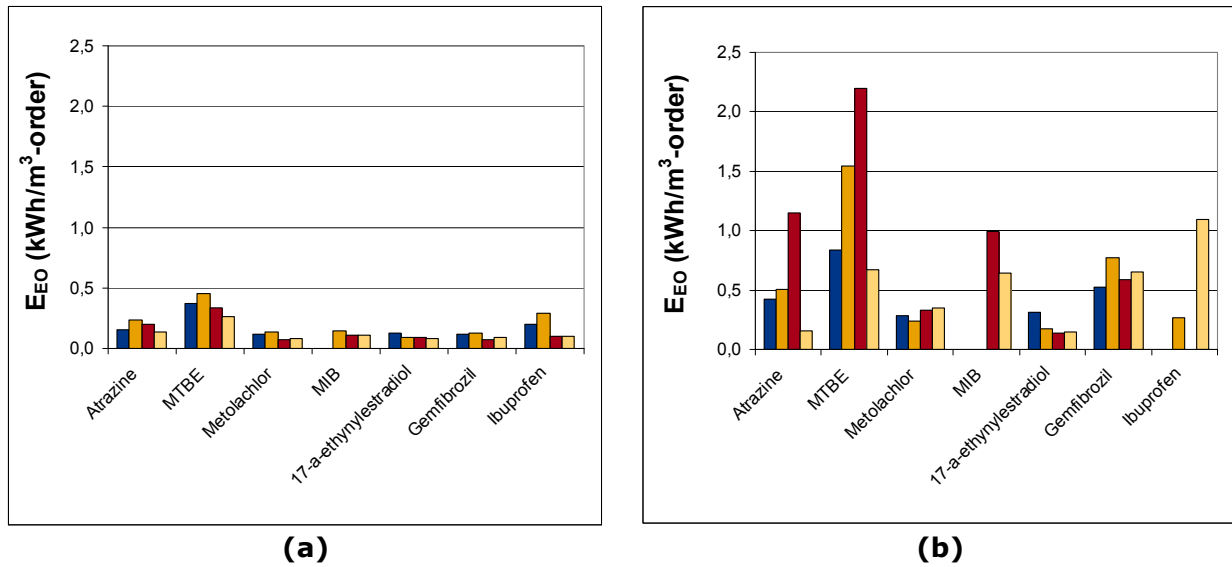
Figure 6-23 Contaminants E_{EO} for LP reactor in Post-GAC water by (a) UV/H_2O_2, (b) UV photolysis. (■) Fall 2007, (■) Winter 2008, (■) Spring 2008, (■) Summer 2008 (1 kWh/m^3-order = 0.634 kWh/kgal-order)

Table 6-10 Average E_{EO} (kWh/m^3-order) of contaminants for LP reactor under UV/H_2O_2 and UV photolysis (1 kWh/m^3-order = 0.634 kWh/kgal-order)

	Atrazine	MTBE	Metolachlor	MIB	EE2	Gemfibrozil	Ibuprofen
UV/H_2O_2	0.18	0.31	0.10	0.12	0.10	0.10	0.17
UV photolysis	0.56	1.31	0.30	0.82	0.19	0.63	0.68
E_{EO} Ratio UV photolysis / UV/H_2O_2	3.1	4.2	2.9	6.7	1.9	6.2	3.9

6.4.4 Effectiveness of GAC in Removing Spiked Contaminants

GAC adsorption was very effective in removing spiked contaminants, and provided an impenetrable barrier when preceded by UV/H_2O_2. Each of the seven compounds spiked into the process were removed to below the detection levels (Table 6-4) in the GAC effluent streams when the GAC influent stream was pretreated with UV/H_2O_2. GAC without UV/H_2O_2 pretreatment removed six of the seven compounds to below detectible concentrations for all four quarters. MTBE was the only compound detected in the fourth quarter of GAC run (day 286). MTBE was detected at a concentration of 0.31 and 0.26 µg/L, respectively in control columns 1 and 2. It should be noted that these detections represent a 94 to 95% removal, which was significantly better than the 54 to 56% removal achieved by UV/H_2O_2 alone. Table 6-3 presents the partition coefficients (K_{OW} values) that confirm that MTBE has the lowest logK_{ow} and highest solubility in water and was therefore expected to be the least adsorbed of the contaminants tested. Greater Cincinnati Water Works (GCWW) reactivates their GAC to maintain an average run day less than 200 days. Therefore, if this contaminant was present at the spiked levels, 4 µg/L, GAC alone may be able to adequately control this contaminant at GCWW operating conditions.

6.4.5 Biofilm formation potential

Assimilable organic carbon (AOC) through UV/H$_2$O$_2$ pilot using CONV influent

Non-chlorinated AOC samples were collected throughout the pilot run to reflect variations in water quality in the process streams when the pilot was normalized for 80% atrazine destruction. When using the CONV process stream as influent to the pilot plant, the total AOC concentration increased through the UV/H$_2$O$_2$ reactors from an average of 106 µg/L, to an average of 141 µg/L (33% increase) for the LP process train and from an average of 106 µg/L, to an average of 137 (30% increase) for the MP process train (Figure 6-24, and Table 6-11). However, GAC was very effective in reducing the total AOC concentration from an average of 106 µg/L, to an average of 39 to 45 µg/L (63%-58% reduction) through the control GAC contactors. Note that the total AOC concentration means of the two GAC control effluent streams were similar, 14% difference (Figure 6-24, Table 6-11, and Table 6-12). GAC adsorption following the UV/H$_2$O$_2$ process was effective in reducing the total AOC concentration from an average of 141 µg/L for LP process train, to an average of 54 µg/L (62% reduction) in the associated GAC effluent and from an average of 137 µg/L for MP process train, to an average of 45 µg/L (67% reduction) after GAC adsorption, ultimately resulting in total AOC concentrations similar to the GAC control effluent streams, (Figure 6-24, and Table 6-11). Overall, the removal of total AOC by GAC is very consistent regardless of whether the influent water had received UV/H$_2$O$_2$ treatment.

The quantity and type of AOC formed or reduced by the pilot unit process differed. P-17 AOC concentration was measured by the growth of *Pseudomonas* fluorescens. As discussed in the background information, the P-17 organism is able to utilize various compounds such as proteins, amino acids, carboxylic acids, carbohydrates, alcohols and aromatic acids. This organism can survive using many carbon substrates as carbon sources (van der Kooij *et al.*, 1982 and AwwaRF and KIWA 1988). Spirillium strain NOX is more selective in its growth substrates. Only carboxylic acids and a few amino acids promote growth of the NOX organism. In treatment techniques such as ozonation where compounds not readily utilized by P-17 are formed, the growth of Spirillium strain NOX is a useful indicator of AOC concentration increases. Spirillium strain NOX has been shown to represent carboxylic acids. Also, in cases of low AOC concentration, the Spirillium strain NOX tends to grow better than the P-17 organism, (van der Kooij and Hijnen, 1984 and AwwaRF and KIWA 1988). Therefore it was selected for studying these advanced oxidation processes. An average of 83 µg/L P-17 AOC concentration, and an average of 23 µg/L NOX AOC concentration was found in the CONV pilot influent (Table 6-11). Both parameter concentrations increased through the UV/H$_2$O$_2$ reactors, but as would be anticipated, the NOX AOC concentration increased more. P-17 AOC concentration increased 24% (from an average of 83 to 103 µg/L P-17 AOC) through both the LP and MP reactors (Table 6-12). NOX AOC concentration increased from 23 to 38 µg/L (65% increase) through the LP reactor and from 23 to 35 µg/L through the MP reactor (52% increase). The greater magnitude of the NOX AOC concentration increase was reasonable considering the findings of Sarathy *et al.* (2007 and 2009), i.e, the ratio of hydrophilic to hydrophobic compounds increases with UV/H$_2$O$_2$ treatment.

As was aforementioned, the control GAC effluent concentrations for total AOC were similar, but P-17 AOC was better removed than NOX AOC. This result was expected because GAC was less efficient in removing hydrophilic compounds that would be represented better by NOX AOC concentration (James M. Montgomery, Consulting Engineers, Inc., 1985 and Westerhoff *et al.*, 2005). The NOX AOC was better removed through GAC following the UV/H$_2$O$_2$ process (47-49%) than through the control GAC column (35%) because of the increased bioactivity of the GAC caused by the UV/H$_2$O$_2$ treatment and possibly because the increased NOX AOC concentration through the reactors represented different, more adsorbable compounds than represented by the NOX AOC concentration from the CONV treated process stream (Table 6-12).
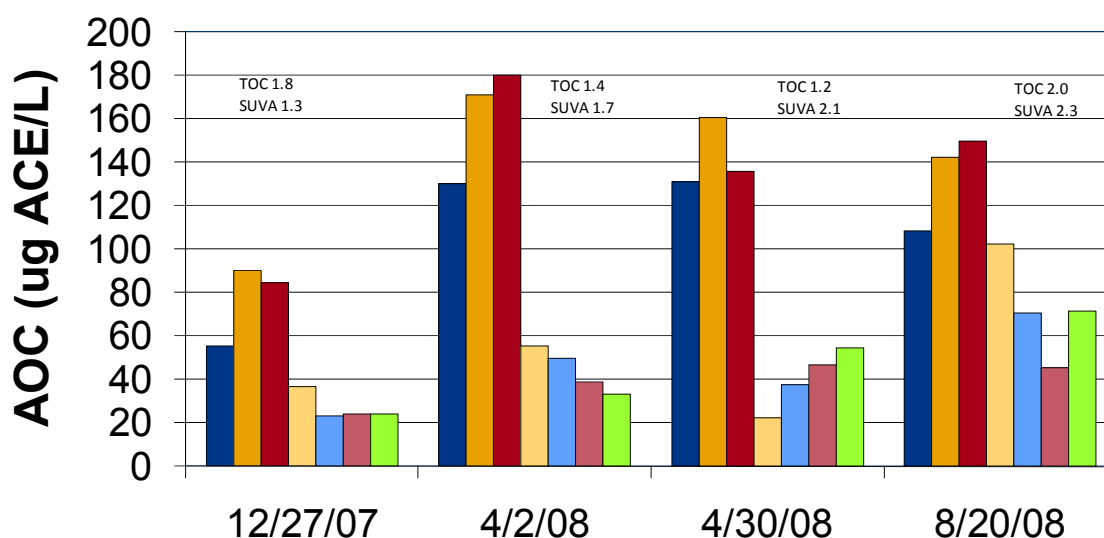
Figure 6-24 UV/H₂O₂ with CONV. Pilot Influent-AOC, (∎) Pilot Influent, (∎) LP Reactor Effluent, (∎) MP GAC Effluent, (∎) LP GAC Effluent., (∎) MP GAC Effluent, (∎) Control #1 GAC Effluent, (∎) Control #2 GAC Effluent (1µg/L = 1.60 µg/gal)

Table 6-11 UV/H₂O₂ with CONV Pilot Influent-AOC µg/L as acetate (1µg/L = 1.60 µg/gal)

	Pilot Inf.	LP Eff.	LP GAC Eff.	MP Eff.	MP GAC Eff.	GAC Control #1	GAC Control #2
P17 Avg.	83	103	34	103	27	24	30
NOX Avg.	23	38	20	35	18	15	15
Total Avg.	106	141	54	138	45	39	45
Sample (n)	4	4	4	4	4	4	4

Table 6-12 UV/H₂O₂ with CONV Pilot Influent-Changes in AOC (as acetate) through Treatment Processes

	LP Reactor	MP Reactor	LP GAC	MP GAC	GAC Control #1	GAC Control #2
P17	24%	24%	-67%	-74%	-71%	-64%
NOX	65%	52%	-47%	-49%	-35%	-35%
Total	33%	30%	-62%	-67%	-63%	-58%

AOC through UV/H₂O₂ pilot using Post-GAC influent

The total AOC concentration in the pilot influent was 40% lower (64 µg/L vs. 106 µg/L) when Post-GAC water was used as the pilot influent rather than CONV treated water (Figure 6-25, and Table 6-13). Because the Post-GAC pilot influent contained less UV absorbable organics, 80% atrazine reduction was obtained with less UV energy. The total AOC concentration increased slightly through the reactors during the Post-GAC influent phases, from 64 µg/L to 73 µg/L (14%) for both the LP and MP reactors. This increase in total AOC concentration was less than the 30 to 33% increase in total AOC concentration when CONV treated water was used as pilot influent. The lesser increase in total AOC concentration when Post-GAC served as pilot influent was because the TOC concentration was lower and of a different nature. Larger molecular weight humic compounds, potentially precursors of AOC, are well-removed by GAC (Sontheimer et al., 1988 and Morris and Newcombe, 1993). Thus, there is a lower concentration

of these humics in the Post-GAC pilot influent to act as AOC precursors. The P-17 AOC concentration did not increase through the reactors when Post-GAC water was used as pilot influent. The lower concentration of organics in this process stream and the reduction of the larger molecule AOC precursors by the GAC pretreatment contributed to this result. The NOX AOC concentration increased from 20 to 30 – 31 µg/L, about 50%, again indicative of carboxylic acid formation through the UV/H_2O_2 reactors (Table 6-14).
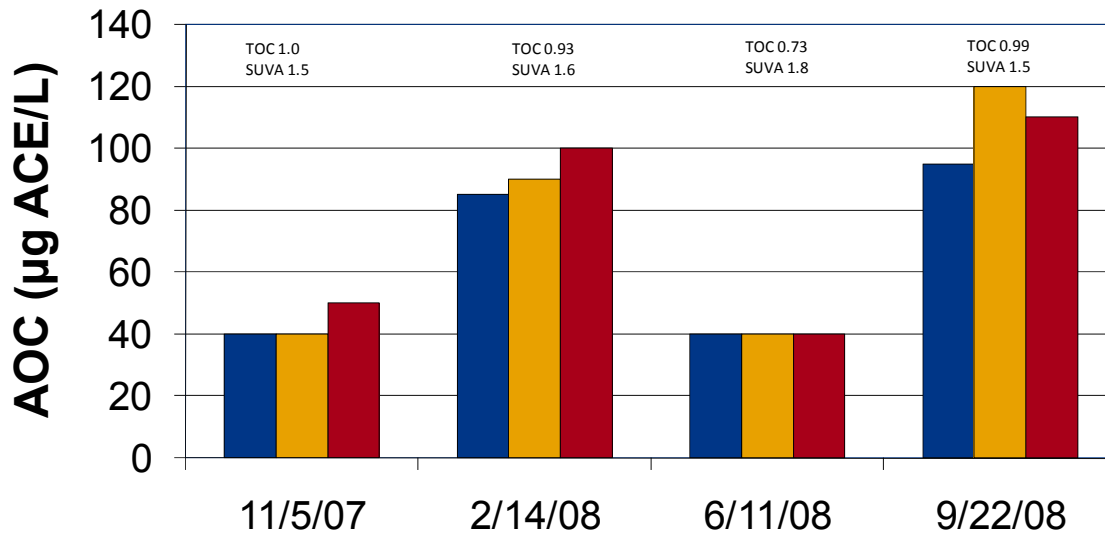
Figure 6-25 UV/H_2O_2 with Post-GAC pilot influent-AOC, (■) Pilot Influent, (■) LP Reactor Effluent, (■) MP Reactor Effluent (1µg/L = 1.60 µg/gal)

Table 6-13 UV/H_2O_2 with Post-GAC Pilot Influent AOC µg/L as acetate (1µg/L = 1.60 µg/gal)

	Pilot Inf.	LP Eff.	MP Eff.
P-17 Avg.	44	42	43
NOX Avg.	20	31	30
Total Avg.	64	73	73
Sample (n)	4	4	4

Table 6-14 UV/H_2O_2 with Post-GAC Pilot Influent
Changes in AOC as acetate through Treatment Processes

	LP Reactor	MP Reactor
P-17 Avg.	-5%	-2%
NOX Avg.	55%	50%
Total Avg.	14%	14%

AOC through UV photolysis pilot using Post-GAC influent

Three experimental pilot runs were performed using photolysis alone. However, these results were not able to be directly compared to the UV/H_2O_2 results for AOC concentration because an 80% atrazine degradation was not achievable. Also because of the aforementioned technical considerations, the LP reactor UV dose (approximately 800 mJ/cm^2) was higher than the MP reactor dose (approximately 280 mJ/cm^2). Nevertheless, the relative increases in P-17 and NOX AOC concentrations are of interest. When using Post-GAC pilot influent, photolysis created no increase in NOX AOC concentration, because without the H_2O_2, less oxidation takes place and few carboxylic acids are formed (Figure 6-26). The P-17 AOC concentration (Table 6-15) increased through the LP reactor, but not through the MP reactor. This increase was likely associated with the higher LP reactor dose focused near the 254 nm wavelength. This wavelength is known to be well-absorbed by humic materials. Photolysis of the humic materials would thus proceed. As was previously discussed, the P-17 AOC represents a wide variety of smaller molecular weigh assimilable compounds (Table 6-16).
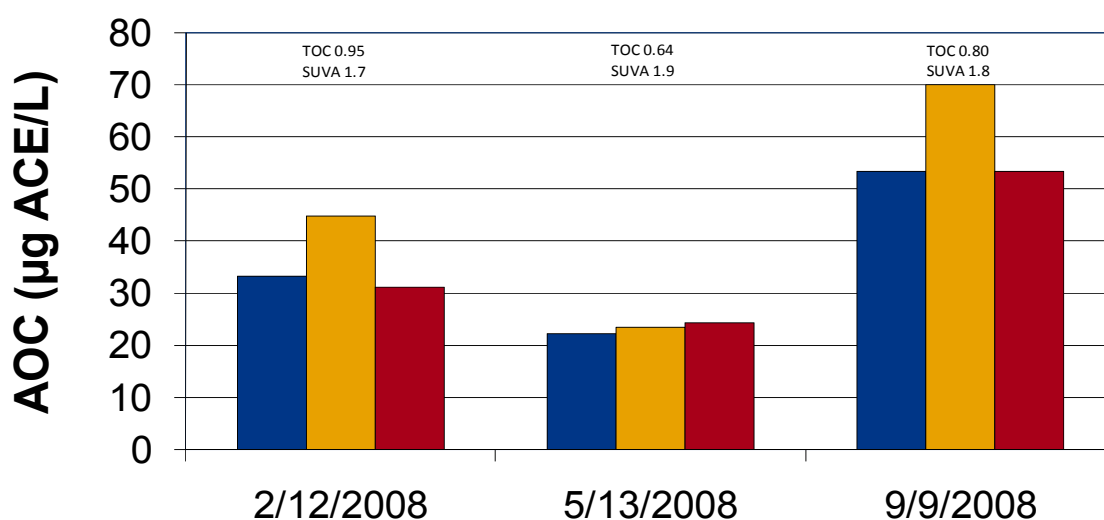
Figure 6-26 Photolysis with Post-GAC pilot influent-AOC, (■) Pilot Influent, (■) LP Reactor Effluent, (■) MP Reactor Effluent (1µg/L = 1.60 µg/gal)

Table 6-15 Photolysis with Post-GAC Pilot Influent AOC µg/L as acetate

	Pilot Inf.	LP Eff.	MP Eff.
P-17 Avg.	33	45	31
NOX Avg.	22	23	24
Total Avg.	55	68	56
Sample (n)	3	3	3

Table 6-16 Photolysis with Post-GAC Pilot Influent
Changes in AOC as acetate through Treatment Processes

	LP Reactor	MP Reactor
P-17 Avg.	36%	-5%
NOX Avg.	5%	10%
Total Avg.	24%	1%

Van der Kooij (1992) recommended that unchlorinated systems maintain AOC concentrations below 10 µg/L. Even the GAC effluent samples had total AOC concentrations above this value (Table 6-11, Table 6-13, and Table 6-15). If a utility with a source water similar to GCWW's wished to maintain a total AOC concentration less than 10 µg/L, a GAC empty bed contact time greater than the pilot condition of 15 minutes may be required. LeChevallier *et al.* (1990 and 1996) provided some evidence that chlorine disinfected systems may limit regrowth and coliform occurrence by maintaining AOC concentrations less than 50 to 100 µg/L. Only the UV/H_2O_2 reactor effluent streams and the CONV pilot influent samples had total AOC concentrations exceeding this range (Figure 6-24, and Figure 6-25).

Biofilm annular reactors after GAC pilot contactors

Because the pilot GAC effluent streams had relatively low AOC concentrations, annular biofilm reactors were employed to examine biofilm production more closely. The annular reactors were operated continuously on the undisinfected GAC effluent streams. The experiments were begun during the most biologically active stage of GAC, i.e., near the end of the run and during warm weather conditions. The experiment ran from September 4, 2008 to October 2, 2008, which corresponded to run-day 300 to 328 of the GAC. The temperature ranged from 27 to 28°C and the TOC from 0.82 to 1.95 mg/L for this time period. The biofilm from the coupons was extracted from the reactors and analyzed by two methods: the traditional HPC method and a ATP-bioluminescence method developed internally. HPC is a microbiological parameter and tends to have more scatter in the data than a chemical parameter. Thus, a log scale was used to display the data. When analyzing biofilm by this method, one can only discern differences in magnitudes of order. Even with this caveat, the reproducibility of individual coupons was not as good as would be desired. Overall, the GAC process streams for the two controls produced similar HPCs. The HPCs of these control samples were less than those receiving water from the UV/H_2O_2 reactors. The LP reactor process stream data was the least precise. However, the coupons from this process stream tended to have slightly lower HPCs than the coupons from the MP process stream (Figure 6-27).
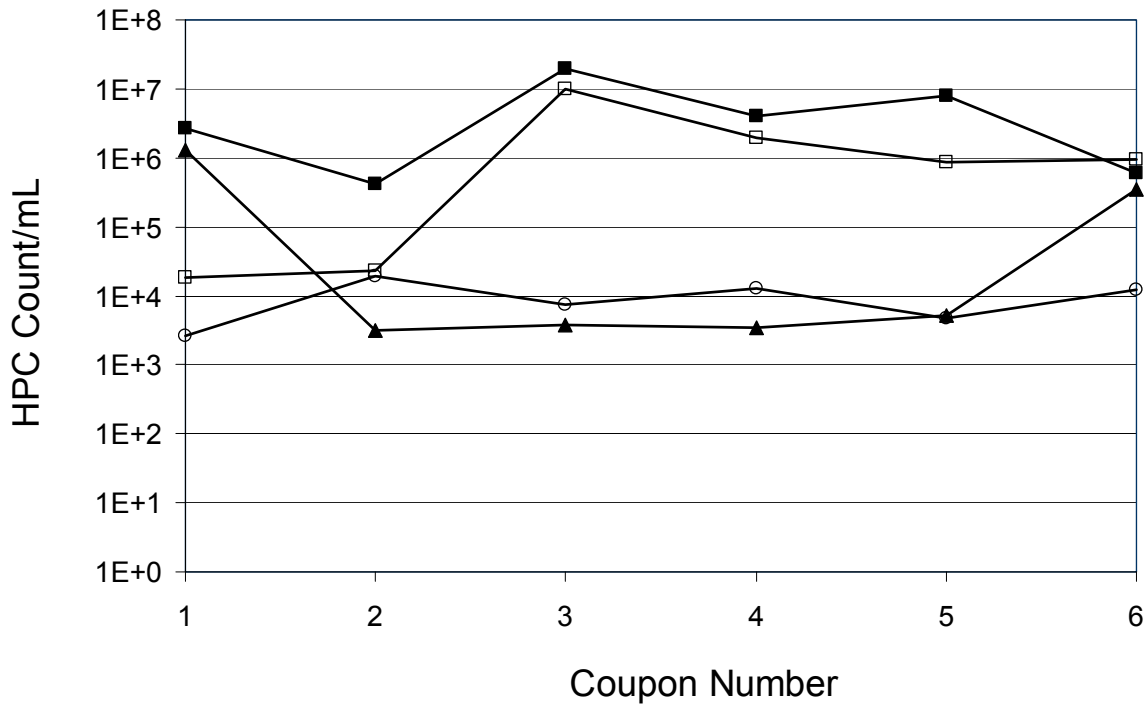
Figure 6-27 Effluent Results-HPC, (■) Medium-pressure GAC Effluent, (□) Low-pressure GAC Effluent, (▲)GAC Control #1, (○) Control #2 (count/mL = 1.60 count/gal)

The ATP-bioluminescence method of biofilm quantification was based on the amount of ATP present. This method was dependant on viability of the organisms. Because the ATP-bioluminescence method was a chemically based analysis, and does not have the problem of cell separation, the data tend to be more precise. For this reason a linear scale can be used for the concentration axis (Figure 6-28). However, there are still situations that can cause the test to produce outlying data points. ATP is common to all microbes and larger cells such as protozoa require more energy to thrive. Therefore, if larger cells are present, they can skew the ATP data. The data exhibited good precision, with two outlying data points, likely caused by the presence of a larger microorganism. Nevertheless, it was clear that the control GAC column effluent streams produced similar results. The GAC effluent following the LP reactor also produced results similar to the controls. The MP stream GAC effluent produced the highest results. The HPC and the ATP-bioluminescence methods showed different results because the HPC method grew the organisms in a nutrient media under ideal conditions.

Injured cells had the opportunity to repair (LeChevallier *et al.*, 1990). The ATP-bioluminescence method results represented cell viability at the time that the coupons were removed from the annular reactors and biofilm extracted. The data would suggest that the organisms produced by the MP process stream were more viable than those produced by the LP process stream, even though the HPCs for the two streams were similar.
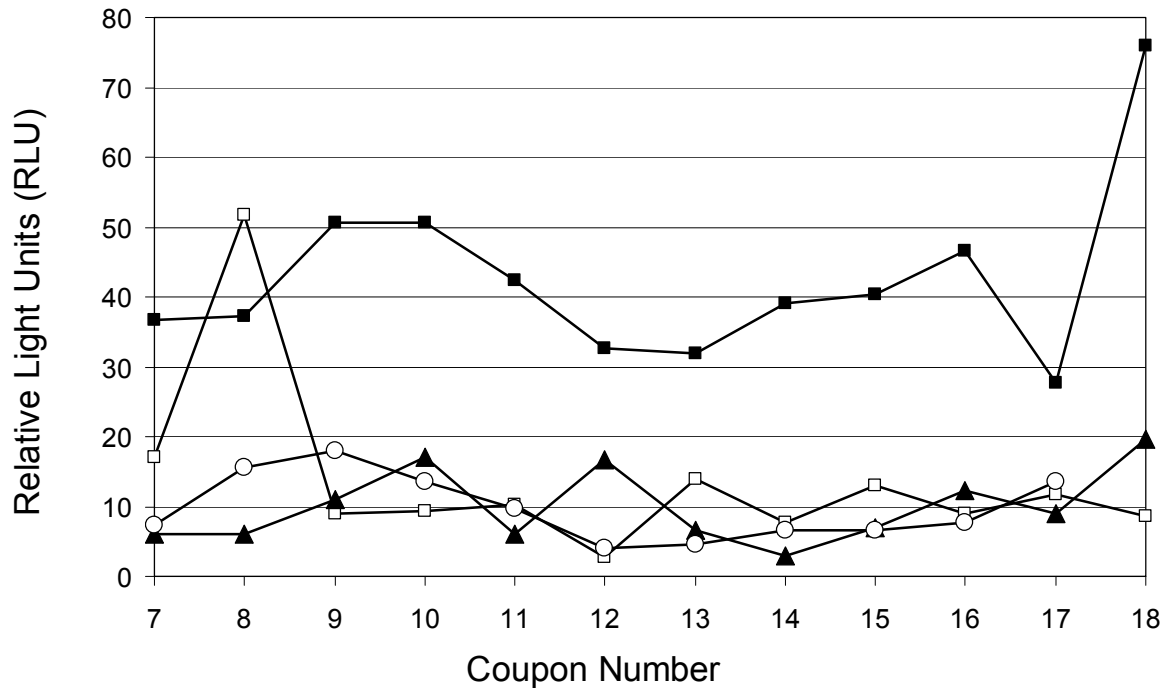
Figure 6-28 GAC Effluent Results-ATP, (■) Medium-pressure GAC Effluent, (□) Low-pressure GAC Effluent, (▲) Control #1, (○) Control #2

6.5   Conclusions

- The pilot results indicate that when the two reactors were benchmarked at 80% atrazine degradation conditions, a similar degree of degradation among the selected contaminants was achieved regardless of the type of reactor (MP and LP) or the influent water (CONV and Post-GAC). The only contaminant with lower degradation than atrazine was MTBE, while the remaining compounds showed very good destruction at study conditions.

- For the MP reactor, the E_{EO} increased between 1.2-1.6 times when the influent water was switched from Post-GAC to CONV water, while for the LP reactor, the increase was between 1.5-2.0 times. This was an indication that the efficiency of the LP reactor increased more than the efficiency of the MP reactor when the UVT of the water increased.

- Overall, the MP reactor's E_{EO} values for all the contaminants were greater than those of the LP reactor's, as was expected by the efficiencies of these two lamp technologies.

- The seasonal variations in the TOC concentration of the CONV water affected the E_{EO} values calculated for the MP reactor.

- There was a significant advantage in using advanced oxidation with UV/H_2O_2 versus photolysis alone for the degradation of MTBE, MIB, Gemfibrozil and Ibuprofen when the MP reactor was used. Due to their relatively poor destruction by photolysis, 17-α-ethynylestradiol, atrazine and metolachlor required almost twice the energy to degrade by photolysis versus UV/H_2O_2. Similarly for the LP reactor for all the contaminants, except 17-α-ethynylestradiol, the best treatment for destruction would be UV/H_2O_2 rather than photolysis.

- After GAC run day 220, the GAC effluent streams that had received UV/H_2O_2 treatment , exhibited 16% lower TOC concentrations than the control GAC effluent streams that had not

received UV/H$_2$O$_2$ pretreatment. Increased bioactivity was assumed responsible for this reduction.

- GAC adsorption was very effective in removing the contaminants that were spiked quarterly. Only MTBE broke through the control GAC columns during the final quarter (286 GAC run days). The removal of MTBE was 94 to 95% through the control GAC columns the fourth quarter.

- When atrazine destruction was normalized at 80% through the UV/H$_2$O$_2$ pilot reactors, AOC concentration increased through the reactors.
    - The average Total AOC concentration increased 33% through the LP reactor and 30% through the MP reactor when CONV water was used as pilot influent
    - The average Total AOC concentration increased 14% through the reactors when Post-GAC water was used as pilot influent
    - The average P-17 AOC concentration increased 24% through the LP and MP reactors when CONV water was used as pilot influent
    - The average P-17 AOC concentration did not increase through the reactors when Post-GAC water was used as pilot influent
    - The average NOX AOC concentration increased 65% through the LP reactor and 52% through the MP reactor when CONV water was used as pilot influent
    - The average NOX AOC concentration increased 55% through the LP reactor and 50% through the MP reactor when Post GAC water was used as pilot influent

- LP UV photolysis at a dose of approximately 800 mJ/cm^2, produced a 36% average P-17 AOC concentration increase, but no NOX AOC concentration increase was observed when using Post GAC as pilot influent.

- MP UV photolysis at a dose of approximately 280 mJ/cm^2, produced no appreciable AOC concentration increase when using Post GAC as pilot influent.

- Biofilm coupon studies indicated that biofilms with greater HPCs were observed in the GAC effluent steams receiving UV/H$_2$O$_2$ pretreatment.

- Biofilm coupon studies indicated that the effluent streams of the GAC column preceded by the MP reactor exhibited more viable biofilm than the other GAC effluent streams based on an ATP bioluminescence method. More research should be performed in this area.

Pilot plant research II (DBD lamp)

Work package 8; Dunea

Authors: **A.H. Knol, K. Lekkerkerker-Teunissen, E. F. Beerendonk, C.H.M. Hofman-Caris**

7 Work package 8: Pilot plant research II (DBD lamp) (Dunea)

7.1 Introduction

"Dunea duin en water" produces drinking water for 1.2 million customers in the Western part of the Netherlands. High drinking water quality and customers confidence are important objectives of Dunea. Dunea has a multiple barrier treatment approach to produce biologically stable and pathogen free drinking water (its water soucrce is the Meuse river), which can be distributed without post disinfection such as chlorination. The treatment consists of coagulation, sedimentation, microstraining, rapid sand filtration, artificial recharge and recovery, softening, aeration, dosage of powdered activated carbon, rapid sand filtration and slow sand filtration.
Improved analytical techniques and increasing use of chemical compounds in our society have increased the detection and concentration of organic micropollutants (OMPs) in the Meuse river to levels higher than the Dutch drinking water standards. Although Dunea has already a well-developed treatment process, Dunea is considering an additional treatment step to ensure an adequate removal of organic micropollutants.

At the end of 2005, Dunea started the "additional treatment" project, which is still ongoing. The project consists of several sub projects, one of them being the research towards an advanced oxidation process consisting of UV and hydrogen peroxide. This research was a perfect fit with the Dutch/U.S. collaboration (Philips, KWR and GCWW) on evaluating the effectiveness of using low pressure (LP) and medium pressure (MP) UV in direct photolysis and with H_2O_2 to degrade micro-pollutants.

Besides the removal of organic micropollutants in drinking water, the additional treatment step (e.g. UV/H_2O_2) has to fulfill two other requirements. In the first place, the drinking water quality should not deteriorate after implementing the technique. A second objective, if the additional treatment is installed before the dunes, is to fulfill the requirements of the "Infiltration Decree" (in Dutch: Infiltratiebesluit). Dunea and the Dutch Government agreed that starting in 2016 the current agreement will end and infiltration in the dune area will only be allowed if the concentration of a single pesticide in the infiltration water is below 0.1 µg/L and the sum of all pesticides is below 0.5 µg/L. Furthermore, it is anticipated that for OMPs such as endocrine disruptors, pharmaceuticals, etc., the same guidelines will be pursued (according to the drinking water standard).
The fact that the maximum concentration in dune influent water should be 0.1 µg/L, while the maximum concentration in the river at the intake is 0.5 µg/L, implies that the UV/H_2O_2 step has to achieve at least 80% degradation of pesticides. To enable the comparison between the different lamp technologies, atrazine has been selected as a reference compound, because of the extensive literature and knowledge on this compound. In addition, atrazine is degraded by UV photolysis and by ·OH radical oxidation.

The research project of Dunea consists of three phases:
1) pilot plant research with intermittent operation, three lamp types (LP, MP and DBD).
2) pilot plant research with continuous operation, two lamp types (selection after phase 1).
3) demonstration unit with one lamp type (selection after phase 2).

In this report, only phase 1 is reported as WP8 in the joint project with GCWW, KWR and Philips. The first phase started in 2009 and ended in the beginning of 2010. Phase 1 mainly focused on the degradation of organic micropollutants by UV/H_2O_2 with three different lamp types. The second phase started in March 2010 and has focused on long term experiments, on the conditioning of the UV-reactor influent water, and on the remaining research issues. The final goal of the research is to achieve a set of design parameters for a demonsration installation at the end of 2010. Research with this demonstration

installation will lead to the design and operational parameters for a full scale installation that will degrade organic micropollutants and other emerging contaminants during pretreatment (i.e., before dune infiltration).

Phase 1 lasted 10 months and a variety of seasonal variations was examined. Additionally, operational requirements and organic and inorganic byproduct formation were studied. Because hydroxyl radicals react non-selectively with organic compounds, unintended byproduct formation was expected to occur. The formation of byproducts, assimilable organic carbon, and the regrowth potential was investigated.

Initially the following hypotheses/assumptions were developed:

1) Based on collimated beam studies performed at KWR (WP1), it was assumed that the DBD-lamp can produce more radicals than the LP- and MP-lamp. Therefore, the conversion of a selection of contaminants by a DBD-reactor was compared to the conversion of the same contaminants by an LP- and MP-reactor.

2) It was expected that the MP reactor would require more energy to achieve equal conversion because a major part of the wavelength spectrum of an MP lamp is not used for hydroxyl radical production or photolysis of contaminants. It was assumed that conversion by direct photolysis with MP lamps, although more effective than photolysis with LP- and DBD-lamps, is less efficient than the combination with oxidation by OH radicals..

3) It was hypothesized that the natural organic matter would be chemically altered by the UV/H_2O_2 process, increasing the content of microbiologically assimilable organic compounds and thus the biofilm formation potential.

4) Adsorption with GAC following the UV/H_2O_2 process would be necessary to quench excess H_2O_2 and reduce nitrite, AOC and degradation by -products that are expected to be formed during UV/H_2O_2-oxidation .

5) Results of the different reactors with different lamp types can be compared, even though each reactor has not been fully optimized beforehand. Optimizing reactors may result in different effects on EEO, formation of byproducts, etc. in those reactors.

The scope of this research included the following:
  ➢ Exploring the feasibility of two modes of contaminant removal by UV, i.e., UV/H_2O_2 and photolysis (confirmation of the expected better performance of UV/H_2O_2 above only UV irradiation).
  ➢ Determining the effect of seasonal variations in water quality on UV/H_2O_2 and photolysis processes.
  ➢ Comparing MP, LP and DBD lamp performance for both UV/H_2O_2 and photolysis processes.
  ➢ Evaluating the Electrical Energy per Order (E_{EO}) and compare MP to LP and DBD technology for both UV/H_2O_2 and photolysis processes.
  ➢ Determining the effect of GAC after the UV/H_2O_2 process on H_2O_2, AOC, and organic micropollutants
  ➢ Evaluating enhanced removal of contaminants with UV/H_2O_2 followed by (biologically active) GAC.
  ➢ Determining AOC increase by the UV-reactors with different lamp types.

7.2 Experimental set-up

7.2.1 Facilities

A pilot scale installation was built at the pretreatment location of the full scale water treatment plant. The pretreatment plant is located in Bergambacht. Dunea's intake is located in Brakel, on the banks of a dead-end side stream of the Meuse River. Ferrous sulphate is dosed (average dose = 3.4.mg/L, 2 mg Fe^{2+}/L) at the entrance of the side-stream resulting in coagulation, flocculation and sedimentation. Furthermore, there is a certain extend of self-cleaning during seven weeks dwelling time in the side stream. At the Wilhelminasluis site, the water is taken in and micro straining is applied during spring and summer, because of the higher concentration of organic material and organisms in the water. From Brakel the water is pumped over a distance of 35 km to the pre-treatment in Bergambacht. At Bergambacht the water is treated by rapid sand filtration (filtration rate =5.5 m/h).

The location of the pre-treatment is explained from Dunea's history: before 1975, water from the river Lek (a tributary to the river Rhine) was used. When the intake was relocated to the Afgedamde Maas, it was decided to maintain the pre-treatment in Bergambacht. Whenever a calamity occurs in the Afgedamde Maas or the transport pipeline, the Lek water can still be withdrawn and pretreated on site. This configuration increased Dunea's supply reliability. From Bergambacht, the water is transported to the dune areas via two pipelines, one with a length of 46 km, the other with a length of 57 km (Lekkerkerker-Teunissen, 2009).
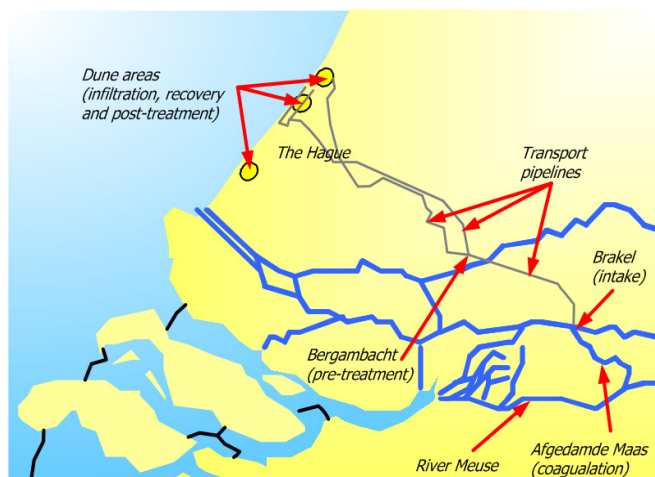
Figure 7-1 Infrastructure Dunea

Pretreated river water is used as influent, and its quality varies seasonally. The temperature for instance can vary from approximately 0 °C during winter times 25 °C during summer. The temperature has been measured and recorded for every performed experiment. Seasonal variations can also be noticed for UVT, DOC concentrations, alkalinity (bicarbonate), nitrite, and nitrate. DOC concentrations are highest during the spring (4 mg/L) and gradually decrease to 3 mg/L in September. From September onwards, DOC concentrations rise again. Nitrate concentrations are highest during winter and spring (near 17 mg/L NO_3^-) and lowest in summer periods (8.6 mg/L NO_3^-). Concentrations of nitrite are generally well below the detection limit of 0.007 mg/L NO_2^-.

7.2.2 Pilot plant design

A pilot scale installation was built at the pretreatment location with a design flow of 5 m^3/h per reactor. Figure XX-1 in Appendix XX shows the process and instrumentation diagram (P&ID) of the pilot installation in Bergambacht including the location of the chemical injection and sampling points. There is a sampling point placed after the point where model compounds are spiked, and one after H_2O_2 is added to the water. Three reactors have been installed, one for each lamp technology:

1. The LP reactor (LBX 10) was obtained from ITT Wedeco (Herford, Germany) and was equipped with four 330 W mercury lamps with an automatic wiping system, thus a total installed power of 1.32 kW. The frequency for automatic wiping of the quartz tubes was set to 1 hour. The electrical ballast used at the LP reactor has an efficiency of 95%. The reactor also included an immersed pre-calibrated UV monitor sensitive to UVC wavelength.
2. The MP reactor (B 2020) was obtained from Berson UV Technology (Nuenen, the Netherlands) and was equipped with two 2200 W mercury lamps with an automatic wiping system, thus a total installed power of 4.4 kW. The frequency for automatic wiping of the quartz tubes was set to 1 hour. The electrical ballast used at the MP reactor has an efficiency of 92%. The reactor also included an immersed pre-calibrated UV monitor sensitive to UVC wavelength
3. The DBD reactor was specially designed by KWR, Philips and LIT UV-technology and constructed by Melamo (Helmond, The Netherlands). The DBD reactor was equipped with four 300 W lamps and no wiping system. The electrical ballast used in the set-up has an efficiency of 93%. The total installed power was 1.2 kW.

The maximum UV dose in the reactors has been calculated by means of CFD modeling (see chapter 8). The average dose (D_{mean}), and the D_{10}/D_{mean} are given in Table 7-1. D_{10}/D_{mean} can be considered as a measure for the performance of a reactor: for an ideal reactor this ratio will be "1", a reactor with a ratio of about 0.66 can be considered as a "good performing" reactor, whereas a standard reactor on the average will show a ratio of about 0.5.

Table 7-1 Mean dose (D_{mean}) and 10th percentile of the dose (D_{10}) for the various UV reactors under different conditions. The lamp power is defined as the UVC output of all the lamps in the reactor. (m^3/h = 0.624 kgal/h)

	Flow rate [m^3/h]	UVT [%]	Lamp power [W]	D_{mean} [mJ/cm²]	D_{10}/D_{mean} [-]
Dunea LP	5	75	600	741	0.57
	5	82	600	927	0.61
Dunea MP	5	75	834	875	0.41
	5	82	834	1150	0.49
Dunea DBD	1	78	145.2	1179	0.56
	3	78	145.2	392	0.56

Dunea's pilot plant consisted of a constant head tank, the peroxide and contaminant feed systems, the UV reactors and the GAC columns.

The influent used for the experiments consisted of river water pretreated by coagulation, microstraining and dual media filtration and was directly withdrawn from the full-scale treatment plant. From the constant head tank the water was pumped to the UV reactors while the water flow for each UV reactor was measured by a magnetic flow meter located after each reactor. Pictures of the LP, MP and DBD pilot reactors at Dunea are shown in Figure 7-3 and Figure 7-4.

In the main line, before splitting the water flow to each reactor, H_2O_2 and other compounds were dosed. Because the composition of the river water shows seasonal variations, experiments were performed frequently during a ten-month period to assess the overall sensitivity of AOP to seasonal variations.

Two GAC columns were used in the setup. Each with a diameter of 0.60 m and a bed height of 2.40 m. With a water flow of 1 m^3/h, this resulted in a empty bed contact time (EBCT) of 40 min and a filtration rate of 3.5 m/h (Figure 7-2). The activated carbon used was Chemviron TL830. During the ten-month

research in phase 1, the GAC columns were fed with rapid sand filtered water. Post UV reactor water was pumped to the GAC columns only during the spiking experiments.

Figure 7-2 GAC columns used in pilot plant at Dunea

Figure 7-3 shows the LP (on the left) and MP (on the right) pilot reactors at Dunea. The DBD reactor is shown in Figure 7-4.

Figure 7-3 LP (on the left) and MP (on the right) pilot plant at Duena

Figure 7-4 DBD pilot reactor at Dunea

7.2.3 Pilot plant operation

During the first phase of the research project at Dunea, the pilot plant was operated intermittently. To capture the seasonal variations of the influent water quality, the selected contaminants were spiked weekly (or at least every other week) and the necessary parameters were consistently monitored. Dosing experiments were conducted with a typical duration of 1.5 hours. Each reactor was de-aerated before starting the experiment. During each experiment, the conditions and settings were monitored and recorded. When a UV setting was changed, it took 15 minutes for the reactor to stabilize and when the H_2O_2 dose was adjusted, it took approximately 4 minutes to reach a steady-state condition, so samples were taken after 6 minutes. To prevent unnecessary spills of the organic micropollutants, the dosing pump was switched off when UV settings were changed.

During the experiments, several set points for water flow were tested. In this report, only results obtained with a flow of 5 m^3/h are shown for the LP and MP lamps, and with 1, 3 or 5 m^3/h for the DBD lamps. The hydrogen peroxide concentration was varied from 0 to 5 or 10 mg/L and the UV dose was adjusted by changing the energy level of the lamp ballasts. The settings for the weekly experiments are shown in Table 7-2.

Table 7-2 Standard experimental settings

Setting number	UV Ballast (%)	Dose H$_2$O$_2$ (ppm)	Model compounds (all settings)
1		10	
2	100	5	
3		0	
4		10	10 µg/L Atrazine
5	80	5	10 µg/L Bromacil
6		0	20 µg/L Ibuprofen
7		10	10 µg/L NDMA
8	60	5	
9		0	

Note: UV dose is not mentioned in this table because it depends on the actual UVT of the treated water.
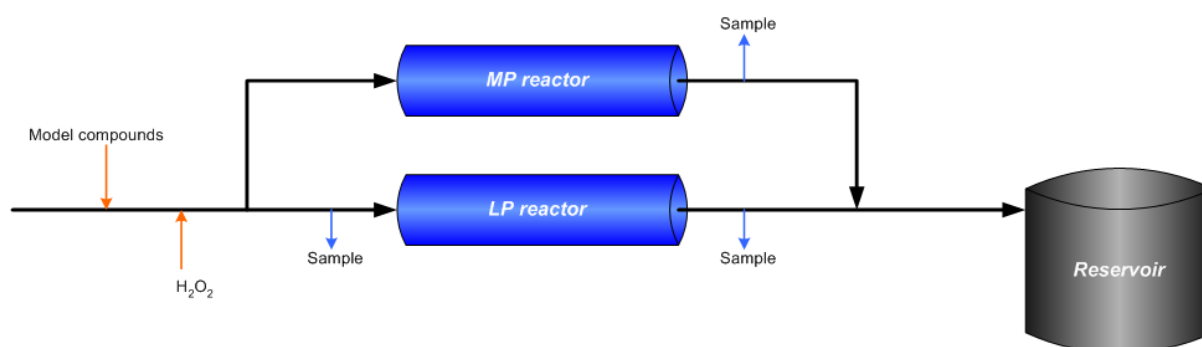
Figure 7-5 Overview experimental set-up

As mentioned before (section 7.1), the excess of H$_2$O$_2$ in the effluent has to be dealt with before infiltration in the dunes.It was studied to what extent water itself is capable of converting this excess. Effluent of the AOP was transferred to 2 L polyethylene bottles, prohibiting the penetration of light. The bottles were stored in a crate suspended in the supernatant water level above the dual media filters in the full-scale treatment plant to guarantee a constant and representative water temperature. Samples were taken and residual peroxide concentrations were determined via spectrophotometry at 420 nm, using TiOSO$_4$ as the reagent.

Samples from the pilot-plant experiments were taken at the indicated sample points (see Figure 7-5), transferred to 40 mL glass flasks and stored in a cooler. Samples were also taken for analysis of the water matrix (nitrite, ammonium, DOC, pH, bicarbonate, UVT) and AOC. All samples were collected within 2 days and transported to a laboratory specialized in water analysis (Het Water Laboratorium (HWL), Haarlem, the Netherlands).

During the experiments several water quality, operational and performance parameters were monitored at the pilot, as shown in Table 7-3. The pilot reactors were monitored during each experiment on a daily basis for flows, UV reactor intensity, and applied UV dose. The UVT of the pilot influent was monitored and the H$_2$O$_2$ concentration was determined before and after the reactors and after the GAC columns. Additionally several other water quality parameters, such as TOC, alkalinity, nitrate and nitrite concentration were tested at various frequencies across the pilot.

Table 7-3 Water quality sampling protocol and pilot performance monitoring

Parameter	Sampling/monitoring frequency
Operational/Performance	
Hydrogen peroxide	Once per day
Flows	Continuously
Reactor UV intensity	Continuously
UV dose (MP)	Continuously
Lamps on/off & run hours	Continuously
Water Quality	
UVT	Each dosing test
pH/Temperature	Each dosing test
TOC	Each dosing test
Alkalinity	Each dosing test
UV scan 200-300nm	Each dosing test
Nitrate	Each dosing test
Nitrite	Each dosing test
Ammonium	Each dosing test
AOC	Each dosing test
Atrazine	At each test condition
Bromacil	At each test condition
Ibuprofen	At each test condition
NDMA	At each test condition

A summary of the standard settings is given in Table 7-2. The installed power (P) was 4.4 kW for the MP reactor, 1.32 kW for the LP reactor, and 1.29 kW for the DBD reactor. In case of the MP and LP reactors, the UV dose was varied during the experiment by changing the ballast power of the reactor. The flow was kept constant at 5 m^3/h. In this way, hydraulic conditions were kept constant during all tests. In case of the DBD reactor, the ballast percentage could not be changed, therefore the flow through the reactor had to be changed, in order to get a different UV dose for the water.

The quartz tubes were wiped automatically every hour. It was visually verified that no fouling had occurred.
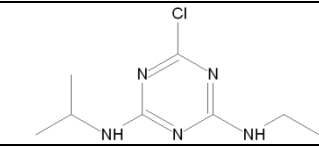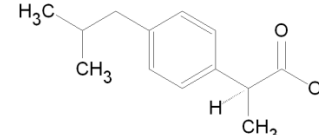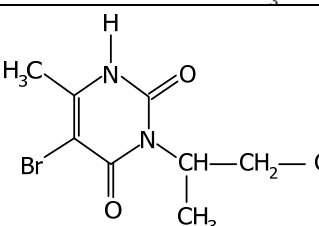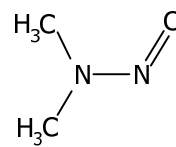
7.2.4 Materials and analytical methodologies

Several contaminants of interest were reviewed by Dunea to be used in this study. Criteria considered for their selection were:
- Past detection in river Meuse and removal by existing treatment processes.
- Representation of major emerging contaminant groups.
- The chemical composition: atomic bonds, and structure of the compounds.
- The degree of degradation by UV advanced oxidation based on the results from the collimated beam tests performed by KWR.
- The potential for destruction by photolysis.
- Analysis capability by HWL.
- Costs and availability of the compounds.

The contaminants selected as reference compounds for spiking were atrazine, ibuprofen, bromacil and NDMA. Their structures and constants related to advanced oxidation and adsorption are shown below. The constant k_{OH} is the second order reaction rate constant between the compound and hydroxyl radicals, while K_{ow} is the octanol-water partition coefficient. K_{ow} is defined as the ratio of the concentration of a chemical in octanol and in water, and it has been correlated to the water solubility of the chemical.

Table 7-4 Selected contaminants for pilot spiking at Dunea

Compound	Structure	Major Groups	k_{OH} $(M^{-1}s^{-1})$	$\log K_{ow}$
Atrazine		Triazine ring, secondary amines	$2.6 \cdot 10^9$ (Haag, 1992)	2.61 (Snyder et al, 2007)
Ibuprofen		Aromatic ring, carboxylic acid	$6.67 * 10^9$ (Yuan et al., 2009)	3.97 (Snyder et al, 2007)
Bromacil		Br-atom, two double oxygen bonds and two alkyl groups		
NDMA		double oxygen bond and two methyl groups	95 ± 5 (Wink et al., 1991)	

10 L spike solutions were prepared at HWL in milli-Q water, containing 100 mg of atrazin (Fluka, 97,5% pure), bromacil (Fluka, 98,6% pure) and N-nitrosodimethylamine (NDMA, pure solution of 1.006 g/cm³ ,Sigma-Aldrich). Separate spike solutions were prepared of 200 mg of ibuprofen (dissolved as sodium salt) in 10 L Milli-Q All compounds were obtained from Sigma-Aldrich, Zwijndrecht, The Netherlands. Both solutions were dosed into a reservoir and diluted further with regular tap water, yielding concentrations of 1 ppm atrazine, bromacil and NDMA and 2 ppm ibuprofen. The influent water was spiked continuously with the solution to obtain a concentration of 10 µg/L of atrazine, bromacil and NDMA and 20 µg/L of ibuprofen in both reactors. A hydrogen peroxide solution (10%) was purchased from Quaron (Zwijndrecht, the Netherlands). The hydrogen peroxide was dosed inline, obtaining a concentration of 0, 5 or 10 ppm H_2O_2 in both reactors. Static mixers had been installed to ensure a homogenous mixture in the reactors.

For analyses of several parameters, the following methods were used:
- The UV transmission of the water was measured at 1 nm intervals using a spectrophotometer and values measured at 254 nm were reported.
- Bicarbonate concentrations weare determined via titration of hydrochloric acid (0.1 n increments) using methyl orange as an indicator.
- Nitrate concentrations were determined with continuous flow analysis (Skalar San⁺⁺). Nitrate is reduced to nitrite using metallic cadmium. A phosphoric acid reagent solution is added and both the nitrite, that was initially present, as well as the nitrite resulting from the reduction of nitrate will diazotize sulphanilamide in the acid solution to diazonium salt which is then coupled with N-s-naphtyl ethylenediamine, forming a red colored complex. The extinction measured at 540 nm is a measure for the amounts of nitrate and nitrite that were already present. Subtracting the concentration of nitrite yields the nitrate level (NEN-EN-ISO 13395, 1997).

- Concentrations of ammonium and nitrite have been determined with an automated discrete photometric analyzer (Aquakem). The spectrometric extinction measured at 660 nm of a blue compound formed by a reaction of ammonium with salicylate and hypochlorite ions in the presence of sodium nitroprusside, is a measure for the level of ammonium (NEN 6604, 2007). Nitrite concentrations are determined using the same method as described above.
- Dissolved organic carbon (DOC) concentrations are determined with Non-Purgeable Organic Carbon Analysis (Shimadzu TOC-V$_{CPH}$). A sample is acidified to a pH of 2-3 with hydrochloric acid and the inorganic carbon is eliminated with a spurge gas (O_2). The remaining TC is measured to determine total organic carbon, and the result is generally referred to as TOC. The sample is introduced in the TC combustion tube, filled with an oxidation catalyst and heated to 680 °C, burning the sample and converting the TC components to carbon dioxide. A carrier gas (flow rate of 150 ml/min) carries the combustion products to an electronic dehumidifier, cooling and dehydrating the gas. The sample combustion products are passed through a halogen scrubber, removing chlorine and other halogens. Finally, the carrier gas delivers the sample combustion products to the cell of a non-dispersive infrared (NDIR) gas analyzer, where the carbon dioxide is detected. The NDIR outputs an analog detection signal that forms a peak, which is proportional to the TC concentration of the sample. With a calibration curve expressing the relationship between the peak area and the TC concentration, the total concentration of DOC can be determined.
- Analysis of the model compounds was performed at HWL using a method especially designed for the efficient analysis of the multiple samples of treatment plant research. An Ultra Performance Liquid Chromatograph (UPLC, Waters Acquity) was equipped with a quaternary pump, combined with a Quattro Xevo triple quadrupole Mass Selective Detector (Waters Micromass). A sample of 15 µL was injected on a UPLC BEH C18 column (5 cm, particle size 1.7 µm, internal diameter 2.1 mm, Waters Acquity) with a flow rate of 0.45 mL/min. The eluent consisted of a mixture of two solvents: A (0.1% formic acid in water) and B (Methanol). Limits of detection were determined by analysis of nine drinking water samples spiked with 0.05 µg/L atrazine and bromacil and 5 µg/L ibuprofen. Recoveries were 0.063±0.003 µg/L atrazine, 0.058±0.004 µg/L bromacil, 4.0±0,6 µg/L ibuprofen. The limit of detection of NDMA was determined using an unspiked process water sample containing about 1.5 µg/L NDMA. Limits of detection, determined as 3 times the standard deviation of these results, were calculated to be 0.008 µg/L for atrazine, 0.013 µg/L for bromacil, 0.61 µg/L for NDMA and 1.8 µg/L for ibuprofen (Houtman, personal communication). Spike compounds for the dosing experiment with the extended spike mixture on the 11th of February 2010 were dissolved in milli-Q-water at HWL and analysed in the samples using GC-MS with purge and trap extraction for the volative compounds and large volume injection for others).
- AOC analysis is done with a bioassay which quantifies the concentration of bacterial cells that have grown on the available carbon in a water sample. Pseudomonas fluorescens P-17 and Spirillum sp. strain NOX are used as test organisms. A 600 mL water sample is inoculated with the bacteria and incubated at 15°C for 10-14 days. During incubation microbacterial growth is measured with plating on nutrient agar. The average net growth is related to the growth of the test organisms on pure solutions of acetate (P-17) or oxalate (NOX) with pre-derived yield values. The final result is reported as acetate C-equivalents (Hammes, 2008).

  Measurements of AOC have an error percentage of 24% (Luc Zandvliet, HWL) and are therefore performed in duplicate. Moreover, the presence of disinfectants such as H_2O_2 interferes with the measurements since it will inhibit bacterial growth. Residual H_2O_2 was not quenched by the addition of sodium thiosulphate. Storage of AOC samples may increase the AOC levels up to 65% (Escobar et al., 2000) within a week. This was determined to be the result of fermentation of biodegradable organic matter (BOM) to AOC by a yeast, Cryptococcus neoformans. The P-17 bacteria particularly benefit from the fermentation products since they have a greater diversity in terms of ability to utilize a larger variety than carbon sources compared to NOX bacteria (Escobar et al, 2000), as a consequence AOC levels determined with P-17 were a lot higher than AOC levels determined with NOX strains.

  The H_2O_2 was analyzed spectrofotometrically at Dunea. The accuracy of the measurement was about 0.5 mg/L

7.3 Results

As mentioned in chapter 7.1, the pilot was operated during the period from March 2009 until January 2010 for the LP and MP reactors. The DBD reactor was operated between November 2009 and January 2010.

7.3.1 Water matrix /Operational parameters

The LP and MP reactors were in operation once or twice a week from March 2009 until January 2010. The DBD-reactor once or twice a week from November 2009 until January 2010. Each experiment lasted approximately 2 hours. During the research period, the pilot influent water showed seasonal variations or changes in water quality due to natural surface water fluctuations and the upstream treatment processes. The influent water quality parameters potentially affecting the performance of the UV advanced oxidation process were UVT, TOC, alkalinity, nitrate and iron concentration. Influent UVT, nitrate and TOC concentration were expected to fluctuate during the year.

The average composition was determined from samples taken during the experimental period, (see below). The quality of the water matrix is described by a multitude of parameters such as the UV transmission, nitrogen compounds, pH, temperature, and dissolved organic matter, collectively called the water matrix.

Table 7-5 presents the water quality data for the pilot influent.

Table 7-5 Quality influent water (pre-treated water from river Meuse)

Parameter	Unit	Minimum	Maximum	Mean
Temperature	°C	5.3	23.7	18.7
UV transmission at 254 nm	%	43.4	82.7	78
pH		7.70	8.1	7.9
Bicarbonate	mg/L HCO_3^-	133	174	147
Ammonium	mg/L NH_3	0.00	0.04	0.01
Nitrite	mg/L NO_2^-	0.0006	0.1603	0.0197
Nitrate	mg/L NO_3^-	8.6	15.9	11.4
DOC	mg/L C	2.97	4.01	3.48
AOC	µg/L C			13

The water matrix negatively influences direct photolysis of a target compound via absorption of ultraviolet light. As a result the UV transmission is reduced. Moreover, absorption of ultraviolet light results in reduced photolysis of hydrogen peroxide and thus a reduced formation of hydroxyl radicals. If the concentration of radical scavenging species in the water matrix (DOC, bicarbonate, nitrite/nitrate) is higher, scavenging for hydroxyl radicals is increased, resulting in a lower availability of hydroxyl radicals for advanced oxidation of the target compounds.

UV-transmission (UVT)

The influent primarily absorbs UV irradiation at wavelengths shorter than 240 nm; at 254 nm the absorbance is 0.105 which corresponds to a UVT of 78%. For wavelengths shorter than 235 nm, nitrate is a more efficient UV absorber than DOC. UV absorbance of bicarbonate and peroxide are relatively low over the entire spectrum. At 254 nm, the absorbance of DOC and nitrate are 0.15 and 0.1 respectively, and the absorbances of bicarbonate (0.015) and peroxide (0.011) are low. The UV absorbance of the pretreated Meuse water shows characteristics of the absorbance spectrum of nitrate, indicating that competition for UV light between the model compounds and nitrate will be relatively high.

Temperature

The intensity of LP lamps is temperature dependent (Stefan, 2004); efficiency can decrease to 30% near temperatures near 0° C (Kramer, 2002). The surface temperature of a low pressure lamp is relatively low, the influence of water temperature may be significant. The optimal water temperature is about 20°C and variations above or below result in lower UV output by low pressure lamps. At temperatures below 5° C, UV output becomes unpredictable and low pressure lamps can fail to start. Medium pressure lamps have higher surface temperatures and are not influenced by the water temperature (Berson UV, 2009).
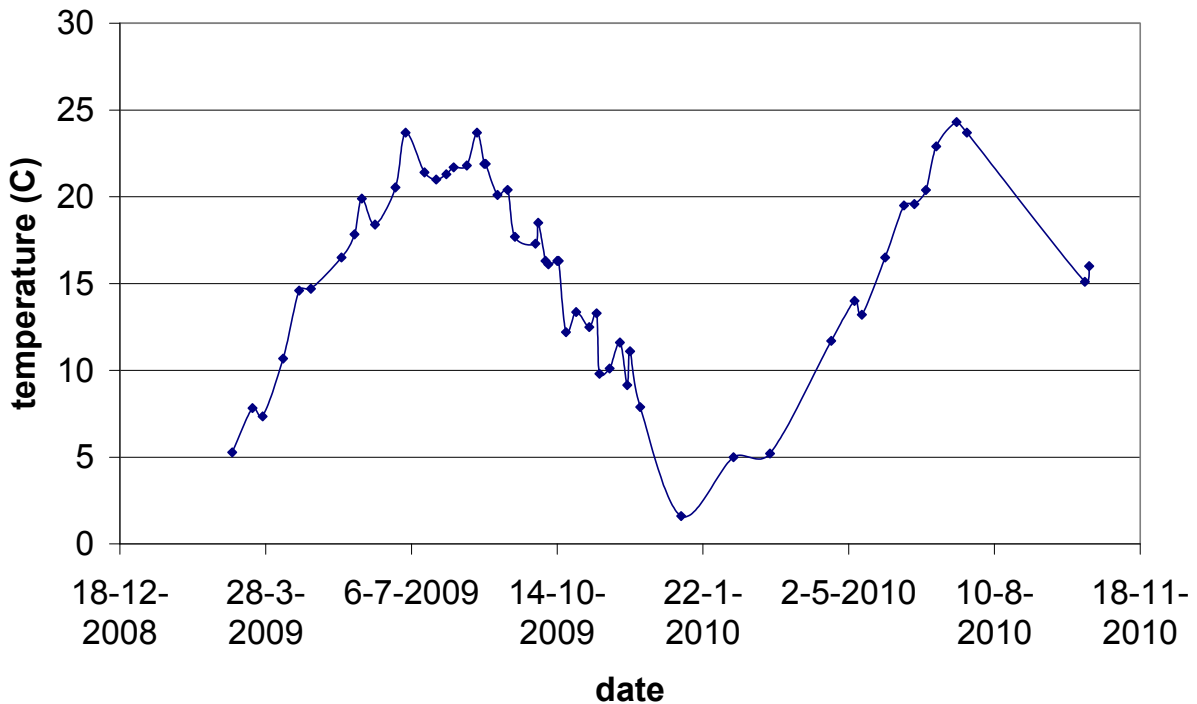
Figure 7-6 Measured temperature of influent water

The lowest and highest water temperatures observed were 5.3 °C (March 5th, 2009) and 23.7 °C (August 8th, 2009) respectively. Unfortunately just one test was performed at a water temperature below 10 °C. During the best performance the water temperature was 21.4 °C. However, during the test performed on June 11[t]h, the water temperature was high (18.3 °C) while the performance of both reactors was poor. Obviously, water temperature is not the only factor affecting the performance (composition may also play an important role).

DOC

Table 7-5 shows that the DOC concentration in the water before UV-oxidation varies between 3 and 4 mg/L with an average of 3.5 mg/l. Between July and October 2009 (i.e., not for the DBD-reactor), the effect of UV/H_2O_2 on DOC concentration in the water was analyzed 8 times and the decrease in DOC concentration from the observed average is shown in Table 7-6. The observed DOC conversion is highest at 10 ppm H_2O_2 addition, regardless of the lamp type, confirming the fact that dissolved organic material acts as a hydroxyl radical scavenger too. A significant amount of DOC conversion occurs when no peroxide is added. This can be a result of direct photolysis of the organic material or through reaction with radicals that are formed from compounds that are already present in the water. DOC conversion is relatively higher using MP lamps compared to using LP lamps. This can be explained from the broad emission spectrum of MP lamps, which results in a far more effective photolysis of organic compounds.

Table 7-6 Average conversion of DOC

| H₂O₂ dose (ppm) | DOC (mg/L C) | | | DOC (µg/L C) | |
	Influent	*Effluent LP*	*Effluent MP*	*ΔDOC_LP*	*ΔDOC_MP*
10	3.48	3.226	3.186	196	237
5	3.48	3.250	3.229	99	120
0	3.48	3.308	3.274	82	105

UV absorbance by atrazine is almost equal to the UV absorbance by DOC at wavelengths >250 nm (see Figure 7-7), which means that the competition for UV light in this part of the spectrum is high. It was observed earlier that the lowest degradation of atrazine was obtained with the highest concentration of DOC (4 mg/L C). This confirms the hypothesis that DOC has a negative impact on the performance of the MP reactor because the UV transmission is reduced.

The absorbance spectra (Figure 7-7) of the model compounds show that photolysis of atrazine (a broad, high peak between 210 and 240 nm) and NDMA (absorbs UV light over the whole spectrum) is possible. The absorbance spectra of bromacil (a broad, low peak between 265-295 nm) and ibuprofen (a broad high peak) show that photolysis of these two compounds is more difficult.
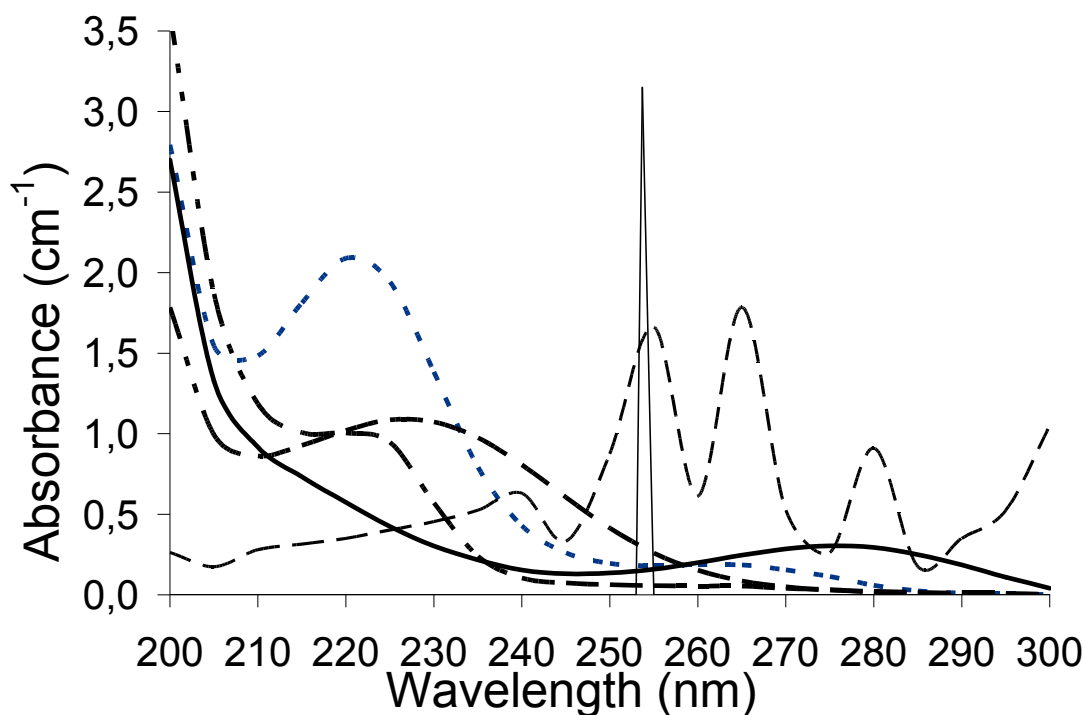
Figure 7-7 Emission spectra of LP and MP lamps and absorbance of of model compounds
Absorption spectra model compounds (HWL, 2009)

         _____ *LP lamp,*   _ _ _ _ _ *MP lamp,* ·········· *atrazine,*   _ ··_ ··_ ·· *ibuprofen,*
         _____ *bromacil,* _ ·_ ·_ ·_ · *NDMA*

Note: emission spectra lamps do not reflect the true scale

UVT and Nitrate

The average nitrate concentration of the pre-treated river water during the experiments was 11.4 mg/L with the lowest concentrations (8.6 mg/L) in summer. It was observed that, when nitrate concentration is high, UVT is low (see Figure 7-8). Degradation levels of the model compounds thus are expected to be high when UVT is high and nitrate concentration is low, and the opposite is expected when the nitrate concentration is high and UVT is low.
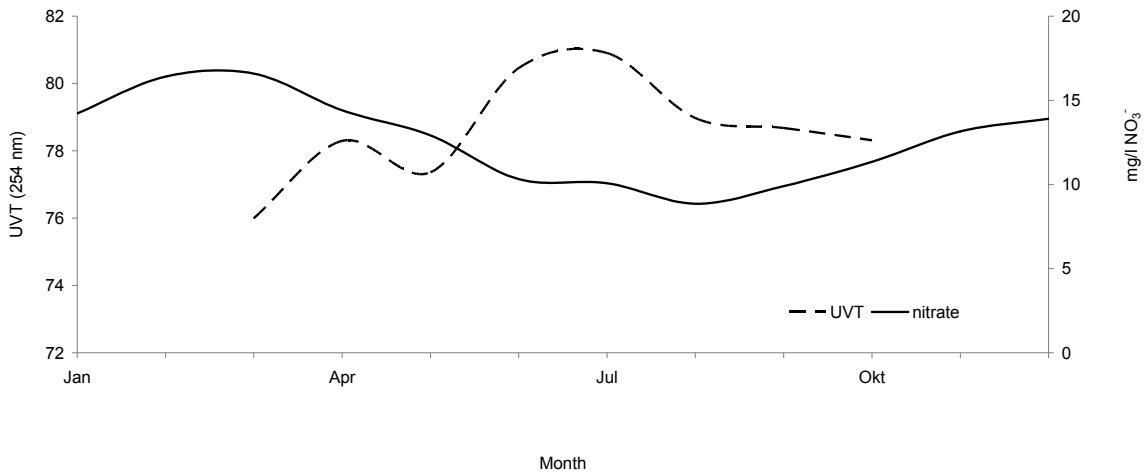
Figure 7-8 Seasonal variations in UVT (monthly average 2009) and nitrate concentration (monthly average 2007 tot 2009) of influent Bergambacht.

According to Figure 7-7 and Figure 7-9 the absorbance of atrazine is higher than that of DOC, whereas the absorbance peak of ibuprofen is lower than the peak of DOC. Nitrate absorbs more UV light than bicarbonate and DOC, especially between 200-250 nm (see Figure 7-9). Consequently the influence of higher nitrate concentrations on the degradation of model compounds is expected to be higher than the influence of DOC and bicarbonate.
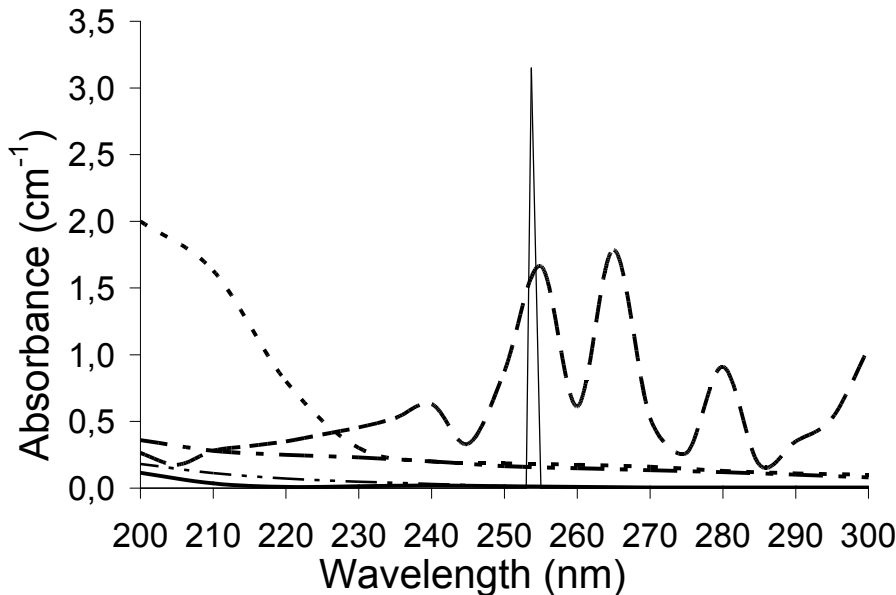
Figure 7-9 Absorbance of nitrate, DOC and H_2O_2 and HCO_3- vs. emission spectra; emission spectra lamps (Berson, Wedeco), bicarbonate (adapted from de Ridder, 2006). Note: emission spectra lamps do not reflect the true scale.

——— LP lamp, ––––– MP lamp, ••••••••••• nitrate,–··–··– H_2O_2 10 mg/L, -··–··–··- DOC 3 mg/L
━━━ bicarbonate

Alkalinity and bicarbonate

Based on literature and knowledge of pH influence, the influent water used in the tests does not contain carbonate, or only in a very low (negligible) concentration: the pH of the water is around 8 (calcium-carbonate equilibrium). This is relevant as the radical scavenging rate of carbonate (3.9×10^8 M^{-1}s^{-1}) is higher than the scavenging rate of bicarbonate (8.5×10^6 M^{-1}s^{-1}). The value of the pH itself was relatively constant (see Table 7-5) during the experimental period and no effect on the degree of degradation could be distinguished.

The average bicarbonate concentration during the experiments was 147 mg/L HCO$_3^-$ with a maximum and minimum of 133 and 174 mg/L, respectively. From Figure 7-9 it can be concluded that the competition for UV light between bicarbonate and the model compounds is small: the UV absorbance of bicarbonate is considerably lower than the UV absorbance of the model compounds over the entire spectrum. As the changes in bicarbonate concentration are relatively small and competition for UV light is negligible, the influence of bicarbonate on the degradation of model compounds will be low.

7.3.2 Degradation of organic micropollutants

The achieved degradation depends on the water quality, which varies over the year. For MP and LP, 24 experiments were performed, mostly in summer with good performance because of the relatively high UVT. For DBD, 6 experiments were performed in winter (worst case, because of lower UV-transmission).

The degradation of the model compounds is defined as the reduction in concentration:

$$-\frac{dC}{dt} = \frac{C_i - C_e}{C_i} * 100\%$$

Degradation of model compounds

The conversion of atrazine, bromacil, ibuprofen and NDMA in the MP and LP pilot plant was measured as a function of the season. The data are shown in *Figure 7-10* to Figure 7-13. When these figures are compared with Figure 7-8, it can be observed that generally the conversion of organic micropollutants increases with increasing UV transmittance. Thus, seasonal variations in UV-T, composition and temperature are a parameter to take into account when deciding on process conditions.
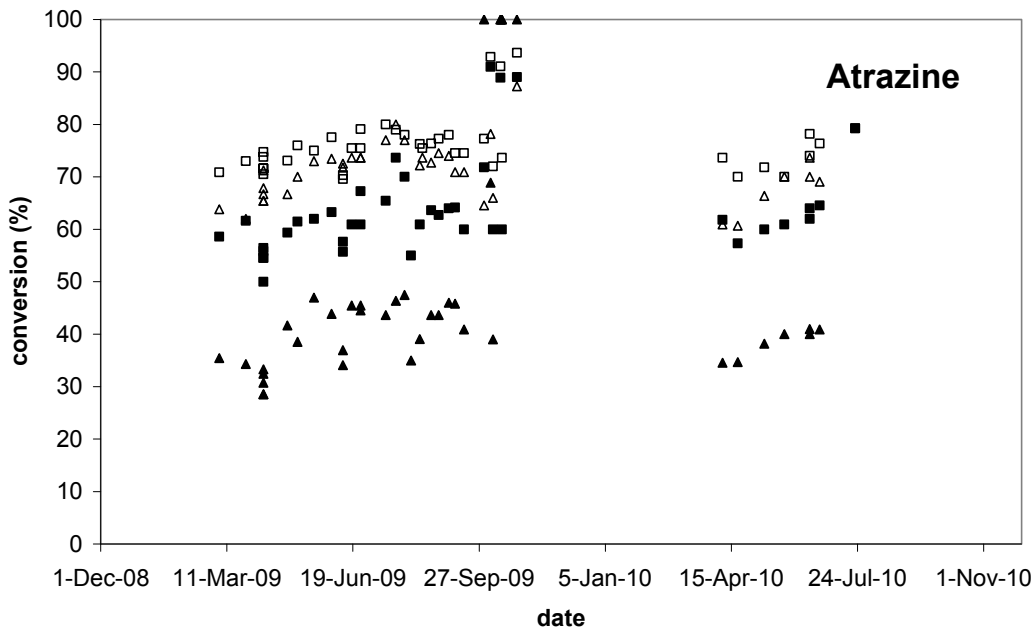
Figure 7-10 Degradation of atrazine in the Dunea pilot reactors (100% power, 5 m³/h) ■ *MP photolysis (0 mg H₂O₂/L),* □ *MP 10 mg H₂O₂/L,* ▲ *LP photolysis (0 mg H₂O₂/L),* △ *LP 10 mg H₂O₂/L*
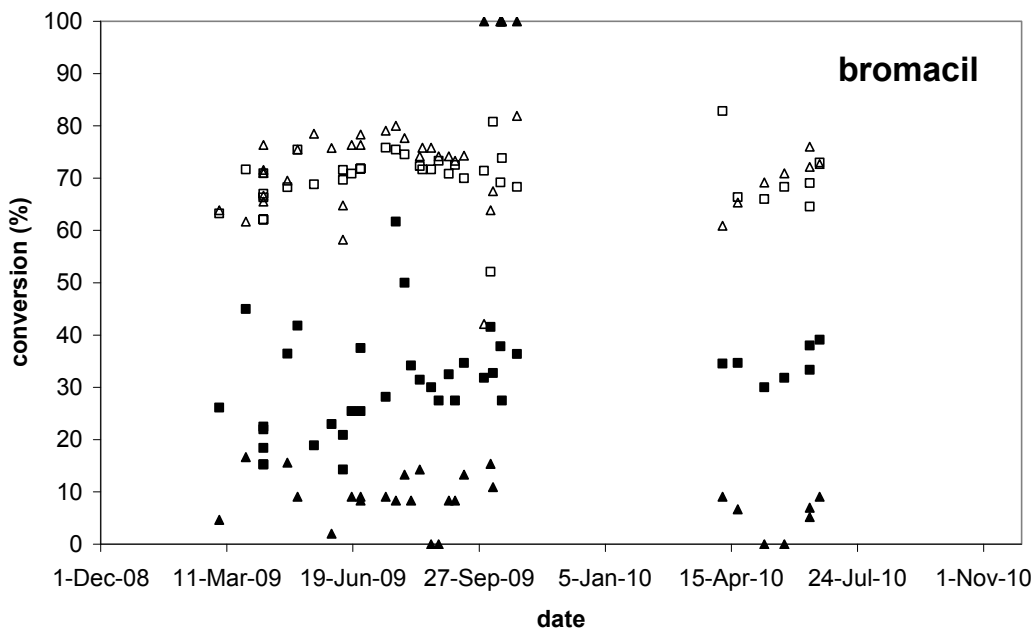
Figure 7-11 Degradation of bromacil in the Dunea pilot reactors (100% power, 5 m³/h) ■ *MP photolysis (0 mg H₂O₂/L),* □ *MP 10 mg H₂O₂/L,* ▲ *LP photolysis (0 mg H₂O₂/L),* △ *LP 10 mg H₂O₂/L*
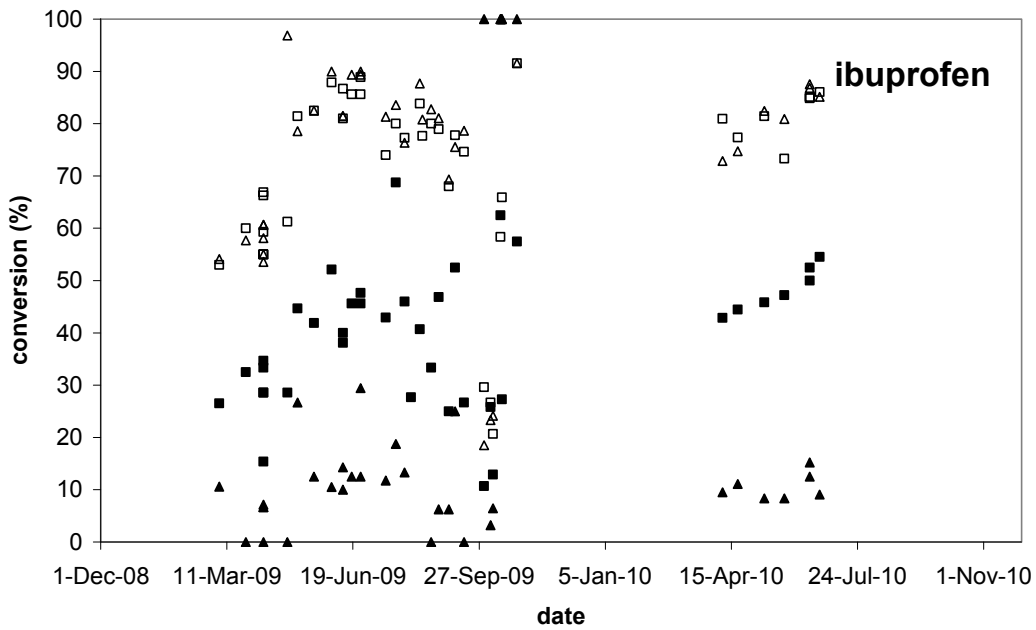
Figure 7-12 Degradation of ibuprofen in the Dunea pilot reactors (100% power, 5 m³/h) ■ MP photolysis (0 mg H₂O₂/L), □ MP 10 mg H₂O₂/L, ▲ LP photolysis (0 mg H₂O₂/L), △ LP 10 mg H₂O₂/L
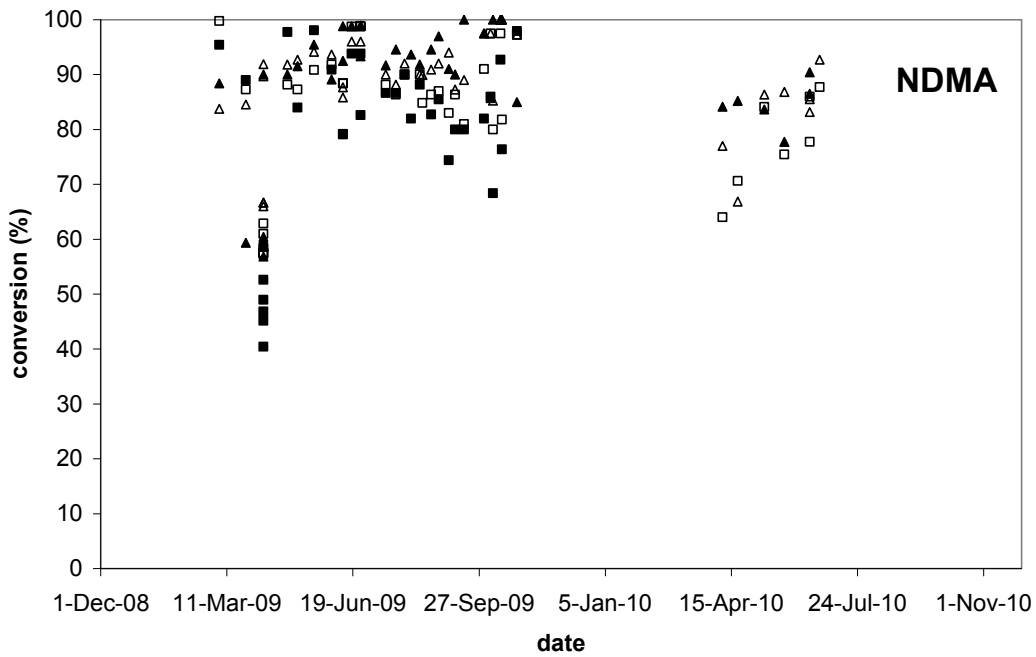
Figure 7-13 Degradation of NDMA in the Dunea pilot reactors (100% power, 5 m³/h) ■ MP photolysis (0 mg H₂O₂/L), □ MP 10 mg H₂O₂/L, ▲ LP photolysis (0 mg H₂O₂/L), △ LP 10 mg H₂O₂/L

The conversion obtained in the DBD reactor is shown in Figure 7-14 . The flow in the DBD reactor was varied, resulting in a varying UV dose. In chapter 8 the dose distribution in the reactor is calculated for a flow of 1 and of 3 m³/h, using CFD. In Figure 7-14 it can be seen, that by increasing the flow, and thus decreasing the UV dose applied, the conversion of all four compounds decreases.
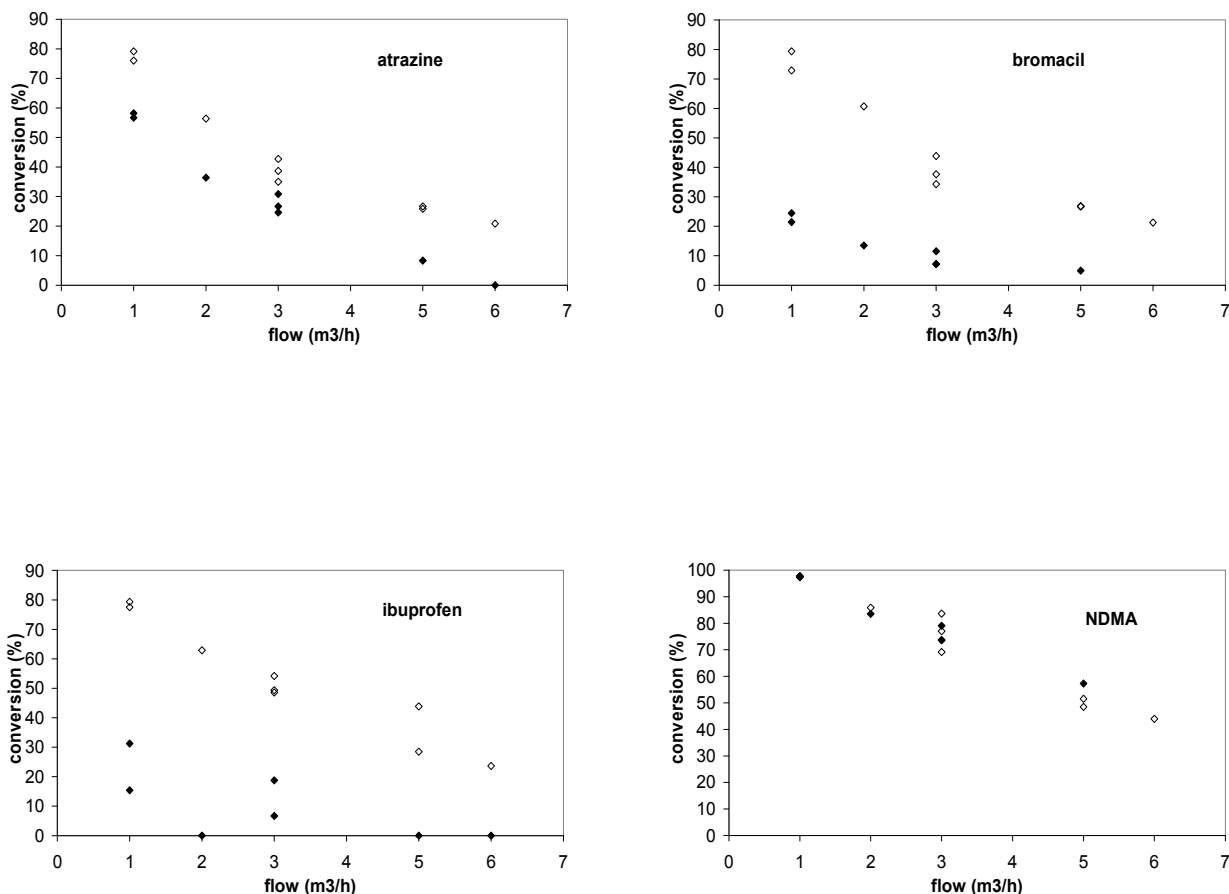
Figure 7-14 Conversion of model compounds in the DBD reactor as a function of flow. ◆ photolysis (no H_2O_2), ◇ 10 mg H_2O_2/L

Comparing the degradation achieved by the three reactors, the following observations were made:
- For the 4 model compounds, degradation by MP-UV/H_2O_2 and LP-UV/H_2O_2 is approximately at the same level. Degradation by DBD-UV/H_2O_2 at the same UV dose seems to be always lower or equal to the degradation obtained with MP or LP lamps.
- Without H_2O_2 (i.e. with photolysis only), degradation of atrazine, bromacil and ibuprofen is highest for the MP reactor and lowest for the DBD-reactor. Degradation with the LP reactor lies between that of the MP and DBD reactors. For NDMA, a compound that is known to be easily degraded by photolysis (absorption maximum at 227 nm (Lee 2005), the degradation by both LP and MP is large, and, at the same level in these pilot reactors at the applied UV doses. Again, the DBD reactor shows the lowest degradation. The MP-lamps emit a broad spectrum of polychromatic light (coinciding with the absorbance spectra of the model compounds) while the DBD-lamps emit a small spectrum

of polychromatic light around 237 nm and the LP-lamps emit monochromatic light (254 nm). Therefore, in general the photolytic capacity of MP lamps will be higher than that of the LP and DBD lamps, as the chances that a compound is irradiated at a wavelength it can absorb are larger when a broader spectrum is applied.

The fact that the degradation in the LP and MP reactors is comparable is more or less a coincidence. The actual conversion obtained depends on the UV dose applied, flow conditions, the reaction rate constants (which for photolysis depend on the wavelength) and the quantum yield at the wavelengths involved. However, more interesting is the comparison based on the amount of energy that is needed to degrade organic micropollutants. For this comparison, the E_{EO} calculation is needed (see chapter 3).

E_{EO} for the 4 model compounds has been plotted in Figure 7-15 and Figure 7-16 for (settings 5 m³/h, 100% ballast power) 10 mg/L H_2O_2 and 0 mg/L H_2O_2, respectively. For DBD two bars are shown:
- DBD, which shows the E_{EO} that is calculated with the current energy efficiency (7%) of the ballast system.
- DBD potential, which shows the E_{EO} that has been corrected to a future expected energy efficiency of 24%. However, it is not certain yet that this energy efficiency will be achieved.
- The efficiency of the MP reactor was relatively low (see also Table 8-4). This means that the results for an MP reactor potentially could be about 20% better than what was measured in this pilot reactor.

For UV/H_2O_2-oxidation it can be concluded that in general MP has the highest E_{EO}, LP the lowest. The E_{EO} for the present DBD lamp is in between the E_{EO} for MP and LP lamps. When the DBD energy efficiency is corrected for the potential efficiency, the DBD reactor performs almost at the same level as the LP-reactor.
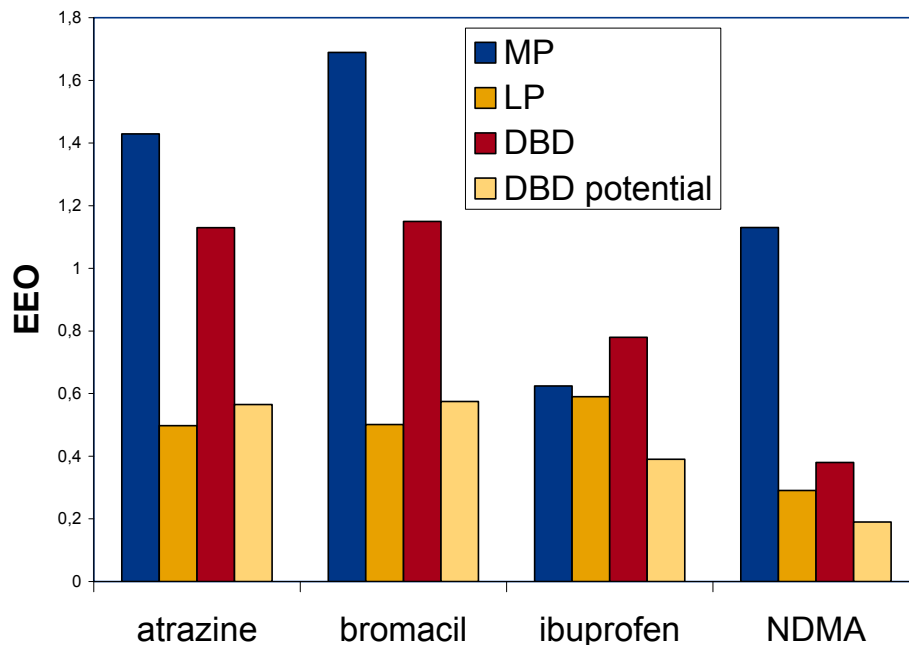
Figure 7-15 Average E_{EO} (kWh/m³) for the model compounds during UV/H_2O_2-oxidation (10 mg/L H_2O_2 and 100% ballast power) 5 m³/h for MP and LP reactors, and 3 m³/h for the DBD reactor .(1 kWh/m³ = 0.264 kWh/kgal).
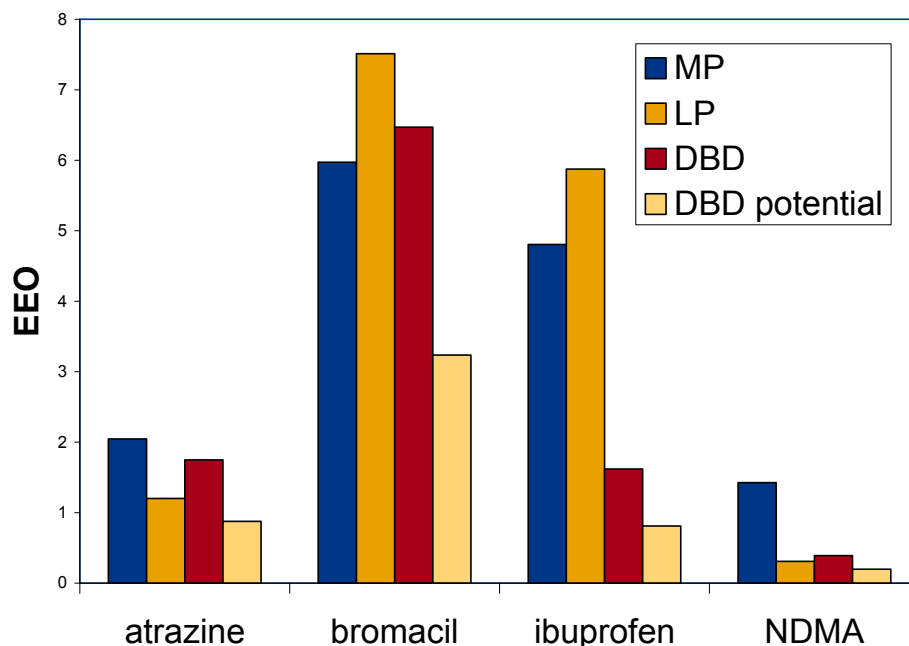
Figure 7-16 Average E_{EO} (kWh/m³-order) for the model compounds during UV-photolysis (0 mg/L H_2O_2 and 100% ballast power) 5 m³/h for MP and LP reactors, and 3 m³/h for the DBD reactor .(1 kWh/m³ = 0.624 kWh/kgal)

For UV-photolysis (without H_2O_2) it can be concluded that in general uncorrected DBD has a high E_{EO}, DBD potentially the lowest. As the DBD lamp still is in the development phase, it will strongly depend upon the final energy efficiency of the DBD lamp that will be reached, whether or not this lamp will be an interesting alternative to LP or MP lamps.
NDMA is the compound with the lowest Eeo and most efficient photolysis as expected from literature.

Degradation of other organic micropollutants

On February 11th 2010, several other organic micropollutants were spiked and the effect of the three UV/H_2O_2 reactors was determined. The results are shown in Figure 7-17. For the LP and MP reactors, a flow of 5 m³/h was set, the flow through the DBD reactor was 3 m³/h. H_2O_2-concentration was 10 mg/L for all three reactors.

From the figure below the following conclusions can be drawn:
- All compounds are degraded 20% or more.
- Atrazine and diuron are the compounds hardest to convert by UV/H_2O_2 oxidation. This had not been expected. From the experiments carried out at KWR and at GCWW (see chapters 3 and 6) it already had been observed that MTBE is relatively hard to degrade by UV/H_2O_2 oxidation, or in other words, that the E_{EO} for the conversion of MTBE is the highest (so, the conversion of MTBE requires more energy than the conversion of the other compounds studied). At the moment we have no real explanation for this observation, other than that the flow conditions in the pilot may play an important role.
- The degradation percentages of the DBD-reactor are the lowest. But to compare DBD-performance with performance of the other reactor, E_{EO} values need to be compared. Since this was only a single experiment, E_{EO} was not calculated and used to compare reactors.
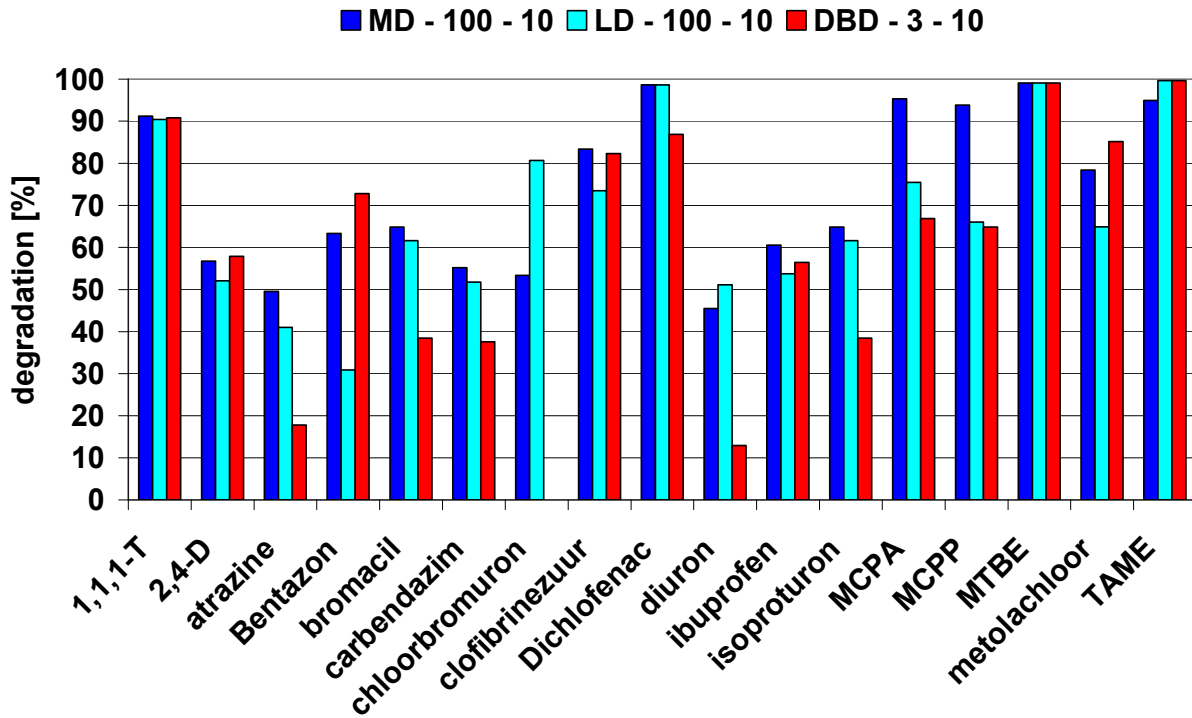
Figure 7-17 Degradation of various organic micropollutants by the three UV-reactors of Dunea (10mg/L H_2O_2 and 100% ballast power).

7.3.3 Formation of by -products

In this sub paragraph, formation of byproducts nitrite and AOC is described. Research into formation of genotoxic by-product is described in chapter 9.

Nitrite formation

Concentrations of nitrite measured in the influent were below the detection limit (<7 µg/L) and significantly increased using MP lamps. The concentration of nitrite observed in the effluent of the MP reactor varied from 0.44 to 0.68 mg/L NO_2^-, depending on the H_2O_2 dose (see Figure 7-18).
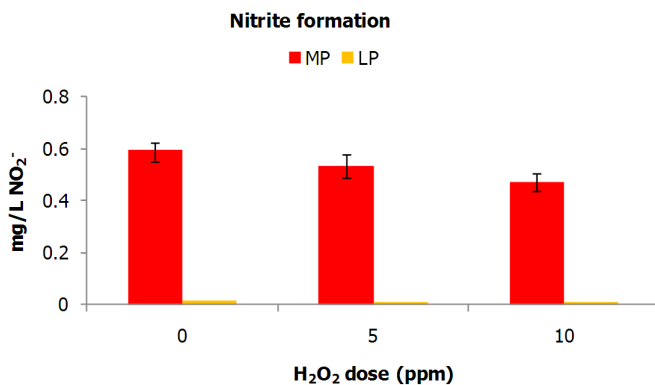
Figure 7-18 Average nitrite formation resulting from AOP using LP lamps and MP lamps, N=7, error bars represent minimum and maximum.

Nitrite concentrations observed in the MP effluent during the research in Bergambacht were highest in the absence of H_2O_2 (0.61 mg/L). Dosing 5 and 10 ppm H_2O_2 yielded nitrite concentrations of 0.56 and 0.48 mg/L NO_2^- respectively. However, results from collimated beam experiments performed by Sharpless et al. (2003) show that H_2O_2 addition during polychromatic UV irradiation significantly increases the levels of nitrite formed compared to solutions without hydrogen peroxide. Nitrite production rate is increased when the hydrogen peroxide concentration is increased from 5 to 10 mg/L (Sharpless et al., 2003). The differences between the results in Bergambacht and Sharpless et al (2003) can not be explained yet.

PWN Water Supply Company observed that nitrite concentrations increase to 100-300 µg/(average 160 µg/L) with a MP-UV dose of 600 mJ/cm² and 6 ppm H_2O_2 at their full scale UV/H_2O_2 plant in Andijk (The Netherlands). The nitrate concentrations in pre-treated IJssel Lake water in general are 6-12 mg/L, and during the research in Bergambacht a range of 8.5-12 mg/Lwas measured. This fact combined with the higher UV dose applied can explain why nitrite levels found in this research are higher.

Observed nitrite formation applying LP UV is generally well below 0.015 mg/L, regardless of the hydrogen peroxide doses and can be considered negligible in relation to background concentrations, which is in accordance with results found in other experiments.

AOC formation

AOC levels in the pre-treated river water (without H_2O_2 addition) were between 9.5 to 16.3 µg/L, with an average of 12.9 µg/L. Influent concentrations with 10 ppm H_2O_2 addition show large variations (0 – 24 µg/L) but half of the measured concentrations were close to 0 µg/L. It is possible that H_2O_2 in those samples had not been completely quenched. Influent concentrations with 5 ppm H_2O_2 addition were measured only twice and in both cases the results were as expected (10.2 and 13 µg/L). It is concluded that AOC determination in samples taken from the influent water is unreliable in the presence of high peroxide concentrations when quenching is incomplete. Based on the measured concentrations (0 and 5 ppm H_2O_2), it is concluded that the average AOC concentration in pre-treated river water was about 13 µg/L.

Measured AOC levels in the effluent (10 ppm H_2O_2) of both LP and MP reactors show a large variation (possibly due to incomplete quenching of the H_2O_2). This makes it difficult to make a conclusive statement about the extend of AOC formation. The AOC level may increase up to 100 µg/L, but as the results obtained are neither consistent nor conclusive, it was decided not to include any graphs on the AOC formation in this report.
Effluent AOC levels for advanced oxidation with 5 ppm H_2O_2 were only determined twice, and in both cases resulted in higher AOC concentrations using LP lamps than using MP lamps: 81 and 47 µg/L and 65 and 40 µg/L, respectively. This does not correspond well with results found in other research (IJpelaar et al., 2006, 2007) in which LP UV lamps were found to result in a lower AOC formation than MP UV lamps. However, since AOC concentrations only were determined twice, this could simply be a coincidence; more measurements are required to confirm these results.

AOC levels measured in the effluent when 0 ppm H_2O_2 was applied (i.e., photolysis only) show a more constant pattern and are approximately 25 µg/L in the LP effluent and 47 µg/L in the MP effluent. It is concluded that AOC formation resulting from photolysis using LP lamps is twice as low as AOC formation using MP lamps.

PWN Water Supply Company applies UV/H_2O_2 in a full scale drinking water plant for disinfection and degradation of organic micropollutants. The applied MP UV dose of 600 mJ/cm² and H_2O_2 dose of 6 ppm results in AOC levels of 100-150 µg/L C (influent levels 5-33 µg/L), which is considerably higher than levels found in this research: 46-89 µg/L (10 ppm H_2O_2, 850 mJ/cm²) and 40-65 µg/L (5 ppm H_2O_2, 850 mJ/cm²). DOC levels found in pre-treated Lake IJssel water are 2.5 mg/L (Martijn et al, 2007) while pre-treated Meuse water contains 3.5 mg/L of DOC.

Conclusions regarding AOC formation

The concentration of AOC in the influent water is approximately 13 µg/L. AOC formation is significantly enhanced in the presence of H_2O_2 using LP lamps and MP lamps. Effluent AOC levels applying advanced oxidation (5 and 10 ppm H_2O_2) show that AOC concentrations after LP UV/H_2O_2 and MP UV/H_2O_2 are at about the same level. In case there is no significant increase, no further polishing steps are required. Applying only direct photolysis yielded AOC concentrations of 25 µg/L (LP lamps) and 47 µg/L (MP lamps). At such an increase in AOC an additional polishing step will be required, as otherwise the regrowth potential will be too high.

From literature it was concluded that UV doses <100 mJ/cm² do not result in significant AOC formation (IJpelaar et al, 2007) regardless of the lamp type applied. Recent research (van der Maas et al, 2009) showed that LP UV resulted in a 1.5-time increase in AOC concentrations (from 11 to 16 µg/L) at a dose of 40 mJ/cm². Since the applied LP UV dose in this research is 20 times greater, it is not surprising to find considerably higher AOC concentrations in the effluent during photolysis. AOC formation is at the same level or higher using MP lamps compared with LP lamps.

Based on the results obtained in this work package, in combination with results of other companies, it seems that AOC formation increases during advanced oxidation compared with photolysis. This may be caused by reactions with hydroxyl radicals, but it is difficult to determine, as the remaining peroxide is disturbing the measurements. In general, the AOC formation observed in both reactors is relatively low and similar in the presence of hydrogen peroxide (i.e., when treated by UV/H_2O_2).

7.4 Conclusions

7.4.1 General remarks on results

- The experiments with DBD lamps were performed in winter (lowest UVT), the experiments for MP and LPmostly in summer (highest UVT). As a result of the higher UVT, all UV reactors will be more effective in summer than in winter. In this case this was a disadvantage for the comparison of the DBD-reactor, which was tested in winter.
- The ballast efficiency of the DBD reactor was poor (7%) because the lamps are prototypes and still need to be optimized. The expected efficiency of a full scale lamp is 24%. Although this high energy efficiency has not been proven yet, corrected E_{EO} values for a system with 24% energy efficiency were also used.
- Because the typical lifespan of MP and LP lamps is in thousands of hours, the decrease of the UV output within the timeframe of the pilot tests is negligible. The lifespan of the prototype DBD lamp is expected to be a few hundred hours and decrease of UV output was observed already within the 6 experiments performed.

7.4.2 Conclusions

- Overall, the MP reactor E_{EO} values for the four selected contaminants (atrazine, bromacil, ibuprofen and NDMA) were greater than those of the LP reactor, as was expected by the efficiencies of these two lamp technologies. The E_{EO} values of the DBD reactor seemed to be relatively high, but when values were considered for future expected energy efficiency of the ballast system, the E_{EO} values became the lowest.
- For UV photolysis (without H_2O_2) it can be concluded that in general DBD with the present efficiency has a relatively high E_{EO}, whereas potentially E_{EO} for DBD may be the lowest. NDMA is the compound with the lowest E_{EO}, so NDMA is the compound that is photolyzed efficiently as expected from its absorption spectrum.

- When a wide variety of organic micropollutants was tested (once), atrazine and diuron were the hardest compounds to convert by UV/H_2O_2-oxidation, whereas MTBE showed a good conversion. This had not been expected, as from other experiments it is known that MTBE is hard to degrade by UV/H_2O_2-oxidation. However, this may strongly depend on the water matrix. In literature it has been shown that the presence of scavengers in the water, for example, has a negative effect on MTBE degradation (Tawabini, 2009). Other authors also found, that the degradation of MTBE is largely affected by the water quality, and thus by the pretreatment applied (Alnaizy, 209; Li, 2008).
- Regarding by-product formation: nitrite concentration increased significantly using MP lamps. The concentration of nitrite observed in the effluent of the MP reactor varies from 0.44 to 0.68 mg/L NO_2^-. Unexpectedly, nitrite concentrations seemed to be lower when the H_2O_2 dose increased. Observed nitrite formation applying LP UV is generally well below 0.015 mg/L, regardless of the H_2O_2 dose and can be considered negligible, which is in line with results found in other experiments.
- Measured AOC levels in the effluent (10 ppm H_2O_2) of both the LP and MP reactor show a large variation which makes it difficult to make a conclusive statement about the amount of AOC formation. It is concluded that formation of AOC increases resulting from advanced oxidation (10 ppm H_2O_2) processes.
- AOC levels measured in the effluent without H_2O_2 (i.e., photolysis only), show that AOC formation resulting from photolysis using LP lamps is twice as low as AOC formation using MP lamps. Both with LP as well as with MP lamps, however, the AOC level seems to increase after photolysis. As a result, a polishing step will be required after the UV process, in order to prevent regrowth.

7.4.3 Future plans

Based on the remarks and conclusions above, Dunea decided to extend the pilot research with LP and MP lamps. The anticipated lamp life for DBD was too short to conduct experiments with continuous operation of the DBD system.

This research was part of a larger investigation at Dunea, in which several technologies are compared in order to develop a robust purification process for the future. Part of this investigation already has been published (Lekkerkerker 2009), and it will be published in future papers and the PhD thesis of K. Lekkerkerker-Teunissen.

Modeling of reactor performance

KWR

Authors: B.A. Wols, C.H.M. Hofman-Caris

8 Modeling of reactor performance

8.1 Introduction

The efficacy of UV systems is largely determined by the hydrodynamic processes occurring within the system. The movement of water parcels inside the UV system defines the amount of UV radiation received by these water elements (UV dose). The spatial differences in the UV radiation field and the differences in residence times of the water elements cause a certain distribution of UV doses. From this UV dose distribution, the disinfection and/or oxidation performance can be determined. For a proper estimation of the dose distribution in a UV system, knowledge of the transfer and mixing processes is therefore essential. Computational fluid dynamics (CFD) is a powerful tool to simulate these processes (Sozzi and Taghipour, 2006; Wols, 2010)

A large variation exists in the geometries of UV reactors, which may result in completely different hydrodynamic processes occurring within each system. As a result, the dose distribution, disinfection and oxidation may be different, even though the flow rate, lamp power and water absorbance are similar. Because of the large number of reactor types available, the reactor type with the best performance could not be identified prior to the research. Therefore, the different reactors used in this research were assessed by CFD to calculate their UV dose distribution and "efficiency".

8.2 Material and methods

A finite element package, COMSOL v3.5a, was used for the CFD modeling. The Reynolds averaged Navier-Stokes equations, with a closure given by the equations for the turbulent kinetic energy and turbulent dissipation (k-ε model), were solved using this model. The equations were solved using a direct matrix solver (PARDISO) and convergence was obtained when the relative error on the solution was less than 0.001. The domain is discretized with tetrahedrons using quadratic finite elements.

In the resolved flow field, particles were released that traced the pathways of the fluid parcels. Particles were assumed to be small enough to move in conjunction with the flow. The particle movements consist of an advection displacement induced by the computed velocity field and a displacement induced by turbulent diffusion, which is determined from the computed k and ε. In order to account for this latter contribution, a diffusive velocity is constructed by drawing a random variable from a uniform distribution with mean zero and a standard deviation which is in agreement with the turbulent diffusion coefficient. The UV irradiance was calculated by a MSSS model (Liu et al., 2004), which divided the UV lamp into 200 segments and calculated the optical pathway and corresponding UV irradiance from each segment of the lamp to each mesh point of the computational domain. The radiation model accounted for refraction and reflection at the interfaces (air-quartz and quartz-water), UV absorbance in quartz and in water. Due to refraction at the quartz surface, the light rays are diverged into a smaller area than without refraction, which too has to be corrected in the calculation of the UV irradiation. This factor is called focusing (Liu et al., 2004).

The UV dose of a particle was calculated by integrating the UV irradiance over the particle's path. The UV dose distribution was determined from the doses of the particles that crossed the reactor outlet. The reactor outlet was selected at a position where the UV irradiance was diminished to zero. Validation of the predicted flow fields and particle tracks are reported in Wols (2010).

Advanced oxidation model (UVperox)
In advanced oxidation processes, hydrogen peroxide is added to the UV reactor. Organic compounds can be degraded by the effect of direct photolysis and/or the reaction with hydroxyl (*OH•)* radicals. The hydroxyl radicals form when the hydrogen peroxide is irradiated by the UV lamps. The reaction by photolysis for a certain compound N_i (for example organic compound or hydrogen peroxide) is given by (Sharpless and Linden, 2003)

$$[4] \qquad \frac{d[N_i]}{dt} = -E_{CFD} \frac{1-10^{-A}}{A} \Phi_{N_i} \varepsilon_{N_i} [N_i],$$

where Φ represents the quantum yield (a measure of the photon efficiency of a photochemical reaction, defined as the number of moles of reactant removed or product formed per einstein of photons absorbed), ε the molar extinction (L/mol/cm) and A represents the absorption, which can be calculated from the summation of the molar extinction multiplied by the concentration over all the compounds in the water ($A = L \sum \varepsilon_{N_i}[N_i]$) or from the 1 cm transmittance (T_{10}) of the water ($A = -10\log(T_{10})$). E_{CFD} is the UV photon flux (mmol/cm²/s), for which a unit conversion is needed from the UV intensity I (mW/cm²) as calculated by the CFD model:

$$[5] \qquad E_{CFD} = \frac{I}{N_A E_f},$$

where E_f is the energy of a photon (J) and N_A is Avogadro's constant (1/mol).

It is assumed that upstream of the reactor the hydrogen peroxide mixes perfectly with the water. The $OH\bullet$ radicals react very quickly with different contaminants in the water so that a steady-state concentration of $OH\bullet$ radicals immediately forms (Sharpless and Linden, 2003; De Laat et al, 1999). The equilibrium concentration for the $OH\bullet$ radicals is then calculated by:

$$[6] \qquad [OH\cdot] = 2E_{CFD} \frac{1-10^{-A}}{A} \frac{\Phi_{H_2O_2} \varepsilon_{H_2O_2} [H_2O_2]}{\sum k_i[N_i]},$$

where k_i represents the reaction rate of contaminant i (L/mol/s) with $OH\bullet$ radicals and $[N_i]$ the concentration of contaminant i (mol/L). The factor two is introduced because two $OH\bullet$ radicals form when the hydrogen peroxide is irradiated by UV. The factor $\sum k_i[N_i]$ contains the reactions with all the compounds (including peroxide and bicarbonate) in the water. Since the number of compounds can be very large, the reactions with the background components in the water were not individually solved for all the background components but treated as one overall reaction with a rate of 50,000 (s⁻¹).

The background reaction rate was determined from the collimated beam results in Dunea water. For all the reactors assessed by CFD, this value was assumed for the background reaction rate. Although different water types were used (Dunea water and GCWW water), the collimated beam results showed little differences of atrazine removal between these waters (44% Dunea water versus 41% GCWW water at 300 mJ/cm² and 65% Dunea water versus 74% GCWW water at 600 mJ/cm²).

The (first order) conversion of a contaminant N_0 by direct photolysis and reaction with $OH\bullet$ radicals can be written as (where one contaminant reacts with one $OH\bullet$ radical):

$$[7] \qquad \frac{dN_0}{dt} = -E_{CFD} \frac{1-10^{-A}}{A} \left(\Phi_N \varepsilon_N + 2 \frac{\Phi_{H_2O_2} \varepsilon_{H_2O_2} [H_2O_2]}{\sum k_i[N_i]} k_0 \right) N_0,$$

which represents a first-order reaction. The reduction of H_2O_2 due to the production of $OH\bullet$ radicals is assumed to be small, so that the H_2O_2 concentration remains constant in the calculation. Equation 7 is solved over the path of a particle, so that the conversion is calculated for each particle. The chemical properties of the compounds of interest are shown in Table 8-1.

Table 8-1 Reaction constants used for the UVPerox model calculations

compound	Molar mass (g/mol)	Quantum yield (mol/Einstein) Φ	Molar ext. coeff. (mol^{-1}cm^{-1}) ε_N	Reaction constant (L/mol/s) k_N	Lit. ref.
H$_2$O$_2$	34	0.5	18.6	$2.7*10^7$	De Laat 1999
Atrazine	215.72	0.045	$3.86*10^3$	$2.7*10^9$	Nick 1992
NDMA	74.08	0.30	$1.974*10^3$	$3.3*10^8$	Sharpless 2003
Bromacil	--	--	--	--	--
Ibuprofen	206.3	0.1923	256	$6.77*10^9$	Yuan 2009

Advanced oxidation model (UVperoxII)

A more simplified method to calculate the degradation of chemicals is applied by using the dose-response behavior of chemicals. Similar as for disinfection predictions, the UV sensitivity of a compound is determined from collimated beam experiments. The dose-response behavior (k is the sensitivity to UV [cm^2/mJ]) of the compounds of interest is shown in Table 8-2, which are determined from collimated beam results. From the dose distribution calculated by the CFD model, the degradation can now be predicted.

Table 8-2 Reaction constants used for the UVPeroxII model calculations (MP lamps).

	k [cm^2/mJ]		
	0 mg/L H$_2$O$_2$	5 mg/L H$_2$O$_2$	10 mg/L H$_2$O$_2$
Atrazine	$6.79*10^{-4}$	$8.51*10^{-4}$	$9.63*10^{-4}$
NDMA	-	$5.90*10^{-4}$	$1.13*10^{-3}$
Bromacil	$4.58*10^{-4}$	$6.82*10^{-4}$	$8.64*10^{-4}$
Ibuprofen	$5.60*10^{-4}$	$8.58*10^{-4}$	$9.63*10^{-4}$

Geometry reactors

The geometries of the reactors that were simulated by the CFD model are shown in Figure 8-1. The reactors were simulated for a range of experimental conditions (flow rate, lamp power and 10 cm transmittance), which are shown in Table 8-3. The number of particles for the Dunea reactors and GCWW reactors was lower than for the KWR reactor to reduce computational times, whereas the lower number was still sufficient to obtain accurate results.

Table 8-3 Conditions for the different reactors used in the CFD calculation. The lamp power is defined as the UVC output of all the lamps in the reactor. N_{part} represents the number of particles used in the CFD.

Reactor	Number of lamps	Flow rate [m^3/h]	Lamp power UVC [W]	UVT [%/cm]	N_{part}
KWR LP	4	2.1 -3	88	78	4900
KWR MP	4	1.3 – 2	113	78	4900
Dunea LP	4	5	600	75-82	1,000
Dunea MP	2	5	834	75-82	1,000
Dunea DBD	4	1-3	145.2	78	1,000
GCWW LP	8	2.32	192	86-98	1,000
GCWW MP	1	9.3	484	86-98	1,000
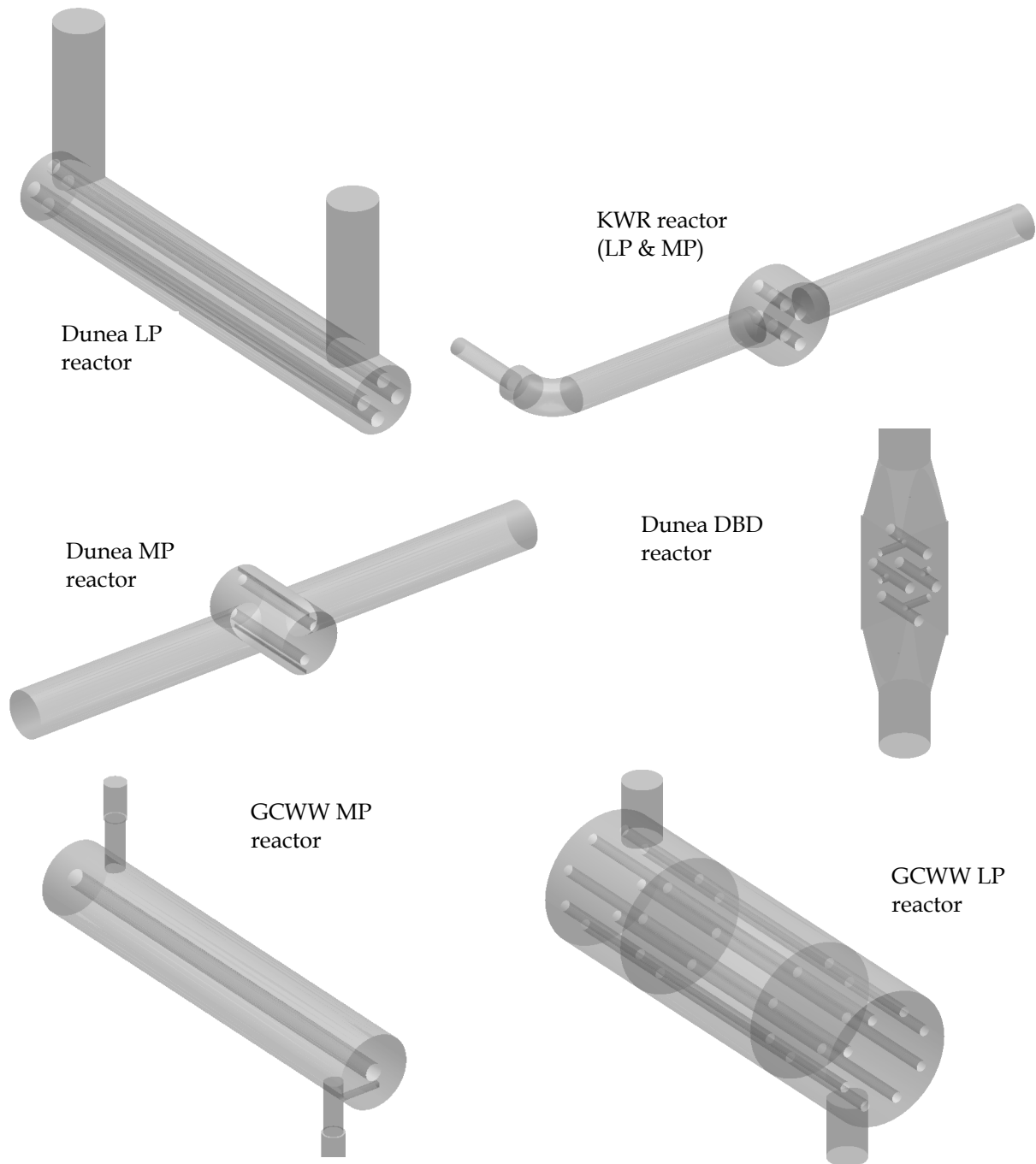
Figure 8-1 Geometries of the UV reactors that were modelled by CFD

8.3   Results

The predicted dose distributions are shown in Figure 8-2 and Figure 8-3. The mean dose and 10th percentile of the dose (D_{10}) are shown in Table 8-4. For all the reactors, a first peak is observed at the lower UV dose range, which represents particles that move in conjunction with the main flow. Also, a long tail at higher UV doses is observed, which is caused by particles that are trapped in recirculation zones in the reactor. The widest, most asymmetrical distribution is observed for the Dunea MP reactor, whereas the Dunea DBD reactor and the GCWW LP reactor showed the most symmetrical shape. The hydrodynamic performance of the UV reactors is captured in the factor D_{10}/D_{mean}. In the ideal case, the D_{10}/D_{mean} for a UV reactor would be 1, a good working in general has a D_{10}/D_{mean} of about 0.65, but

most standard reactors show a value of 0.5. The best performance was observed for the Dunea LP reactor, the Dunea DBD reactor and the GCWW reactors, whereas the Dunea MP reactor showed the worst performance.

As expected, by increasing the flow rate or decreasing the transmittance of the water, the UV doses are decreased. The shape of the dose distribution is slightly affected by changes in discharge or UVT. Increasing the UVT leads to an increase in the factor D_{10}/D_{mean}, because the spatial differences in UV radiation are reduced.

Table 8-4 Mean dose (D_{mean}) and 10th percentile of the dose (D_{10}) for the various UV reactors under different conditions. The lamp power is defined as the UVC output of all the lamps in the reactor. (m³/h = 0.624 kgal/h)

	Flow rate [m³/h]	UVT [%]	Lamp power [W]	D_{mean} [mJ/cm²]	D_{10}/D_{mean} [-]
KWR LP	2.1	78	88	306	0.51
	3	78	88	212	0.52
Dunea LP	5	75	600	741	0.57
	5	82	600	927	0.61
GCWW LP	2.32	88	192	609	0.57
KWR MP	1.3	78	113	633	0.50
	2.1	78	113	390	0.52
Dunea MP	5	75	834	875	0.41
	5	82	834	1150	0.49
GCWW MP	9.3	96	484	752	0.58
Dunea DBD	1	78	145.2	1179	0.56
	3	78	145.2	392	0.56
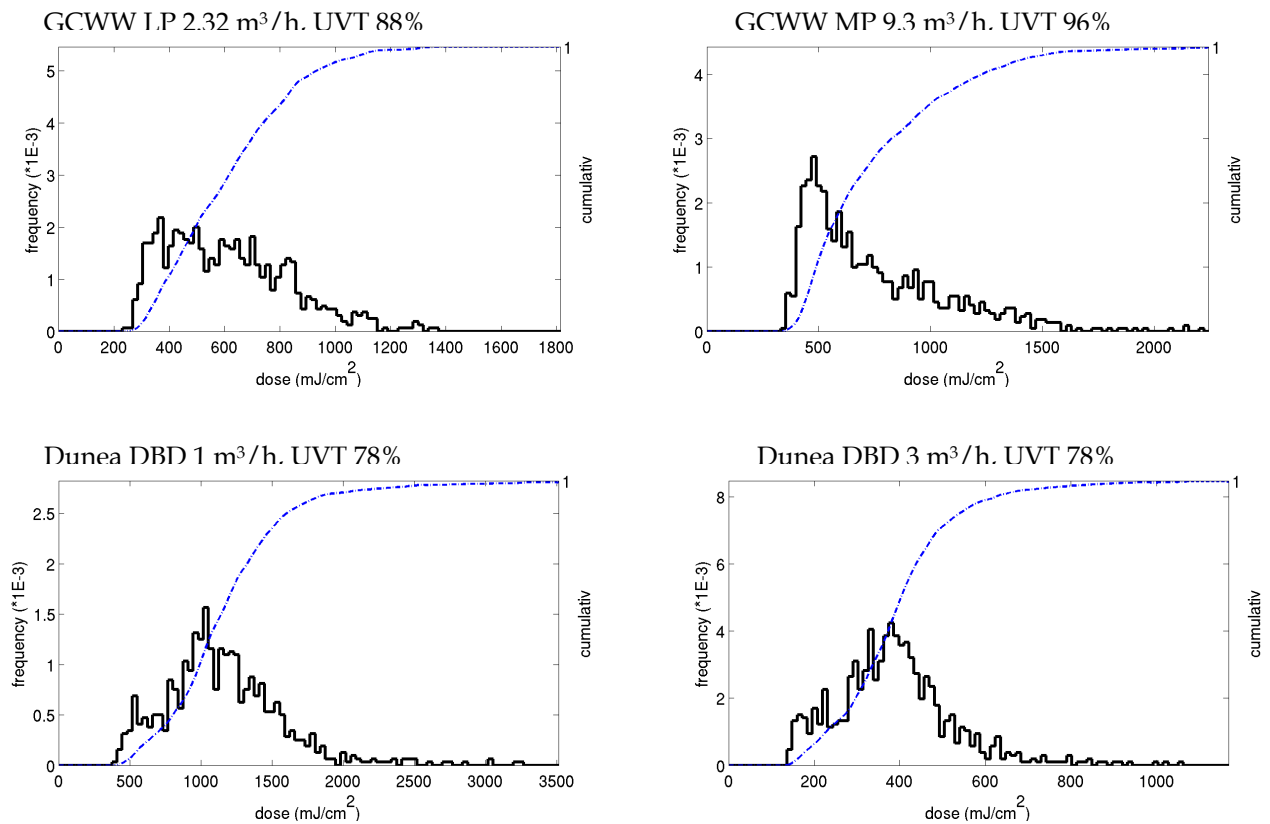
Figure 8-2 UV dose distribution in the Dunea DBD reactor and GCWW reactors, dose distribution (-), cumulative dose distribution (- -)
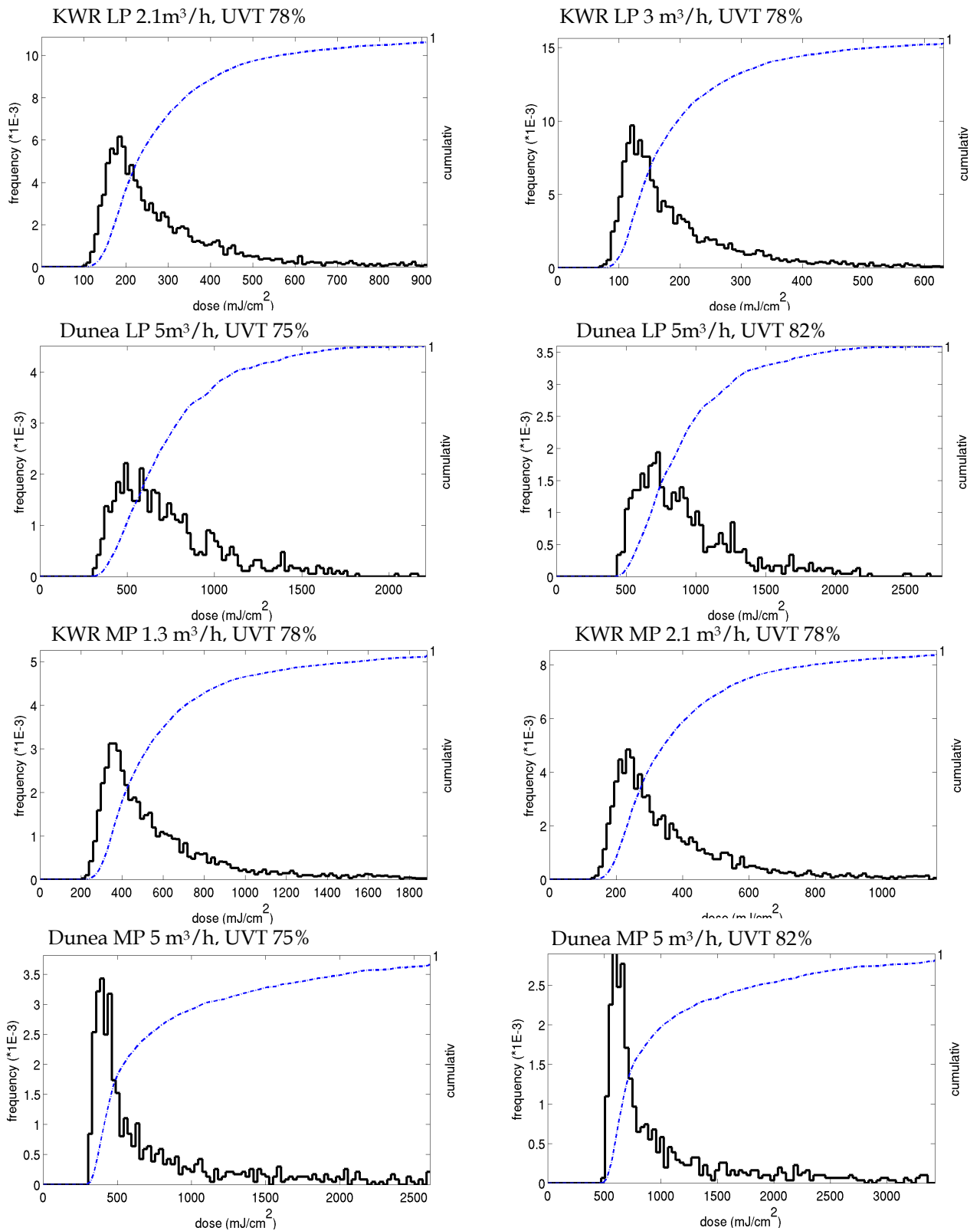
Figure 8-3 UV dose distribution in the Dunea and KWR reactors (LP and MP), dose distribution (—), cumulative dose distribtution (-·-)

Table 8-5 Degradation results from the CFD model are compared to the measured data. A good agreement (within 10%) is indicated by the green fields (xx); a moderate agreement (within 25%) is indicated by the orange fields (xx); a disagreement is indicated by the red fields (xx). Total power is the UVC output (W). ATZ = atrazine, IBU = ibuprofen

KWR LP, 2.1 m³/h, 78% UVT				Total power: 88 W, D_{mean} = 306 mJ/cm²			
Degradation results [%]	H_2O_2 [mg/L]	ATZ		IBU		NDMA	
		CFD	Meas	CFD	Meas	CFD	Meas
	0	20	21	6	0	50	-
	10	40	43	54	66	51	-

KWR LP, 3 m³/h, 78% UVT				Total power: 88 W, D_{mean} = 212 mJ/cm²			
Degradation results [%]	H_2O_2 [mg/L]	ATZ		IBU		NDMA	
		CFD	Meas	CFD	Meas	CFD	Meas
	0	14	14	4	0	39	-
	10	30	29	42	58	40	-

Dunea LP, 5 m³/h, 75% UVT				Total power: 600 W, D_{mean} = 741 mJ/cm²			
Degradation results [%]	H_2O_2 [mg/L]	ATZ		IBU		NDMA	
		CFD	Meas	CFD	Meas	CFD	Meas
	0	41	36	14	11	80	88
	5	59	52	67	32	81	100
	10	70	64	84	54	82	84

Dunea LP, 5 m³/h, 82% UVT				Total power: 600 W, D_{mean} = 927 mJ/cm²			
Degradation results [%]	H_2O_2 [mg/L]	ATZ		IBU		NDMA	
		CFD	Meas	CFD	Meas	CFD	Meas
	0	49	43	18	10	88	91
	5	69	61	76	63	88	92
	10	79	73	91	69	89	89

GCWW LP, 2.32 m³/h, 88% UVT				Total power: 192 W, D_{mean} = 609 mJ/cm²			
Degradation results [%]	H_2O_2 [mg/L]	ATZ		IBU		NDMA	
		CFD	Meas	CFD	Meas	CFD	Meas
	0	38	-	13	-	78	-
	10	67	62	82	81	79	-

KWR MP, 1.3 m³/h, 78% UVT				Total power: 113 W, D_{mean} = 633 mJ/cm²			
Degradation results [%]	H_2O_2 [mg/L]	ATZ		IBU		NDMA	
		CFD	Meas	CFD	Meas	CFD	Meas
	0	57	52	50	2	-	-
	10	68	73	68	90	58	-

KWR MP, 2.1 m³/h, 78% UVT				Total power: 113 W, D_{mean} = 390 mJ/cm²			
Degradation results [%]	H_2O_2 [mg/L]	ATZ		IBU		NDMA	
		CFD	Meas	CFD	Meas	CFD	Meas
	0	42	43	-	0	-	-
	10	53	58	53	74	73	-

Dunea MP, 5 m³/h, 75% UVT				Total power: 834 W, D_{mean} = 875 mJ/cm²			
Degradation results [%]	H_2O_2 [mg/L]	ATZ		IBU		NDMA	
		CFD	Meas	CFD	Meas	CFD	Meas
	0	63	59	57	27	-	95
	5	70	66	70	50	58	100
	10	73	72	73	53	78	100

Table 8-5 Continued

Dunea MP, 5 m³/h, 82% UVT				Total power: 834 W, D_{mean} = 1150 mJ/cm²			
Degradation results [%]	H_2O_2 [mg/L]	ATZ		IBU		NDMA	
		CFD	Meas	CFD	Meas	CFD	Meas
	0	74	62	68	32	-	78
	5	80	72	80	70	69	83
	10	83	76	83	69	87	83

GCWW MP, 9.3 m³/h, 96% UVT				Total power: 484 W, D_{mean} = 752.1 mJ/cm²			
Degradation results [%]	H_2O_2 [mg/L]	ATZ		IBU		NDMA	
		CFD	Meas	CFD	Meas	CFD	Meas
	0	66	64*	59	36*	-	-
	10	77	81**	77	75**	82	-

Dunea DBD, 1 m³/h, 78% UVT				Total power: 145.2 W, D_{mean} = 1179 mJ/cm²			
Degradation results [%]	H_2O_2 [mg/L]	ATZ		IBU		NDMA	
		CFD	Meas	CFD	Meas	CFD	Meas
	0	56	58	22	25	92	100
	5	76	74	82	68	93	98
	10	85	78	94	78	93	98

Dunea DBD, 3 m³/h, 78% UVT				Total power: 145.2 W, D_{mean} = 392 mJ/cm²			
Degradation results [%]	H_2O_2 [mg/L]	ATZ		IBU		NDMA	
		CFD	Meas	CFD	Meas	CFD	Meas
	0	25	23	8	5	61	74
	5	40	33	47	33	62	74
	10	50	40	66	50	63	77

* The measured values for the GCWW were averaged over 2 measurement series under similar conditions.

** Averaged over 3 measurement series under similar conditions

The results obtained by applying the UVPerox model to the conversion of atrazine, ibuprofen and NDMA for all the LP reactors are shown inTable 8-5. For the MP reactors, the kinetic constants (such as quantum yield, molar extinction, reaction rates) were unknown over the whole range of wavelengths, therefore the UVPeroxII model was used. For the DBD reactor, the lamps were treated as LP lamps to calculate the dose distribution and degradation results. The results were compared with experimental results, which are also shown inTable 8-5.

LP lamp results
For atrazine there is a very good agreement between the predicted and measured conversion in the KWR pilot reactor. For the Dunea pilot reactor the predicted values are a little higher than the actually measured values. This may be due to uncertainties in the lamp output. The agreement between model and actual data is good in all types of reactors, not only for photolysis (0 mg H_2O_2/L), but also for the combined system of photolysis and oxidation by •OH radicals.
For ibuprofen in the KWR reactor the model predicts lower values than actually measured, whereas for the Dunea reactor the model predicts considerably higher values for the UV/H_2O_2 process than measured. In the GCWW reactor, there is a good agreement between the measured and calculated degradation.
The conversion of NDMA in the KWR reactor appeared to be fast, which dropped the concentration immediately below the lower detection limit. In the Dunea reactor some measurements could be carried out, but here too the resulting NDMA concentration quickly became very low. For the Dunea and GCWW reactor these high conversions are also predicted by the CFD model, showing a good agreement between model results and experimental results.

MP lamp results

Again, for atrazine, there is a very good agreement between the model and the experimental data for the KWR reactor and the GCWW reactor. For the Dunea pilot reactor, the difference between the predicted and the measured conversion is a little larger, although still less than 10%. The difference between both reactors can be explained from uncertainties in the lamp output of the Dunea pilot plant the actual lamp output in the Dunea pilot reactor could not be measured, so data from the lamp supplier were used, and it was assumed that the lamp output would be about 100%.For ibuprofen, the difference with the experimental data may be larger, especially for photolysis (0 mg H_2O_2/L). This is probably due to larger uncertainties in the ibuprofen concentration determination.

For NDMA, the model results at the highest UVT seem to be in reasonable agreement with the experimental data. At the lower transmission (75%) the measured conversion of NDMA is higher, which seems to be contradictory, because the UV dose is lower. This may be caused by uncertainties in the analysis of NDMA.

DBD lamp results

The CFD model shows a good agreement with the measured degradation in the DBD reactor with a flow of 1 m^3/h, especially for atrazine and NDMA. At the higher flow rate of 3 m^3/h, the model prediction deviates from the measured data up to 25% for atrazine and NDMA. There is a small over prediction for NDMA, whereas a small under prediction by the model was found for atrazine. These differences between model and experiment are similar as for the other lamp types. The largest differences were found for ibuprofen, which was already observed for the other lamps and reactors. These deviations may be caused by inaccuracies in the analysis of ibuprofen. Since no special irradiation model was developed for the DBD lamp (it was modelled similarly as for the LP lamps), the agreement between model and experimental results seems to be satisfactory.

8.4   Conclusions

For atrazine there is a good agreement between the predicted and measured conversion in all reactor types. Also for other compounds rather good results were obtained. The CFD model combined with a kinetic model (UVPerox I) can be applied to describe and predict the performance of a pilot reactor, equipped with LP, MP lamps and even DBD lamps. Thus, this performance can be calculated under different circumstances. The main problem for the UVPerox I model is that accurate constants (reaction rate constant with hydroxyl radicals, quantum yield) are required for all compounds and these are not always available yet. In systems equiped with MP UV lamps, these compounds even are required at every wavelength of the spectrum emitted. As these values hardly ever are available, the UVPerox I model will only be applicable in UV reactors with LP lamps.

The dose distributions determined by the CFD model reveal the hydrodynamic behavior of the UV reactors. There is a large peak at the lower UV dose region, which contain the particles that move in conjunction with the main flow. Also, a long tail was observed at higher UV doses that is caused by particles trapped inside recirculation regions. This behaviour was most clearly observed for the Dunea MP reactor, whereas the Dunea DBD reactor and the GCWW LP reactor showed the most symmetrical dose distribution.

The UVPerox I model is a useful tool to evaluate reactor efficiency.

Formation and removal of genotoxicity during UV/H₂O₂-GAC treatment

Work package 9; KWR

Author: M.B. Heringa

9   Work package 9: Formation and removal of genotoxicity during UV/H$_2$O$_2$-GAC treatment (KWR)

9.1   Introduction

It is known and expected that water treatment based on chemical/oxidative degradation processes may lead to the formation of by-products, e.g. trihalomethanes (THMs) during chlorination and bromate during ozonation of (pre-treated) natural water (e.g. Rook, 1974; Richardson *et al.*, 2007; Najm and Trussell, 2001; von Gunten and Hoigne, 1994). Similarly, UV/H$_2$O$_2$ treatment of water may induce the formation of by-products. It appears that typical UV/H$_2$O$_2$ process conditions do not fully mineralize contaminants to water and carbon dioxide. Indeed, formation of organic intermediates has been reported (e.g. Lau *et al.*, 2005). By-products may result from the direct photolysis or from oxidation of compounds in the water matrix. Known by-products are nitrite (photolysis of nitrate) and assimilable organic carbon (AOC; photolysis and oxidation of dissolved organic carbon (DOC)). Most organic contaminants strongly absorb light in the UVC range (200 – 285 nm) of the electromagnetic spectrum and this absorbed energy may lead to changes in the molecular structure of the compounds, resulting in (by-)products. Also the omni-present natural compounds in surface water, collectively grouped as natural organic matter (NOM), absorb in the UVC wavelength range and can therefore be degraded into various (by-)products. Because the identity of the by-products of UV-oxidation processes is largely unknown, the formation of toxic compounds during UV/H$_2$O$_2$ treatment of natural water should be considered.

So far, only a few studies have been conducted on the toxicity of water after UV/H$_2$O$_2$ treatment, including studies on estrogenicity and acute toxicity (e.g. Linden *et al.*, 2004). The formation of genotoxic (i.e. DNA-damaging) by-products by the oxidative reactions of ozone and chlorine are a reason to study the generation of genotoxic activity by AOPs such as UV/H$_2$O$_2$ treatment. However, although it has been shown that bromate or trihalomethane compounds (THMs) were not formed (Kruithof *et al.*, 2007; Kashinkunti *et al.*, 2004), no direct effect genotoxicity studies (detecting any possible genotoxin) have been reported for UV/H$_2$O$_2$ treatment.

Quite a few studies have been conducted on the effects of UV disinfection (without H$_2$O$_2$) on the formation of genotoxicity. Conflicting results have been reported, with some finding an increase in genotoxicity after UV disinfection and others that do not. These differences might be attributed to the use of different water qualities, applied UV lamps (medium pressure (MP) vs. low pressure (LP)), UV dose and genotoxicity tests (e.g. Helma *et al.*, 1994; Carnimeo *et al.*, 1995; Haider *et al.*, 2001 and 2002).

The present study therefore had the following objective: to study the genotoxic activity of surface water before and after treatment with UV/H$_2$O$_2$ AOP and after subsequent GAC, for both MP and LP lamps. Additionally, a comparison was performed between the three lamp types (MP, LP and DBD) in the formation of genotoxic activity.

Several assays are available for evaluating the genotoxic potential of water extracts. To detect gene mutations, the Ames II assay (Gee *et al.*, 1998; Fluckiger-Isler *et al.*, 2004) was selected. This modified version of the well-known classic Ames test uses less sample volume. For a complementary assay detecting chromosomal damage, the Comet assay in HepG2 liver cells was selected. The Comet assay is a sensitive test that can be performed with any cell type and allows rapid detection of chromosomal damage such as single and double DNA strand breaks (Tice *et al.*, 2000). The human HepG2 liver cell line has the advantage of having endogenous metabolic capacity and liver cells are one of the first cell types chemicals encounter after intestinal absorption.

9.2   Experimental set-up

Three studies were performed:
- one in October 2007 with pretreated Meuse water from Bergambacht (the Netherlands) in a pilot reactor at KWR with MP or LP lamps
- one in September 2008 with pretreated Ohio River water from Cincinnati (OH, USA) in two pilot reactors simultaneously with different lamps (MP and LP)
- one in February 2010 with the same pretreated Meuse water as in the first study, in three pilot reactors simultaneously with three different lamps (MP, LP and DBD) at Dunea for comparison.

Experimental details (e.g. materials) can be found in appendix XXI

9.2.1 Water treatment and sampling
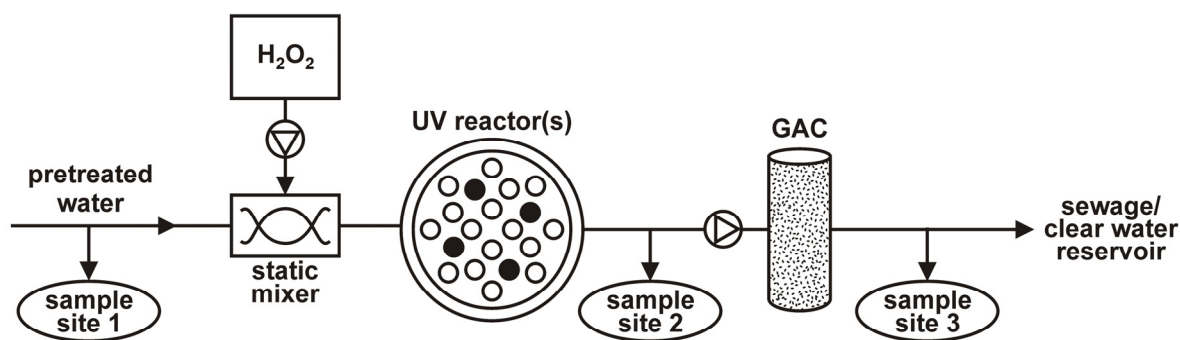
Figure 9-1 Schematic of the general treatment setup for the studies with pretreated Meuse water and pretreated Ohio river water.

In the Meuse water study at KWR, samples were taken at three different flow velocities at site 2 and for the lowest flow velocity only at site 3. In the Ohio river water study, samples at site 2 were collected both after UV treatment with H_2O_2 and after UV treatment without H_2O_2. Samples at site 3 were taken only after UV treatment with H_2O_2. In the Meuse water comparison study at Dunea, three different UV reactors were applied (an MP-, and LP- and a DBD-reactor) and no GAC filtration was performed.

Figure 9-1 shows the general scheme of the three treatment setups and shows at which points samples were taken. Table 9-1 gives the most important details of the different treatment steps. Further details can be found in appendix XXI.

Table 9-1 Water treatment conditions for the genotoxicity study.

Study	Meuse	Ohio river	Comparison study
Pretreatment	Coagulation ($(Fe)_2(SO)_3$) Sedimentation Micro sieves Rapid sand filtration	Coagulation ($Al_2(SO_4)_3$ and polyDADMAC [c]) Sedimentation pH correction (CaO) Rapid sand filtration	Coagulation ($(Fe)_2(SO)_3$) Sedimentation Micro sieves Rapid sand filtration
UV/H_2O_2-treatment	KWR-design pilot reactor (not optimized) [a] 550 mJ/cm^2 (chemidosimetry) 10 mg/L H_2O_2 1. 4 MP lamps: HOK 20/100 2 kW (Philips Lighting; Roosendaal, the Netherlands) 2. 4 LP lamps: TUV PL-L 95W HO (Philips Lighting; Roosendaal, the Netherlands)	Aquionics pilot reactor (optimized) ± 400 mJ/cm^2 (instrument read-out) 10 mg/L H_2O_2 1. 1 MP lamp: 3.5 kW Super TOC (Aquionics; Erlanger, KY, USA) 2. 8 LP lamps: 80W Super TOC (Aquionics; Erlanger, KY, USA)	10 mg/L H_2O_2 1. MP reactor (Berson UV Technology, 2 lamps, 4.4 kW) 5 m^3/h, at 100% power (78% atrazine conversion) 2. LP reactor (ITT Wedeco, 4 lamp, 1.32 kW) 5 m^3/h, at 100% power (72% atrazine conversion) 3. DBD reactor (designed by KWR, Philips and lIT UV technology, constructed by Melano, 4 lamps, 1.2 kW) 3 m^3/h., at 100% power (approx. 80% atrazine conversion)
GAC treatment	Virgin Chemviron F400 GAC (Chemviron Carbon; Feluy, Belgium) Column 40 × 9 cm EBCT [b] 30 min. Flow 5 L/h	Reactivated Calgon F400 (Calgon Carbon; Pittsburgh, PA, USA), 325 d service Column 1.73 × 0.1 m EBCT [b] 15 min. Flow 57 L/h	Not applied

[a] The KWR reactor was used for comparative research and was therefore not optimally configured for any specific lamp.

[b] EBCT = empty bed contact time

[c] polyDADMAC = cationic polymer (poly-diallyldimethylammonium chloride

Table 9-2 Water quality parameters of pre-treated river Meuse and Ohio water after coagulation and rapid sand filtration.

	Nitrate (mg NO$_3^-$/L)	pH	Alkalinity (mg HCO$_3^-$/L)	TOC [1] (mg C/L)	UV-T$_{254}$ (%, cm^{-1})
Meuse (LP lamps)	8.0	8.09	148	3.8	79
Meuse (MP lamps)	5.8	7.06	151	3.9	78
Ohio	3.1	7.7	93.3	1.95	90.6

[1] Measured as NPOC: Non-Purgeable Organic Carbon

Table 9-2 shows the water quality parameters of the sand filtrate prior to the oxidation step in the Meuse and Ohio river study. To all samples treated with UV/H$_2$O$_2$ for the Meuse and comparison study, 300 mg Na$_2$SO$_3$/L was added to quench residual H$_2$O$_2$. To all samples treated with UV/H$_2$O$_2$ for the Ohio River study, 500 mg Na$_2$SO$_3$/L was added, hereafter the samples were frozen and shipped to the Netherlands for analysis.

9.2.2 Sample extraction and concentration

The detailed extraction procedure can be found in appendix XXI. In brief, within 24 hours after collection or thawing, three replicates of one liter of every sample were extracted by solid phase extraction (SPE) with 200-mg Oasis® HLB cartridges (Waters Corporation, Milford, USA) at pH 2.3. In the study with Ohio river water, mineral water samples (Evian from glass bottles) were included as procedure controls. Elution was performed with 3 serial additions of 2.5 mL of 20% methanol in acetonitrile. The 7.5-mL eluates were evaporated and taken up in 50 µL of DMSO yielding 20,000-fold concentrated extracts. All extracts were stored at -18°C until analysis.

9.2.3 Ames II tests

The Ames II test strains (TA98 and TAMix) and media were purchased from Xenometrix (Basel, Switzerland). The test procedure provided by Xenometrix, also described by Fluckiger-Isler *et al.* (2004), was followed, with minor modifications as described in appendix XXI. In brief, the water extracts were diluted to 100 µL (1:1) with DMSO to obtain a sufficient amount of sample for all tests and the bacteria were finally exposed to a 200-fold concentration of the water samples in culture medium. Water extracts were tested in triplicate, as well as a triplicate negative control (DMSO only), a triplicate positive control for genotoxicity (Table 9-3), and a triplicate positive control for cytotoxicity (1 mg/mL 4-NQO in DMSO). A custom cytotoxicity test was performed with subsamples of the exposure cultures in medium with histidine, to check for possible artifacts due to effects on cell survival and growth. Finally, the number of yellow wells per 48 wells of one sample was counted manually as a measure of genotoxicity.

Table 9-3 Positive controls for the different strains and S9[*)]-conditions

Strain and S9-condition	Positive control (in DMSO)
TA98 –S9	10 (Meuse) or 20 (Ohio) µg/mL 4-NQO
TA98 +S9	5 µg/mL 2-AA
TAMix –S9	5 (Meuse) or 10 (Ohio) µg/mL 4-NQO
TAMix +S9	100 µg/mL 2-AA

[*)] The Ames II assay is performed both with and without S9 liver enzyme extract, in order to detect both direct genotoxic compounds, and indirect genotoxic compounds that need to be converted to a genotoxic metabolite by liver enzymes first.

Ames test responses follow a binomial distribution (Piegorsch *et al.*, 2000), therefore a sample was considered genotoxic if the response of the sample was different from the response of the negative control with a certainty of 99%, based on a binomial distribution (see appendix XXI).

9.2.4 Comet assay

First, a neutral red uptake assay was performed as described in Borenfreund and Puerner (1985) with minor modifications, to check for cytotoxicity on the HepG2 cells. The HepG2 cells were treated for 3 h with 0.25%, 0.5% and 1% of the water extracts in HBSS (v/v). The positive control for cytotoxicity used 1% Triton X-100 (v/v). Details can be found in the appendix XXI

The Comet assay was performed as described by Singh *et al.* (1988), with minor modifications as fully described in appendix XXI. In brief, for the samples from the Meuse water experiment, HepG2 cells were treated for 3 h with HBSS medium containing aliquots of water extract at a concentration of 1% (v/v) in duplicate (exposure to a 200-fold concentration of the water samples). 25 µg/mL MMS in DMSO was used as positive control for genotoxicity. The Comet assays with the Ohio water samples were performed both in presence of S9 (3 h exposure) and in absence of S9 (24 h exposure). The positive control then was 50 µg/mL BaP. For the comparison study, the cells were exposed to the samples for 3h without S9 and for 24 h without S9, as results in the mean time had shown that the HepG2 cells had sufficient metabolic activity themselves and addition of S9 might then be somewhat toxic to the HepG2 cells.

DNA damage was evaluated by calculation of the mean percent tail DNA for a total of 200 cells per water sample (50 cells per slide, two slides per culture and two cultures per water samples). The water extracts were considered positive for genotoxicity when a three-fold increase in tail intensity over the negative control was observed. In addition to the prior neutral red uptake assay, viability was also checked by registering the number of ghost cells, though excluding them from the genotoxicity analysis. The relative proportion of ghost cells should be less than 30%.

9.3 Results and discussion

9.3.1 MP lamp experiments of the Meuse and Ohio river studies

In the neutral red uptake assay for the Comet, water sample concentrations of up to 1% did not show any cytotoxicity in HepG2 cells. Therefore, water extracts were tested at a concentration of 1% (v/v) in the Comet assay, with certainty that a potential genotoxic response could not be induced by cytotoxicity.
The results of the Comet assay are presented in Figure 9-2.
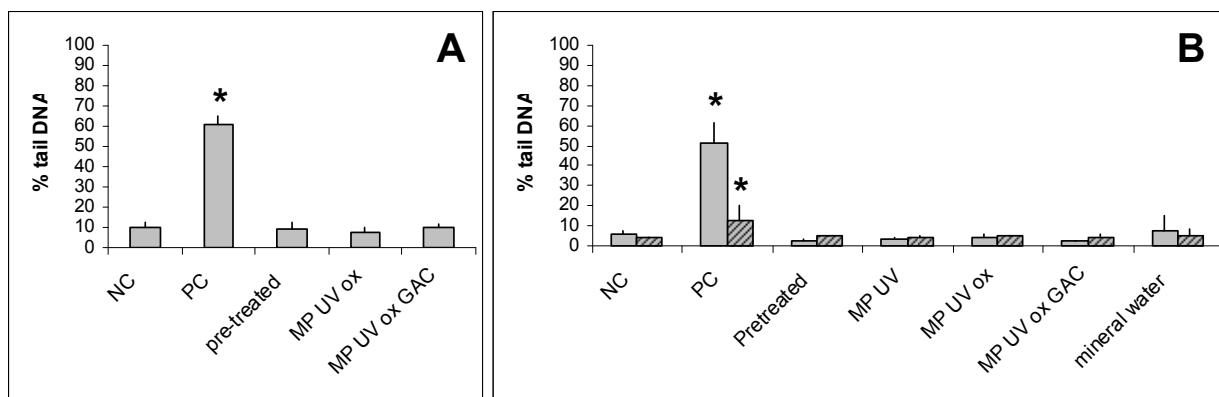
Figure 9-2 Results of the Comet assay with water extracts of the MP lamp experiments in the Meuse river study (A) and Ohio river study (B). Results are given for presence (striped bars) and absence (non-striped bars) of S9. Samples tested were a negative control (NC), a positive control (PC), and extracts of pre-treated water and water after UV treatment alone (UV), UV/H₂O₂ (UV ox) and after subsequent GAC filtration (UV ox GAC). Bars denote average values, error bars denote standard deviations (n = 200). Asterisks denote responses showing genotoxicity, i.e. deviating from the NC. For these samples a significant geontoxicity is assessed.

No genotoxic activity was found with the Comet assay in any of the water samples and procedure controls in either of the two studies. The test system should be sufficiently sensitive to detect a genotoxic potential of water extracts as a genotoxic response has been reported previously in the Comet assay with HepG2 cells with samples of chlorinated drinking water (Buschini *et al.*, 2004; Yuan *et al.*, 2005). However, the compounds involved here can be very different from the compounds formed during UV-oxidation. No data are available in published literature on induction of chromosomal damage by water samples after MP UV/H₂O₂ treatment, for comparison with the results of the present study.

In both studies, the cytotoxicity tests of the Ames II test show clear effects for the positive controls with a complete absence of bacterial growth in these cultures. The water samples and other controls showed no significant cytotoxicity for the applied bacterial strains. This means that absence of genotoxic response in the Ames II test could not have been due to any bacterial death from cytotoxic compounds.
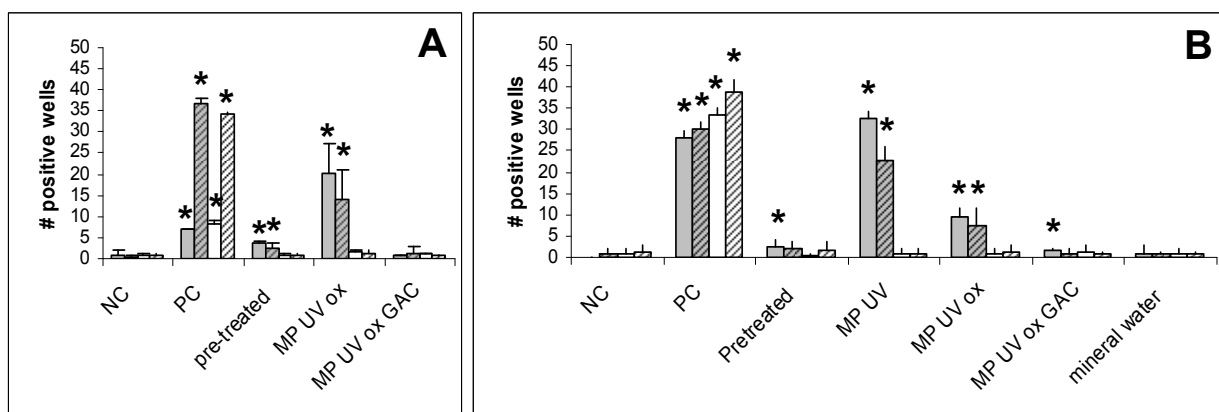
Figure 9-3 Results of Ames II tests with water extracts of the MP experiments of the Meuse river study (A) and the Ohio river study (B). Results are given for strains TA98 (grey bars) and TAMix (white bars), with (striped bars) and without (non-striped bars) S9. Samples tested were a negative control (NC), positive controls (PC), and extracts of pre-treated water and water after UV treatment alone (UV) , UV/H₂O₂ (UV ox) and after subsequent GAC filtration (UV ox GAC). Bars denote average values, error bars denote standard deviations (n = 3). Asterisks denote responses showing genotoxicity, i.e. deviating from the NC with 99% certainty.

Figure 9-3 shows the results of the Ames II test of samples prior to and after MP UV/H$_2$O$_2$ treatment, for the Meuse river study (Figure 9-3A), as well as the Ohio river study (Figure 9-3B). It can be seen here that all negative (DMSO) controls present merely the normal, spontaneous mutations as background. The positive controls show clear increases in mutations, deviating significantly from the background. The positive controls for TA98 -S9 and TAMix - S9 in figure 9-3A were different compounds than in the tests with S9 and were given in lower doses than in the test of figure 9-3B, hence the lower, but still clearly elevated responses there. Therefore, it is concluded that the bacterial strains were functioning normally during the tests and the method was performed correctly.

The Ames II assay is performed both with and without S9 liver enzyme extract, in order to detect both direct genotoxic compounds, and indirect genotoxic compounds that need to be converted to a genotoxic metabolite by liver enzymes first. In the TAMix cultures, no significant increase in mutations was detected in any of the water samples, both with and without metabolic activation (S9). This means there was no increase in the type of mutations detected by this strain, compared to the pre-treated water. No other data for Ames tests on water after MP UV/H$_2$O$_2$ treatment are available for comparison.

In contrast, significant increases in mutations were measured in the TA98 cultures. The pretreated water of both locations showed low genotoxicity either in presence of S9 (Meuse), or in absence of S9 (Meuse and Ohio). These water sources thus contained some compound(s) that are genotoxic directly or become(s) genotoxic after metabolization by liver enzymes. Meuse water has regularly given genotoxic responses in the TA98 strain of the classic Ames test in the past (Veenendaal and van Genderen, 1999). Similar Ames test results, with a predominate response in TA98 + S9, have been found in Dutch groundwater, where the genotoxicity seemed to have a natural origin (Kool and van Kreyl, 1988). It is likely that the genotoxicity found in the three water sources has a natural origin as well, considering that these samples were taken in autumn, when a large load of decomposed plant material is expected in the river.

UV treatment with MP lamps, both with and without H$_2$O$_2$, resulted in a clear increase in the number of mutations in TA98 for both water sources. This increase in genotoxicity was stronger in the absence of S9 in all cases; and in the presence of S9 the increase was still significant. Interestingly, MP UV treatment without H$_2$O$_2$ resulted in a higher response than with H$_2$O$_2$ in the Ohio River study where this was compared. This gives a first indication that the genotoxic by-product(s) are formed by photo-induced processes and not by oxidative processes.

Subsequent treatment of the UV/H$_2$O$_2$-treated water with GAC adsorption removed the genotoxicity to the level of the negative control and of mineral water in the Meuse study (see Figure 9-3A). This observation is similar to that of Guzzella *et al*. (2002). Only in the UV/H$_2$O$_2$-GAC-treated Ohio river water a slight genotoxic response, just above the very low significance limit, was observed in TA98 – S9. This genotoxic response was lower than that of the initial, SF-treated Ohio river water (Figure 9-3B).

9.3.2 LP lamp experiments of the Meuse and Ohio river studies

In the neutral red uptake assay for the Comet, water sample concentrations of up to 1% did not show any cytotoxicity in HepG2 cells. Therefore, water extracts were tested at a concentration of 1% (v/v) in the Comet assay, with certainty that a potential genotoxic response could not be induced by cytotoxicity.

The results of the Comet assay are presented in Figure 9-4.

No genotoxic activity was found with the Comet assay in any of the water samples and procedure controls in either of the two studies. The test system should be sufficiently sensitive to detect a genotoxic potential of water extracts as a genotoxic response has been reported previously in the Comet assay with HepG2 cells with samples of chlorinated drinking water (Buschini *et al*., 2004; Yuan *et al*., 2005). However, the compounds involved here can be very different from the compounds formed during UV-oxidation.

No data are available in published literature on induction of chromosomal damage by water samples after LP UV/H$_2$O$_2$ treatment, for comparison with the results of the present study. After UV-disinfection, however, Helma *et al*. (1994) found an increased response in contaminated groundwater with the micronucleus test with the *Tradescantia* plant (lamp type and dose not given) and also after

UV-treatment of pre-purified contaminated groundwater with a LP-lamp (50-150 mJ/cm²). In contrast, Haider *et al.* (2002) did not find an increase in micronucleus formation with either *Tradescantia* plants or rat liver cells after treatment of Austrian groundwater with low-pressure lamps (80 mJ/cm²).
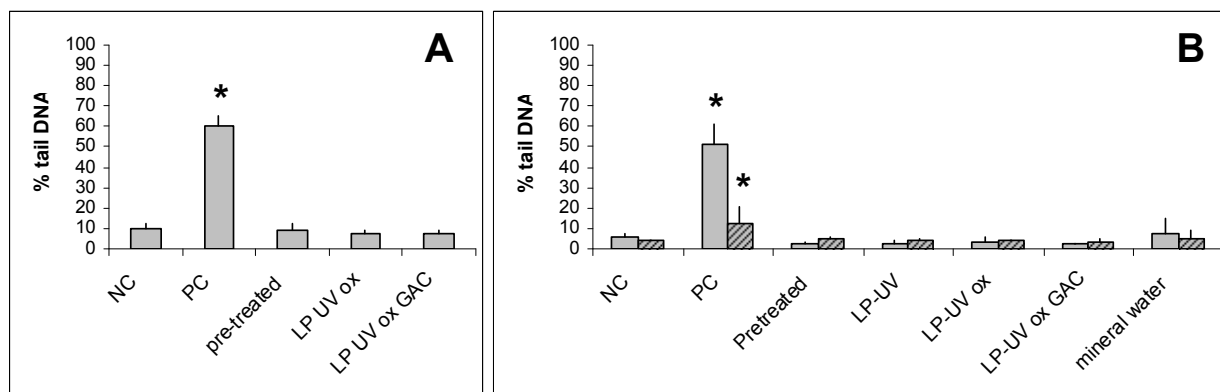
Figure 9-4 Results of the Comet assay with water extracts of the LP lamp experiments in the Meuse river study (A) and Ohio river study (B). Results are given for presence (striped bars) and absence (non-striped bars) of S9. Samples tested were a negative control (NC), a positive control (PC), and extracts of pre-treated water and water after UV treatment alone (UV), UV/H₂O₂ (UV ox) and after subsequent GAC filtration (UV ox GAC). Bars denote average values, error bars denote standard deviations (n = 200). Asterisks denote responses showing genotoxicity, i.e. deviating from the NC.

In both studies, the cytotoxicity tests of the Ames II test show clear effects for the positive controls with a complete absence of bacterial growth in these cultures. The water samples and other controls showed no significant cytotoxicity for the applied bacterial strains. This means that absence of genotoxic response in the Ames II test could not have been due to any bacterial death from cytotoxic compounds.
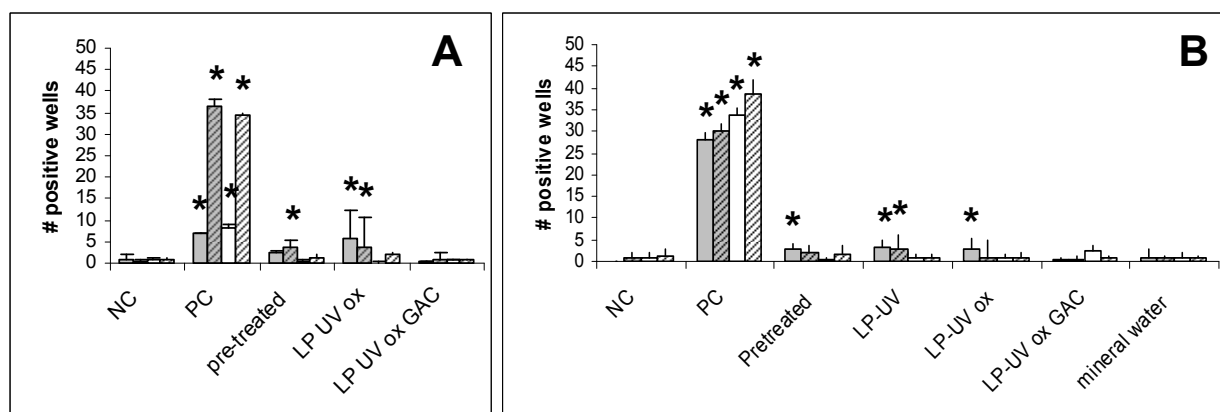
Figure 9-5 Results of Ames II tests with water extracts of LP lamp experiments of the Meuse river study (A) and the Ohio river study (B). Results are given for strains TA98 (grey bars) and TAMix (white bars), with (striped bars) and without (non-striped bars) S9. Samples tested were a negative control (NC), positive controls (PC), and extracts of pre-treated water and water after UV treatment alone (UV), UV/H₂O₂ (UV ox) and after subsequent GAC filtration (UV ox GAC). Bars denote average values, error bars denote standard deviations (n = 3). Asterisks denote responses showing genotoxicity, i.e. deviating from the NC with 99% certainty.

Figure 9-5 shows the results of the Ames II test of samples prior to and after UV/H₂O₂ treatment, for the Meuse river study (Figure 9-5A), as well as the Ohio river study (Figure 9-5B). It can be seen here that all negative (DMSO) controls merely present the normal, spontaneous mutations as background.

The positive controls show clear increases in mutations, deviating significantly from the background. Therefore, it is concluded that the bacterial strains were functioning normally during the tests and that the method was performed correctly.

In the TAMix cultures, no significant increase in mutations was detected in any of the water samples, both with and without metabolic activation (S9). This means there was no increase in the type of mutations detected by this strain, compared to the pre-treated water. No other data for Ames tests on water after UV/H_2O_2 treatment are available for comparison. However, these findings are in agreement with the results of the UV disinfection research of Haider *et al*. (2002). They used LP lamps for UV disinfection and found no response with TA100 (comparable strain to TAMix) in UV-disinfected groundwater samples (80 mJ/cm^2). Guzzella *et al*. (2002) also found no increase in TA100 response after O_3/UV and O_3/UV/H_2O_2 treatment (UV dose 40 Vs/cm^3; lamp type not given).

In contrast, increases in mutations were measured in the TA98 cultures. The pretreated water of both locations showed low genotoxicity either in presence of S9 (Meuse), or in absence of S9 (Ohio), where the Meuse samples of this experiment were different from the MP-lamp experiment and the Ohio samples were the same for both experiments. As discussed in paragraph 9.3.1., these results are not uncommon.

UV treatment with LP lamps, both with and without H_2O_2, resulted in a slight increase (Meuse study) or no increase (Ohio study) in the number of mutations in TA98 for both water sources. There was no clear difference in the response after LP UV treatment without H_2O_2 compared to that with H_2O_2 in the Ohio study. No other data for Ames tests on water after UV/H_2O_2 treatment are available for comparison. In UV-disinfection experiments, Haider *et al*. (2002) found an increase in TA98 –S9 response after UV-irradiation only for one of the five tested water samples, while for one other sample, the response decreased after UV-irradiation.

Subsequent treatment of the UV/H_2O_2-treated water with GAC adsorption removed any genotoxicity to the level of the negative control and of mineral water. This observation is similar to that of Guzzella *et al*. (2002).

It is tempting to directly compare the TA98 responses of the LP-lamp experiments to those of the MP-lamp experiments, especially as the LP and MP samples of each study were analyzed in the same Ames II batch. However, this is complicated by the fact that these lamps were applied in a non-optimized reactor (Meuse study) or not fully optimized reactors (Ohio study). Better optimized, full scale reactors can give different results, as also seen in Heringa *et al*. (2011), where samples of PWN's full scale MP reactors show lower responses than those of the pilot reactors. Additionally, it must be kept in mind that the ratio of photolysis and oxidation conversion of atrazine (for which the applied UV-dose was chosen) is different for LP and MP lamps, with MP lamps providing a higher proportion of photolytic conversion. A pure, fundamental comparison is therefore not possible between these lamps, only a holistic comparison based on conditions used in practice (e.g. 80% atrazine conversion). Under such conditions, with these not fully optimized pilot reactors, the results shown here give an indication that LP lamps produce less genotoxic by-product(s). Considering the difference in the photolytic power of both lamp types, this observation is another indication that photo-induced processes are responsible for the formation of the observed genotoxic activity.

9.3.3 Comparison of three lamps

In the neutral red uptake assay for the Comet, water sample concentrations of up to 1% did not show any cytotoxicity in HepG2 cells. Therefore, water extracts were tested at a concentration of 1% (v/v) in the Comet assay, with certainty that a potential genotoxic response could not be induced by cytotoxicity.

The results of the Comet assay are presented in *Figure 9-6*. No genotoxic activity was found with the Comet assay in any of the water extracts and in the procedure control, as in the other studies (paragraph 9.3.1 and 9.3.2)
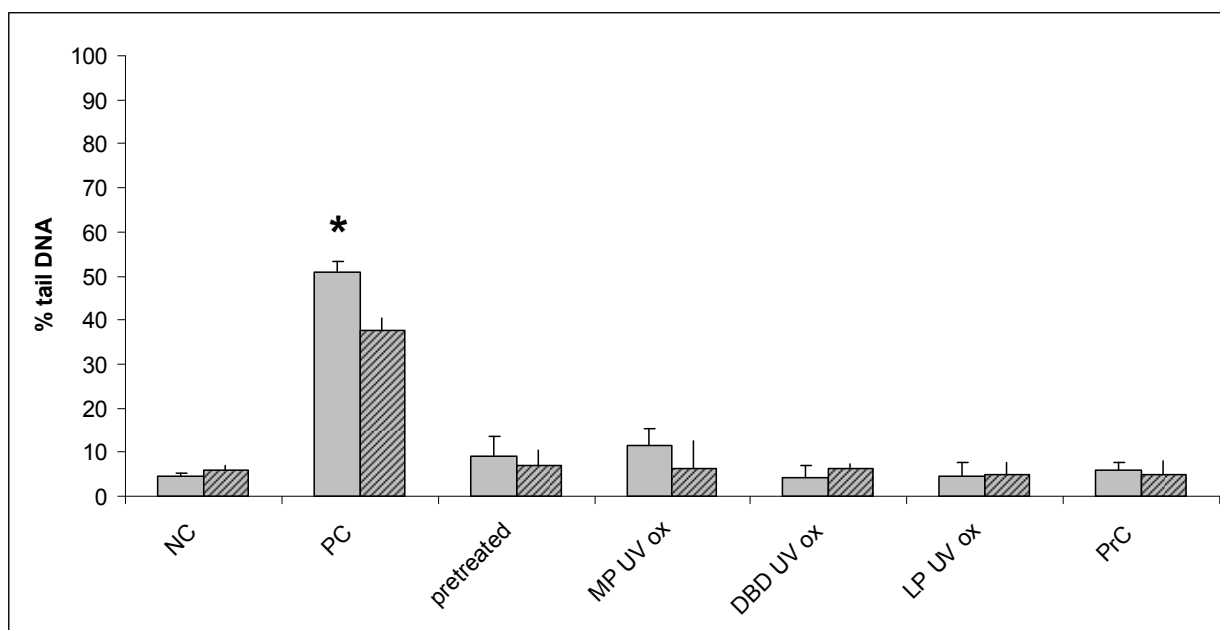
Figure 9-6 Results of the Comet assay with water extracts of the lamp comparison study. Results are given for 24h (striped bars) and 3h (non-striped bars) exposure in absence of S9. Samples tested were a negative control (NC), a positive control (PC), a procedure control (PrC), and extracts of pre-treated water and water after UV/H$_2$O$_2$ treatment with MP (MP UV ox), LP (LP UV ox) and DBD (DBD UV ox) lamps. Bars denote average values, error bars denote standard deviations (n = 200). Asterisks denote responses showing genotoxicity, i.e. deviating from the NC.

Figure 9-7 shows the Ames II results of the comparison study at Dunea. A similar pattern is seen as before: the TAMix strain does not show any response. The pretreated water shows a slightly genotoxic response in the TA98, both in absence and presence of S9, and this response is increased after UV/H$_2$O$_2$ treatment with MP lamps. The increase in genotoxic response is clearly lower after UV/H$_2$O$_2$ treatment with DBD or LP lamps, and comparable among these two. This increase may even not be significant with regard to the response of the pretreated water.

These results therefore indicate that the LP and DBD lamps cause less formation of genotoxic by-products than MP lamps, under the practical process conditions giving a similar conversion of the model compound atrazine. This is similar to the observations in paragraph 9.3.1. and 9.3.2. The main difference between the MP lamps on the one side, and the DBD and LP lamps on the other side, is the spectrum of emitted UV-light. The LP lamps emit monochromatic UV irradiation at a wavelength of 253.7 nm. The MP-lamps emit a broad spectrum of polychromatic light while the DBD-lamps emit a small spectrum of polychromatic light around 237 nm. As a result, photo-induced processes are a far more important process for MP lamps than for LP lamps, and for DBD lamps it will be in between. These results are therefore another indication that photo-induced processes play an important role in the formation of the genotoxic by-products.
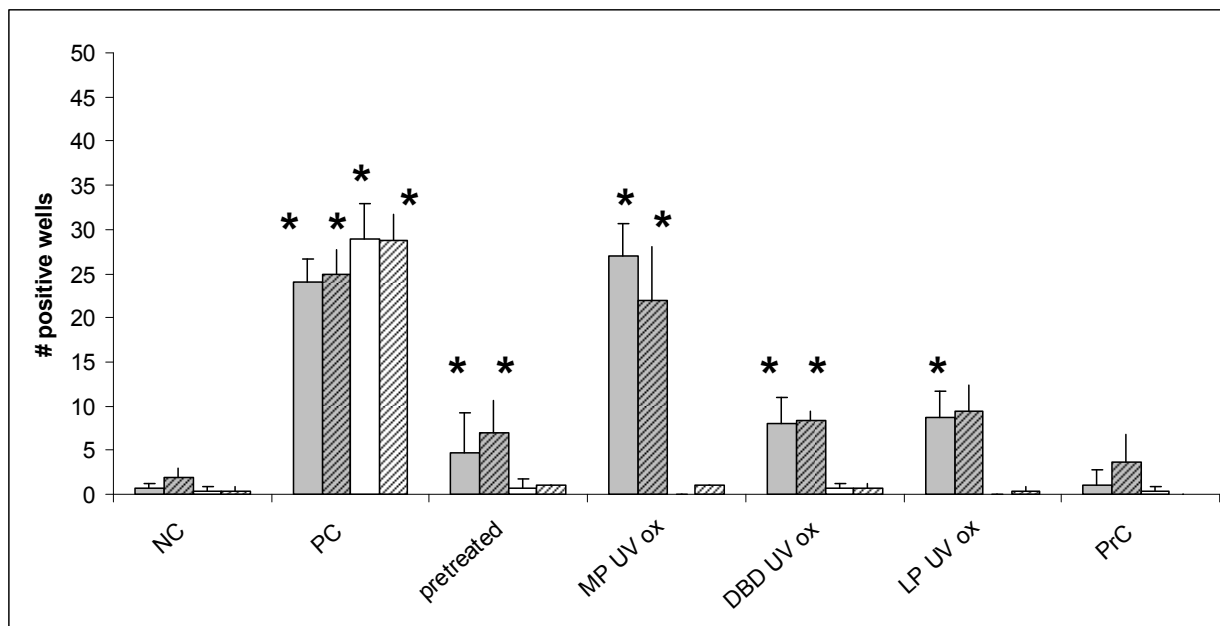
Figure 9-7 Results of Ames II tests with water extracts of the comparison study. Results are given for strains TA98 (grey bars) and TAMix (white bars), with (striped bars) and without (non-striped bars) S9. Samples tested were a negative control (NC), positive controls (PC), a procedure control (PrC), and extracts of pre-treated water and water after UV/H₂O₂ treatment with MP (MP UV ox), LP (LP UV ox) and DBD (DBD UV ox) lamps. Bars denote average values, error bars denote standard deviations (n = 3). Asterisks denote responses showing genotoxicity, i.e. deviating from the NC with 99% certainty.

9.3.4 Difference between strains and responsible compounds

The striking difference between the results found with the two bacterial cultures (TA98 and TAMix) can be explained by the difference in the type of mutations detected by these (mixes of) strains. The TAMix is a mixture of six strains, detecting six different base-pair substitutions (Gee *et al.*, 1994). The TA98 strain is a single strain, which detects frame shift mutations caused by deletions or additions of base pairs in the DNA. Although the TAMix culture in theory has 1/6th of the sensitivity of the TA98 culture, this cannot explain the absence of TAMix response for samples where the TA98 response is 33 positive wells, i.e. 8 times the detection limit (Figure 9-3B).

It is more probable that the compounds in the samples simply do not cause base-pair substitutions, but only frame shift mutations. The Comet results are complementary to the results of the Ames II in this respect, as it is known that some base-pair substitutions may lead to chromosomal breaks under the alkaline conditions applied in this Comet assay. This strengthens the observation that the formed compounds do not cause base-pair substitutions.

9.3.5 Effect of setup, water type, hydrogen peroxide and sulfite

UV/H₂O₂ advanced oxidation was applied to pre-treated surface water without additional treatment or additions of any kind. Comparisons between the two setups (a KWR designed and built pilot reactor and a commercially available pilot reactor) are difficult to make, as the analyses were performed in different batches. Furthermore, the KWR pilot reactor had not been optimized for either LP or MP lamps, whereas commercial reactors are optimized for either one of these types of lamps. Different batches give some variation in the test response (12-22% in TA98) due to the biological variation of the bacterial cultures. The genotoxic activity after treatment in the KWR pilot reactor (Meuse river) was higher than in the (partly optimized) commercial pilot reactor (Ohio River study),

which may be caused by a non-optimal dose distribution, resulting in less effective oxidation of (by-)products. This is in accordance with CFD calculations (see Table 8-4), which show that the D_{10}/D_{mean} for the KWR reactor is about 0.51, whereas the D_{10}/D_{mean} value for the GCWW MP reactor is about 0.58.

The increase in genotoxic response after UV/H_2O_2 treatment is observed in two different waters whose systems are hydrologically not connected. This may indicate that the genotoxic compound(s) is/are formed from ubiquitous contaminants or aquatic substances, such as natural organic matter (NOM). Although these contaminants or substances have not been identified, all locations applying UV/H_2O_2 treatment should be aware of this effect.

The extent to which any observed increase in genotoxic response after UV/H_2O_2 treatment could be caused by sulfite or residual H_2O_2 was verified. Based on the results of earlier and unpublished research, it was shown that dosage of an excess sulfite ion, as applied in these studies, effectively reduces the H_2O_2 concentration to below the detection limit of 0.06 mg/L before toxicological analysis. Chemical analysis of the Meuse water after UV/H_2O_2 treatment in this study confirmed concentrations <0.06 mg/L. Furthermore, according to Aeschbacher *et al.* (1989), H_2O_2 appeared not genotoxic in the classic Ames test with TA98 ± S9 up to 150 µmol per plate (~ 1650 mg/L, assuming a distribution volume of 3 mL). Because control tests with chemical analysis of sulfite levels in the Meuse water extracts showed that the extraction method applied does not extract sulfite ion, the extracts of the water samples will not have contained detectable levels of sulfite. Therefore, any observed increase of the genotoxic response cannot be the result of sulfite or residual H_2O_2 in the treated water. This is confirmed by the lack of substantial increase of the genotoxic response in pretreated Meuse water samples to which sulfite ion alone or sulfite ion and H_2O_2 were added (see Figure 9-8). In the Ohio River samples, 500 mg/L sulfite was added instead of 300 mg/L, but as sulfite appears not to be extracted, these higher levels are also not expected to have reached the ultimate extracts.
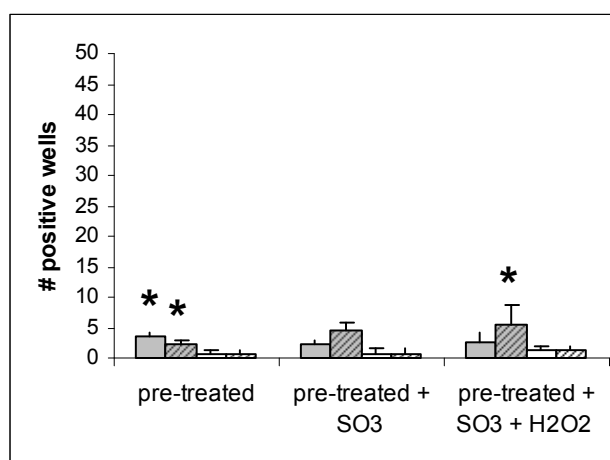
Figure 9-8 Results of Ames II tests with TA98 (grey bars) and TAMix (white bars) with (striped bars) and without (empty bars) S9 on extracts of the pre-treated Meuse water with and without additions of H_2O_2 (10 mg/L) and Na_2SO_3 (300 mg/L). Bars denote average values, error bars denote standard deviations (n = 3). Asterisks denote responses determined to show genotoxicity, i.e. deviating from the NC with 99% certainty.

9.3.6 Effect of UV-photolysis and UV/H₂O₂ oxidation

The increase of the genotoxic response in the LP- and MP-UV/ H_2O_2 treated waters are clearly due to formation of new compounds during the treatment, as the genotoxic response was absent or lower than before the treatment. To further investigate how these new compounds may have been formed, Ohio River water was treated with both photolysis by UV (without H_2O_2) and oxidation by UV in combination with H_2O_2. As can be seen in Figure 9-3B, the genotoxic responses after UV were higher

in the absence of H_2O_2. This gives a first indication that the formation of genotoxic compounds is (mainly) due to photo-induced processes. These processes include direct bond breaking by photons as well as bond breaking by radicals formed by the photons (i.e. photosensitization).
Additionally, the experiments treating Meuse and Ohio river water with LP UV/H_2O_2 showed no or a much lower increase in genotoxic response, while MP UV/H_2O_2 treatment showed a clear increase at the same atrazine conversion level. Finally, the Ames II results of the comparison study (Figure 9-7) showed lower genotoxic responses after treatment with LP and DBD lamps than with MP lamps at the same atrazine conversion level. LP and DBD lamps emit a smaller bandwidth of UV-wavelengths and provide a lower proportion of photolytic conversion of atrazine than MP lamps. It must be kept in mind that these experiments were performed in not fully optimized pilot reactors, and that results in full scale reactors may be different. But, altogether, these results at least give a strong indication that photo-induced processes are the responsible processes for the formation of the genotoxic by-product(s).This remains to be further investigated.

These results yield another question: can an increased genotoxic response be expected during UV disinfection with MP lamps? If direct photolysis does contribute to genotoxicity, there probably is a relation between the induction of genotoxicity and the applied UV dose. The UV dose during UV disinfection is typically 10 – 15 times lower than the UV dose applied in this research. Thus, the induction of genotoxicity would be expected to be much lower or even undetectable during UV disinfection of water. In fact, the results of earlier research have shown that, although not qualified as significantly genotoxic, there was a slight increase in mutations in TA98 without S9 after MP UV disinfection of pre-treated surface water at a biocide UV dose of about 90 mJ/cm^2 in a 300 liter/h laboratory-scale UV disinfection apparatus (IJpelaar *et al.*, 2005). Under the same conditions, with the same water quality, an increase in mutations in TA98 without S9 was also found when treating the water in a 180-m^3/h MP UV pilot, indicating that the scale of the laboratory research did not give false positive results (IJpelaar *et al.*, 2005). Similarly, Haider *et al.* (2002) found one weak increased response in TA98 without S9 in UV-disinfected groundwater using an LP lamp. Carnimeo *et al.* (1995) reported negative Ames test results for UV/H_2O_2-disinfected raw river water using LP lamps.

However, when different MP-UV doses were applied in the Meuse water tests, the responses did not show an effect of UV dose on the height of the genotoxic response (Figure 9-9). We have no solid explanation for this observation, given the discussion above. A possibility is that there was some kind of saturation in the formation process of the genotoxic compounds. Further studies are necessary to confirm our observation that photolysis seems to be responsible for the observed induction of genotoxicity.
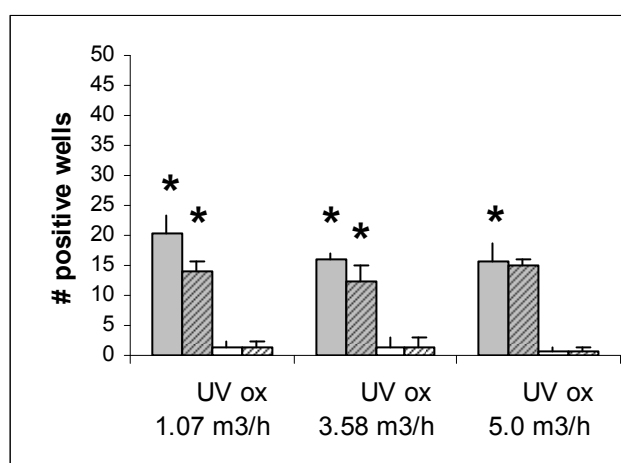
Figure 9-9 Results of Ames II tests with TA98 (grey bars) and TAMix (white bars) with (striped bars) and without (empty bars) S9 on extracts of Meuse water after MP-UV treatment at different flow velocities, resulting in UV doses of 547, 313 and 180 mJ/cm^2, respectively. Bars denote average values, error bars denote standard deviations (n = 3). Asterisks denote responses determined to show genotoxicity, i.e. deviating from the NC with 99% certainty

9.3.7 Human health

A final question is what these results actually mean in terms of risks to human health. It must be emphasized that the applied genotoxicity tests can only indicate a health <u>hazard</u>: namely the presence of genotoxic compounds in that water. It is impossible at this stage to derive a health <u>risk</u>, as it is unknown what compounds are responsible for the measured genotoxicity and what doses of these compounds a consumer could tolerate. Additionally, further research is required to determine whether these mutagenic effects also occur in mammalian cells or in mammalian organisms.

Most importantly, the increased genotoxic response as observed in treated water was removed to below the detection limit or below the level of the pretreated water by GAC adsorption in both studies (even when GAC was not fresh). Because water treatment plants that currently apply UV oxidation also typically use subsequent GAC adsorption, genotoxic compounds are not expected to be present in the finished drinking water. Therefore, no health risk from the finished drinking water is expected. Clearly, new installations should include GAC adsorption after UV/H_2O_2 treatment. As the adsorption capacity of GAC decreases in time, and because there was one instance of GAC-contacted water exceeding the detection limit, it is important to monitor the effectiveness of GAC contactors when removing compounds that contribute to a genotoxic response.

In the design of new installations and selection for treatment methods, the UV/H_2O_2 technique should be compared to other techniques. It is well-known that chlorination, chloramination and ozone-oxidation lead to genotoxic by-products, too (e.g. Rook, 1974; Richardson *et al.*, 2007; Najm and Trussell, 2001; von Gunten and Hoigne, 1994). It is unclear if the generation of the genotoxic response observed in these methods is comparable because they have been measured in different tests (e.g. classic Ames test vs. Ames II). This issue should be investigated. Furthermore, other factors, such as micropollutant removal, disinfection power, and costs of the different methods are also important to consider in a treatment method comparison.

9.4   Conclusions

- The results of these studies show no genotoxic activity after UV/H_2O_2 treatment in the Comet assay and in the Ames II TAMix strain with and without S9 under all applied conditions.
- An increase in genotoxic activity in the Ames II TA98 strain both with and without S9 was measured in three tested waters after MP UV/H_2O_2 treatment.
- After LP and DBD $UV//H_2O_2$ treatment a lower or no increase was observed in the same strain, in the same waters, at the same atrazine conversion level, but in not fully optimized reactors.
- The genotoxicity observed after DBD UV/H_2O_2 treatment was comparable to what was observed with LP lamps at the same atrazine conversion level.
- The increase in genotoxic activity was also seen after MP UV treatment without H_2O_2, to a higher level than with H_2O_2, indicating that a photo-induced process may be the responsible process for the formation of genotoxic compounds.
- GAC post treatment effectively reduced the formed genotoxic activity to control levels for all but one study and to below the level of the pre-treated water in the other study; no health risks are expected as long as UV/H_2O_2 is followed by GAC adsorption.
- Further research should primarily include other natural water qualities (e.g. with and without chemical pollutants; low or high DOC), chemical identification of the responsible products, UV dose – genotoxic effect relations, further comparisons between LP and MP lamps, studies on the responsible process for the by-product formation, and comparisons to byproduct formation in other treatment methods. This research already is being done within the framework of a new project on byproduct formation.

Design of combined full scale oxidation unit

Work package 10; KWR

Authors: C.H.M. Hofman-Caris, E.F. Beerendonk

10 Work package 10: Design of combined full scale oxidation unit

10.1 Introduction

At the start of the project "New concepts for UV/H_2O_2 oxidation", it was expected that it is essential for organic contaminant control that an oxidation process like UV/H_2O_2 is combined with GAC filtration. Based on the research in this project it was concluded that the UV/H_2O_2 process, followed by GAC filtration results in a good drinking water quality. One of the hypotheses in the project, however, was that the concept could be further improved by applying a novel treatment concept in which the UV/H_2O_2 oxidation process and a GAC filtration are integrated. This concept might result e.g. in lower costs, a smaller footprint of the complete installation based on two barriers, lower energy use, and capacity-expandable modules. A suggestion for a possible, integrated process is given in Figure 10-1. In WP10 ideas were drawn up on new concepts (e.g., combining a UV/H_2O_2 reactor with a granular activated carbon (GAC) contactor) that would minimize the space in a water treatment plant and would reduce (operational and/or investment) costs. CFD calculations can be used to design the optimum reactor.

Several ideas were generated on how such a combination can be achieved. In this chapter, an overview is given on the results of this brainstorm. Several suggestions were made, and for every option a short description is given on the expected advantages and disadvantages.
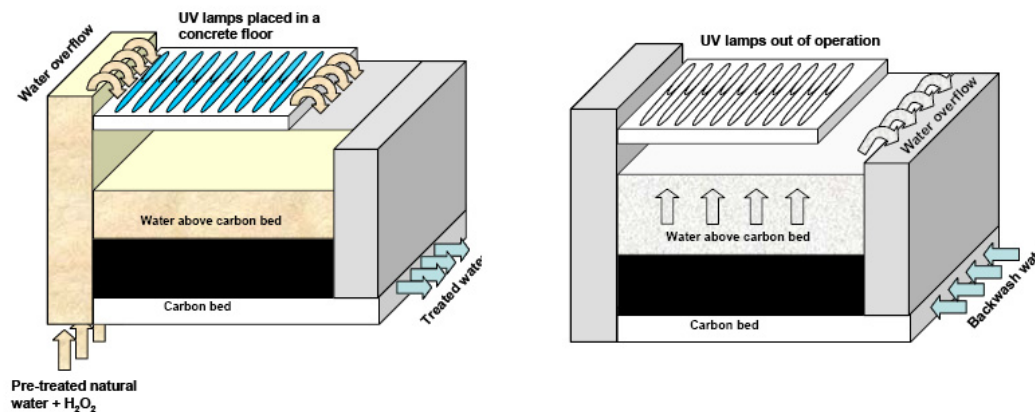
Figure 10-1 An optional schematic representation of the UV-oxifilte. The left part of this figure shows the unit in oxidation and filtration mode. The right part presents the backwash mode of the unit.

Various options

The following sections describe several options that were suggested. The following legend is used (Figure 10-2).
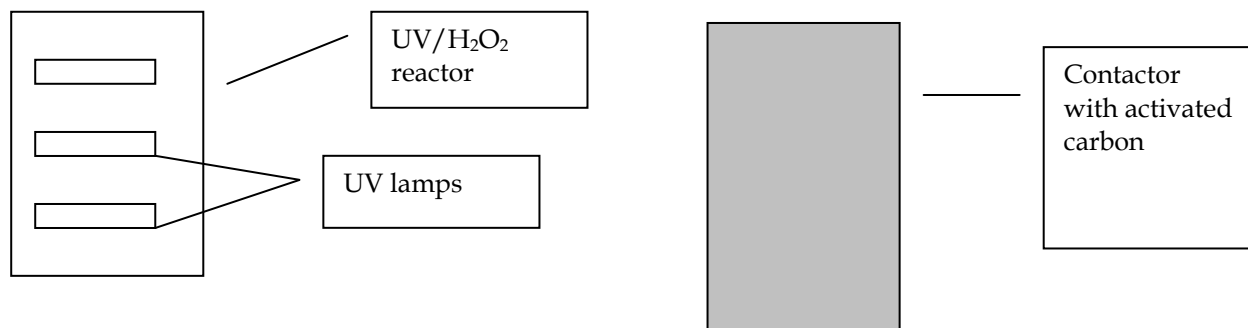
Figure 10-2 Legend for the schemes used in the various options presented in chapter 10.

The merit of any of the options described below also depends on whether its implementation is for an existing or new treatment plant.
Further aspects that would have to be considered include the following:
- Capacity of the treatment process (m^3/h)
- Water quality and UV transmission before UV treatment: which UV system will be used (LP, MP or maybe DBD lamps), targeted conversion of organic micropollutants, and required UV dose (mJ/cm^2 or kWh/m^3)
- Water quality after UV treatment, before GAC adsorption: type of GAC contactor (conventional or biological, up flow or down flow) and required empty bed contact time of the GAC contactor
- Required final water quality after UV/H_2O_2 and GAC
- Space available for the installation (UV combined with GAC)
- Housing and space of the electrical part of the installation
- Frequency and time required for GAC regeneration and its effect on the total process: the process may become less flexible, if the UV part is connected to the GAC contactor (i.e., taking out the GAC contactor for maintenance will temporarily put the UV installation out of order).

In a UV/H_2O_2 treatment plant a large amount of lamps is used. It is possible that energy (and money) may be safed by placing multiple reactors in a cascade. One passage through a combined UV/H_2O_2/GAC reactor may not sufficient to obtain the desired conversion of micropollutants, but in such a cascade the process can be repeated. The advantage may be that for the subsequent reactors in the cascade different operation conditions may be required, as the water quality is improving during the process. It will be important to monitor water quality in between the separate steps to be able to adjust process conditions to the actual situation. For example: if after the first passage the UVT of the water has improved, the UV dose in the second reactor may be lower than in the first reactor.

10.1.1 Option 0: current situation

In the present situation, both in pilot and in full scale plants, a separate UV/H_2O_2 reactor is combined with separate GAC contactors. This is schematically shown in Figure 10-3.
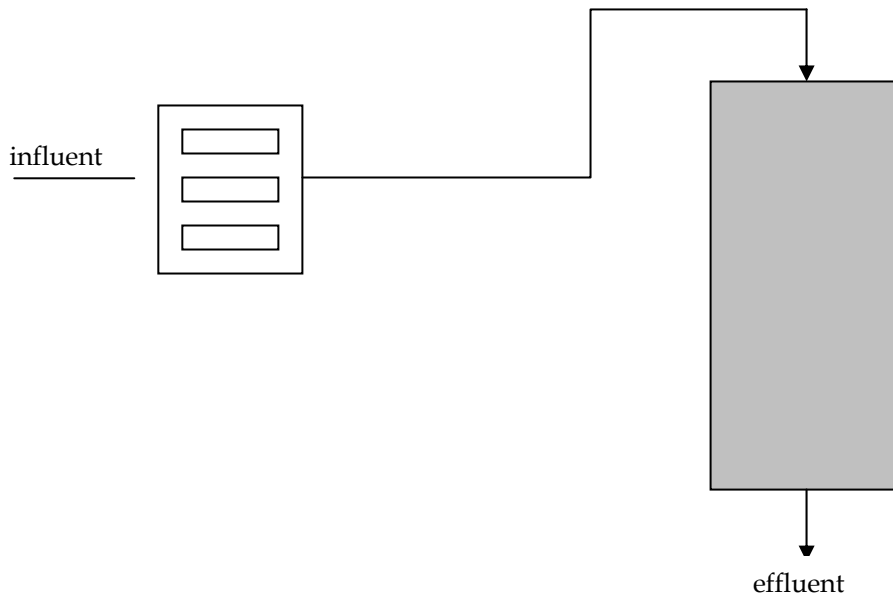
Figure 10-3 Option 0: separate UV/H₂O₂ reactor and separate GAC contactor

A combination of several UV/H_2O_2 reactors (in series and parallel) could be used with a number of contactors in parallel. Collecting the water from the UV/H_2O_2 reactors in a separate equalization tank before it is pumped to the contactors would be possible.

10.1.2 Option 1: UV lamps above the filter

The simplest combination would be to place the UV lamps in the space above the GAC contactor (the idea that was presented when the project was started in 2005/2006), as shown in Figure 10-4. It would be relatively easy to implement this option in an existing plant, and would not require much extra space. In principle there are two possibilities for this option: placing the lamps horizontally or vertically above the contactor.

influent   influent

effluent   effluent
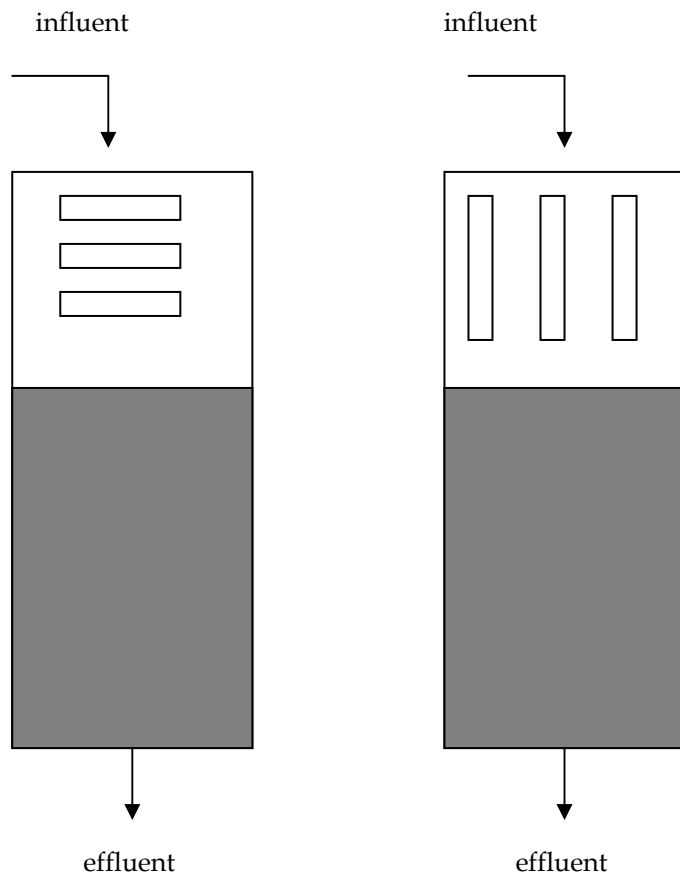
Figure 10-4 UV/H$_2$O$_2$ reactor placed above the GAC contactor

If the UV lamps are placed as shown in Figure 10-4, it is very important to take into account whether the filters will be operated at a constant flow or at a constant water level above the contactors. As the UV/H$_2$O$_2$ reactor is in direct contact with GAC, the carbon will adsorb the excess H$_2$O$_2$, resulting in a concentration gradient for this compound. This effect should be calculated or estimated on forehand to determine the required H$_2$O$_2$ concentration. Furthermore, H$_2$O$_2$ should be injected into the main water inlet, before the water enters the UV compartment, to obtain an optimum UV/H$_2$O$_2$ process. Since the lamps will be spread on top of the GAC there will be a need for an optimal spatial configuration for maximum efficiency (and sufficient UV dose distribution) at different flow rates. It may be best to operate lamps that could be dimmed to different power levels. Appropriate placement of sensors may also be a challenge.

Special attention should be paid to mixing of the water in the UV/H$_2$O$_2$ reactor in this case to ensure that all water receives a sufficient UV dose. In conventional reactor systems, a sufficient UV dose is guaranteed by applying turbulence in the UV reactor. In this set-up, turbulent flow would result in carbon particles whirling through the UV compartment, thus rendering the UV process less efficient (higher turbidity, more H$_2$O$_2$ consumption). Furthermore, the residence time of the water in the UV/H$_2$O$_2$ reactor will be longer than is common in the current reactors. For AOP, this may be of importance as reaction time is a critical parameter. As the water with the organic micropollutants spends more time in the UV reactor, the UV output of the lamps (W) may be reduced, which may be an advantage (lower energy demand) Furthermore, there are no additional costs of a separate UV reactor. On the other hand, care should be taken that the water temperature does not become too high, and that a sufficient UV dose is obtained for all water. Besides, adsorption of H$_2$O$_2$ by GAC will become more important when longer residence times and effective mixing conditions are applied.

Because the UV lamps are close to the filter bed, the sleeves may be affected during contactor backwashing. Therefore, a device will have to be developed to enable the operators to easily remove

the lamps when maintenance is required (contactor backwashing, replacement of lamps and/or quartz sleeves). This should be a rather robust system because contactor backwashing would occur on a regular basis.

It is possible to implement a UV/H$_2$O$_2$ reactor above several contactors, or to use a series of such combined reactors. The failure of one UV/H$_2$O$_2$ reactor would not affect the entire plant.

10.1.3 Option 2: UV lamps below the filter beds.

This option, with horizontally or vertically placed lamps, is schematically shown in Figure 10-5.
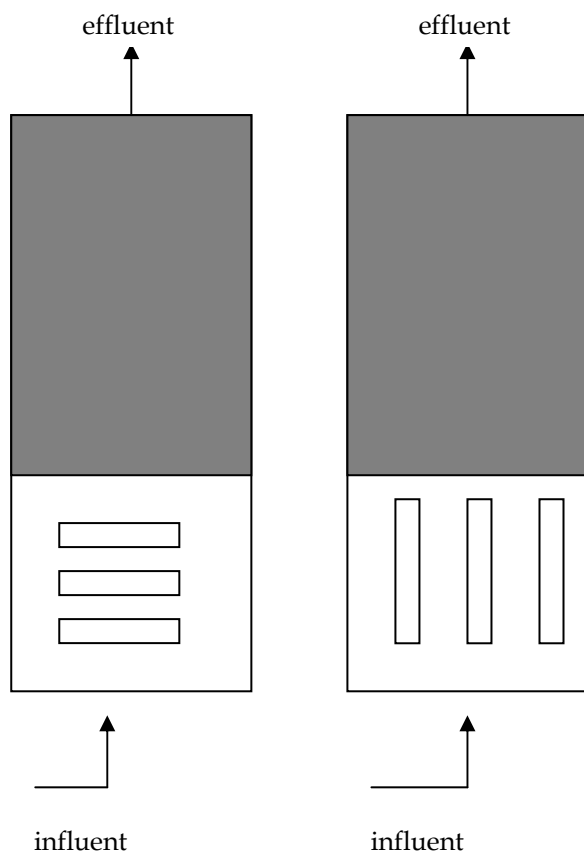
Figure 10-5: UV/H$_2$O$_2$ reactor placed below the GAC contactor

This option will not be as easy to implement in an existing situation as option 1, as there should be enough space available below the contactors. The contactors also have to be kept in place somehow, and special attention should be paid to a practical design to be able to backwash the contactors, and to replace the lamps. It may be an option if the system is designed for a new plant. Mixing of the water, UV intensity, and possible temperature effects should be taken into account in this option also. As in option 1, the residence time of the water will be longer than is usual in option 0, and thus a lower UV intensity and lower energy costs may be required. If GAC contacts H$_2$O$_2$, a concentration gradient may exist for H$_2$O$_2$, and extra H$_2$O$_2$ dosage may be required (like in option 1).

Carbon particles should be avoided in the UV/H$_2$O$_2$ reactor because they will decrease the H$_2$O$_2$ concentration and increase the turbidity of the solution. This option only can be applied in case of upflow GAC contactors.

10.1.4 Option 3: UV/H₂O₂ reactor placed above or below the filter bed, with a separating shield in between.

This option, in which direct contact between the carbon and the solution during UV/oxidation is decreased, is schematically shown in Figure 10-6.
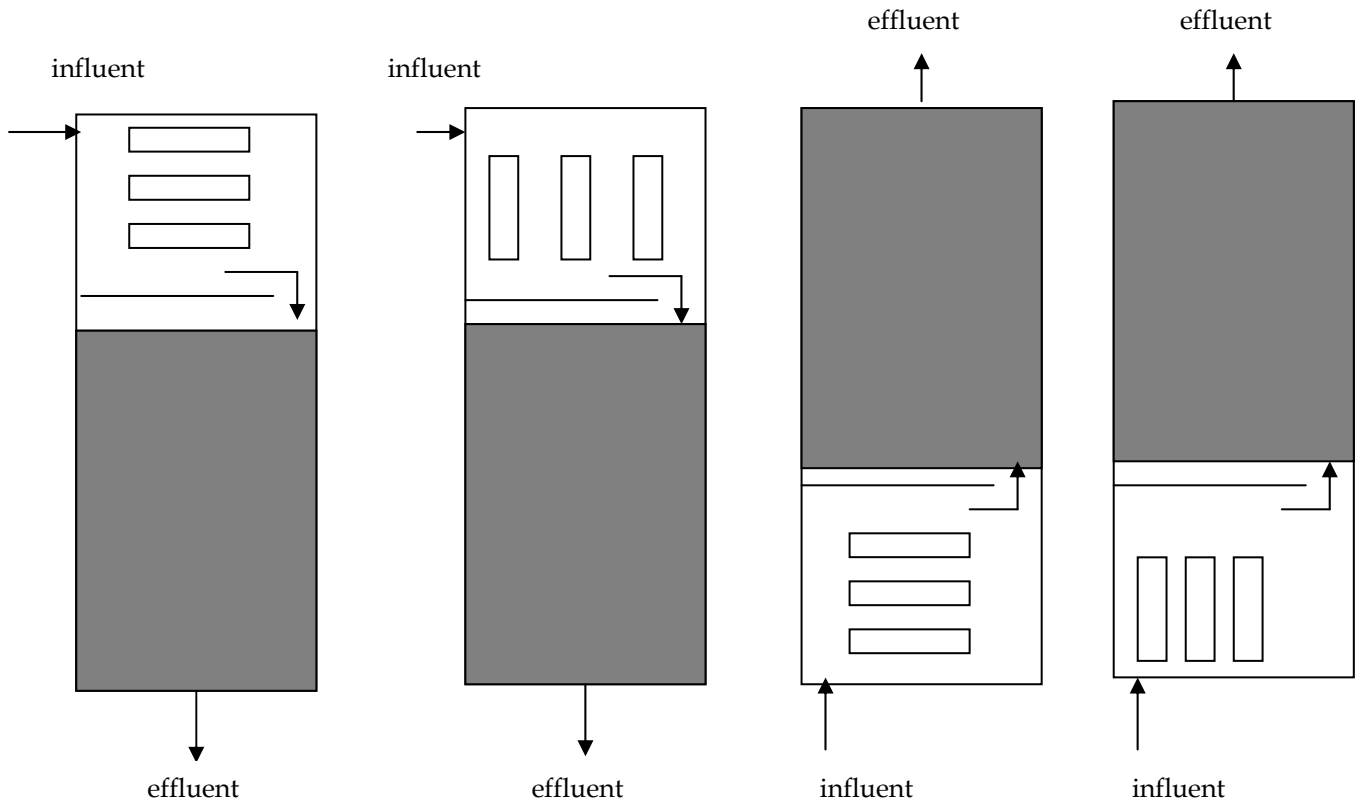
Figure 10-6 UV/H₂O₂ reactor placed above (or below) the filter bed, using a separating shield in between the contactor and the reactor.

This system is more or less comparable to options 1 and 2. The main difference is that direct contact between carbon and the water in the UV/H₂O₂ reactor is prevented. Thus, less peroxide will be required, and the chance to obtain an inefficient oxidation process is lower because carbon particles would not cause turbidity in the UV reactor. It should be taken into account that the convection velocity from the UV/H₂O₂ reactor to the contactor can be rather high, which may have consequences for the mixing conditions in the UV reactor. Because of flow short-circuiting, the efficiency of the UV reactor may decrease.

Because the shield between the UV lamps and the GAC contactor essentially forms a separate UV reactor, the UV dose distribution and the process efficiency could be improved and controlled easier than in option 1. Like in options 1 and 2, a special robust device would also be required for maintenance (contactor backwashing and lamp replacement).

10.1.5 Option 4: UV/H₂O₂ reactor placed in a channel between the filter beds.

In some plants several contactors are fed from one central channel (e.g., Richard Miller Treatment Plant in Cincinnati). In that case it may be possible to place the UV lamps and H_2O_2 dosage system in this channel, as schematically shown in Figure 10-7.
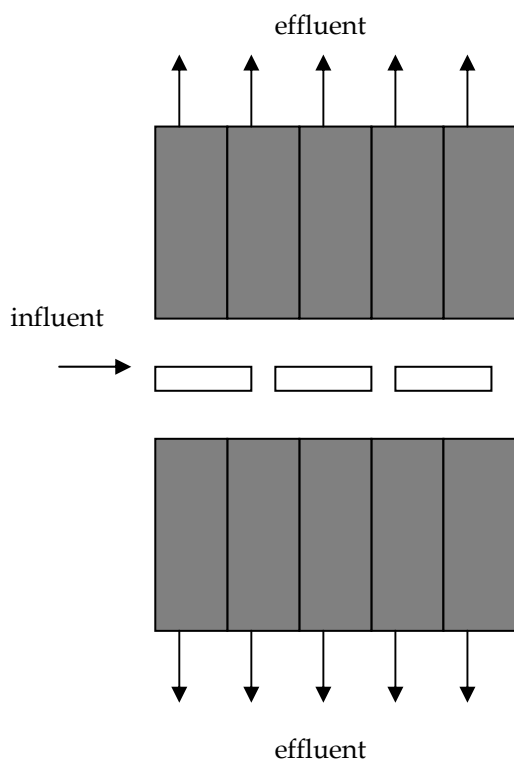
Figure 10-7 UV/H₂O₂ reactor placed in the central channel between the contactors

In this case no practical problems are expected to occur with respect to turbidity due to the presence of carbon particles in the UV/H_2O_2 reactor, to H_2O_2 consumption due to contact with GAC, and to maintenance. A device has to be developed for lamp replacement and sleeve cleaning, but this system does not need to be as robust because as for the preceding options because these events would occur less frequently (i.e., not on the regular basis of options 1-3 where the lamps would have to be removed every time the contactor has to be backwashed).

A special point of attention will be the UV dose distribution in the channel, as all water should obtain a sufficient dose. However, this point will be less critical than in options 1 and 2, because there is no direct contact between the contactor and the UV compartment, and thus turbulent flow can be applied. Temperature in the channel should be controlled. The peroxide should probably be injected before the water enters the channel where the UV lamps will be located to ensure sufficient mixing. As in the previous options, the residence time of the water in the UV/H_2O_2 reactor will also be relatively long resulting in a lower applied output of the lamps (and possibly resulting in lower energy costs). However, because of the possible long distance between the water and the UV lamps, adequate mixing inside the channel will have to be considered.

The practical implementation of this system is another factor that requires special attention . It will not be very difficult to implement the UV/H$_2$O$_2$ reactor in an existing channel, but redundancy should be ensured. Problems can be expected when lamp failure occurs. If the UV/H$_2$O$_2$ reactor is present in the central channel and failure occurs, all contactors will be affected and water production may be at risk. Therefore, UV/H$_2$O$_2$ reactors should preferably be placed in compartments (e.g., small channels in between the main channel and the separate contactors). This will also simplify maintenance and ensure a sufficient UV dose for the water. If the lamps are placed in an existing channel, access to the lamps, sleeves or sensors may be a challenge.

10.1.6   Option 5: GAC contactor inside the UV/H$_2$O$_2$ reactor

This option can only be considered if a totally new plant should be designed, as it will not be possible to implement this in an existing drinking water treatment plant.
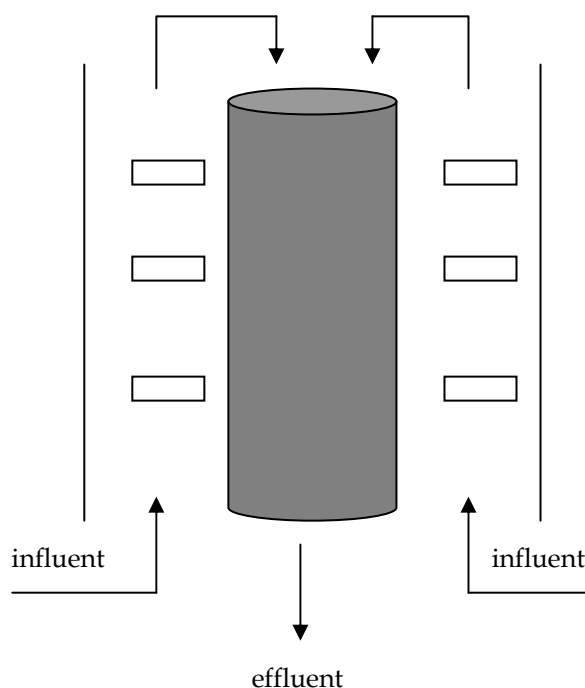
Figure 10-8: UV/H$_2$O$_2$ reactor around a GAC contactor

In this case, like in option 4, no problems are to be expected with respect to contact between GAC and H$_2$O$_2$ or to turbidity in the UV/H$_2$O$_2$ reactor. Mixing and the UV dose can be controlled, and if necessary the water can be directed through the contactor multiple times. It will also be possible to place several of such reactors in series. By doing so, the UVT in the subsequent UV/H$_2$O$_2$ reactors will improve resulting in a lower UV dose and possibly less peroxide. This design can be considered as a separate UV/H$_2$O$_2$ reactor before the GAC bed, with a different position of the reactor around the GAC contactor. In principle, it would have similar benefits as options 3 and 4.

The major drawback of this option is the actual size of the contactor. Normally a GAC contactor is relatively large compared to the size of a UV/H$_2$O$_2$ reactor, and this would require building a huge UV/H$_2$O$_2$ reactor. Of course the UV/H$_2$O$_2$ reactor does not have to be that large, and a small reactor, placed on the side the contactor would be much more practical. Identical considerations regarding the UV dose and implementation can be made for this smaller reactor. Maintenance and lamp failure are not expected to be a problem in this option.

10.1.7 Option 6: UV/H₂O₂ reactors placed inside the GAC contactor

In this case the UV/H_2O_2 reactor is not placed outside the contactor, but inside, as shown in Figure 10-9.
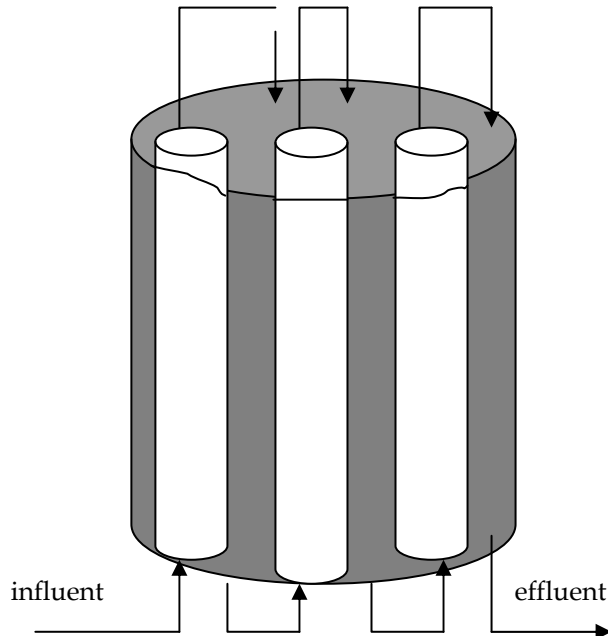
Figure 10-9: UV/H_2O_2 reactor inside the GAC contactor

In this set-up, the water can be directed through the UV/H_2O_2 reactors in series. Thus, for the subsequent UV/H_2O_2 reactors a lower UV dose and lower H_2O_2 concentrations may be required. In this set-up, problems with increasing temperature can also be prevented. In between the passage through the UV/H_2O_2 reactors the water can be directed through the filter In that case, the peroxide concentration in the water will be reduced to 0, as a result of which H_2O_2 will have to be added before each UV reactor. This may result in an increase in the total amount of H_2O_2 required. Special attention will have to be paid to the construction of the contactor to prevent flow short-circuiting between the UV reactors. Apart from this problem, separate compartments for the GAC will also be required to prevent the entire system from blending within the contactor, which would result in each UV reactor receiving the same influent. This, of course, will not be a problem if a single pass system is applied. Furthermore, H_2O_2 should be injected and mixed in the water before each UV reactor.
Some special devices will be required to facilitate maintenance, but this will not be a problem. Because a plant will consist of several of these integrated contactors and reactors, failure of a lamp or contactor will not cause a problem. Implementation in an existing plant depends on the plant design. Each reactor could be lowered into the GAC contactor when the bed is fluidized.

10.2 Discussion, conclusions and recommendations

Table 10-1 shows an overview of the options and their advantages and disadvantages compared with the existing situation (option 0: separate UV/H_2O_2 reactor and GAC filter). Although all criteria are scaled + or -, it should be kept in mind that some criteria will be of more importance than others. Therefore, a column is included with an estimation of the "importance" of the criteria, ranging from 1 (not very important) to 7 (very important).

Table 10-1 overview of the advantages and disadvantages for options 0-6

criteria	options							importance
	0	1	2	3	4	5	6	
Implementation in existing plants	0	+	-	+	+	- -	- -	5
Required space (excluding the electrical device)	0	+	+	+	+	- -	+	1
Energy consumption	0	+	+	+	+	+	+	7
Investment costs	0	+	+	+	+	- -	- -	6
Maintenance	0	-	-	-	0	0	- -	2
Redundancy	0	0	0	0	--	0	0	3
H_2O_2 consumption	0	-	-	0	0	+	+	4

Whether or not an option would be favorable, strongly depends on the actual situation. One of the most important factors is whether the new reactor should be incorporated into an exisiting plant, or whether a totally new plant is being built.
According to the overview in Table 10-1 and the considerations described in section 2, it seems that options 3 (with the lamps placed above the filter bed) and 4 (the UV reactor placed in a channel in between the filter beds) would merit to be further explored.

When a new plant is to be built, or in case an existing plant should be optimized, one of the options mentioned above may be considered. "Computational Fluid Dynamics" (CFD) modeling can be very valuable to obtain information on the possible performance improvement this option would offer. However, this can only be applied when a more or less detailed reactor design is available. In that case, CFD can give information on the mixing conditions in the UV reactor, the residence time distribution and the possibility of GAC entering the reactor. Furthermore, it can be calculated whether the reactor performance may be improved by applying some changes to this reactor design (e.g. by placing baffles or by changing the water inlet or outlet, or the residence time).

General overview, conclusions, practical implementation and suggestions for further research

KWR

Authors: C.H.M. Hofman-Caris, E.F. Beerendonk

11 General overview and conclusions

11.1 General discussion

11.1.1   UV/hydrogen peroxide process

UV irradiation has been used for decades to achieve disinfection of drinking water. UV light can also be absorbed by some types of organic compounds, which become converted into degradation compounds by photolysis. Ultimately, this conversion will result in the formation of CO_2 and H_2O, but for drinking water treatment in general, it will be sufficient if these "organic micropollutants" are converted into into smaller easily biodegradable compounds. The disadvantage of photolysis reactions, however, is that not all molecules can absorb UV irradiation, and if they can, these molecules will only be able to absorb UV at a certain wavelength. As a result, UV irradiation in itself cannot be used to obtain sufficient conversion of all micropollutants. This problem can be solved by adding H_2O_2 to the system. H_2O_2 is able to absorb UV irradiation to yield •OH radicals that attack all organic compounds that are sensitive towards oxidation. Thus the goal of a significant decrease in the concentration of organic micropollutants can be attained by combining H_2O_2 addition with UV irradiation.

11.1.2   Various UV lamps

The UV/H_2O_2 advanced oxidation process (AOP) has been studied by various authors, and also is applied in a few full-scale drinking water treatment processes. In principle, two types of UV lamps can be used: Medium Pressure and Low Pressure UV lamps. Both lamps contain mercury, and their main difference is that MP lamps emit a broad spectrum of wavelengths, whereas LP lamps only emit at 253.7 nm (making these lamps less suitable for photolysis). However, the LP lamps have a high energy efficiency (25-30% compared to 15% for MP lamps), and a longer expected life span (9,000-12,000 hours in contrast to 4,000-6,000 hours for MP lamps). Because these LP lamps are less effective for photolysis, they would generate less by-products than MP lamps. On the other hand, because of their higher power fewer MP lamps are required in a reactor compared with LP lamps to achieve an equivalent dose, which results in a smaller footprint of the reactor. Therefore, most commercially available UV reactors are presently equipped with MP UV lamps. However, because of the advantages of LP lamps, the question was raised whether LP lamps can also be used to achieve an effective UV/oxidation reactor.

Philips Lighting has been developing two new types of lamps. One is an LP UV-lamp, with higher power than conventional LP lamps, thus mitigating a disadvantage of LP lamps. The Philips LP lamp was studied in the collimated beam set-up and pilot reactor at KWR.

The other Philips Lighting lamp is a Dielectric Barrier Discharge (DBD) lamp that does not contain mercury and emits UV light over a smaller range of wavelengths than the MP lamp. This lamp would combine the advantages of both MP and LP lamps. A prototype was used in the studies carried out at KWR (collimated beam and pilot reactor) and in the pilot plant of Dunea.

11.1.3   Hydroxyl radical formation by means of MP, LP and DBD UV lamps

H_2O_2 generally absorbs UV irradiation at a wavelength between 200 and 235 nm. The emittance of MP lamps in this area is rather weak, but still higher than that of LP lamps. LP lamps emit UV irradiation at a wavelength of 253.7 nm. At this wavelength, the molar extinction coefficient of H_2O_2 is 19.6 $M^{-1}s^{-1}$

(Tuhkanen, 2004), which is very low. This means that in order to generate a sufficiently high level of •OH radicals in a solution, the concentration of H_2O_2 has to be rather high. However, natural compounds present in water, like DOC and nitrate, show a strong absorbance in the range of 200-235 nm, whereas their absorbance at 254 nm is very low. Therefore, although the extinction of H_2O_2 at 253.7 nm is low, the radical formation by LP lamps may be rather efficient because of the very low absorbance of the water matrix at this wavelength. Calculations showed that H_2O_2 may absorb 21.4% of the total photon flow from an LP lamp compared with only 15.5% from an MP lamp. These calculations were verified using pretreated water from both Dunea and GCWW. The model compound pCBA is known to be relatively insensitive toward photolysis, but very sensitive to oxidation by •OH radicals. Figure 3-6 shows the conversion of pCBA as a function of UV doses in Dunea water, and Figure 3-7 in GCWW water, both in the absence and in the presence of 10 mg H_2O_2 / L. The experiments were carried out with either LP or MP lamps. Obviously, only irradiation with LP lamps hardly results in any conversion of the pCBA, whereas a small conversion can be observed when MP lamps are used for photolysis. The DBD lamp gives a conversion which is in between the conversions of the other two lamps. However, when H_2O_2 is added, the conversion increases with H_2O_2 addition: the highest conversion was achieved for the reactor with a DBD lamp, followed by the reactor equipped with LP lamps, for both types of water.

The hypothesis was thus confirmed that a lower UV absorption by the water matrix at a wavelength of 254 nm (which is specific for LP lamps) increased the hydroxyl radical formation at this wavelength compared with lower wavelengths, despite the fact that at 254 nm the UV absorption by H_2O_2 is lower.

11.1.4   Comparison of different UV reactors

Subsequently, the conversion of organic micropollutants by the three different lamp types in combination with H_2O_2 in a collimated beam setup was studied.
The comparison of reactors, equipped with different types of lamps, requires some discussion. On one hand, it would be preferable to use one type of reactor, that can be equipped with all types of lamps. Thus, the performance of the lamps can be compared under the same flow conditions. On the other hand, it can be argued that a full scale reactor always will be optimized for the type of lamp it will be equipped with. As for a reactor with MP lamps another flow will be optimum than for a reactor equipped with LP or DBD lamps, another eactor design will have to be applied. In order to compare the efficiency and costs involved with all different types of lamps, it can be argued that this ideally should be done under real full scale conditions. In general, this will mean that reaction vessels, optimized for the type of lamps they have been equipped with, will be used, and that the operating conditions will be set in such a way, that a certain conversion of a model compound or set of model compounds will be achieved. The KWR pilot reactor was designed according to the first concept: comparing lamps under similar flow conditions, whereas both other pilot reactors were designed according to the second concept: comparing reactors under conditions, partly optimized for this specific application.

11.1.5   Conversion of hormones and triazines

In collimated beam experiments it was found that MP lamps convert hormones like 17-β- estradiol, estriol and estrone very well. For 17-α-estradiol a higher UV dose appeared to be required to achieve sufficient conversion.
Under similar experimental conditions, the DBD lamp appeared to give more or less the same results as the MP lamp. At a dose of 300 mJ/cm² in GCWW water, a conversion of at least 86% was obtained, and in Dunea water of at least 92%. At a dose of 600 mJ/cm² the DBD lamp gave complete conversion of all hormones tested in all cases.

The LP lamp appeared to give a lower conversion of hormones than the MP or DBD lamp, as was expected. However, even with this lamp type, a conversion of about 75% was obtained at a dose of 300mJ/cm², and about 90% of the hormones appeared to be converted at 600 mJ/cm².

It should be noted, that applying only UV irradiation (without H_2O_2 present) results in a notably lower conversion of the hormones tested, than when also H_2O_2 is used. Photolysis is not a very important process especially for LP lamps because they emit only one distinct UV wavelength. This also explains the somewhat lower overall conversion obtained with LP lamps, because the conversion essentially depends on oxidation by hydroxyl radicals, whereas with the other lamps a combination of photolysis and oxidation takes place.

The results obtained for the conversion of triazines with all three types of lamps appeared analogous to the results obtained with hormones, as discussed above.

11.1.6   Conversion of organic micropollutants

When several organic micropollutants were tested in the pilot reactor of KWR, comparable results were obtained for the three types of lamps. The best results were obtained with MP lamps, followed by DBD lamps and finally LP lamps. The differences can be explained from the contribution of photolysis in the overall process. In general, the conversion obtained was a little lower than in the collimated beam set-up, which can be explained from the fact that the pilot reactor had not yet been optimized. By adapting the reactor configuration based on Computational Fluid Dynamics (CFD) modeling, a more efficient flow through the reactor can be obtained, resulting in a better conversion.

11.1.7   Nitrite formation

From the experiments carried out in the KWR reactor, it could be concluded that most nitrite is formed when MP lamps are used, followed by DBD and LP lamps respectively.

11.1.8   Disinfection capacity

The disinfection capacity of the UV/H_2O_2 process was studied using MS2 Phages as model microorganisms. For all three types of lamps, at a UV dose of 450 mJ/cm², an 8-log reduction of the MS2 phages was achieved. Thus, regardless of the type of UV lamps used, the water would be well disinfected.

11.1.9   Effect of UV Transmittance

It also became clear that the UV/H_2O_2 process will be more effective in water with a higher UV transmittance (UVT). This had been expected, as UV irradiation can be used for photolysis of organic micropollutants and H_2O_2 more optimally, if it is not absorbed by other substances.

11.1.10   Electrical energy per order (E_{EO})

It was not very easy to make an objective comparison of the three types of lamps. One way of comparing the lamps is by using the E_{EO} (electrical energy per order). This is the amount of energy (kWh) required to convert 90% of a certain compound in a certain reactor in 1 m³ of water. Because the pilot reactor at KWR could be equipped with all three types of lamps, a good comparison could be made of the performance of the lamps under the same flow conditions (see discussion above. The E_{EO} was calculated for several organic micropollutants, as shown in Figure 3-18. The LP lamps gave the lowest E_{EO} values. The E_{EO} values obained for MP lamps seemed to be about twice as high. For the DBD lamps, assuming a potential efficiency of 24% (based on information by Philips Lighting), the E_{EO}

values fell in between the values obained for MP and LP lamps, although they were closer to the values obtained for LP lamps. Unfortunately, so far the efficiency of the DBD lamps has not been optimized yet (7% efficiency was reached during the experiments at KWR in WP1, and 12% during the experiments at Dunea in WP8).

11.1.11 Pilot plants

Based on the results obtained at KWR, guidelines and requirements were described for the pilot plants at Dunea and GCWW. At GCWW two commercially available UV reactors were used: one equipped with one MP lamp and one equipped with eight (conventional) LP lamps. For this purpose, commercially available LP lamps were used, not the improved type developed by Philips and used by KWR in the investigation described above. The LP lamps used in the GCWW and Dunea pilot plant are conventional LP lamps, which have a lower power than the HO-LP lamps used previously by KWR.

At GCWW the pilot unit was run during a full year, thus treating water with seasonal variations, and the resulting UV transmission varying between 84 and 95%. A water treatment plant would most likely adopt the strategy of varying operational parameters This difference can greatly affect the amount of UV dose required to obtain 80% conversion of atrazine. It was decided to achieve a target conversion, rather than have a fluctuating conversion under fixed operating conditions. Therefore, with 80% atrazine conversion set as a reference, both reactors gave a comparable degree of degradation of the selected organic micropollutants, regardless of lamp type (LP or MP) or influent water source. The efficiency of the LP reactor increased more than the efficiency of the MP reactor when UVT increased. When comparing both types of reactors, the E_{EO} for the MP reactor appeared to be higher than for the LP reactor, which agrees well with the results obtained by KWR. The difference in conversion of organic micropollutants between the MP- and Lp-reactor can be attributed to the higher efficiency of LP lamps. Furthermore, as in the experiments at KWR, GCWW found that adding H_2O_2 to a UV reactor significantly increased compound conversion. In agreement with the findings at KWR, GCWW observed that more energy was required to convert 17-α-ethynylestradiol.

AOC and biofilm formation at GCWW
Applying the UV/H_2O_2 process, regardless of the types of lamp used, increased the AOC concentration in the GCWW pilot plant. For conventionally pretreated water this increase was about 30% for both lamps. When post-GAC water was used as influent (i.e., conventionally pretreated water that had passed through GAC before being treated with UV/H_2O_2), this increase was only about 14%, probably as a result of the higher bioactivity in this water. A similar effect was observed for P-17 AOC: a 24% increase with conventional water versus no increase with post-GAC water. For NOX AOC these data were 65% and 55%, respectively.

Some experiments were carried out applying GAC adsorption after UV/H_2O_2 treatment. This is very often done, also in water treatment plants to remove excess H_2O_2. At GCWW it was found that more biofilm formation can be observed in the GAC effluent streams that received UV/H_2O_2 pretreatment. For MP reactors the biofilms also appeared to be more viable.

Pilot plant research at Dunea
Similar experiments like at GCWW were carried out at Dunea, also using MP and LP reactors equipped with commercially available UV lamps. The reactors used there were also commercially available pilot reactors. A special reactor had to be designed only for the DBD lamp.
For comparison of the three types of lamps at Dunea, like at GCWW, the second concept, of comparing optimized reaction vessels, was applied. CFD modelling can be used to determine how well a reactor has been optimized. In case of the Dunea reactors, it was found that the MP reactor design is less optimal compared with the other two reactors. Although the E_{EO} is a good way to

compare lamp performance, its value also strongly depends on the flow through the reactor, which in this case for the MP reactor was less optimal than for the LP and DBD reactor.

Similarly to the results obtained by GCWW and KWR, Dunea also found that the E_{EO} of the reactor equipped with LP lamps was lowest, whereas the E_{EO} for theMP reactor showed the highest value. As expected, the E_{EO} for the DBD lamp seemed to fall in between the other two E_{EO} values. The reactor with LP lamps required the lowest amount of energy to achieve 80% atrazine reduction compared to the other two types of reactors. However, the reactor with the DBD lamps at Dunea seemed to require more energy than the one with the MP lamps. There are three explanations for this observation:

- The experiments with the DBD lamps were carried out in winter, with a relatively low UVT, whereas the other reactors were tested with water at a higher UVT.
- Prototypes of the DBD lamps were used, for which the efficiency is only 12% (for the DBD lamps used in the Dunea pilot plant. The former types, used in the KWR pilot plant, had an efficiency of only 7%). It is expected that for a fully developed DBD lamp this efficiency will increase up to 24%, which would make them twice as energy efficient, reducing the energy demand for this reactor with a factor two.
- The prototype DBD lamp does not yet have a very long expected life span, so the UV output may already have decreased during the experiments. For the LP and MP lamps, with a higher life span, no decrease in UV output is to be expected during the time the experiments were carried out.

Comparison of pilot plants

In general there is good agreement in the conversion of organic micropollutants between experiments at KWR, Dunea and GCWW. All compounds are converted to a high level (>80%), except for MTBE. MTBE can be converted, but it may require a relatively high UV dose (and thus a lot of energy), depending on the actual water composition. Besides, it should be remarked that the E_{EO} obained for MTBE at KWR is unlikely high. This is caused by the low conversion measured, but this is based on only one measurement, where probably something went wrong in the dosing or analysis of the MTBE. To compare the various reactors, the E_{EO} can be applied. In Table 11-1 a summary of the E_{EO} data obtained in this report is given. In general the E_{EO} values for the KWR pilot reactor seem to be a little higher than those in the pilot reactors at Dunea and GCWW. This is caused by the fact that the E_{EO} depends on e.g. reactor geometry, and that this KWR reactor had not been optimized for one of the types of lamps. Taking this into account, it can be concluded that there is a fairly good accordance in the E_{EO} results obtained. In general the E_{EO} values for LP systems are lower than those for MP systems. For the DBD lamps, all calculations were based on the optional electric efficiency of 24%. In this case, the E_{EO} for the DBD lamps is nearly as low as for the LP lamps. However, at the moment the efficiency of the present DBD lamps has not yet reached 24%.

Table 11-2 provides an overview of the E_{EO} approximate values (the amount of energy required to convert the compounds for 90%) for the various pilot plants.

Table 11-1: Overview of E_{EO} values (kWh/m³-order) shown in this report. For GCWW two values are given: obtained with conventionally pretreated water/ obtained with post-GAC water. For the DBD lamp the present energy efficiency of 12% is taken into account, although according to Philips Lighting the optional future efficiency will be 24% (resulting in an E_{EO} value that is only half as high).

compound	MP			LP			DBD	
	KWR	GCWW	Dunea	KWR	GCWW	Dunea	KWR	Dunea
MTBE	1.80	1.42/0.90		55.44*)	0.48/0.31		2.24	
alachlor	0.71			0.35			0.8	
atrazine	1.06	0.59/0.41	1.43	0.62	0.30/0.18	0.50	1.18	1.14
Cyanazine	1.47			0.80			1.48	
Metazochlor	0.58			0.34			0.68	
Erythromycine	1.00			0.42			1.20	
Bezafibrate	0.64			0.26			1.18	
Carbamazepine	0.77			0.40			0.76	
Diclofenac	0.27			0.10			0.24	
Ibuprofen	0.58	0.54/0.43	0.62	0.32	2.27/0.17	0.59	0.80	0.78
Lincomycine	0.48			0.24			0.52	
metropolol	0.78			0.43			0.84	
Phenazone	0.66			0.30			0.72	
Sotalol	0.38			0.20			0.40	
Sulfamethoxazole	0.53			0.14			0.68	
Metolachlor		0.35/0.23			0.20/0.10			
MIB		0.49/0.32			0.20/0.12			
EE2		0.31/0.15			0.17/0.10			
Gemfibrozil		0.43/0.27			0.17/0.10			
Bromacil			1.69			0.50		1.16
NDMA			1.13			0.29		0.38

*) This value is unlikely high, as was already mentioned in paragraph 3.9.

Table 11-2 General overview of average E_{EO} values (kWh/m³) for various compounds in the different pilot plants. The values for GCWW were obtained with conventionally treated water as influent.

Pilot Plant	MP	LP	DBD
KWR	~ 0.7	~ 0.4	~ 0.4
Dunea	~ 1.4	~ 0.4	0.3 - 2
GCWW autumn	0.4-1.8	~ 0.3-1.0	
GCWW winter	~0.2-1.2	~ 0.2-0.6	
GCWW spring	~0.2-1.2	~ 0.1-0.5	
GCWW summer	0.4-1.5	~ 0.1-0.3	

These data can give an indication on the performance of a reactor, although the E_{EO} value is also influenced by the water matrix. This becomes clear from the data from GCWW, which indicate a difference throughout the year due to seasonal variations (i.e., UVT changes), resulting in a more or in a less effective UV/H_2O_2 process. This also agrees with other findings of Dunea and GCWW: the E_{EO} found after GAC treatment of the water (eliminating seasonal variations) decreases notably. The effectiveness of a UV/H_2O_2 process for water treatment thus depends on water quality.

Apart from this observation, optimization of the reactor design (the water flow through the reactor) may result in a substantial decrease in energy costs for the process. In this regard, modeling (CFD in

combination with kinetic models) may be very helpful to predict the performance of a reactor design, and to optimize reactors.

11.1.12   Integrated UV/H$_2$O$_2$-reactor and GAC contactor

All pilot plants consisted of a separate UV reactor and separate GAC contactors. For a full scale plant it may be economically interesting to integrate both treatment steps into a single reactor. In WP10 some suggestions were made on how this can be realized. It is not possible to determine which option will be most suitable beforehand, as this will strongly depend on the actual conditions at a treatment plant. If a totally new plant is to be designed, a totally new concept may be interesting (e.g., lamps placed in a (separate) section above the filter bed). However, if the reactor has to be implemented into an existing purification plant, a less innovative concept (e.g., UV lamps placed in a channel in between the filter beds) may be more likely. In any case, first applying some CFD modeling to the various reactor concepts may result in a more efficient reactor design, and thus to a more energy efficient treatment process.

11.1.13   Possible formation of genotoxic byproducts

As was mentioned before, GAC adsorption removes excess H$_2$O$_2$ present after the UV reactor. Additionally, byproducts may also be removed from the water. This very important aspect was shown in WP9, where genotoxicity studies were carried out with the UV/H$_2$O$_2$ processes described above, using both pretreated water from Dunea and from GCWW. In water treated with MP UV lamps, increased genotoxicity may be observed with the Ames II test (TA98 strain). It seems that for an MP UV lamp the genotoxicity is a little lower in the presence of H$_2$O$_2$ than in its absence. This indicates that photolysis may be causing this effect. Fortunately, in all cases it was observed that all genotoxicity was removed after GAC filtration.

A comparison between treatment with MP, LP and DBD lamps at similar atrazine conversion showed that LP and DBD lamps caused a lower increase in genotoxicity than MP lamps. This is another indication that photolysis has an important role in the formation of the genotoxic byproduct(s). From the genotox data in this report no real comparison between all three lamps can be made, as not all reactors had been optimized for the types of lamps used. For application in a full scale plant, an optimized reactor would be installed, and the operating conditions then would be set in order to achieve a certain conversion of a certain compound or set of compounds. Under such conditions, a true comparison of the effect of the lamps could be made, but these conditions were not available at the time of this investigation.

Based on the results obtained by Dunea and GCWW GAC adsorption is very effective in removing excess H$_2$O$_2$ required to obtain an efficient UV/H$_2$O$_2$ process. This adsorption may also remove any possible genotoxicity that may have been generated during the process. It is hypothesized this genotoxicity originates from converted natural organic matter. GAC adsorption prior to UV/H$_2$O$_2$ treatment then may also prevent the formation of genotoxic compounds, if GAC completely removes the genotoxic precursors.

When a totally new plant has to be designed, it also may be worthwhile to consider an integrated design, as suggested in chapter 10. If the UV/H$_2$O$_2$ process is followed by infiltration in a dune area, the GAC adsorption step may possibly be omitted, although at least the H$_2$O$_2$ content has to be reduced before infiltration.

In all cases, modeling of the reactor design will help in obtaining an efficient process.

E$_{EO}$ is a very useful tool to compare processes and reactors. However, E$_{EO}$ should not be the only factor to consider. The available footprint for a UV/H$_2$O$_2$ process is also a factor that has to be taken into account. Processes equipped with LP and DBD lamps require more lamps and a larger footprint than processes based on MP technology. Furthermore, there will be international or regional differences in costs of energy, investments etc. This means that for every case a thorough consideration of the local circumstances will be required to be able to decide whether or not the UV/H$_2$O$_2$ process may be a suitable process to remove contaminants from drinking water.

11.2 General conclusions

During recent years in literature a lot of research on UV/H_2O_2 processes has been described. Some general conclusions were confirmed by our work:

- In general, the process becomes far more effective if H_2O_2 is added to a UV reactor.
- In general, a higher conversion of organic micropollutants was observed with MP lamps, as a result of oxidation combined with photolysis, whereas conversion with LP reactors are mainly based on oxidation processes.
- The UV transmission is very important for the efficiency of a UV/H_2O_2 reactor. The higher the UVT, the lower the energy demand will be.

Some new conclusions, based on this particular project are:

- All three types of UV lamps, MP, LP and DBD, can be successfully used to convert a significant amount of organic micropollutants to a high degree.
- All three types of UV lamps, MP, LP and DBD, can be successfully used to obtain disinfection of the treated water at UV-dose levels for oxidation purposes.
- Although the efficiency of hydroxyl radical formation at a wavelength of 253.7 nm is low in comparison with the photolysis of H_2O_2 at a lower wavelength, the hydroxyl radical formation process is still more efficient with LP lamps than with MP lamps, due to the lower UV absorption by the water matrix at 254 nm.
- In general it was found that the E_{EO} of reactors equipped with LP lamps is the lowest, whereas the E_{EO} for MP lamps is the highest.
- To optimize a reactor design, CFD modeling will be very useful. By applying an optimized reactor, the energy efficiency of the process can be significantly decreased.
- DBD lamps may be a very interesting alternative for both MP as well as LP lamps, as they may combine the advantages of both types of lamps and besides do not contain any mercury. Unfortunately, it was not yet possible to make a fair comparison, as only a prototype of the lamp could be used. Water utilities may be very interested in applying this type of lamp, if a fully developed DBD lamp is available for testing or even for application in a full scale treatment plant. However, because this is not yet the case, such water utilities will probably refer to conventional MP or LP lamps. On the other hand, Philips may be more interested in fully developing the DBD lamp, if more water utilities would intend to use them. Since this is not yet the case, development of a commercial type of DBD lamp is not a first priority. This is unfortunate, as our results indicate that this may be a very interesting alternative.
- In practice a UV/H_2O_2 process will be followed by GAC adsorption. This not only removes excess H_2O_2, but also the by-products formed during the process. As some of these byproducts may be genotoxic, this will be a very important step to include into the total treatment process.
- More research will be required to fully understand the risk of possible generation of genotoxic byproducts.
- To obtain a safe process, with a multiple barrier for organic micropollutants, a UV/H_2O_2 process has to be combined with GAC adsorption. Maybe in the future both process steps can be combined into a single reactor design.

12 Practical implementation of UV/H$_2$O$_2$ technology in water treatment plants

12.1 Introduction

Within the framework of the project "New concepts UV/H$_2$O$_2$ oxidation" research has been carried out into all kinds of aspects of UV/H$_2$O$_2$ technology. It was concluded that it is a very interesting technology to convert organic micropollutants in water. However, various factors, depending on the particular situation, influence the application of this technology, as a result of which it is not possible to give a general advice on how the UV/H$_2$O$_2$ process should be designed and operated. In this chapter some indications are given whether or not UV/H$_2$O$_2$ may be an interesting technology in a particular case, and which parameters will have to be taken into account when implementing this technology.

Before deciding whether or not UV/H$_2$O$_2$ technology may be implemented, the treatment company which wants to convert or remove organic micropollutants from water will have to chose between several processes available. These processes include adsorption, oxidation and membrane filtration processes. Based on company strategy and plant and site specific criteria and considerations, oxidative technologies, possibly in combination with an adsorption process, may be chosen. Several oxidative processes may be applied, like eg.:

- Ozone (O$_3$)
- Fenton
- Fenton/UV
- O$_3$/UV
- O$_3$/H$_2$O$_2$
- UV/H$_2$O$_2$
- O$_3$/H$_2$O$_2$/UV
- TiO$_2$/UV

In most cases research will have to be conducted in order to determine which technology would be best suitable in the specific circumstances. Important parameters will be the conversion of organic micropollutants realized, the energy requirement of the process, the possible formation of byproducts, and the implementation of the process in the total existing or new treatment process.

12.2 Where can UV/H$_2$O$_2$ technology be used for?

Some organic micropollutants, like for example NDMA, are very sensitive towards photolysis, where other compounds, like e.g. ibuprofen, are difficult to photolyze, but can very easily be oxidized by means of hydroxyl radicals. By combining UV irradiation with the presence of hydrogen peroxide (and thus of hydroxyl radicals) both processes, photolysis and oxidation, can be combined. Research showed that this UV/H$_2$O$_2$ technology is very suitable to convert organic micropollutants. In principle, it is possible to mineralize these compounds, but this will require high UV doses. In general, however, it will not be necessary to obtain complete mineralization: in most cases conversion into smaller, often less harmful or better degradable compounds will be sufficient.

An additional advantage of UV/H$_2$O$_2$ technology is that the process is very effective in inactivating microorganisms. In general, the UV dose required for UV/H$_2$O$_2$ processes (500-1000 mJ/cm^2) is about 10 times as high as the dose required for disinfection purposes.

12.3 Which UV dose and H$_2$O$_2$ concentration will be required?

In general a H$_2$O$_2$ concentration of 5-10 mg/L appears to be enough to guarantee sufficient conversion of organic micropollutants.

The UV dose required strongly depends on the type and concentration of the organic micropollutants which will have to be converted. First it will be necessary to establish which degree of conversion will be required for which particular compounds, based on the quality of the wate to be treated, the demands on water quality after treatment and the effect of the total treatment process. The compound requiring the highest UV dose then can be used as a model compound, to determine the reactor settings. In order to determine this UV dose, a literature search, laboratory experiments (using a collimated beam set-up) or pilot plant experiments can be carried out. Futhermore, models have been developed which can be used to optimize the reactor design and/or the practical settings.

12.4 Which type of lamp will be suitable?

In principle two types of UV lamps are commercially available:
- Medium pressure (MP) lamps
- Low pressure (LP) lamps (presently also High Output Low pressure lamps are available)

These lamps and the corresponding reactors (designed for a particular type of lamp) all show their specific advantages and disadvantages. Which combination will be the best, will depend on each specific case. A concise overview of the differences of these lamps is shown in Table 12-1.

Table 12-1: overview of differences between LP and MP lamps.

property	LP	MP
Power	Low (≤ 1kW)	High (≤ 60kW)
Footprint	large	small
Energy efficiency	25-30%	10-15%
Expected lifespan	3.000-12.000 hours	4.000-6.000 hours
Costs of lamp	€ 500	€ 1500
Formation of byproducts*	"Low"	"High"
E_{EO}[**] (kWh/m^3-order)	Ca. 0,35	Ca. 0,70

*) This is being investigated within the framework of a new project.

**)E_{EO} is is the amount of energy per m^3, required to convert a certain compound by one order of magnitude. The actual E_{EO} depends on water quality, type of compound, type of lamp and reactor design, but the order of magnitude will be between about 0.3-0.7 kWh/m^3-order (according to the research described in this project the E_{EO} varied between 0.1 and 2.0 kWh/m^3-order depending on water quality and type and concentration of micropollutants present).

12.5 What is the influence of the water matrix?

The water matrix is an important parameter to take into account to assess the (economic) feasibility of the technology. Water showing a low UV-transmission will require a higher UV-dose, and thus will lead to a larger energy demand. This disadvantage may be overcome by pretreatment of the water (eg. by coagulation and filtration, GAC filtration or ion exchange processes), but it will have to be estimated whether or not the costs of such a pretreatment step will match the increasing energy costs.

12.6 Which reactor design will be required?

The reactor design is a very important parameter, affecting the performance of the reactor to a large extend. By adjusting the design, and thus the flow conditions inside the reactor, to the type of lamp, the amount of UV energy required can be minimized. CFD modelling has been proven to be a very important tool in order to optimize the reactor design.

12.7 What kind of posttreatment will be required?

In order to obtain a good conversion of micropollutants, an excess of H_2O_2 will be required. After the UV/H_2O_2 process this excess can be removed by means of filtration over activated carbon. Filtration over activated carbon will also remove any nitrite or AOC formed during the UV/H_2O_2 treatment. Recent measurements have shown that under certain circumstances genotoxic byproducts may be formed during UV processes. Filtration over activated carbon seems also to be very effective in removing possibly genotoxic byproducts. The formation, type and concentration of these byproducts probably depend on the composition of the water matrix and the type of UV-lamps and UV-dose applied.

12.8 Practical approach

When it is considered to apply UV/H_2O_2 technology at a full plant scale, several tools now are available to establish whether in this particular case this would be a suitable technology, and, if so, how it should be implemented.
First of all, in literature a lot of research on the possiblities of UV/H_2O_2 technology has been published in recent years. Kinetic data of several compounds have become available, and knowledge has been generated on the factors that may affect the effecivity of the process.
If certain (kinetic) parameters of organic micropollutants are not available yet, Collimated Beam experiments can be used to obtain them. CFD modeling can be applied to optimize the reactor design. Models, based on the combination of kinetic models (CB experiments) and CFD, can be used to predict the conversion of micropollutants in a UV/H_2O_2 reactor, e.g. as a function of water quality and UV dose. Finally, pilot plant research can be applied to study the effects of several parameters (composition of the water matrix, seasonal variations, etc.) and to determine the E_{EO} of the process, and thus its economic applicability.
As byproducts (AOC, nitrite and possible genotoxic compounds) may be formed during the UV/H_2O_2 process, in each particular case it will have to be investigated what will be the optimum way to deal with it: implementing a pre-treatment step before the UV/H_2O_2 process, or removing the excess of H_2O_2 and the possible byproducts afterwards.

13 Future research

Although at the moment the tools are available to introduce UV/H_2O_2 technology on full scale, there still are many questions left to be answered, which will require additional research:

1. The formation of byproducts and their effects (possible formation of genotoxic compounds) is still unclear. More research will be required to identify genotoxic byproducts(s) and the precursor(s) of these products. Also other byproducts should be investigated in more detail. This will also give information on whether or not post-treatment (like GAC adsorption) will be required in all cases. A project on the factors that affect the formation of byproducts has already been started.
2. The formation of AOC and biofilm depends on the water matrix. To optimize plant operation, it will be very important to know more about these factors. Therefore, research including different types of water will be required.
3. CFD can be used to optimize reactor design. Some improvements will be possible in the models used, giving more accurate information on the water flow through the reactor and the UV doses achieved.
4. Models like UVPerox and UVPeroxII still have to be validated using more types of water and organic micropollutants. A new project on this subject is being started.
5. To successfully apply modeling to optimize reactor operation, adequate sensors for water quality determination will be required. These still have to be developed. In this way, the operating conditions can be adjusted to the actual water composition and temperature.
6. Modeling of other (oxidation) technologies will result in a tool that can be used to compare different technologies for a certain application. Such models in most cases, however, still have to be developed.
7. QSARs (Quantitave Structure-Activity Relationships) can be a very interresting tool to compare the efficiency of different technologies. The development of QSARs for all kinds of organic micropollutants will require a lot of research, but eventually will result in a tool that can be applied to all kinds of micropollutants whose properties are yet unknown. Combining reactor modeling (for various technologies) with QSARS will offer very interesting possibilities.
8. HO-LP lamps are commercially available now. However, the higher the lamp efficiency, the more sustainable UV/H_2O_2 processes can become, as energy costs for such processes are a dominant factor in the operational costs. Furthermore, both LP as well as MP lamps still contain mercury, which from an environmental point of view is a disadvantage. In this respect, further development of DBD lamps would be very interesting.

Literature References

References

Aeschbacher, H.U., Wolleb, U., Loliger, J., Spadone, J.C. and Liardon, R. (1989). "*Contribution of coffee aroma constituents to the mutagenicity of coffee*". Food and Chemical Toxicology 27(4), 227-232

Alnaizy, R., Ibrahim, T.H. (2009); "*MTBE removal from contamined water by the UV/H$_2$O$_2$ process*"; Desal. Wat. Treatm. 10 (1-3), 291-297

American Water Works Research Foundation and Keuringsinstituut Voor Waterleidingartikelen (1988). Collaborative Report: *The Search for a Surrogate American Water Works* Research Foundation Report (1988), Denver, CO.

Ames, B.N., McCann, J. and Yamasaki, E. (1975) "*Methods for detecting carcinogens and mutagens with the Salmonella/mammalian-microsome mutagenicity test*". Mutation Research 31 (6), 347-364.

Arnold, S.M., W.J. Hickey, R.F. Harris (1995) "*Degradation of Atrazine by Fenton's Reagent: Condition Optimization and Product Quantification*", Environ. Sci. Technol., 1995, **29**, pp. 2083-2089.

Asami, Y., T. Satoh, and A. Kuroda (2006). "*Polyphosphate-ATP Amplification Technology: Principle and its Application to Detection of Specific Bacteria.*" Journal of Environmental Biotechnology, 6(2), pp.105-108, 2006

Baribeau, H., N.L. Pozos, L. Boulos, G.F. Crozes, G.A. Gagnon, S. Rutledge, D. Skinner, Z. Hu, R. Hofmann, R.C. Andrews, L. Wojcicka, Z. Alam, C. Chauret, S.A. Andrews, R. Dumancic, and E. Warn (2005). "*Impact of Distribution System Water Quality on Disinfection Efficacy.*" American Water Works Research Foundation Report, 2005. Denver, CO.

Bautista, D.A., J.P. Vaillancourt, R.A. Clarke, S. Renwick, and M.W. Griffiths (1994). "*Adenosine Triphosphate Bioluminescence as a Method to Determine Microbial Levels in Scald and Chill Tanks at a Poultry Abattoir.*" Poult. Science, 73, pp. 1673–1678, 1994

Beltrán, F.J., G. Ovejero, J. Rivas (1996[b]) "*Oxidation of Polynuclear Aromatic Hydrocarbons in Water. 3. UV Radiation Combined with Hydrogen Peroxide*", Ind. Eng. Chem. Res., 35, pp. 883-890.

Berson UV Technologies; Use of UV light for disinfection of water; Referenced on December 28th 2009 via: http://www.bersonuv.com/index.php?id=ourbusiness

Bolton (2001), *Ultraviolet Applications Handbook*, second edition, Bolton Photosciences Inc., ISBN 0-9685432-0-0

Bolton, J.R., K. Bircher, W. Tumas, C.A. Tolman (2001) "*Figures-of-merit for the technical development and application of advanced oxidation technologies for both electrical and solar-driven system*" (IUPAC technical report). Pure Appl. Chem. **73**(4), pp. 627-637.

Bolton J. R., M. Stefan (2002). "*Fundamental Photochemical Approach to the Concepts of Fluence (UV dose) and Electrical Efficiency in Photochemical Degradation Reactions.*" Research on Chemical Intermediates, 28 (7-9), pp. 857-870

Bolton, J.R., Linden, K.G. (2003); "*Standardization of Methods for fluence (UV Dose) Determination in Bench-scale UV Experiments*"; J. Envir. Engrg., Volume 129, Issue 3, pp. 209-215

Borenfreund, E., Puerner, J.A. (1985). "*A simple quantitative procedure using monolayer cultures for cytotoxicity assays*". Journal of Tissue Culture Methods 9, 7-9.

Buschini, A., Carboni, P., Frigerio, S., Furlini, M., Marabini, L., Monarca, S., Poli, P., Radice, S., Rossi, C. (2004) "*Genotoxicity and cytotoxicity assessment in lake drinking water produced in a treatment plant.*" Mutagenesis 19, 341 – 347.

Butterfield, P.W., B. Ellis, A. Camper, and W. Jones (1997). "*Evaluation of Growth Kinetics of Model Drinking Water System Biofilm Cells Utilizing Humic Substances as the Primary Carbon Sources.*" In Proceedings American Water Works Association Water Quality Technology conference, November 9-12, 1997. Denver, CO.

Buxton, G. V., C.L. Greenstock, W.P. Helman, and A.B. Ross (1988). "*Critical Review of Rate Constants for Reactions of Hydrated Electrons, Hydrogen Atoms and Hydroxyl Radicals (·OH/·O-) in Aqueous Solution.*" Journal of Physical and Chemical Reference Data, 17 (2), pp. 513-886, 1988

Carnimeo, D., Di Marino, R.;,Donaldo, F., Liberti, L., Ranieri, E., Pitzurra, M.,Savino, A. (1995). "*Comparison between H_2O_2/UV and ClO_2 disinfection of drinking water*". Water Supply 13, 159-169.

Carr, A., S.B. Baird, and R.B. Baird (2000). "*Mineralization as a Mechanism for TOC Removal: Study of Ozone/Ozone-Peroxide Oxidation using FT-IR.*" Water Research, 34 (16), pp. 4036-4048, 2000

Carvalho, M.F., I.Vasconcelos, and A.T. Bull (2001). "*A GAC Biofilm Reactor for the Continuous Degradation of 4-Chlorophenol: Treatment Efficacy and Microbial Analysis.*" Applied Microbiology Biotechnology, 57, pp. 419-426, 2001

Changlong, W., H. Shemer, K. G. Linden (2007). "*Photodegradation of Metolachlor Applying UV and UV/H_2O_2.*" Journal of Agricultural and Food Chemistry, 55, pp. 4059-4065, 2007

De Laat J., Gallard H., Ancelin S., Legube B. (1999). Comparative study of the oxidation of atrazine and acetone by H_2O_2/UV, Fe(III)/UV, Fe(III)/H_2O_2/UV and Fe(II) or Fe(III)/H_2O_2. Chemosphere, 39:2693-2706.

De Ridder, D.J. (2006). "*UV/H_2O_2 behandeling bij drinkwater bereiding – Onderzoek en ontwerp*". MSc thesis report, TU Delft, Departmetn of sanitary engineering.

Donlan, R.M., and W.O. Pipes (1988). "*Selected Drinking Water Characteristics and Attached Microbial Population Density.*" Jour. AWWA, pp. 70-76, 1988

Driebel, V. (2008). High Tech Detection Methods: *Hygiene Detection using ATP Bioluminescence* Presented at: 3A Standards Meeting Milwaukee, Wisconsin. May 20, 2008.

Elovitz, M.S., U. von Gunten (1999). "*Hydroxyl Radical/Ozone Ratios During Ozonation Processes. I. The R_{CT} Concept*". Ozone Sci. & Eng., 21, pp. 239-260

Escobar, I.C., Randall, A.A. (2000). "Sample storage impact on the assimilable organic carbon (AOC) bioassay; Water Resources." Water Resources, 34 (5), 1680-1686

Fluckiger-Isler, S., Baumeister, M., Braun, K., Gervais, V., Hasler-Nguyen, N., Reimann, R., Van Gompel, J., Wunderlich, H.G. and Engelhardt, G. (2004). "*Assessment of the performance of the Ames II assay: a collaborative study with 19 coded compounds*". Mutation Research 558(1-2), 181-197.

Gee, P., Maron, D.M. and Ames, B.N. (1994). "*Detection and classification of mutagens: a set of base-specific Salmonella tester strains*". Proceedings of the National Academy of Sciences of United States of America 91(24), 11606-11610

Gee, P., Sommers, C.H., Melick, A.S., Gidrol, X.M., Todd, M.D., Burris, R.B., Nelson, M.E., Klemm, R.C. and Zeiger, E. (1998). "Comparison of responses of base-specific Salmonella tester strains with the traditional strains for identifying mutagens: the results of a validation study". Mutation Research 412(2), 115-130.

Geesey, G.G., L. Jang, J.G. Jolley, M.R. Hankins, T. Iwaoka, and P.R. Griffiths (1989). "*Binding of Metal Ions by Extracellular Polymers of Biofilm Bacteria.*" Water Science and Technology, 20(11/12), pp. 161-165, 1989

Glaze, W.H. (1987). "*Drinking Water Treatment with Ozone.*" Environ. Science Technol, 21 (3), pp. 224-230, 1987

Goel, S., R.M. Hozalski, and E.J. Bouwer (1995). "*Biodegradation of NOM: Effect of NOM source and ozone dose.*" Jour. AWWA, 87(1), pp. 90–105, 1995

Gomez-Serrano, V., M. Acendo-Ramo, A.J. Lopez-Peinado, and A. Valenzuela-Calahorro (1994). "*Oxidation of Activated Carbon by Hydrogen Peroxide: Study of Surface Functional Groups by FT-IR.*" Fuel, 73 (3), pp. 387-395, 1994

Guzzella, L., Feretti, D. and Monarca, S. (2002). "*Advanced oxidation and adsorption technologies for organic micropollutant removal from lake water used as drinking-water supply*". Water Research 36(17), 4307-4318.

Haag W. R., C. C. D. Yao (1992). "*Rate constants for Reactions with Hydroxyl Radicals with Several Drinking Water Contaminants.*" Environmental Science and Technology, 26 (5), pp. 1005-1013, 1992

Haddix, P.L., N.J. Shaw, and M.W. LeChevallier (2004). "*Characterization of Bioluminescent Derivatives of Assimilable Organic Carbon Test Bacteria.*" Applied and Environmental Microbiology, 70 (2), pp. 850-854, 2004

Hammes, F.; A comparison of AOC methods used by the different TECHNEAU partners

Techneau, 2008

Harmsen D.; "*Protocol Collimated Beam UV*" Kiwa Water Research, BTO 04.014 Nieuwegein, 2004.

Harmsen, D.J.H., M.B. Heringa, van Genderen J., IJpelaar G.F.; "*Vorming van bijprodukten tijdens UV-desinfectie en UV/H_2O_2 oxidatie*" Kiwa WR BTO 2005.57, Nieuwegein,2005

Haider, T., Sommer, R., Knasmüller, S., Eckl, P., Pribil, W., Cabaj, A. and Kundi, M. (2001). "*Application of a test combination of three different bioassays for the investigation of genotoxic effects induced by UV-irradiation in water*". First International Congress on Ultraviolet Technologies, Washington, D.C., International Ultraviolet Association (IUVA).

Haider, T., Sommer, R., Knasmuller, S., Eckl, P., Pribil, W., Cabaj, A. and Kundi, M. (2002). "*Genotoxic response of Austrian groundwater samples treated under standardized UV (254 nm)--disinfection conditions in a combination of three different bioassays*". Water Research 36(1), 25-32.

Helma, C., Sommer, R., Schulte-Hermann, R. and Knasmuller, S. (1994). "*Enhanced clastogenicity of contaminated groundwater following UV irradiation detected by the Tradescantia micronucleus assay*". Mutation Research 323(3), 93-98.

Hem and Efraimsen (2001). "*Assimilable Organic Carbon in Molecular Weight Fraction of Natural Organic Matter.*" Water Research, 35(4), pp. 1106-1110, 2001

Heringa, M.B., Harmsen, D.J.H., Beerendonk, E.F., Reus, A.A., Krul, C.A.M., Metz, D.H. and IJpelaar, G.F. (2011) "*Formation and removal of genotoxic activity during UV/H$_2$O$_2$-GAC treatment of drinking water.*" Water Research 45(1), 366-374.

Hijnen, W.A.M., Beerendonk, E.F., Medema, G.J. (2006) "*Inactivation credit of UV radiation for viruses, bacteria and protooan (oo)cysts in water: A review*", Water Research, nr. 40, p. 3-22..

Hofman J., Wols B.; "*Applications of CFD modeling for the design of a pilot UV reactor*"Kiwa BTO 2008.011, Nieuwegein, maart 2008

Hovorka, S.W., and C. Schoneich (2001). "*Oxidative Degradation of Pharmaceuticals: Theory, Mechanisms and Inhibition.*" Journal of Pharmaceutical Sciences, 90 (3), pp. 253-269, 2001

Huang, Hsu-Hui, M.C. Lu, J.N. Chen, C.T. Lee (2003). "*Catalytic Decomposition of Hydrogen Peroxide and 4-Chlorophenol in the Presence of Modified Activated Carbons.*" Chemosphere, 51, pp. 935-943, 2003

Huck, P. M. (1990). "*Measurement of biodegradable organic matter and bacterial growth potential in drinking water.*" Jour. AWWA, 82(7), pp. 78–86, 1990

IJpelaar, G.F., A.J. van der Veer, G.J. Medema, J.C. Kruithof (2005), "*Byproduct formation during ultraviolet disinfection of a pre-treated surface water*", J. Environmental Engineering and Science, vol. 4, pp. S51-S56.

IJpelaar, G., Harmsen, D., Sharpless, C.M., Linden, K.G. and Kruithof, J.C.
Fluence Monitoring in UV Disinfection Systems: Development of a Fluence Meter
London: IWA, 2006

IJpelaar, G.F., D.J.H. Harmsen, A.J. van der Veer (2006), "*Zijn reactieproducten tijdens waterzuivering met UV-technologie beheersbaar*" H$_2$O, nr. 14/15, pp. 40 – 41

IJpelaar, G.F., Harmsen, D., Sharpless, C.M., Linden, K.G., Kruithof, J.C. (2006), "*Fluence monitoring in UV disinfection systems: development of a fluence meter*". AwwaRF/Kiwa Water Research report 91110, AwwaRF, AWWA, IWA Publishing.

IJpelaar, G., Harmsen, D., Krijnen, S. and Knol, T.; UV/H$_2$O$_2$-oxidatie mogelijk met middendruk- én lagedruklampen; Schiedam: Nijgh Periodieken BV, article in H2O magazine, volume 40, issue 4, p 44-46, 2007-a

IJpelaar, G., Harmsen, D. and M. Heringa; UV disinfection and UV/H$_2$O$_2$ oxidation: byproduct formation and control; TECHNEAU, 2007-b

Jin S, Mofidi, A.A., Linden K.G. (2006); Polychromatic UV fluence measurement using chemical actinometry, biodosimetry, and mathematical techniques; J. Env. Eng, aug. 2006, 831-841

Kamp P.C., Martijn B.J., Kruithof, J.C. (2007), "*Byproduct formation in Ozone and UV Based Processes A Critical Factor in Process Selection*", proceedings IUVA World Congress Los Angeles, California (VS), 27 – 29 august 2007.

Kaplan, L.A., T.L. Bott, and D.J. Reasoner (1993). "*Evaluation and Simplification of the Assimilable Organic Carbon Nutrient Bioassay for Bacterial Growth in Drinking Water.*" Applied and Environmental Microbiology, 59(5), pp. 1532-1539, 1993

Kaplan, L.A. and T.J. Gremm (1995). *Bioavailability of Humic Substances in Stream Ecosystems*. In Abstracts of the International Humic Substances Society Meeting, Atlanta, GA, 1995

Kaplan, L.A., M. Hullar, L. Sappelsa, D.A. Stahl, P.G. Hatcher, S.W. Frazier (2004). "*The Role of Organic Matter in Structuring Microbial Communities*." American Water Works Research Foundation Report, 2004. Denver, CO.

Karl, D.M. (1980). "*Cellular Nucleotide Measurements and Applications in Microbial Ecology.*" Microbiol. Rev., 44, pp. 739–96, 1980

Kashinkunti, R.D., Linden, K.G., Shin, G.A., Metz, D.H., Sobsey, M.D., Moran, M.C. and Samuelson, A.M. (2004). " *Investigating multibarrier inactivation for Cincinnati*". Journal of the American Water Works Association (AWWA) 96(6), 114-127.

Kavanaugh M., Z. Chowdhury, S. Kommineni, S. Liang, J. Min, J. P. Croue, N. Corin, A. Gary, S. Erich, W. Cooper, P. Tornatore, M. Nickelsen (2003). "*Removal of MTBE with Advanced Oxidation Processes*." AWWA Research Foundation Report, 2003

Khalil, L.B., B.S. Girgis, and T.A. Tawfik (2001). "*Decomposition of H_2O_2 on Activated Carbon obtained from Olive Stones*." Journal of Chemical Technology and Biotechnology, 76 (11), pp. 1132-1140, 2001

Kiwa-huisinstructie; "*Bepaling van het gehalte parachloorbenzoëzuur (pCBA) in water met HPLC-UV*" Kiwa-huisinstruction LOA-007, versie 2.0, 2006

Knowles, B.B., Howe, C.C., Aden, D.P. (1980) "*Human hepatocellular carcinoma cell lines secrete the major plasma proteins and hepatitis B surface antigen*". Science 209, 497 – 499.

Kool, H.J. and van Kreyl, C.F. (1988). "*Mutagenic activity in drinking water prepared from groundwater: a survey of ten cities in The Netherlands*". Science of the Total Environment 77(1), 51-60

Kramer, M.W.; Licht op water: ontwerp voor een UV/H2O2 installatie; MSc thesis, TU Delft, section of sanitary engineering, 2002

Kruithof, J.C., R.Chr van der Leer, W.A.M. Hijnen (1992), "*Practical experiences with UV disinfection in the Netherlands*", J. Water Supply Res. Technol Aqua, pp. 88 – 94.

Kruithof, J.C. en P.C. Kamp (2000), "*UV/H2O2: The ultimate solution for pesticide control*", proceedings van de AWWA Annual Conferentie Denver, Colorado (VS), 11 – 15 juni.

Kruithof, J.C., Kamp, P.C. and Martijn, B.J. (2007). "*UV/H_2O_2 treatment: A practical solution for organic contaminant control and primary disinfection*". Ozone: Science and Engineering 29(4), 273-280.

Lanzhu Shao; "*Degradation of 4TBP by AOP, UV Reactor Modeling and Validation*" TU Delft July 2007.

Lau, T. K., Chu, W., Graham, N. (2005). "*The degradation of endocrine disruptor di-n-butyl phthalate by UV irradiation: A photolysis and product study*". Chemosphere (60) 1045-53.

LeChevallier, M.W.,T.M. Babcock, and R.G.Lee (1987). "*Examination and Characterization of Distribution System Biofilms.*" Applied and Environmental Microbiology, Dec, pp. 2714-2724, 1987

LeChevallier, M.W., B.H. Olson, and G.A. McFeters (1990). "*Assessing and Controlling Bacterial Regrowth Distribution Systems.*" American Water Works Research Foundation Report. 1990. Denver, CO.

LeChevallier, M.W., W.H. Schulz, and R.G. Lee (1991a). "*Bacterial Nutrients in Drinking Water.*" Applied Environmental Microbiology, 57, pp. 857-862, 1991

LeChevallier, M. W., N.J. Welch, and D.B. Smith (1996). "*Full-scale studies of factors related to Coliform Regrowth in Drinking Water.*" Applied and Environmental Microbiology, 62(7), pp. 2201–2211, 1996.

LeChevallier, M.W., C.D. Norton, A.Camper, P.Morin, B.Ellis, W. Jones, A. Rompre, M. Prevost, J. Coallier, P. Servais, D. Holt, A. Deanoue, and J.Colbourne (1998). *Microbial Impact of Biological Filtration*. AWWA Research Foundation. Denver, CO.

Lee, C., Choi, W., Kim Y.G., Yoon, J. (2005). "*UV photolytic mechanism of N-nitrosodimethylamine in water: dual pathways to methylamine versus dimethylamine*". Envrion. Sci., technol., 39, 2101-2106

Lekkerkerker K., Scheideler J., Maeng S.K., Ried A., Verberk J.Q.J.C., Knol A.H., Amy G., van Dijk J.C. (2009); *Advanced oxidation and artificial recharge: a synergistic hybrid system for removal of organic micropollutants*; Water Science and Technology: Water Supply 9 (6), 643-651

Lekkerkerker-Teunissen, K.; *Nieuwe uitdagingen voor de Nederlandse duinen*; In: "Nieuw uitdagingen"-61e vakantiecursus in Drinkwatervoorziening; Delft: Delft University of Technology – Dept. of Sanitary Engineering, 2009

Li, K., Hokanson, D.R., Crittenden, J.C., Trussel, R.R., Minakuta, D. (2008); "*Evaluating UV/H$_2$O$_2$ processes for methyl tert-butylether and tertiary butyl alcohol removal: effect of pretreatment options and light sources*" Wat.Res., 42 (20), 5045-5053

Liao, C-H., Kang, S-F., Wu, F-A. (2001) "*Hydroxyl radical scavenging role of chloride and bicarbonate ions in the H$_2$O$_2$/UV process*". Chemosphere, **44**, pp. 1193-1200.

Linden, K.G., et al (2004). "*Innovative UV Technologies to Oxidize Organic and Organoleptic Chemicals.*" American Water Works Research Foundation Report, 2004

Liu, W., S. A. Andrews, M. I. Stephan, and J. R. Bolton (2003). "*Optimal methods for quenching H2O2 residuals prior to UFC testing.*" Water Research, 37, pp. 3697-3703, 2003

Liu D., Ducoste J.J., Jin S., Linden K., (2004). Evaluation of Alternative Fluence Rate Distribution Models, Journal of Water Supply Research and Technology – Aqua, 53:391-408.

Maas, P. van der, Bruins, J. and Woerdt, D. van der; Effect of Low Pressure UV on the Regrowth Potential of Drinking Water; Amsterdam: IUVA congress proceedings, 2009

Magic-Knezev, A., G. IJpelaar, A.H. Knol (2005), rapport Dunea.

Mark, G., H-G. Korth, H-P. Schuchmann, and C. von Sonntag. 1996. "*The Photochemistry of Aqueous Nitrate Ion Revisited*" Jour. Photochemistry and Photobiology A, 101:89–103.

Maron, D.M. and Ames, B.N. (1983). "*Revised methods for the Salmonella mutagenicity test*". Mutation Research 113 (3-4), 173-215.

Martijn, B.J., J.C. Kruithof, M. Welling. (2006), "*UV/H$_2$O$_2$ Treatment: The Ultimate Solution for Organic Contaminant Control and Primary Disinfection*". WQTC Denver USA, 5-9 November.

Martijn, B.J., Kruithof, J.C and Rosenthal, L.P.M.; Design and implementation of UV/H₂O₂ treatment in a full scale drinking water treatment plant; Velserbroek: PWN, 2007

Meintières, S., Nesslany, F., Pallardy, M., Marzin, D. (2003). "*Detection of ghost cells in the standard alkaline comet assay is not a good measure of apoptosis*". Environmental and molecular mutagenesis 41, 260 – 269

Miller, C. M., and R.L. Valentine (1995). "*Hydrogen Peroxide Decomposition and Quinoline Degradation in the Presence of Aquifer Material.*" Water Research, 29 (10), pp. 2353-2359, 1995

Montgomery, J.M., Consulting Engineers, Inc., (1985). *Water Treatment Principles and Design*. John Wiley & Sons, Inc. New York, NY.

Moore BC, F.S. Cannon, D.H. Metz, J. DeMarco, R. Pohlman, J.A. Westrick, C.A. Shrive and M. Kelsey (2004). "*Reactivating Activated Carbon at Cincinnati: Enhancing Performance.*" American Water Works Research Foundation Report, 2004. Denver, CO.

Morris G. and G. Newcombe (1993). "*Granular Activated Carbon: the Variation of Surface Properties with the Adsorption of Humic Substances.*" J. Colloid Interface Science, 159, pp. 413-420, 1993

Newcombe G, M. Drikas and R. Hayes (1998). "*Influence of Characterized Natural Organic Material on Activated Carbon Adsorption: II. Effect on Pore Volume Distribution and Adsorption of 2-methylisoborneol.*" Water Research, 31(5), pp. 1065-1073, 1998

Nick, K., Schoeler, H., Mark, G. Soylemez, T., Akhlaq, M., Schuchmann, H.-P., von Sonntag, C. (1992). "*Degradation of some triazine herbicides by UV radiation such as used in the UV disinfection of drinking water*". Journal of Water Supply: Research and Technology – AQUQ, 41 (2), 82-87

Najm, I. and Trussell, R.R. (2001). "*NDMA formation in water and wastewater*". Journal / American Water Works Association 93(2), 92-99.

Pereira, V.J., H. S. Weinberg, K. G. Linden, and P. C. Singer (2007). "*UV Degradation Kinetics and Modeling of Pharmaceutical Compounds in Laboratory Grade and Surface Water via Direct and Indirect Photolysis at 254 nm.*" Environmental Science and Technology, 41 (5), pp. 1682-1688, 2007

Piegorsch, W.W., Simmons, S.J., Margolin, B.H., Zeiger, E., Gidrol, X.M. and Gee, P. (2000). "*Statistical modeling and analyses of a base-specific Salmonella mutagenicity assay*". Mutation Research 467(1), 11-19.

PWN (2004), een publicatie door RevueArts bv Publishers.

Razavi, B., W. Song, W. J. Cooper, J. Greaves, J. Jeong (2009). "*Free-Radical-Induced Oxidative and Reductive Degradation of Fibrate Pharmaceuticals: Kinetic Studies and Degradation Mechanisms.*" Journal of Physical Chemistry A, 2009

Reasoner, D.J (1991). "*Assimilable Organic Carbon and Distribution System Quality.*" U.S. Environmental Protection Agency, Office of Research and Development. EPA-600/D-91/203. Cincinnati, Ohio: USEPA.

Richardson, S.D., Plewa, M.J., Wagner, E.D., Schoeny, R. and Demarini, D.M. (2007). "Occurrence, genotoxicity, and carcinogenicity of regulated and emerging disinfection by-products in drinking water: a review and roadmap for research". Mutation Research 636(1-3), 178-242.

Rook, J.J. (1974). "*Formation of haloforms during chlorination of natural waters*". Water Treatment Exam. 23 (2) 234-243.

Rosenfeldt, E.J. en K.G. Linden (2004), "*Degradation of Endocrine Disrupting Chemicals bisphenol A, ethinyl estradiol, and estradiol during UV photolysis and advanced oxidation processes*", Env. Sci. & Technol., vol 38, pp. 5476 – 5483.WQTC Congres, San Antonio, VS.

Rosenfeldt E. J., B. Melcher, K. G. Linden (2005). "*UV and UV/H2O2 Treatment of Methylisoborneol (MIB) and Geosmin in Water.*" Journal of Water Supply: Research and Technology, 54(7), pp. 423-434, 2005

Sarathy, S.R., and M. Mohseni (2007). "*The impact of UV/H2O2 Advanced Oxidation on Molecular Size Distribution of Chromophoric Natural Organic Matter.*" Environmental Science and Technology, 41 (24), pp. 8315-8320, 2007

Sarathy, S.R., and M. Mohseni (2009). "*The Fate of Natural Organic Matter during UV/H2O2 Advanced Oxidation of Drinking Water.*" Canadian Journal of Civil Engineering, 36, pp. 160-169, 2009

Satoh, T., J. Kato, N. Takiguchi, H. Ohtake, and A. Kuroda (2004). "*ATP Amplification for Ultrasensitive Bioluminescence Assay: Detection of a Single Bacterial Cell.*" Biosci. Biotechnol. Biochem, 68, pp. 1216–1220, 2004

Servais, P., A. Anzil, and Ventresque (1989). "*A Simple Method for the Determination of Biodegradable Dissolved Organic Carbon in Water.*" Journal of Appl. Environ. Microbiology, 55, pp. 2732-2734, 1989

Sharp, R. R., A.K. Camper, J.J. Crippen, O.D. Schneider, S. Leggiero (2001). "*Evaluation of Drinking Water Biostability using Biofilm Methods.*" Journal of Environmental Engineering, pp. 403-410, 2001

Sharpless, C.M., and K.G. Linden. 2001. "*UV Photolysis of Nitrate: Effects of Natural Organic Matter and Dissolved Inorganic Carbon and Implications for UV Water Disinfection*" Environmental Science and Technology, 35:2949–2955.

Sharpless C.M., Linden K.G., (2003). Experimental and Model Comparisons of Low- and Medium-Pressure Hg Lamps for the Direct and H_2O_2 Assisted UV Photodegradation of N-Nitrosodimethylamine in Simulated Drinking Water. Environmental Science and Technology, 37:1933-1940.

Sharpless, C.M., Page, M.A. and Linden, K.G (2003). "*Impact of hydrogen peroxide on nitrite formation during UV disinfection*". Water Research, Vol. 37, p 4703-4736,

Sharpless, C.M., and K.G. Linden (2005). "*Interpreting Collimated Beam Ultraviolet Photolysis Rate Data in Terms of Electrical Efficiency of Treatment.*" Journal of Environmental Engineering and Science, 4, pp. S19-S26, 2005

Shi, J., X.D. Zhao, R.F. Hickey, and T.C. Voice (1995). "*Role of Adsorption in Granular Activated Carbon-Fluidized Bed Reactors.*" Water Environment Research, 67(3), pp. 302-309, 1995

Shi-hu, S., Y.Min, G. Nai-yun, H. Wen-Jie (2008). "*Molecular Weight Distribution Variation of Assimilable Organic Carbon during Ozonation/BAC Process.*" Journal of Water Supply: Research and Technology—AQUA, 57 (4), pp. 253-258, 2008

Singh, N.P., McCoy, M.T., Tice, R.R., Schneider, E.L. (1988). "*A simple technique for quantitation of low levels of DNA damage in individual cells*". Experimental Cell Research 175, 184 – 191.

Snyder, A.S. , P. Westerhoff, E.C. Wert, H. Lei, and Y. Yoon (2007). "*Removal of EDCs and Pharmaceuticals in Drinking and Reuse Treatment Processes.*" American Water Works Research Foundation Report, 2007. Denver, CO.

Snyder, A. S., B. J. Vanderford, J. Drewes, E. Dickenson, E. M. Snyder, G. M. Bruce, and R.C. Pleus (2008). *State of knowledge of Endocrine Disruptors and Pharmaceuticals in Drinking Water*. American Water Works Research Foundation Report.

Sontheimer, H., J.C. Crittenden and R.S. Summers (1988). "*Activated Carbon for Water Treatment.*" 2nd ed., DVGW-Forschungsstelle, University of Karlsruhe, Germany, distributed in the USA by AWWA.

Sozzi D.A., Taghipour F., (2006). UV reactor performance modeling by Eulerian and Lagrangian methods, Environmental Science and Technology, 40:1609-1615.

Speitel, G.E., M.M.Wanielista, J.M. Symons, J.M. Davis (1999). "*Advanced Oxidation and Biodegradation Processes for the Destruction of TOC and DBP Precursors.*" American Water Works Research Foundation Report, 1999. Denver, CO.

Staatblad van het Koninkrijk der Nederlanden; 2001. "*Besluit van 9 januari 2001 tot wijziging van het waterleidingbesluit in verband met de richtlijn betreffende de kwaliteit van voor menselijke consumptie bestemd water*", Staatblad 31.

Stanley, P.E (1986). "*Extraction of Adenosine Triphosphate from Microbial and Somatic Cells.*" Methods Enzymol, 133, pp.14–22, 1986

Stefan, M.I. (2004). "*UV photolysis: background*". Advanced oxidation processes for water and wastewater treatment; London: IWA publishing

Stefan, M.I., Kruithof, J.C., Kamp, P.C. (2005), "*Advanced Oxidation Treatment of Herbicides: From Bench-Scale to Full-Scale Installation*", 3rd International Congress on Ultraviolet Technologies, Whistler, Canada, 24-27 May 2005.

Stumm-Zollinger, E., and G.M.Fair (1965). "*Biodegradation of Steroid Hormones.*" Journal of the Water Pollution Control Federation, 37, pp. 1506-1510, 1965

Tabak H. H. and R.L. Bunch (1970). "*Steroid Hormones as Water Pollutants. I. Metabolism of Natural and Synthetic Ovulation-inhibiting Hormones by Microorganisms of Activated Sludge and Primary Settled Sewage.*" Dev. Ind. Microbiol., 11, pp. 367-376, 1970

Tawabini, B., Fayad N., Morsy, M. (2009). "*The impact of groundwater quality on the removal of methyl tertiary butyl ether (MTBE) using advanced oxidation technology*". Water Science and Technology 60, 2161-2165

Tice, R.R., Agurell, E., Anderson, D., Burlinson, B., Hartmann, A., Kobayashi, H., Miyamae, Y., Rojas, E., Ryu, J.C. and Sasaki, Y.F. (2000). "*Single cell gel/comet assay: guidelines for in vitro and in vivo genetic toxicology testing*". Environmental and Molecular Mutagenesis 35(3), 206-221.

Tuhkanen, T.A. (2004), "*UV/H$_2$O$_2$ processes. In: Advanced Oxidation Processes for Water and Wastewater treatment*", S. Parsons (ed.), IWA Publishing, ISBN 1 84339 017 5, pp. 87-88.

van der Kooij, D., D.A.Visser, and W.A. Hijnen (1982). "*Determining the Concentration of Easily Assimilable Organic Carbon in Drinking Water.*" Jour. AWWA, 74(10), pp. 540–545, 1982

van der Kooij, D., and W.A. Hijnen (1984). "*Substrate Utilization by an Oxalate-Consuming Spirillum Species in Relation to Its Growth in Ozonated Water*." Applied and Environmental Microbiology, 47 (3), pp. 551-559, 1984

van der Kooij, D. (1992). "*Assimilable Organic Carbon as an Indicator of Bacterial Regrowth*." Jour. AWWA, 84(2), pp. 57–65, 1992

Van der Pol, A.J.H.P., S. Krijnen (2005), "*Optimal UV output in different application of low-pressure UV-C lamps*" Proceedings IUVA Congres, Whistler (Canada).

Van der Pol, A.J.H.P., S. Krijnen (2005), "*Low mercury containing UV low-pressure lamps*", Proceedings IUVA Congres, Whistler (Canada).

Van der Veer, A.J. (2002), "*Case study Berenplaat, Internationaal UV Workshop* " UV in drinking water treatment – Scientific foundation of succesful application", Kiwa Water Research, 20 – 23 maart.

Veenendaal, H.R. and van Genderen, J. (1999). "*Mutageniteit in Rijn en Maas in 1998*". Kiwa, Nieuwegein (the Netherlands), report KOA 99.088.

Von Gunten, U., J. Hoigné (1994) "*Bromate Formation during Ozonation of Bromide-Containing Waters: Interaction of Ozone and Hydroxyl radical Reactions*", Environ. Sci. Technol., **28(7)**, pp. 1234-1242.

Volk, C.J., C.B.Volk, and L.A. Kaplan (1997). "*The Chemical Composition of Biodegradable Dissolved Organic Matter in Stream water*." Limnology and Oceanography, 42, pp. 39-44, 1997

Watanabe, N., S. Horikoshi, H. Hidaka, N. Serpone (2005) "*On the recalcitrant nature of the triazinic ring species, cyanuric acid, to degradation in Fenton solutions and in UV-illuminated TiO_2 (naked) and fluorinated TiO_2 aqueous dispersions*", J. Photochem. Photobiol. A: Chem., **174**, pp. 229-238.

Watts M.J. and K.G. Linden. 2007. "Chlorine *Photolysis and subsequent OH radical production during UV treatment of chlorinated water*" Water Research, 41(2007), 2871–2878.

Weeks, J.L., Rabani, J. (1966) "*The pulse radiolysis of deaerated carbonate solutions. I. Transient optical spectrum and mechanism. II. pK for OH radicals*", J. Phys. Chem., **70**, pp. 2100-2104.

Weinrich, LA., E. Giraldo, M.W. LeChevallier (2009). "*Development and Application of a Bioluminescence-Based Test for Assimilable Organic Carbon in Reclaimed Waters*." Applied and Environmental Microbiology, pp. 7385-7390, 2009

Westerhoff P., M. Rodriguez-Hernandez, L. Baker, M. Sommerfeld (2005a). "*Seasonal Occurrence and Degradation of 2-Methylisoborneol in Water Supply Reservoirs*." Water Research, 39, pp. 4899-4912, 2005a

Westerhoff, P., Y. Yoon, et al. (2005b). "*Fate of Endocrine Disruptor, Pharmaceutical, and Personal Care Product Chemicals during Simulated Drinking Water Processes*." Environmental Science and Technology, 39(17), pp. 6649-6663, 2005b

Wink, D. A et al; Kinetic Investigation of Intermediates Formed during the Fenton Reagent Mediated Degradation of N-Nitrosodimethylamine: Evidence for an Oxidative Pathway Not Involving Hydroxyl Radical; Chem. Res. Toxicol. Issue 4, p 510-512, 1991

Wols (2010). CFD in drinking water treatment. PhD thesis, Delft University of Technology.

Wu, T.Y. (1991). "*Enhanced Biodegradability of Organic Contaminants by Hydrogen Peroxide and Visible-Ultraviolet Irradiation.*" M.S. thesis. University of Houston, Houston, TX.

Yuan, F., Hu, C., Hu, X., Qu, J. and Yang, M. (2009) "*Degradation of selected pharmaceuticals in aquaeous solution with UV and UV/H_2O_2.*" Water Research 43 (6), p 1766-1774.

Zeid, A.N., G. Nakhla, S.Farooq, E.Osei-Twum (1995). "*Activated Carbon Adsorption in Oxidizing Environments.*" Water Research, 29 (2), pp. 653-660, 1995

Appendices

I Photos of UV bench-scale reactor
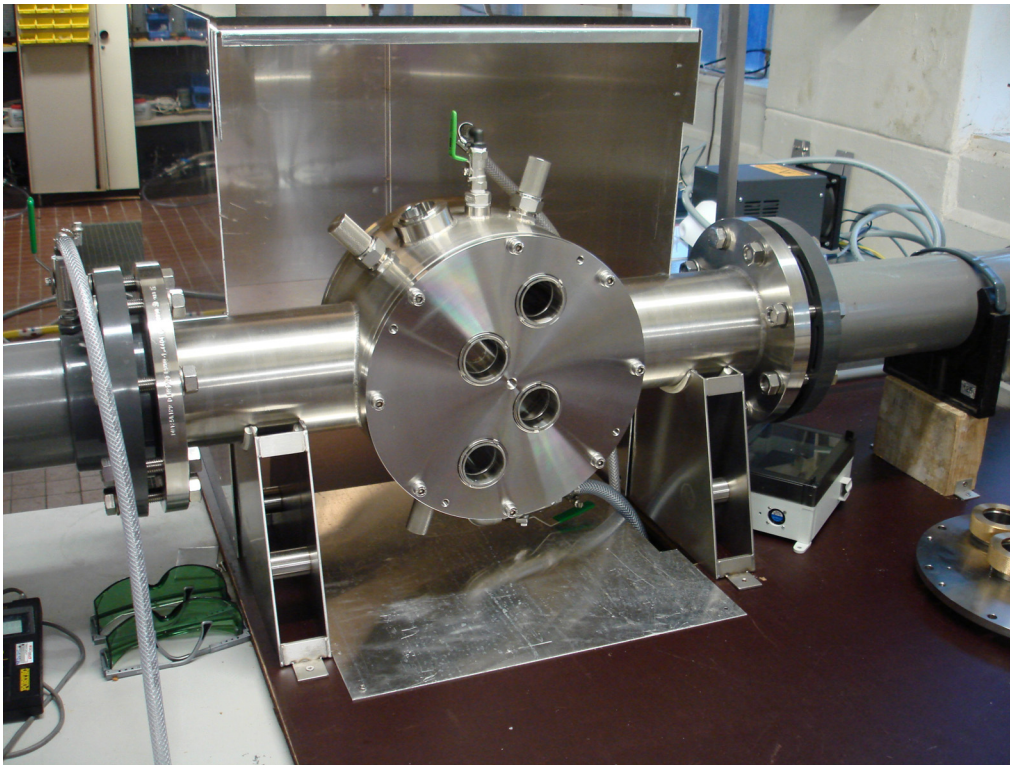
Figure I.1 KWR UV pilot reactor
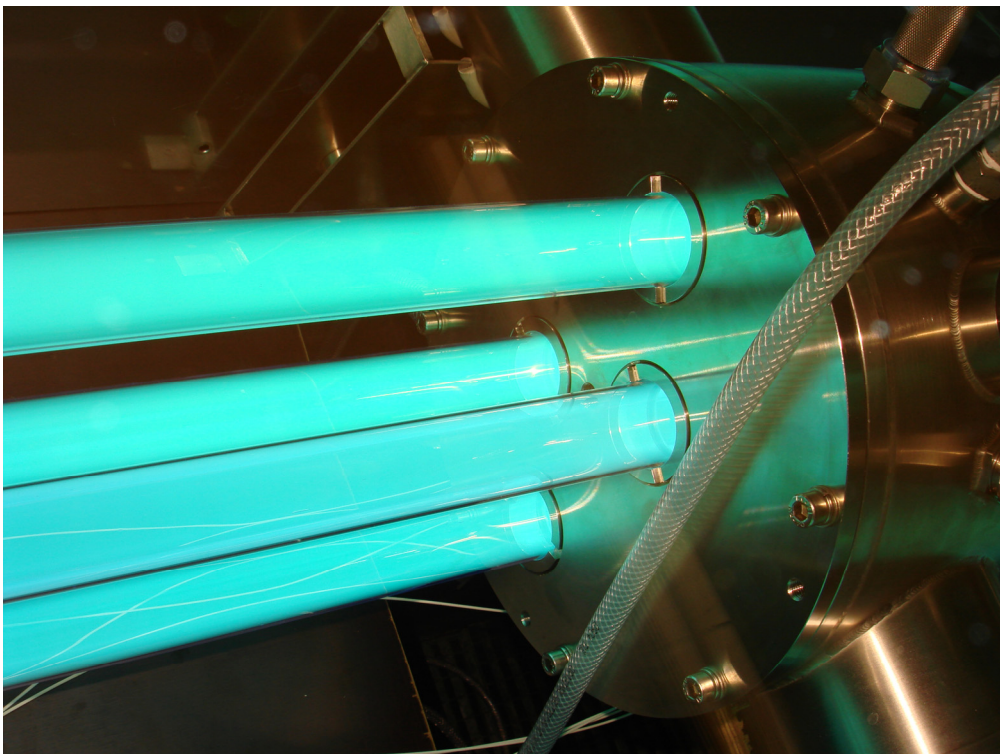
Figure I.2 *KWR UV pilot reactor with LP lamps*

II Treatment Processes of the Dunea plant (Bergambacht) and of the Richard Miller Treatment Plant (GCWW, Cincinnati)

© WAO, 2009

Meuse River

Death end side stream Meuse River

Iron sulphate dosing
ca.2 grFe(II)/m3

Micro sieves

Lek River

Rapid sand filtration Bergambacht

Scheveningen   **Katwijk**   **Monster**

10-15 gr/m3 Fe(III)

Scheveningen	Katwijk	Monster
open infiltration	open infiltration	open infiltration
Coagulation	Coagulation	
Flotation	Flotation	
Rapid filtration	Rapid filtration	
Active carbon filtration	Active carbon filtration	
dune	dune	dune
Deep well infiltration	Deep well infiltration	
Closed winning	Closed winning	Closed winning

Softening (Lime)

Powdered activated carbon

(Norit SA Super 2gr/m3)

Softening (caustic soda)

Powdered activated carbon

(Chemviron type C: 3,5 gr/m3)

Aeration

Powdered activated carbon

(Norit SA Super 3gr/m3)

Aeration

Softening (caustic soda)

Aeration

Rapid filtration

Rapid filtration

Rapid filtration

Slow sand filtration

Slow sand filtration

Slow sand filtration

Clear Water Storage

Clear Water Storage

Clear Water Storage

Treatment	Capacity	x10⁶ m³/jr
Scheveningen	51,5	
Katwijk	24,8	
Monster	7,9	

Figure II.1 Treatment process of Dunea in Bergambacht
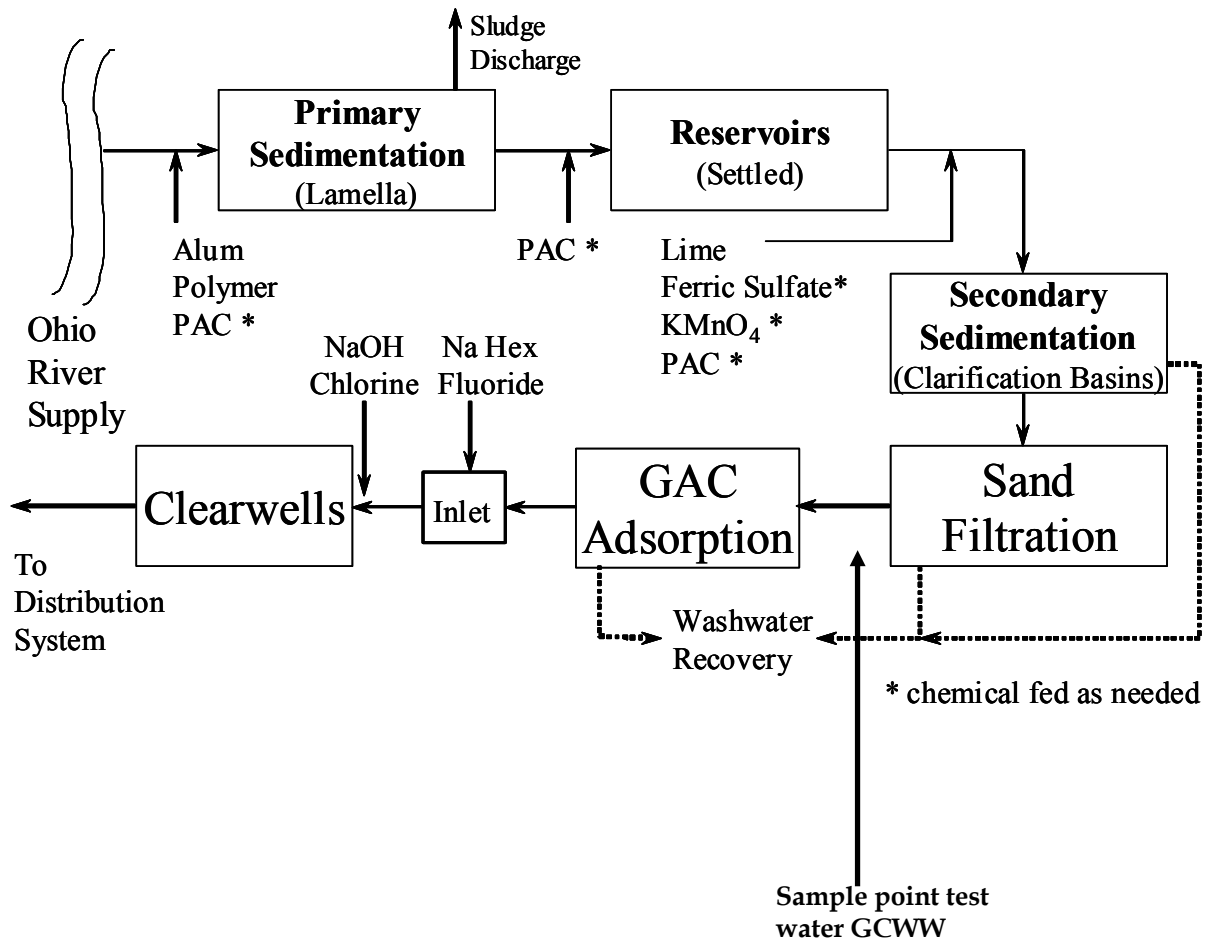
Figure II.2 Treatment process of the Richard Miller Treatment Plant (GCWW)

III Analytic methods used in WP1

All analyses were carried out by the Laboratories of KWR Watercycle Research Institute.

Analyses water quality
Hydrogen peroxide; Instruction LAM-048, in accordance with Kiwa-instruction 1-06-1 (1995)
Hydrogen peroxide forms yellow peroxy-titanal complexes like $[Ti(H_2O_2)]^{4+}$, when treated with titane(IV) ions in the presence of sulfuric acid. The color intensity was measured using the yellow Thermo Spectronic Unicam UV500 spectrophotometer at a wavelength of 400 nm.

UV scan/UV$_{254nm}$; InstructionLAM-033
The UV-scan was made using the Thermo Spectronic Unicam UV500 spectrofotometer at wavelength of 200-300 nm, or 254 nm bij UV$_{254nm}$ applying a 1-cm path length.

Acidity; Instruction LAM-043, in accordance with NEN 6411 (1981)
The pH was determined using a PHM 83 autocal pH meter by Radiometer Copenhagen.

Hydrogen carbonate; Instruction LAM-042, in accordance with NEN 6531 en 6532
Hydrogen carbonate is titrated with chloric acid until a pH of 4.35 is reached. The pH is measured using a PHM 83 autocal pH meter by Radiometer Copenhagen.

Nitrate; Instruction LAM-026, in accordance with EPA 300.0 (1991)
Nitrate is determined directly, after separation by means of ion exchange (Ionpac AG9-SC Guard and the Ionpac SC Analytical) and detection according to conductivity using the DX 500 Ionchromatograaf by DIONEX.

Non-purgeable organic carbon (NPOC); Instruction LAM-041, in accordance with ISO 8245 and NEN-EN 1484
The non-purgable organic carbon is analyzed by means of an infrared gas analyzer from Schimadzu TOC-5000A with TOC control and an ASI-5000A autosampler.

Analyses of hydroxyl radical formation by means of pCBA; Instruction LOA-007
pCBA is analyzed using HPLC-UV (Waters 996 diode array detector).

Analyses conversion of organic micropollutants and disinfection capacity
Collimated beam
Hormones estrone, estradiol, 17alfa estradiol, 17beta estradiol en 17alfa ethynylestradiol have been analyzed using online LC/MS/MS with the Thermo TSQ-7000 triple-Qud LC-MS/MS.

Triazines, atrazine, cyanazine, simazine, desethyl atrazine and desisopropyl atrazine have been analyzed using GCMS-LLE. Target compounds were screened after liquid/liquid extraction using the Thermo, trace GC/MS.

UV-pilot reactor experiments
Medicines erythromycine, benzafibrate, carbamazepine, diclofenac, ibuprofen, lincomycin, metropolal, phenazone, sotalol, sulfamethoxazole were analyzed by means of online LC/MS/MS using the Thermo TSQ-7000 triple-Qud LC-MS/MS.

Pesticides atrazine, cyanazine, alachlor and metazachlor have been analyzed by means of GCMS-SPE. Target compounds were screened after solid extraction, using the Thermo, trace GC/MS.

MTBE; was analyzed by means of purge and trap GC/MS using the GC/MS Thermo Trace DSQ, Tekmar Dohrmann purge and trap system with 3100 sampler concentrator and Aquatek 70 liquid autosampler.

NOM-characterization (LC-OCD = Liquid Chromatography – Organic Carbon Detection); LC-OCD has been carried out by DOC-Labor in Karlsruhe (Germany). An extensive description of this technique can be found in Appendix X.

Nitrite; Instruction LAM-027
Nitrite is diazotized by means of sulfanilamide. The resulting compound reacts with N-(1-naftyl) 1,2 diamino-ethaandihydrochloride to a red azo-dye. The color intensity can be measured using the Thermo Spectronic Unicam UV500 spectrofotometer at a wavelength of 542 nm.

AOC; AOC has been analyzed in accordance with NEN-6271 by Het Waterlaboratorium (Haarlem).

MS2 phages; MS2 phages have been analyzed according to NEN-ISO 10705-1.
The sampled is mixed with liquid agar containing a host compound. This mixture is spread over liquid agar, and after an incubation period of 18 hours at 37 ^{0}C the colonies were counted.

IV pCBA as a hydroxylprobe (WP1)

Validation

In order to test the suitability of pCBA as a hydroxyl probe, an analysis method was implemented by KWR Watercycle Research Institute based on existing analysis methods for pCBA [Elovitz and von Gunten, 1999; Pinkernell and von Gunten, 2001; Min Cho *et al.*,2003]. The analytical method for pCBA was validated for the water of Dunea Bergambacht after rapid sand filtration. The validation results are mentioned in Kiwa instruction LOA-007. In Table IV.1 data are shown.

Table IV.1 Data of pCBA analyses in water of Dunea Bergambacht after rapid sand filtration

µg/L pCBA in SF Bergambacht	Number of analyses n	pCBA µg/L	Standard deviation %
10	7	8	0.9
50	7	44.1	0.9
50 (affter 7 days)	5	45.0	1.2
100	37	97.7	0.5

The recovery in the water (100 µg/L) was 95% with calibration curves (0 – 400 µg/L; n = 11) showing a R^2 larger than 0,999. Based on these data it can be concluded that the analysis method for pCBA is very reliable and accurate, and therefore is a very suitable method.

Furthermore, the influence of hydrogen peroxide on the pCBA concentration was also determined. On July 18th and 19th 2006 an experiment was carried out, in which the pCBA concentration was measured in a peroxide-containing sample of the either pretreated Dunea or GCWW water. The results are shown in Table IV.2.

Table IV.2 Effect of H_2O_2 on the pCBA concentration

Water type	time min	H_2O_2 mg/L	pCBA µg/L
Dunea, Bergambacht,	0	10.5	399
	30		399
GCWW, Cincinnati	0	10.5	169
	30		172

The pCBA concentration does not seem to be affected by the presence of place 10 mg H_2O_2/L during the period in which experiments take. This conclusion has been based on only one measurement, and should be repeated to obtain a more reliable result.

Suitability of pCBA as a hydroxyl probe

Collimated beam tests were carried out using pretreated Dunea water to determine whether or not the tested water matrix affects the analysis of pCBA. pCBA was added to the water sample, and subsequently two experiments were carried out, one with and one without addition of H_2O_2 using MP lamps. To the samples containing H_2O_2 directly after irradiation 100 mg sulfite (Na_2SO_3) was added. These experiments were carried out on May 30th 2006.

The water quality of solutions irradiated was determined and a UV scan was made. The results are shown in Appendix XI.

Results of the collimated beam experiments are shown in Table IV.3 and Figure IV.1.

Table IV.3 Results of collimated beam experiments (MP — lamp) with Dunea water

Test	UV-dose	H_2O_2-concentration	pCBA
	mJ/cm^2	mg/L	$\mu g/L$
1	0	0.20*	410
	750		210
	1125		162
	1500		128
	1875		103
2	0	11.1	403
	750		107
	1125	10.0	53
	1500		38
	1875	10.1	22

* Blank signal, not corrected for during the measurements.

The hydrogen peroxide concentration during the test with H_2O_2 was 10.4 ± 0.6 mg/L. The blank signal corresponding with 0.2 mg H_2O_2 mg/L probably was caused by the color of the water, and not by the presence of H_2O_2 in the water.
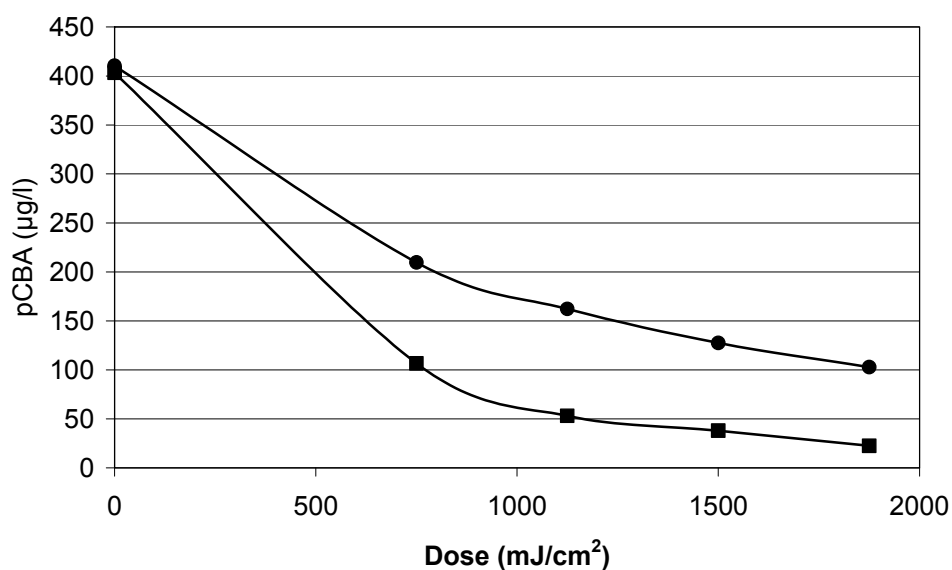
Figure IV.1 Results of collimated beam tests with (MP-lamp) Dunea water; (●) (Dunea): + 0 mg/L H_2O_2 (■) + 10 mg/L H_2O_2.

Obviously, the pCBA concentration decreases with increasing UV dose, independent of the various conditions tested. At an equal UV dose, addition of H_2O_2 increases the pCBA conversion, as a result of the reaction of pCBA with •OH radicals. Increasing the UV dose increases the photolysis of pCBA. Therefore, the results have to be corrected for photolysis to determine the amount of •OH radicals formed. It is assumed that the reaction rate of •OH radicals with pCBA is much higher than the photolysis of pCBA [Watts and Linden, 2007]. Although correction for photolysis is possible, it would be better to use a •OH probe which is less sensitive towards photolysis. However, when these experiments were carried out, such a probe was not available at KWR.
Addition of sulfite to H_2O_2 solutions (to quench excess H_2O_2) does not affect the pCBA analysis, as was concluded from experiments carried out at a dose of 0 mJ/cm^2. In a solution without hydrogen peroxide, 410 µg pCBA /L was measured, whereas with peroxide, 403 µg pCBA /L was found. The solution without hydrogen peroxide did not contain any sulfite.

V Experiments hydroxyl radical formation (WP1)

Suitability of pCBA as a hydroxyl probe
30-05-2006

Experimental conditions
CB parameters
Testing with MP lamp
Distance from lamp to irradiated surface = 80cm
Irradiated volume: 60 mL

Stock solution pCBA = 40 mg/L
Stock solution H_2O_2 = 1 g H_2O_2/L
Water composition: Dunea

For every irradiation a new solution was prepared
Composition solutions:
1. 99 mL Dunea-water + 1mL pCBA 40 mg/L
2. 98 mL Dunea-water + 1mL pCBA 40 mg/L + 1 mL H_2O_2 1 g/L

Table V.1 order of tests + analyses

			Analyses	
Nr.	solution	Dose (mJ/cm^2)	pCBA	H_2O_2
1	2	0	X	X
2	2	300	X	
3	2	450	X	X
4	2	600	X	
5	2	750	X	X
6	1	0	X	X
7	1	300	X	
8	1	450	X	
9	1	600	X	
10	1	750	X	

- Of every solution, 60 mL was irradiated
- First tests 1-5 were carried out randomly, and subsequently this was repeated with tests 6-10.
- After irradiation 100 mg Na_2SO_3 (45x excess) was added to stop the reaction (tests 1 - 5).
- All glassware had been rinsed with milliQ/Acetone/poly ethylene Pipets and cups had been rinsed with PE.

Experiments were carried out in the Collimated Beam (CB) set-up.

Experiments Hydroxyl radical formation

July 4th (4 MP experiments)

Experimental conditions
CB parameters
Testing with MP lamp (2KWHOK)
Distance from lamp to irradiated surface = 80cm
Irradiated volume: 60 mL

Stock solution pCBA = 40 mg/L
Stock solution H_2O_2 = 1 g H_2O_2/L
Water composition: Dunea or GCWW

For every irradiation a new solution was prepared
Composition solutions:
1. 99 mL GCWW-water + 1mL pCBA 40 mg/L
2. 98.5 mL GCWW-water + 1mL pCBA 40 mg/L + 0.5mL H_2O_2 1g/L
3. 98 mL GCWW-water + 1mL pCBA 40 mg/L + 1mL H_2O_2 1g/L
4. 98.5 mL Dunea-water + 1 mL pCBA 40 mg/L + 0.5 mL H_2O_2 1g/L

Table V.2 Order of tests + analyses

		additions			Analyses	
Nr.	Solution	pCBA (μg/L)	H_2O_2 (mg/L)	UV Dose (mJ/cm^2)	pCBA	H_2O_2
1	2	400	5	0	X	X
2	2	400	5	300	X	
3	2	400	5	450	X	X
4	2	400	5	600	X	
5	2	400	5	750	X	X
6	3	400	10	0	X	X
7	3	400	10	300	X	
8	3	400	10	450	X	X
9	3	400	10	600	X	
10	3	400	10	750	X	X
11	4	400	5	0	X	X
12	4	400	5	300	X	
13	4	400	5	450	X	X
14	4	400	5	600	X	
15	4	400	5	750	X	X
16	1	400	0	0	X	X
17	1	400	0	450	X	
18	1	400	0	600	X	

- Of every solution, 60 mL was irradiated
- First tests 1-5 were carried out randomly, and subsequently this was repeated with tests 6-10.
- After irradiation 100 mg Na_2SO_3 (45x excess) was added to stop the reaction (tests 1 - 5).
- All glassware had been rinsed with milliQ/Acetone/PE. Pipets and cups had been rinsed with PE.

July 6th (2 LP experiments)

Experimental conditions
CB parameters
Testing with LP lamp (PLL 95; 1 lamp)
Distance from lamp to irradiated surface = 80cm
Irradiated volume: 60 mL

Stock solution pCBA = 40 mg/L
Stock solution H_2O_2 = 1 g H_2O_2/L
Water composition: GCWW (delivered July 3rd)

For every irradiation a new solution was prepared
Composition solutions:
- 98.5 mL GCWW-water + 1 mL pCBA 40 mg/L + 0.5 mL H_2O_2 1g/L
- 98 mL GCWW-water + 1 mL pCBA 40 mg/L + 1 mL H_2O_2 1g/L

Table V.3 Order of tests + analyses

		Additions			Analyses	
Nr.	Oplossing	pCBA (μg/L)	H_2O_2 (mg/L)	UV Dose (mJ/cm²)	pCBA	H_2O_2
1	1	400	5	0	X	X
2	1	400	5	300	X	
3	1	400	5	450	X	X
4	1	400	5	600	X	
5	1	400	5	750	X	X
6	2	400	10	0	X	X
7	2	400	10	300	X	
8	2	400	10	450	X	X
9	2	400	10	600	X	
10	2	400	10	750	X	X

- Of every solution, 60 mL was irradiated
- First tests 1-5 were carried out randomly, and subsequently this was repeated with tests 6-10.
- After irradiation 60 mg Na_2SO_3 (27x excess) was added to stop the reaction (tests 1 - 10).
- All glassware had been rinsed with milliQ/Acetone/PE. Pipets and cups had been rinsed with PE.

July 7th (2 LP experiments)   (PLL 95; 1 lamp)

Experimental conditions
CB parameters
Testing with LP lamp (PLL 95; 1 lamp)
Distance from lamp to irradiated surface = 80cm
Irradiated volume: 60 mL

Stock solution pCBA = 40 mg/L
Water composition:: Dunea or GCWW (delivered July 3rd)

For every irradiation a new solution was prepared
Composition solutions:
- 99 mL GCWW-water + 1mL pCBA 40 mg/L
- 99 mL Dunea-water + 1mL pCBA 40 mg/L

Table V.4 Order of tests + analyses

		Additions			Analyses	
Nr.	Oplossing	pCBA (μg/L)	H_2O_2 (mg/L)	UV Dose (mJ/cm^2)	pCBA	H_2O_2
1	1	400	0	0	X	X
2	1	400	0	450	X	
3	1	400	0	600	X	
4	2	400	0	0	X	X
5	2	400	0	450	X	
6	2	400	0	600	X	

Of every solution, 60 mL was irradiated
- First tests 1-3 were carried out randomly, and subsequently this was repeated with tests 4-6.
- All glassware had been rinsed with milliQ/Acetone/PE. Pipets and cups had been rinsed with PE.

July 11th (2 LP experimenten)

Experimental conditions
CB parameters
Testing with LP lamp (PLL 95; 1 lamp)
Distance from lamp to irradiated surface = 80cm
Irradiated volume: 60 mL

Stock solution pCBA = 40 mg/L
Stock solution H_2O_2 = 1 g H_2O_2/L
Water composition: Dunea (delivered July 3rd)

For every irradiation a new solution was prepared
Composition solutions:
- 98.5 mL Dunea-water + 1 mL pCBA 40 mg/L + 0.5 mL H_2O_2 1g/L
- 98 mL Dunea-water + 1 mL pCBA 40 mg/L + 1 mL H_2O_2 1g/L

Table V.5 Order of tests + analyses

		additions			Analyses	
Nr.	Solution	pCBA (µg/L)	H_2O_2 (mg/L)	UV Dose (mJ/cm²)	pCBA	H_2O_2
1	1	400	5	0	X	X
2	1	400	5	300	X	
3	1	400	5	450	X	X
4	1	400	5	600	X	
5	1	400	5	750	X	X
6	2	400	10	0	X	X
7	2	400	10	300	X	
8	2	400	10	450	X	X
9	2	400	10	600	X	
10	2	400	10	750	X	X

- Of every solution, 60 mL was irradiated
- First tests 1-5 were carried out randomly, and subsequently this was repeated with tests 6-10.
- After irradiation 60 mg Na_2SO_3 (27x excess) was added to stop the reaction (tests 1 - 10).
- All glassware had been rinsed with milliQ/Acetone/PE. Pipets and cups had been rinsed with PE.

July 13th (3 DBD experiments)

Experimental conditions
CB parameters
Testing with DBD lamp
Distance from lamp to irradiated surface = 40 cm
Irradiated volume: 60 mL

Stock solution pCBA = 40 mg/L
Stock solution H_2O_2 = 1 g H_2O_2/L
Water composition: Dunea (delivered July 3rd)

For every irradiation a new solution was prepared
Composition solutions:
1. 99 mL Dunea-water + 1mL pCBA 40 mg/L
2. 98.5 mL Dunea-water + 1 mL pCBA 40 mg/L + 0.5 mL H_2O_2 1g/L
3. 98 mL Dunea-water + 1 mL pCBA 40 mg/L + 1 mL H_2O_2 1g/L

Table V.6 Order of tests + analyses

| Nr. | Solution | additions | | UV Dose (mJ/cm²) | Analyses | |
		pCBA (µg/L)	H_2O_2 (mg/L)		pCBA	H_2O_2
1	2	400	5	0	X	X
2	2	400	5	300	X	
3	2	400	5	450	X	X
4	2	400	5	600	X	
5	2	400	5	750	X	X
6	3	400	10	0	X	X
7	3	400	10	300	X	
8	3	400	10	450	X	X
9	3	400	10	600	X	
10	3	400	10	750	X	X
11	1	400	0	0	X	X
12	1	400	0	450	X	
13	1	400	0	600	X	

- Of every solution, 60 mL was irradiated
- First tests 1-5 were carried out randomly, and subsequently this was repeated with tests 6-10.
- After irradiation 60 mg Na_2SO_3 (27x excess) was added to stop the reaction (tests 1 - 10).
- All glassware had been rinsed with milliQ/Acetone/PE. Pipets and cups had been rinsed with PE.

July 18th (3 DBD experiments)

Experimental conditions
CB parameters
Testing with DBD lamp
Distance from lamp to irradiated surface = 40 cm
Irradiated volume: 60 mL

Stock solution pCBA = 40 mg/L
Stock solution H_2O_2 = 1 g H_2O_2/L
Water composition: CGWW (delivered July 17th)

For every irradiation a new solution was prepared
Composition solutions:
1. 99 mL GCWWH-water + 1mL pCBA 40 mg/L
2. 98.5 mL GCWW-water + 1 mL pCBA 40 mg/L + 0.5 mL H_2O_2 1g/L
3. 98 mL GCWW-water + 1 mL pCBA 40 mg/L + 1 mL H_2O_2 1g/L

Table V.7 Order of tests + analyses

Nr.	Solution	additions			Analyses	
		pCBA (µg/L)	H$_2$O$_2$ (mg/L)	UV Dose (mJ/cm²)	pCBA	H$_2$O$_2$
1	2	400	5	0	X	X
2	2	400	5	300	X	
3	2	400	5	450	X	X
4	2	400	5	600	X	
5	2	400	5	750	X	X
6	3	400	10	0	X	X
7	3	400	10	300	X	
8	3	400	10	450	X	X
9	3	400	10	600	X	
10	3	400	10	750	X	X
11	1	400	0	0	X	X
12	1	400	0	450	X	
13	1	400	0	600	X	

- Of every solution, 60 mL was irradiated
- First tests 1-5 were carried out randomly, and subsequently this was repeated with tests 6-10.
- After irradiation 60 mg Na$_2$SO$_3$ (27x excess) was added to stop the reaction (tests 1 - 10).
- All glassware had been rinsed with milliQ/Acetone/PE. Pipets and cups had been rinsed with PE.

July 26th (2 MP experiments)

Experimental conditions
CB parameters
Testing with MP lamp (2KWHOK)
Distance from lamp to irradiated surface = 80cm
Irradiated volume: 60 mL
Stock solution pCBA = 40 mg/L
Stock solution H$_2$O$_2$ = 1 g H$_2$O$_2$/L
Water composition: Dunea (delivered July 19th)

For every irradiation a new solution was prepared
Composition solutions:
1. 99 mL Dunea-water + 1mL pCBA 40 mg/L
2. 98 mL Dunea-water + 1 mL pCBA 40 mg/L + 1 mL H$_2$O$_2$ 1g/L

Table V.8 Order of tests + analyses

Nr.	Solution	additions			Analyses	
		pCBA (µg/L)	H$_2$O$_2$ (mg/L)	UV Dose (mJ/cm²)	pCBA	H$_2$O$_2$
1	2	400	10	0	X	X
2	2	400	10	300	X	
3	2	400	10	450	X	X
4	2	400	10	600	X	
5	2	400	10	750	X	X
6	1	400	0	0	X	X
7	1	400	0	450	X	
8	1	400	0	600	X	

- Of every solution, 60 mL was irradiated
- First tests 1-5 were carried out randomly, and subsequently this was repeated with tests 6-8.
- After irradiation 60 mg Na$_2$SO$_3$ (27x excess) was added to stop the reaction (tests 1 - 8).
- All glassware had been rinsed with milliQ/Acetone/PE. Pipets and cups had been rinsed with PE.

VI Conversion of organic micropollutants in collimated beam experiments (WP1)

Collimated beam testen
July 20th (2 DBD experiments)

Experimental conditions
CB parameters
Testing with DBD lamp
Distance from lamp to irradiated surface = 40 cm
Irradiated volume: 100 mL

Stock solution hormones/triazines = (200 µg/L triazines and 4 µg/L hormones)
Stock solution H_2O_2 = 1 g H_2O_2/L
Water composition: CGWW (delivered July 12th) or Dunea (delivered July 19th)

For every irradiation a new solution was prepared
Composition solutions:
1. 196 mL GCWW-water + 2 mL 200 µg/L triazines and 4 µg/L hormones + 2 mL H_2O_2 1g/L
2. 196 mL Dunea-water + 2 mL 200 µg/L triazines and 4 µg/L hormones + 2 mL H_2O_2 1g/L

Table VI.1 Order of tests + analyses

| Nr. | Solution | Additions | | | | analyses | | |
		Hormones (ng/L)	Triazines (µg/L)	H_2O_2 (mg/L)	UV Dose (mJ/cm²)	Hormones	triazine	H_2O_2
1	1	40	2	10	0	X		X
2	1	40	2	10	300	X		X
3	1	40	2	10	600	X		
4	1	40	2	10	0		X	X
5	1	40	2	10	300		X	
6	1	40	2	10	600		X	X
7	2	40	2	10	0	X		X
8	2	40	2	10	300	X		X
9	2	40	2	10	600	X		
10	2	40	2	10	0		X	X
11	2	40	2	10	300		X	
12	2	40	2	10	600		X	X

- Of every solution, 100 mL was irradiated
- First tests 1-6 were carried out randomly, and subsequently this was repeated with tests 7-12.
- After irradiation 100 mg Na_2SO_3 (27x excess) was added to stop the reaction (tests 1 - 10).
- All glassware had been rinsed with milliQ/Acetone/PE. Pipets and cups had been rinsed with PE.

July 25th (2 LP experiments)

Experimental conditions
CB parameters
Testing with LP lamp (PLL 95; 1 lamp)
Distance from lamp to irradiated surface = 30 cm
Irradiated volume: 100 mL

Stock solution hormones/triazines = (200 µg/L triazines and 4 µg/L hormones)
Stock solution H_2O_2 = 1 g H_2O_2/L
Water composition: CGWW (delivered July 12th) or Dunea (delivered July 19th)

For every irradiation a new solution was prepared
Composition solutions:
- 196 mL GCWW-water + 2 mL 200 µg/L triazines and 4 µg/L hormonen + 2 mL H_2O_2 1g/L
- 196 mL Dunea-water + 2 mL 200 µg/L triazines and 4 µg/L hormonen + 2 mL H_2O_2 1g/L

Table VI.2 Order of tests + analyses

| Nr. | Solution | additions | | | | analyses | | |
		Hormones (ng/L)	Triazines (µg/L)	H_2O_2 (mg/L)	UV Dose (mJ/cm²)	Hormones	triazine	H_2O_2
1	1	40	2	10	0	X		X
2	1	40	2	10	300	X		X
3	1	40	2	10	600	X		
4	1	40	2	10	0		X	X
5	1	40	2	10	300		X	
6	1	40	2	10	600		X	X
7	2	40	2	10	0	X		X
8	2	40	2	10	300	X		X
9	2	40	2	10	600	X		
10	2	40	2	10	0		X	X
11	2	40	2	10	300		X	
12	2	40	2	10	600		X	X

- Of every solution, 100 mL was irradiated
- First tests 1-6 were carried out randomly, and subsequently this was repeated with tests 7-12.
- After irradiation 100 mg Na_2SO_3 (27x excess) was added to stop the reaction (tests 1 - 10).
- All glassware had been rinsed with milliQ/Acetone/PE. Pipets and cups had been rinsed with PE.

July 26th (2 MP experiments)

Experimental conditions
CB parameters
Testing with MP lamp (2KWHOK)
Distance from lamp to irradiated surface = 80cm
Irradiated volume: 100 mL

Stock solution hormones/triazines = (200 µg/L triazines and 4 µg/L hormones)
Stock solution H_2O_2 = 1 g H_2O_2/L
Water composition: CGWW (delivered July 17th) or Dunea (delivered July 19th)

For every irradiation a new solution was prepared
Composition solutions:
1. 196 mL GCWW-water + 2 mL 200 µg/L triazines and 4 µg/L hormonen + 2 mL H_2O_2 1g/L
2. 196 mL Dunea-water + 2 mL 200 µg/L triazines and 4 µg/L hormonen + 2 mL H_2O_2 1g/L

Table VI.3 Order of tests + analyses

Nr.	Solution	additions				analyses		
		Hormones (ng/L)	Triazines (µg/L)	H_2O_2 (mg/L)	UV Dose (mJ/cm²)	Hormones	triazine	H_2O_2
1	1	40	2	10	0	X		X
2	1	40	2	10	300	X		X
3	1	40	2	10	600	X		
4	1	40	2	10	0		X	X
5	1	40	2	10	300		X	
6	1	40	2	10	600		X	X
7	2	40	2	10	0	X		X
8	2	40	2	10	300	X		X
9	2	40	2	10	600	X		
10	2	40	2	10	0		X	X
11	2	40	2	10	300		X	
12	2	40	2	10	600		X	X

- Of every solution, 100 mL was irradiated

- First tests 1-6 were carried out randomly, and subsequently this was repeated with tests 7-12.

- After irradiation 100 mg Na_2SO_3 (27x excess) was added to stop the reaction (tests 1 - 10).

- All glassware had been rinsed with milliQ/Acetone/PE. Pipets and cups had been rinsed with PE.

VII Conversion of organic micropollutants and determination of disinfection capacity in the KWR pilot reactor (WP1)

Validation experiments UV pilot reactor

Collimated beam tests
November 20

LP lamp
Experimental conditions
CB parameters
Testing with LP lamp (PLL 95; 1 lamp)
Distance from lamp to irradiated surface = 30 cm
Irradiated volume: 100 mL

Stock solution Atrazine = 200 µg/L
Watert ype: Dunea Bergambacht (delivered November 17th)

A solution was prepared containing Dunea water + 2 µg/L atrazin (2 L for tests on November 20th)

Table VII.1 Experimental conditions CB experiments with LP lamp.

Nr.	Atrazine (µg/L)	UV-Dose(mJ/cm²)
1	2	0
2	2	100
3	2	300
4	2	500
5	2	700

- A sample of 100 mL was irradiated.
- all experiments were carried out randomly.
- all glassware used was dishwasher clean.

MP lamp
Experimental conditions
CB parameters
Testing with MP lamp (2KWHOK)
Distance from lamp to irradiated surface = 80 cm
Irradiated volume: 100 mL

Stock solution Atrazine = 200 µg/L
Water type: Dunea Bergambacht (delivered November 17th)

A solution was prepared containing Dunea water + 2 µg/L atrazine (2 L for tests on November 20th)

Table VII.2 Experimental parameters CB tests MP lamp

Nr.	Atrazine (µg/L)	UV Dose (mJ/cm²)
1	2	100
2	2	300
3	2	500
4	2	700

- UV dose = 0 is similar to these tests carried out with the DBD lamp (if carried out at the same day).
- Of all solutions, 100 mL was irradiated.
- All experiments were carried out randomly.
- all glassware used was dishwasher clean.

November 23rd

DBD lamp
Experimental conditions
CB parameters
Testing with DBD-lamp
Ddistance from lamp to irradiated surface = 40 cm
Irradiated volume: 100 mL

Stock solution Atrazine = 200 µg/L
Water type: Dunea Bergambacht (delivered November 17th; 10 L)

A solution was prepared containing Dunea water + 2 µg/L atrazin (2 L for tests on November 20th)

Table VII.3 Experimental parameters CB tests DBD lamp

Nr.	Atrazin (µg/L)	UV-Dose (mJ/cm²)
1	2	0
2	2	100
3	2	300
4	2	500
5	2	700

- Of all solutions, 100 mL was irradiated.
- All experiments were carried out randomly.
- all glassware used was dishwasher clean.

Pilot plant testing
21 november

MP lamp
Experimental conditions

Water type: Dunea Bergambacht (delivered November20th; about 2,5 m³)
Stock solution atrazine 1200 µg/L

Table VII.4 Pilot testing with MP lamp

Nr.	Flow (m³/h)	Atrazine (µg/L)
1	0.2	2
2	1.0	2
3	4.0	2

Planning

The MP lamp had already been put into the system

- Connect tank with Dunea water and stirrer to UV-unit
- Remove air from tubes between tank and pump
- add atrazine (tank 700 L, so 1.167 L stock solution atrazine
- water removal via drainage (using valve). All valves not used for removal of air should be closed.
- Remove air by using drinking water
- Set flow to 4 m³/h
- Turn lamps on
- Drain off water to collection tank for pesticides (using valve)
- If possible check lamp (voltage and current), check sensor and temperature
- Replace drinking water by test water
- Fill system 5x with test solution (takes 3 min.)
- Sampling: first effluent, than influent
- Turn flow to 1 m³/h
- Check lamp (voltage and current) and sensor.
- Fill system twice with test solution (takes 6 min.)
- Sampling: first effluent, than influent
- Turn flow to 0.2 m³/h
- Check lamp (voltage and current) and sensor.
- Fill system twice with test solution (takes 26 min.)
- Sampling: first effluent, then influent

November 22nd

LP lamp
Experimental conditions

Water type: Dunea Bergambacht (delivered November20th; about 2,5 m³)
Stock solution atrazine 1200 µg/L

Table VII.5 Pilot testing with LP lamp

Nr.	flow (m³/h)	Atrazine (µg/L)
1	0.2	2
2	1.0	2
3	4.0	2

November 24th

DBD lamp
Experimental conditons

Water type: Dunea Bergambacht (delivered November20th; about 2,5 m³)
Stock solution atrazine 1200 µg/L

Table VII.6 pilot testing with LP lamp

Nr.	Flow (m³/h)	Atrazine (µg/L)
1	0.2	2
2	1.0	2
3	4.0	2

Experiments with UV pilot reactor at KWR

December 4th

DBD-lamp
Experimental conditions

Water type: Dunea Bergambacht (delivered December 1st; about 2,5 m³)
Stock solution phages 100 mL concentration 5x10^{11} in 1 m³ Dunea water
Stock solution BM see section 3.4.4.

Table VII.7 Process parameters for experiments in the KWR UV pilot reactor.

Nr.	Test	Phase	H_2O_2 (mg/L)	Flow (m³/h)	analyses
1	Desinfection	2e	10	1	6x MS2 phages (3x influent; 3x effluent) 2x H_2O_2 (influent with and without H_2O_2)
2	BM	2d	10	1	2x pesticides/pharmaceuticals/MTBE (1x influent; 1x effluent); 1x H_2O_2 (influent);2x NOM, AOC + nitrite (effluent + influent zonder H_2O_2)
3			10	2	1x pesticides/pharmaceuticals/MTBE (effluent); 1x H_2O_2 (influent) 1x AOC+nitrite (effluent)
4			0	2	2x pesticides/pharmaceuticals/MTBE (1x influent; 1x effluent) 1x H_2O_2 (influent)
5			0	1	1x pesticides/pharmaceuticals/MTBE (effluent) ; 1x NOM (effluent)

- Disinfection: Influent without H_2O_2
- Disinfection: 100 mg Na_2SO_3 (3x excess) was added to the samples in order to quench the peroxide reaction.
- BM: 1 g Na_2SO_3 (27x excess) per liter is added to samples containing H_2O_2 both influent as well as effluent) in order to quench the reaction with peroxide.
- All glassware was rinsed by means of a dishwasher. The sample bottles for MTBE were pretreated with methanol, purged and trapped.

N.B.
Sampling of the influent + H_2O_2 pesticides/pharmaceuticals/MTBE only took place during experiments with the DBD lamp, and not with other types of lamps. The solution was kept for 30 min., and then neutralized by means of sulfite (Na_2SO_3 1g per liter)

Experimental
The DBD lamp had been placed in the UV reactor

- Connect tank 1 with Dunea water and the mixer to the UV-unit
- Remove air from tubes between tank and pump
- Add phages (tank 650 liter so 65 mL of stock solution phages)
- water removal via drainage (using valve). All valves that are not being used for air removal have to be closed.
- Remove air from system using drinking water
- Set flow of 1 m^3/h
- dose H_2O_2 (2.5 g/L) with 4 l/h
- check dosage after having flushed the total system once.
- Turn on the lamps
- If possible check lamp (voltage + current) + check sensor + temperature
- Replace drink water by test water
- Fill system 5x with test solution (takes 13 min)
- Sampling: first effluent, subsequently influent (after peroxide dosing had been stopped)

End of disinfection experiment
- Sampling Dunea water (HCO$_3$/CO$_3$/pH/nitrate;DOC; UV-T)
- Connect tank2 with Dunea water and mixer to UV-unit
- Remove air from tubes between tank and pump.
- add BM (tank 700 liter so 1,4 l stock solution of BM)
- water removal via drainage (using valve). All valves that are not being used for air removal have to be closed
- remove air from system by using drinking water
- set flow to 1 m^3/h
- start dosage of H_2O_2 2.5 g/L at 4 l/h
- check dosage after after having flushed the total system once
- turn the lamps on
- Drain off water to collection tank for pesticides (using valve)
- If possible check lamp (voltage + current) + check sensor + temperature
- Change from drinking water to test water
- Fill system 4x with test solution (this takes 10 min.)
- Sampling: first effluent, subsequently influent
- Change flow to 2 m^3/h
- Start dosing H_2O_2 2.5 g/L at 8 l/h
- Check lamp (voltage + current) + check sensor.
- Fill system twice with test solution (this takes 3 minutes)
- Sampling: first effluent, subsequently influent
- Stop H_2O_2 dosage
- Check lamp (voltage + current)+ check sensor.
- Fill system 4x with test solution (this takes 5 minutes)
- Sampling: first effluent, subsequently influent
- Change flow to 1 m^3/h
- Check lamp (voltage + current)+ check sensor.
- Fill system 2x with test solution (this takes 5 minutes)
- Sampling: first effluent, subsequently influent
- Recirculate solution with pesticides (±30 minutes)

End of BM experiments

- Replace DBD lamps with MP lamps

N.B. Sampling of influent without H$_2$O$_2$ should probably take place in the tank or before the water enters the installation

December 5th

LP and MP lamps
Experimental conditions

Water type: Dunea Bergambacht (delivered december 1st; about 2,5 m^3)
Stock solution of phages 100 mL 5x10^{11} in 1m^3 Dunea water

Table VII.8 Process parameters for experiments in the KWR UV pilot reactor

Nr.	lamp	Test	Phase	H$_2$O$_2$ (mg/L)	flow (m^3/h)	analyses
1	MP	disinfection	2e	10	1	6x MS2 phages (3x influent; 3x effluent) 2x H$_2$O$_2$ (influent met en zonder H$_2$O$_2$
2	LP	disinfection	2e	10	1	6x MS2 fagen (3x influent; 3x effluent) 1x H$_2$O$_2$ (influent)

- Influent is solution without H$_2$O$_2$
- 100 mg Na$_2$SO$_3$ (3x excess) is added to the samples in order to quench the peroxide reaction.

December 6th
LP and MP lamps
Experimental conditions

Water type: Dunea Bergambacht (delivered december 1st; about 2,5 m^3)
Stock solution of BM see section 3.4.4.

Table VII.9 Process parameters for experiments in the KWR UV pilot reactor

Nr.	lamp	Test	Phase	H₂O₂ (mg/L)	Dose (mJ/cm²)	Flow (m³/h)	Analyses
1	LP	BM	2c	0	300	2.99	1x pesticides/pharmaceuticals/MTBE (1x effluent);
2				0	450	2.16	2x pesticides/pharmaceuticals/MTBE (1x influent; 1x effluent); 1x H₂O₂ (influent); 1x NOM (effluent)
3				10	450	2.16	1x pesticides/pharmaceuticals/MTBE (effluent); 1x H₂O₂ (influent);1x NOM, AOC and nitrite (effluent) extra nitrite influent
4				10	300	2.99	1x pesticides/pharmaceuticals/MTBE (effluent); 1x H₂O₂ (influent) 1x AOC+nitrite (effluent)
5	MP	BM	2b	0	300	2.12	1x pesticides/pharmaceuticals/MTBE (1x effluent);
6				0	450	1.37	2x pesticides/pharmaceuticals/MTBE (1x influent; 1x effluent); 1x H₂O₂ (influent); 1x NOM (effluent)
7				10	450	1.37	1x pesticides/pharmaceuticals/MTBE (effluent); 1x H₂O₂ (influent); 1x NOM, AOC and nitrite (effluent) extra nitrite influent
8				10	300	2.12	1x pesticides/pharmaceuticals/MTBE (effluent); 1x H₂O₂ (influent) 1x AOC+nitrite (effluent)

- BM: 1 g Na_2SO_3 per L (27x excess) is added to samples containing H_2O_2 (both influent as well as effluent samples) in order to quench the reaction with peroxide.
- All glassware was rinsed by means of a dishwasher. The sample bottles for MTBE were pretreated with methanol, purged and trapped.

VIII Validation of UV-pilot reactor (WP1)

Experimental set up of validation

The pilot UV reactor was validated before experiments were carried out. The required flow to obtain a certain UV dose was determined. Validation was carried out for every lamp and type of water, because the UV dose depends on the water composition (e.g. UV-T, TOC, nitrate concentration), and the type of lamp used. Atrazine was used as a chemidosimeter in the test water (Dunea, Bergambacht).

First experiments were carried out in the collimated beam set-up. Atrazine was added to Dunea water, and a UV scan of the water was made to check whether the water quality was equal in all cases. Subsequently, the dose response curve was measured for atrazine, using 100 mL of water. The conversion of atrazine was calculated according to equation 1:

$$\text{Conversion} = \frac{C_0 - C_t}{C_0} * 100\% \qquad (1)$$

with:
conversion = (%)
C_0 = starting concentration atrazine
C_t = concentration of atrazine after UV treatment

This formula can be applied to every compound. The dose response curve is determined according to equation 2:

Conversion of atrazine (%) = a* dose (mJ/cm^2) + b   (2)

Subsequently, experiments were carried out using the UV pilot reactor, and Dunea water containing atrazine. The pretreated Dunea water was transported in stainless steel tanks (700 L) from Bergambacht to Nieuwegein. For every test, a new atrazine solution was made. During the experiments the solution was stirred to obtain a homogeneous mixture. Before the start of the experiment, a sample was taken from the tank for atrazine analysis and to make a UV scan. Post-UV samples for atrazine analysis were taken from the effluent sampling point placed after the static mixer. The UV samples were taken after a residence time of at least three times the reactor volume.

During the experiments the equation for the conversion of atrazine as a function of water flow was established:

Atrazine conversion (%) = c* flow (m^3/hour) +d   (3)

Based on equations 2 and 3 the flow required for a certain UV dose can be calculated. For practical reasons the conversion was calculated instead of "log conversion". The equations are more or less linear (see Figure VIII.1).

The atrazine conversion at the required dose is calculated according to equaton 2. This conversion is used in equation 3 to calculate the flow required to obtain this dose (or atrazine conversion).

The set- up and implementation of the validation have been described in detail in paragraph 3.4. The process parameters during the validation experiments are shown In table VIII.1.

Table VIII.1 Proces conditons during validaton of the UV pilot reactor; Dunea water

		Collimated Beam	UV-pilot reactor
Lamp	Atrazine	UV-Dose	Flow
	µg/L	mJ/cm²	m³/h
MP	2	0-100-300-500-700	0 - 0.2 – 1 - 4
LP	2	0-100-300-500-700	0 - 0.2 – 1 - 4
DBD	2	0-100-300-500-700	0 - 0.2 – 1 - 4

Results of validation

The validation was carried out in November 2006, before the installation was used for experiments with pretreated water from Dunea. The UV scans made are shown in Appendix XV, Figure XV.1. From these results it can be concluded that the water quality during all tests was equal, and thus that the results of the various experiments can be compared. The results obtained with the collimated beam set up are shown in table VIII.2. In Figure VIII.2 the dose response curve of atrazine with various lamps is shown.

Table VIII.2 results of collimated beam experiments with atrazine

	MP-lamp		LP-lamp		DBD-lamp	
Dose	Atrazine	Conversion	Atrazine	Conversion	Atrazine	Conversion
mJ/cm²	µg/L	%	µg/L	%	µg/L	%
0	1.8	0	1.8	0	1.6	0
100	1.2	33.3	1.5	16.7	1.4	12.5
300	0.89	50.6	1.3	27.8	1.2	25.0
500	0.65	63.9	1.2	33.3	0.96	40.0
700	0.48	73.3	0.96	46.7	0.74	53.8
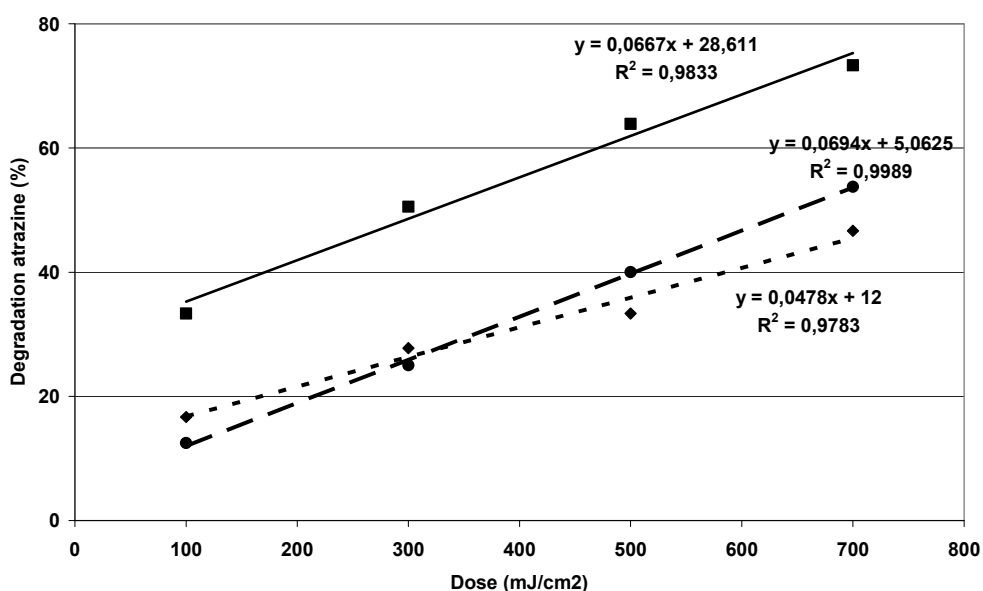
Figure VIII.1 Dose response curves for atrazine; (■) MP-lamp; (♦) LP-lamp; (●) DBD-lamp

Besides the measurement of dose reponse curves for atrazine, also the conversion of atrazine (without H_2O_2) was determined in the pilot reactor, using various flows. The results of these experiments are

shown in Table VIII.3. In figure VIII.2 the conversion of atrazine as a function of the water flow through the UV reactor is shown for all three types of lamps.

Table VIII.3 Results of validation of KWR UV pilot reactor

flow	MP-lamp		LP-lamp		DBD-lamp	
	Atrazine	Conversion	Atrazine	Conversion	Atrazine	Conversion
m³/h	μg/L	%	μg/L	%	μg/L	%
0	1.7	0	1.7	0	1.7	0
0.2	0.26	84.7	0.55	67.6	0.56	67.1
1.0	0.62	63.5	0.96	43.5	1.1	35.3
4.0	1.3	23.5	1.4	17.6	1.6	5.9
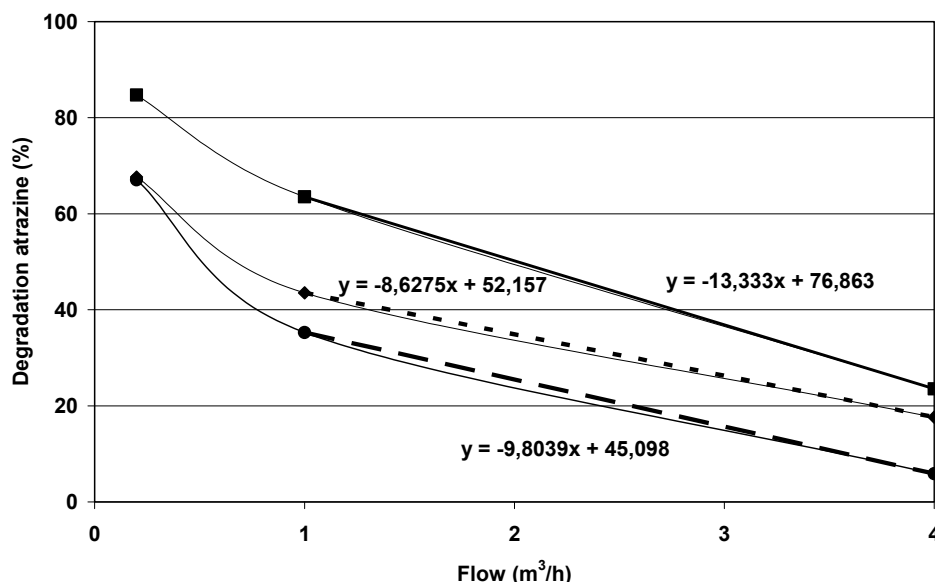
Figure VIII.2 Conversion of atrazine (%) versus water flow (m³/h) during pilot reactor experiments; (■) MP-lamp; (♦) LP-lamp; (●) DBD-lamp

At flows lower than 1 m³/h, larger deviations were found. This can be explained from the fact that at a flow below 1 m³/h the flow profile is laminar, whereas above 1 m³/h, turbulent flow through the reactor was obtained. This can be concluded from calculations of the Reynolds number. To obtain reliable results with the pilot set-up, it will be necessary to apply a turbulent flow profile. Therefore, it was decided to only use the results obtained at flows of 1 and 4 m³/h.

The flows required to obtain the desired UV dose were calculated. The results are shown in table VIII.4.

Table VIII.4 Flows required for experiments with conversion of organic micropollutants and disinfection capacity in the UV pilot reactor

Lamp	UV-dose required	Flow
	mJ/cm^2	m^3/h
MP	300	2.12
	450	1.37
LP	300	2.99
	450	2.16
DBD	300	1.96
	450	0.90

IX Results of NOM characterization (WP1)

Natural organic matter (NOM) is always present in water. The presence of NOM affects drinking water quality (odor, taste and color). Furthermore, as a result of the biodegradability of NOM, regrowth in the distribution network can occur. NOM partly consists of humic acids and fulvic acids, and can be characterized by means of LC-OCD. This technique also can be used to analyze inorganic colloids.

In order to check whether NOM can be converted by UV/H_2O_2 samples were taken and analyzed before and after UV at a dose of 450 mJ/cm^2, with and without addition of 10 mg/L H_2O_2, using various types of lamps. The results of LC-OCD analyses are shown in Table IX -1.

Table IX -1 Results of LC-OCD analyses[*)] at a UV dose of 450 mJ/cm^2

Lamp	H_2O_2	DOC	SUVA	PS-DOC	HA-DOC	BB-DOC	LMA-DOC	Inorganic colloids
	mg/L	mg/L	l/mg-m	mg/L	mg/L	mg/L	µg/L	m^{-1}
Influent		3.67	2.78	0.21	2.07	0.67	bld	0.23
MDMP	0	3.89	2.52	0.17	1.99	0.67	bld	0.03
	10	3.72	2.26	0.19	1.95	0.69	45	0.20
LDLP	0	3.51	2.86	0.16	1.98	0.65	bld	0.02
	10	3.68	2.45	0.16	1.97	0.62	8	0.03
DBD	0	3.45	2.12	0.16	1.88	0.64	19	0.05
	10	3.61	2.59	0.17	1.92	0.70	bld	0.01

* Explanation of abbreviations; *bdl=below detection limit; DOC=dissolved organic carbon; SUVA=UV/DOC; PS=biopolymers; HA=humic acids; BB=buildinig blocks of humic acids; LMA=low molecular acids.*

Based on the analytical results, the conversion of various compounds was determined for photolytic processes, and UV/H_2O_2 processes, using different types of lamps. The results are shown Figure IX -1 and Figure IX -2.
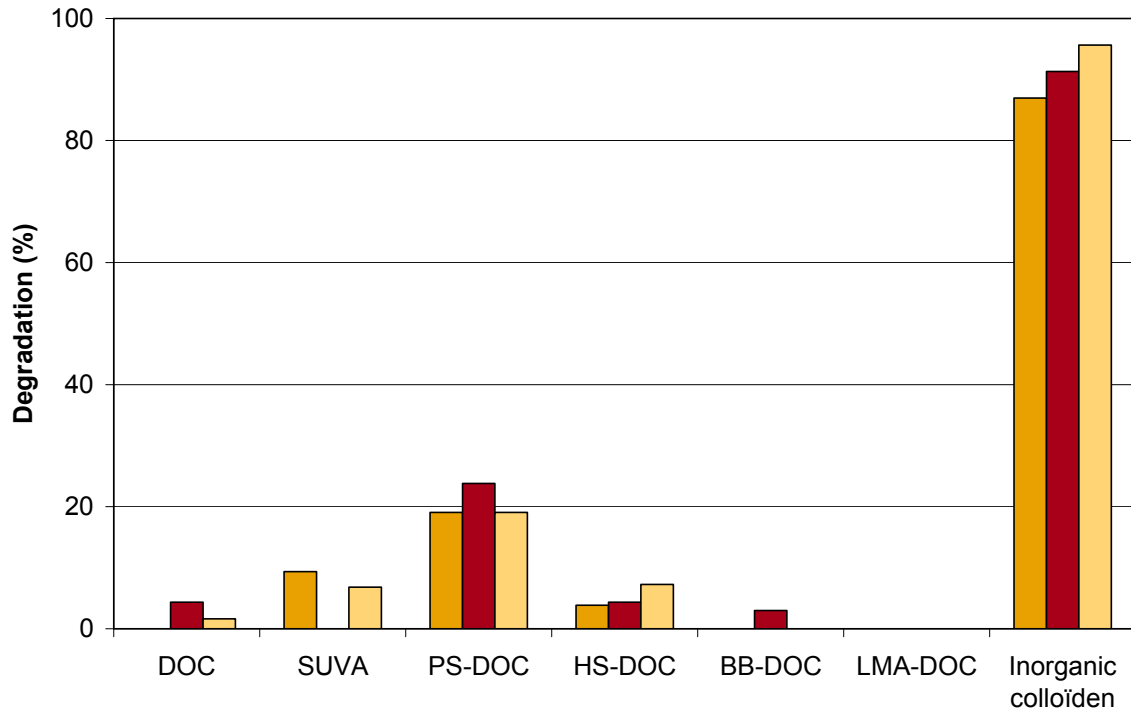
Figure IX -1 Conversion of NOM and inorganic colloids during UV pilot testing; pretreated water of Dunea, without H_2O_2 at a UV dose of 450 mJ/cm²; (■) MP; (■)LP; (■) DBD
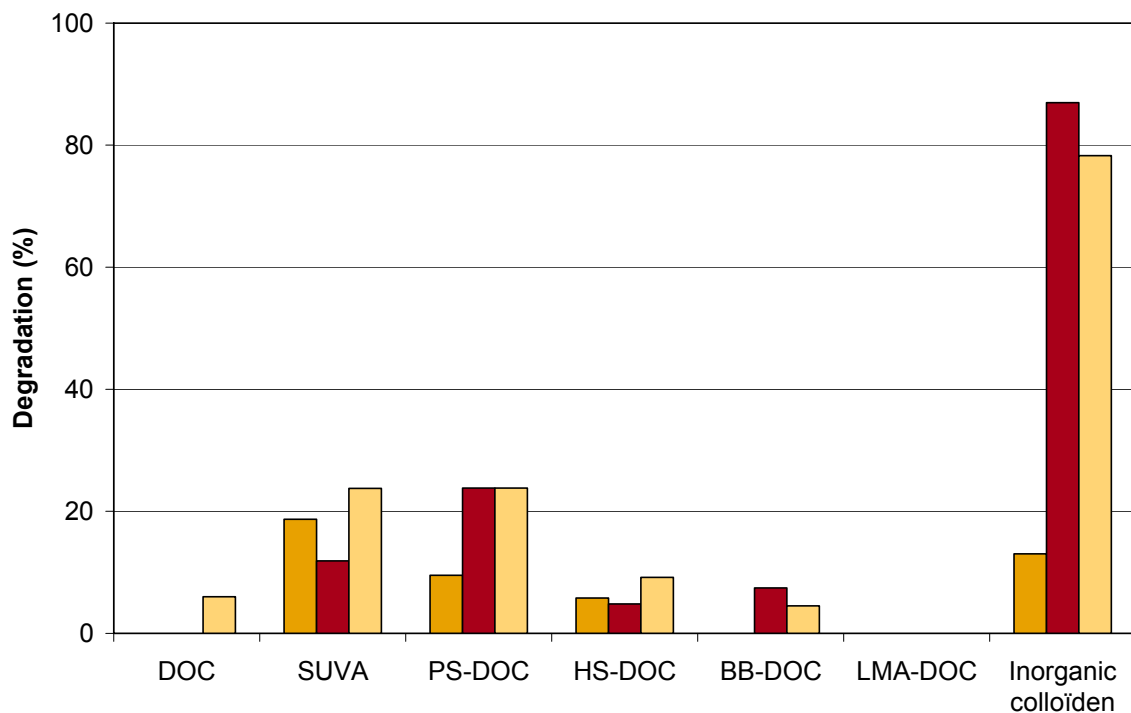
Figure IX -2 Conversion of NOM and inorganic colloids during UV pilot testing; pretreated water of Dunea, 10 mg H_2O_2/L at a UV dose of 450 mJ/cm²; (■) MP; (■)LP; (■) DBD

NOM hardly seems to be converted by means of UV photolysis. Of all types of NOM, the biopolymers (PS-DOC) seem to be the most sensitive towards photolysis. Independent of the type of lamp used, their conversion is about 20%.

Application of UV/H$_2$O$_2$ hardly results in a better conversion. Only for SUVA a 10-15% higher conversion is observed if H$_2$O$_2$ is added. This can be explained from a reaction of the hydroxyl radicals with the double bonds in the molecules.
Inorganic colloids, like iron oxides and silica, seem to be sensitive to photolysis. Addition of H$_2$O$_2$ in combination with MP lamps has a negative effect on the conversion (which decreases up to 75%). For DBD and LP lamps this decrease seems to be negligible.

In general it can be concluded, that the highest conversion is obtained for DBD lamps, followed by LP lamps and finally MP lamps.

Conclusions:
-   NOM is hardly converted by means of UV photolysis.

-   Among all types of NOM, bio polymers (PS-DOC) seem to be the most sensitve towards UV.

-   Conversion of biopolymers is about 20%, independent of the type of lamp.

-   Application of UV/H$_2$O$_2$ hardly results in a higher conversion of NOM, when compared with photolysis. Only in case of SUVA an improvement of 10-15% can be observed.

-   The highest conversion of NOM in a UV/H$_2$O$_2$ process is observed for:
    DBD > LP > MP

-   UV, with or without hydrogen peroxide, can be applied to convert inorganic colloids.

-   Application of UV/H$_2$O$_2$ with MP lamps results in a lower conversion of inorganic colloids.

X NOM-characterization by means of LC-OCD (WP1)

LC-OCD (Liquid Chromatography – Organic Carbon Detection) is a rather new analytical technique that can be applied to analyze Natural Organic Material.

Natural Organic Matter (NOM) is first fractionated by means of liquid chromatography (LC of SEC). Subsequently, the NOM concentrations of the different fractions are measured using an organic carbon detector (OCD). A UV sensor (254 nm) is integrated into the system in order to obtain information on the aromaticity of the fractions.
The sensitivity of the measurements is 2 – 10 ppb for the TOC determination, and 5 – 50 ppb for the different fractions. As a result of this high sensitivity, water with a very low NOM concentration can be analyzed, without pre concentration of the samples.

Analyses were carried out by DOC-Labor in Karlsruhe.
Samples are taken in specially prepared 50 mL bottles. After pasteurizing them for 40 minutes at a temperature between 60 and 80°C, these were sent to Germany in a thermostated box.

Characterization
First the TOC (total organic carbon) is measured. Then, the solution is filtered through a 0.45-μm filter, separating the DOC (dissolved organic carbon) and POC (Particulate organic carbon). The amount of POC is calculated as the difference between TOC and DOC.

The dissolved part of the DOC can be both hydrophilic (Chromatographic DOC; CDOC) as well as hydrophobic (Hydrophobic Organic Carbon; HOC). The CDOC fraction can move through the chromatograph column, whereas the HOC is adsorbed in this column. The amount of HOC is calculated from the difference between DOC and CDOC.

The hydrophilic CDOC is subsequently divided into five parts according to molecular weight. This is shown in table IX.1 according to increasing molecular mass. Figure IX.1 shows how the DOC-Labor carries out the characterization. Table IX.2 gives a description of the various parts, and table IX.3 shows the accuracy of the LC-OCD measurements.

Table X.1 determination of MM over the various parts

Fraction	Abbreviation	MM
Free organic acids	OZ	< 350
Neutral and amphiphilic compounds	N/A	< 350
Building blocks	BB	350 – 500
Humic materials	Humics	500 - 1200
Polysaccharides	PS	> 10,000
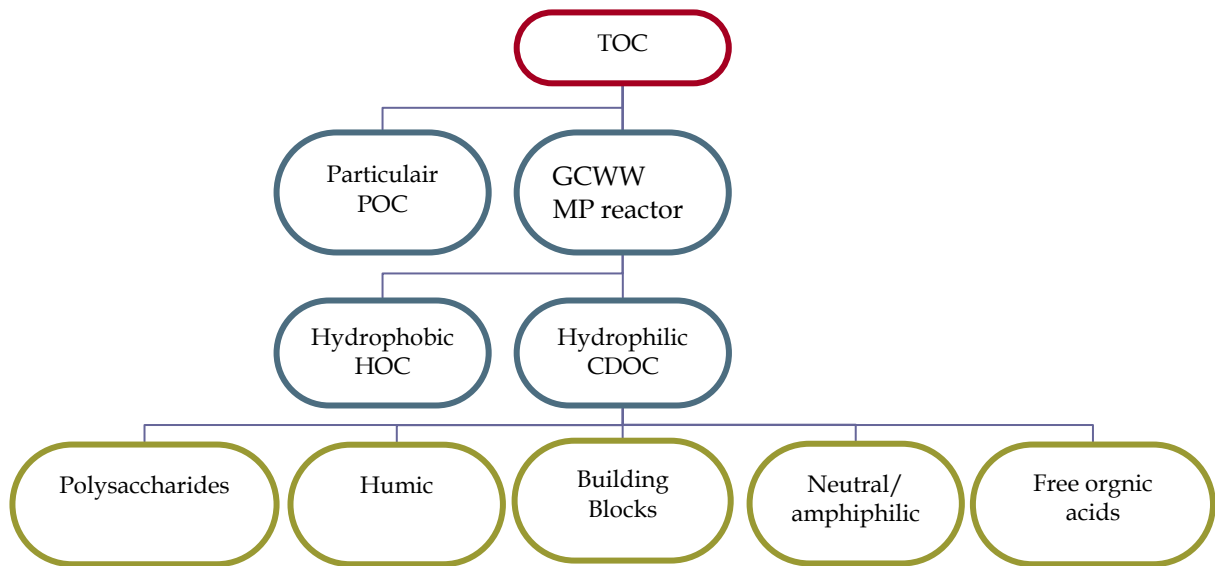
Figure X.1 Characterization scheme according to DOC Labor

Table X.2 fraction determined by means of LC-OCD

Abbreviation	Name	Explanation
TOC	Total organic carbon	The Total amount of organic carbon in the original sample, before entering the chromatographic column.
DOC	dissolved OC	Dissolved fraction of organic carbon, passing a 0.45-µm filter.
POC	particulate OC	The fraction retained on the 0.45-µm filter before entering the chromatographic column. This fraction is the difference between TOC and DOC
CDOC	chromatographic dissolved OC	The fraction passing the chromatographic column, mostly hydrophilic.
HOC	hydrophobic OC	The fraction remaining in the column. This strongly hydrophobic fraction is determined as the difference between DOC and CDOC. This fraction includes mainly lipides.
PS	polysaccharides	This fraction contains amino sugars, polypeptides and peptides with a high molecular weight
Humic	Humic acids	Humic compounds, mainly polycarboxylic acids and substituted phenols.
BB	building blocks	Oxidation products of humic acid, mainly polycarboxylic acids.
N/A	neutral and amphiphilic compounds	Small organic compounds like alcohols, aldehydes, ketones and amino acids.
OZ	Free organic acids	Low molecular weight acids

Table X.3 Accuracy of LC-OCD

Chromatographic fractions	Detection limit (ppb)	Confidence interval (%)
TOC	1	5
HOC	50	11
Humic	20	2
BB	10	6
PS	2	5
N/A	5	5
OZ	5	10

Reports

A. <u>Chromatogram and table</u>

The result is a chromatogram, which is edited by means of FIFFIKUS-software to obtain a table with results in ppb and the percentage of TOC.

B. <u>HS-diagram</u>

The humic substances can be divided into humic acids, fulvic acids and humin, based on a difference in solubility. This difference cannot be used for dissolved humic substances. Therefore, DOC-Labor used a HS diagram. In this diagram, the average molecular mass and the SAC (Spectral Absorption coefficient at 254 nm divided by the humic concentration) of the fraction of humic substances are shown graphically. The SUVA value obtained is specific for a certain fraction of humic substances. Humic acid can be found in the upper right of the diagram, and show the more aromatic compounds. The fulvic acids, coming from microbiological acitivity and thus having a lower aromaticity and molecular mass, are found in the lower left corner of the diagram. As NOM of groundwater is characterized by a higher aromaticiy and molecular mass, ground water will be found in the upper right corner of the diagram, whereas surface water is expected to be found in the lower left corner. The HS diagram (Figure IX.2) shows the degree of humification.
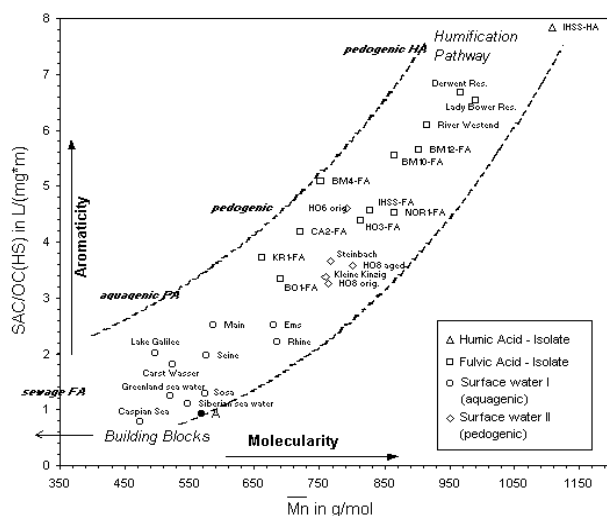
Figure X.2 HS-diagram

XI Water quality data of collimated beam experiments (WP1)

Table XI.1 water quality of rapid sand filtered water from Dunea (Bergambacht) during the collimated beam experiments at KWR

Date	Nitrate mg N/L	Nitrate mg NO$_3$/L	pH	HCO$_3^-$ mg HCO$_3$/L	NPOC mg C/L	UV-254nm %
05-30-2006[1]	2.7	12.1	7.87	165	3.5	79
07-04-2006[2]	1.5	6.6	8.07	136	3.5	79
07-07-2006[2]			8.20	135		79
07-11-2006[2]			8.16	136		81
07-13-2006[3]	2.0	8.9	8.01	135	3.7	79
07-20-2006[4]	1.5	6.6	7.92	133	2.5	80
07-25-2006[4]			8.12	133		80
07-26-2006[4]			8.2	136		80

1   nitrate analyses at 07-10-2006
2   Dunea water at 07-03-2006
3   Duneawater at 07-12-2007
4   Dunea water at 07-19-2008

Table XI.2 Water quality of GCWW water during collimated beam experiments

Date	Nitrate mg N/L	Nitrate mg NO$_3$/L	pH	HCO$_3^-$ mg HCO$_3$/L	NPOC mg C/L	UV-254nm %
07-04-2006[1]	1.1	4.9	7.94	87	2.4	86
07-06-2006[1]			8.06	89		86
07-07-2006[1]	1.2	5.3	7.98	89	2.2	87
07-18-2006[2]	0.9	4.0	7.90	71	1.5	87
07-20-2006[2]			7.80	70		87
07-25-2006[2]			7.90	71		87
07-26-2006[2]	0.9	4.0	8.04	73	2	87

1   GCWW water at 06-29-2006 (GAC influent)
2   GCWW water at 07-10-2006 (GAC influent)
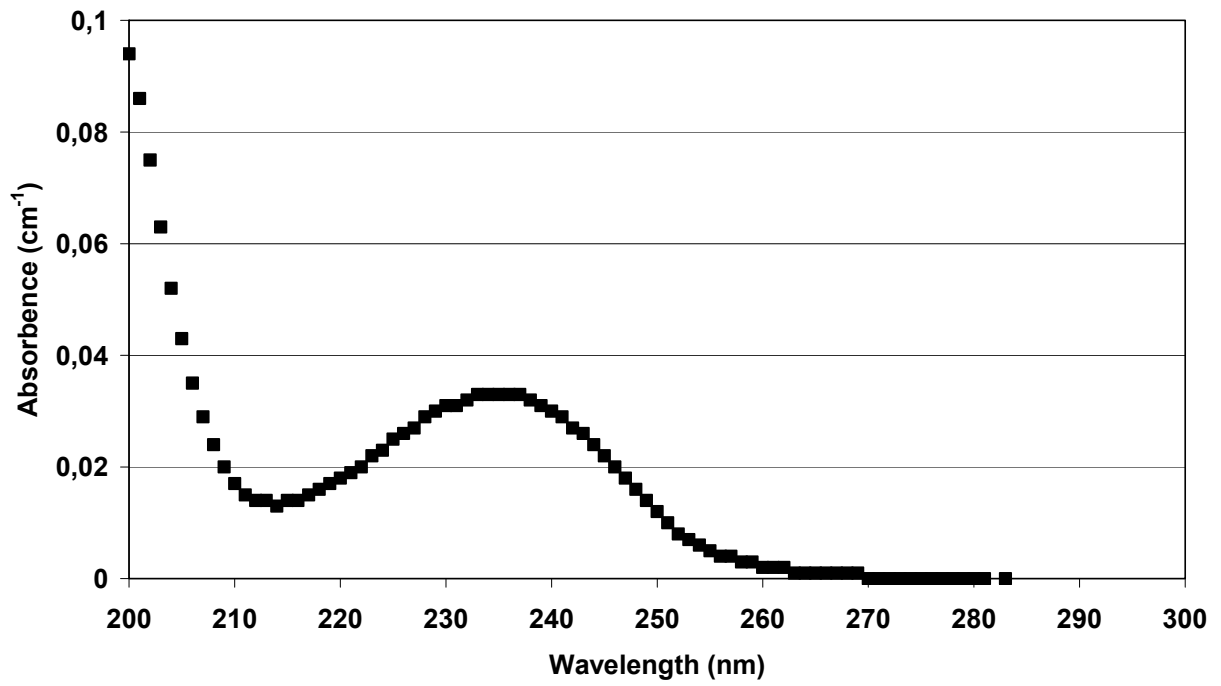
Figure XI.1 Absorption scans of pCBA in collimated beam experiments with MP lamps
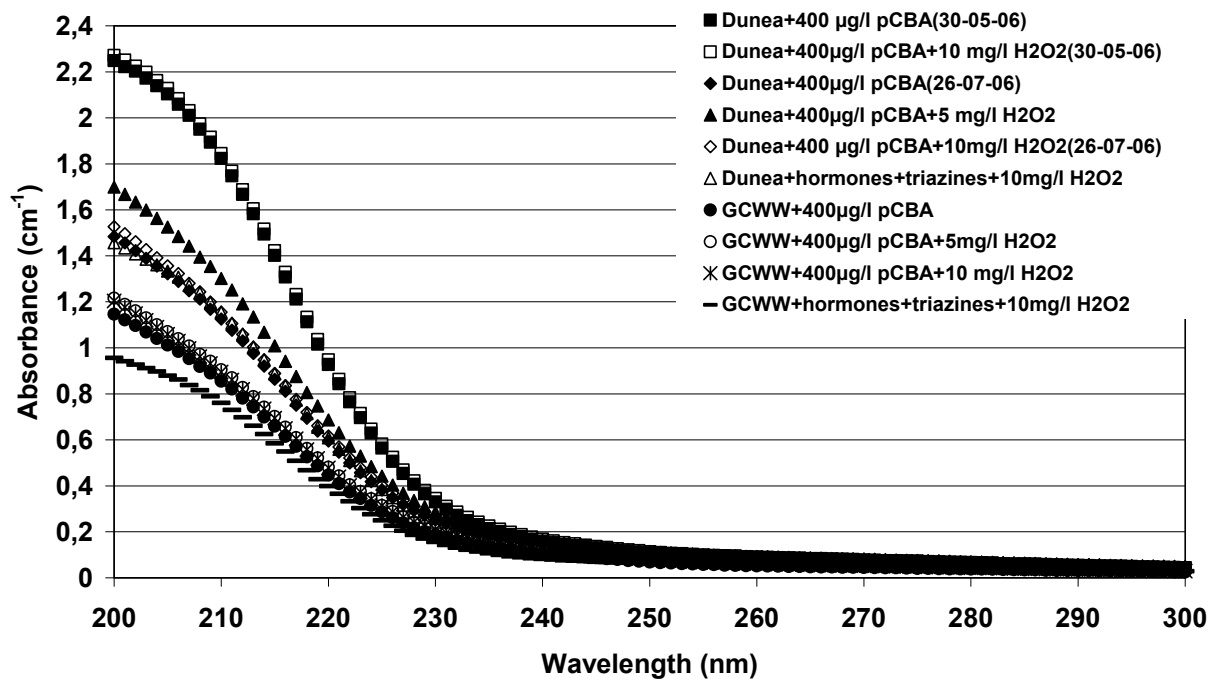
Figure XI.2 Absorption scan of irradiated water in collimated beam experiments with MP lamps
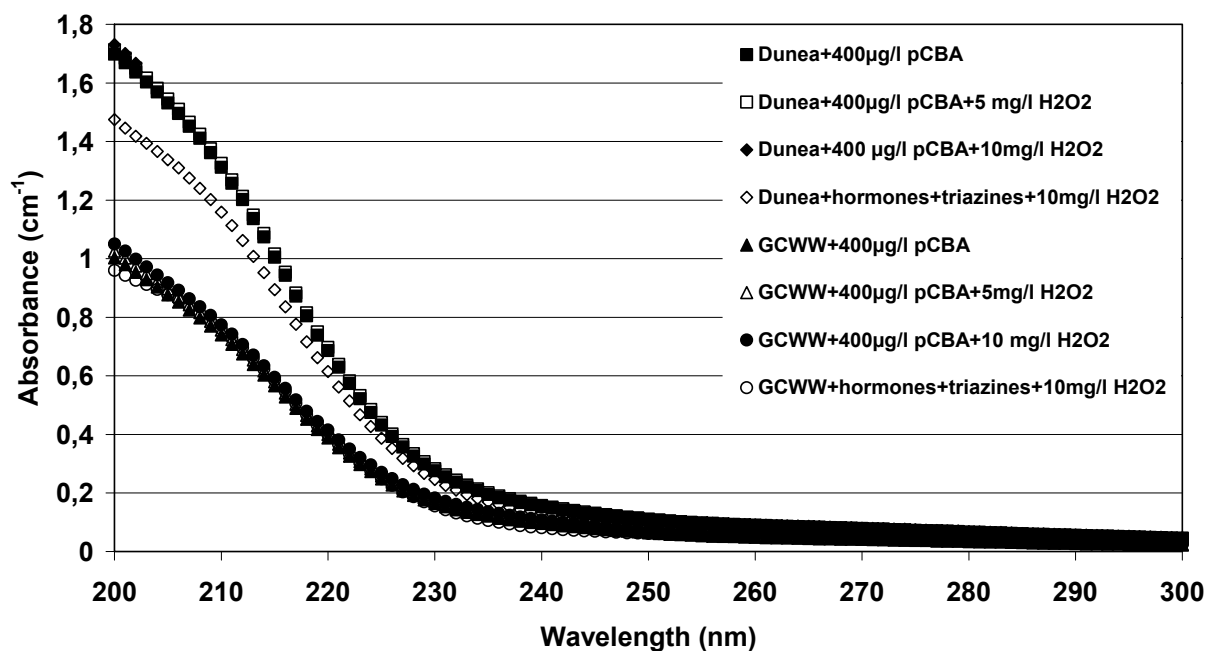
Figure XI.3 Absorption scans of irradiated water in collimated beam experiments with DBD lamps
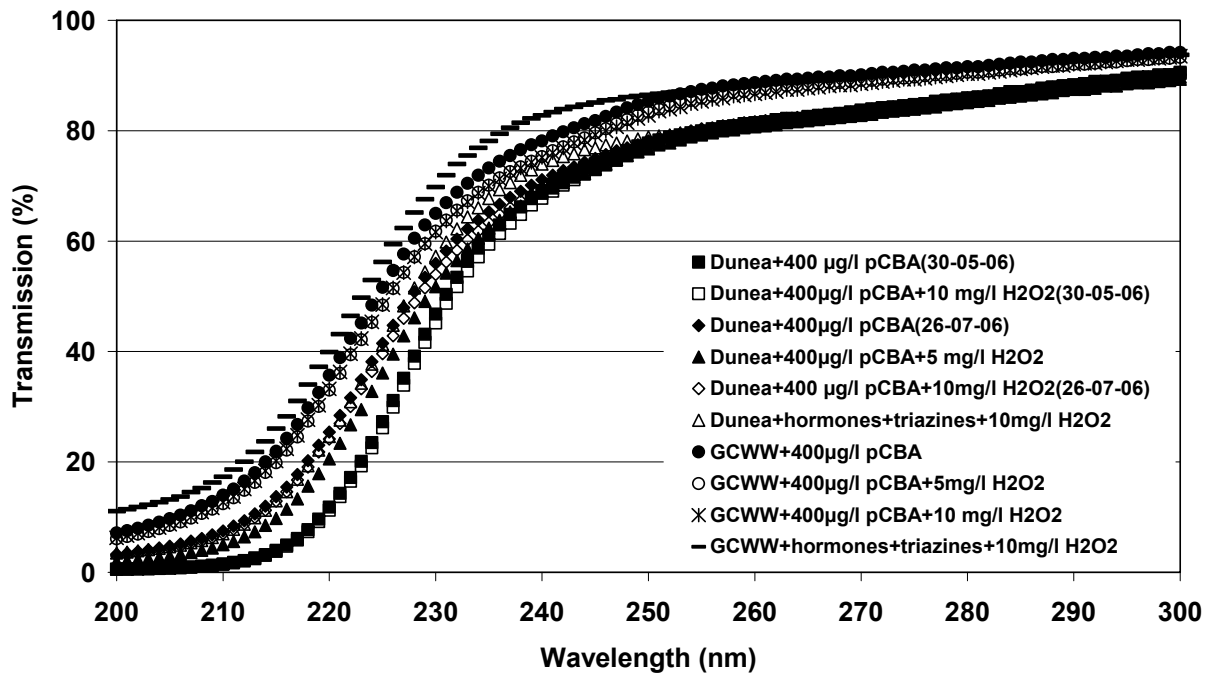
Figure XI.4 Transmission scans of irradiated water in collimated beam experiments with MP lamps
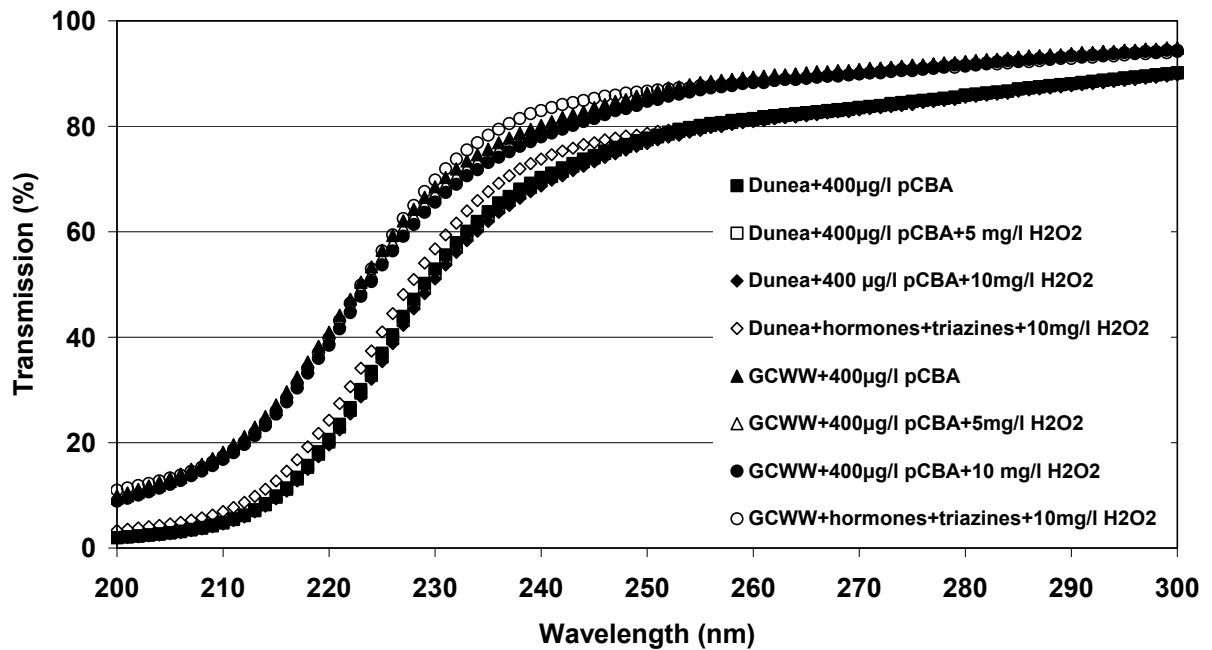
Figure XI.5 Transmission scans of irradiated water in collimated beam experiments with DBD lamps

XII Calculation of conversion of pCBA and contribution of photolysis to the conversion (WP1)

Table XII.1 Calculations for the conversion of pCBA in the MP-UV/H_2O_2 process with Dunea water

without H_2O_2

Dose	pCBA	pCBA without H_2O_2	Degradation	Degradation without H_2O_2	log pCBA/pCBA$_0$	log pCBA/pCBA$_0$ without H_2O_2
(mJ/cm^2)	(µg/L)	(µg/L)	(%)	(%)		
0	404		0.0		0	
450	242		40.1		-0.223	
600	210		48.0		-0.284	

5 mg/L H_2O_2

Dose	pCBA	pCBA without H_2O_2	Degradation	Degradation without H_2O_2	log pCBA/pCBA$_0$	log pCBA/pCBA$_0$ without H_2O_2
(mJ/cm^2)	(µg/L)	(µg/L)	(%)	(%)		
0	393	393	0.0		0	0
300	265		32.6		-0.171	
450	225	387	42.7	1.5	-0.242	-0.020
600	184	378	53.2	3.8	-0.330	-0.045
750	173		56.0		-0.356	

10 mg/L H_2O_2

Dose	pCBA	pCBA without H_2O_2	Degradation	Degradation without H_2O_2	log pCBA/pCBA$_0$	log pCBA/pCBA$_0$ without H_2O_2
(mJ/cm^2)	(µg/L)	(µg/L)	(%)	(%)		
0	398	398	0.0	0.0	0.000	0
300	179		55.0		-0.347	
450	127	289	68.1	27.4	-0.496	-0.274
600	96	290	75.9	27.1	-0.618	-0.333
750	73		81.7		-0.737	

Table XII.2 Calculations for the conversion of pCBA in the MP-UV/H$_2$O$_2$ process with GCVW water

without H$_2$O$_2$

Dose	pCBA	pCBA without H$_2$O$_2$	Degradation	Degradation without H$_2$O$_2$	log pCBA/pCBA$_0$	log pCBA/pCBA$_0$ without H$_2$O$_2$
(mJ/cm^2)	(µg/L)	(µg/L)	(%)	(%)		
0	395		0		0	
450	223		43.5		-0.248	
600	271		31.4		-0.164	

5 mg/L H$_2$O$_2$

Dose	pCBA	pCBA without H$_2$O$_2$	Degradation	Degradation without H$_2$O$_2$	log pCBA/pCBA$_0$	log pCBA/pCBA$_0$ without H$_2$O$_2$	log pCBA/pCBA$_0$	pCBA zonder H$_2$O$_2$	log pCBA/pCBA$_0$ zonder H$_2$O$_2$
(mJ/cm^2)	(µg/L)	(µg/L)	(%)	(%)				(µg/l)	
0	312	312	0	0	0			312	0
300	284		9.0			284	-0.041		
450	187	359	40.1	-15.1	-0.222			359	0.026
600	124	76	60.3	75.6	-0.401			248	-0.237
750	119		61.9		-0.419				

10 mg/L H$_2$O$_2$

Dose	pCBA	pCBA without H$_2$O$_2$	Degradation	Degradation without H$_2$O$_2$	log pCBA/pCBA$_0$	log pCBA/pCBA$_0$ without H$_2$O$_2$	log pCBA/pCBA$_0$	pCBA without H$_2$O$_2$	log pCBA/pCBA$_0$ without H$_2$O$_2$
(mJ/cm^2)	(µg/L)	(µg/L)	(%)	(%)				(µg/l)	
0	396	396	0	0	0			396	0
300	160		59.6		-0.394				
450	130	302	67.2	23.7	-0.484			302	-0.235
600	145	269	63.4	32.1	-0.436	145	-0.436	269	-0.273
750	53		86.6		-0.873				

Table XII.3 Calculations for the conversion of pCBA in the LP-UV/H$_2$O$_2$ process with Dunea water

without H$_2$O$_2$

Dose	pCBA	pCBA without H$_2$O$_2$	Degradation	Degradation without H$_2$O$_2$	log pCBA/pCBA$_0$	log pCBA/pCBA$_0$ without H$_2$O$_2$
(mJ/cm^2)	(µg/L)	(µg/L)	(%)	(%)		
0	402		0		0	
450	371		7.7		-0.035	
600	366		9.0		-0.041	

5 mg/L H$_2$O$_2$

Dose	pCBA	pCBA without H$_2$O$_2$	Degradation	Degradation without H$_2$O$_2$	log pCBA/pCBA$_0$	log pCBA/pCBA$_0$ without H$_2$O$_2$
(mJ/cm^2)	(µg/L)	(µg/L)	(%)	(%)		
0	406	406	0	0	0	0
300	290		28.6		-0.146	
450	241	272	40.6	33.0	-0.227	-0.192
600	203	239	50.0	41.1	-0.301	-0.260
750	173		57.4		-0.370	

10 mg/L H$_2$O$_2$

Dose	pCBA	pCBA without H$_2$O$_2$	Degradation	Degradation without H$_2$O$_2$	log pCBA/pCBA$_0$	log pCBA/pCBA$_0$ without H$_2$O$_2$
(mJ/cm^2)	(µg/L)	(µg/L)	(%)	(%)		
0	403	403	0	0	0	0
300	219		45.7		-0.265	
450	159	190	60.5	52.9	-0.404	-0.369
600	120	156	70.2	61.3	-0.526	-0.485
750	91		77.4		-0.646	

Table XII.4 Calculations for the conversion of pCBA in the LP-UV/H₂O₂ process with GCWW water

without H₂O₂

Dose	pCBA	pCBA without H₂O₂	Degradation	Degradation without H₂O₂	log pCBA/pCBA₀	log pCBA/pCBA₀ without H₂O₂
(mJ/cm²)	(µg/L)	(µg/L)	(%)	(%)		
0	405		0		0	
450	371		8.4		-0.038	
600	364		10.1		-0.046	

5 mg/L H₂O₂

Dose	pCBA	pCBA without H₂O₂	Degradation	Degradation without H₂O₂	log pCBA/pCBA₀	log pCBA/pCBA₀ without H₂O₂
(mJ/cm²)	(µg/L)	(µg/L)	(%)	(%)		
0	408	408	0	0	0	0
300	258		36.8		-0.199	
450	209	243	48.8	40.4	-0.291	-0.252
600	176	217	56.9	46.8	-0.365	-0.319
750	140		65.7		-0.465	

10 mg/L H₂O₂

Dose	pCBA	pCBA without H₂O₂	Degradation	Degradation without H₂O₂	log pCBA/pCBA₀	log pCBA/pCBA₀ without H₂O₂
(mJ/cm²)	(µg/L)	(µg/L)	(%)	(%)		
0	405	405	0	0	0	0
300	184		54.6		-0.343	
450	127	161	68.6	60.2	-0.504	-0.466
600	88	129	78.3	68.1	-0.663	-0.617
750	60		85.2		-0.829	

Table XII.5 Calculations for the conversion of pCBA in the DBD-UV/H₂O₂ process with Dunea water

without H₂O₂

Dose	pCBA	pCBA without H₂O₂	Degradation	Degradation without H₂O₂	log pCBA/pCBA₀	log pCBA/pCBA₀ without H₂O₂
(mJ/cm²)	(µg/L)	(µg/L)	(%)	(%)		
0	405		0		0	
450	311		23.2		-0.115	
600	293		27.7		-0.141	

5 mg/L H₂O₂

Dose	pCBA	pCBA without H₂O₂	Degradation	Degradation without H₂O₂	log pCBA/pCBA₀	log pCBA/pCBA₀ without H₂O₂
(mJ/cm²)	(µg/L)	(µg/L)	(%)	(%)		
0	400	400	0	0	0	0
300	204		49.0		-0.292	
450	147	241	63.3	39.8	-0.435	-0.320
600	106	218	73.5	45.5	-0.577	-0.436
750	78		80.5		-0.710	

10 mg/L H₂O₂

Dose	pCBA	pCBA without H₂O₂	Degradation	Degradation without H₂O₂	log pCBA/pCBA₀	log pCBA/pCBA₀ without H₂O₂
(mJ/cm²)	(µg/L)	(µg/L)	(%)	(%)		
0	404	400	0	0	0	0
300	125		69.1		-0.509	
450	70	182	82.7	54.5	-0.761	-0.647
600	39	151	90.3	62.3	-1.015	-0.901
750	23		94.3		-1.245	

Table XII.6 Calculations for the conversion of pCBA in the DBD-UV/H₂O₂ process with GCWW water

without H₂O₂

Dose (mJ/cm²)	pCBA (µg/L)	pCBA without H₂O₂ (µg/L)	Degradation (%)	Degradation without H₂O₂ (%)	log pCBA/pCBA₀	log pCBA/pCBA₀ without H₂O₂
0	405		0		0	
450	318		21.5		-0.105	
600	297		26.7		-0.135	

5 mg/L H₂O₂

Dose (mJ/cm²)	pCBA (µg/L)	pCBA without H₂O₂ (µg/L)	Degradation (%)	Degradation without H₂O₂ (%)	log pCBA/pCBA₀	log pCBA/pCBA₀ without H₂O₂
0	401	401	0	0	0	0
300	176		56.1		-0.358	
450	120	207	70.1	48.4	-0.524	-0.419
600	82	190	79.6	52.6	-0.689	-0.584
750	24		94.0		-1.223	

10 mg/L H₂O₂

Dose (mJ/cm²)	pCBA (µg/L)	pCBA without H₂O₂ (µg/L)	Degradation (%)	Degradation without H₂O₂ (%)	log pCBA/pCBA₀	log pCBA/pCBA₀ without H₂O₂
0	399	399	0	0	0	0
300	93		76.7		-0.632	
450	47	134	88.2	66.4	-0.929	-0.824
600	23	131	94.2	67.2	-1.239	-1.105
750	13		96.7		-1.487	

XIII Results and calculations for the conversion of hormones and pesticides in collimated beam experiments (WP1)

Table XIII.1 Results obtained with hormones in a MP-UV/H$_2$O$_2$ process

Date	Description	Dose	Hormones					H$_2$O$_2$	T$_{254nm}$
			17-alpha estradiol	17-alpha ethynylestradiol	17-beta estradiol	estriol	estrone		
		mJ/cm^2	ng/L	ng/L	ng/L	ng/L	ng/L	mg/L	%
26-7-2006 GCWW		0	76*	63*	65*	18	21	9.8	87.29
		300	2	< 2 (0.7)	< 2	< 2	< 1	9.6	
		600	15	< 2	< 2 (0.6)	< 2	< 1 (0.5)		
	Dunea	0	72*	63*	71*	17	24	10.1	79.80
		300	< 2	< 2 (0.6)	< 2	< 2	< 1		
		600	< 2	< 2	< 2	< 2	< 1	9.8	

* These values are inductive because they are obtained by extrapolation of the calibration curve

Table XIII.2 Results obtained with hormones in a LP-UV/H$_2$O$_2$ process

Date	Description	Dose	Hormones					H$_2$O$_2$	T$_{254nm}$
			17-alpha estradiol	17-alpha ethynylestradiol	17-beta estradiol	estriol	estrone		
		mJ/cm^2	ng/L	ng/L	ng/L	ng/L	ng/L	mg/L	%
25-7-2006 GCWW		0	69*	50*	57*	17	20	10.2	87.5
		300	13	8	11	6	6	10.3	
		600	2	2	2	2	1		
	Dunea	0	80*	62*	57*	18	22	10.5	
		0**	68*	57*	72*	18	22		
		300	15	14	14	5	7		
		600	6	3	5	3	3	10.5	

* These values are inductive because they are obtained by extrapolation of the calibration curve
** after 30 minutes

Table XIII.3 Results obtained with hormones in a DBD-UV/H$_2$O$_2$ process

Date	Description	Dose	Hormones					H$_2$O$_2$	T$_{254nm}$
			17-alpha estradiol	17-alpha ethynylestradiol	17-beta estradiol	estriol	estrone		
		mJ/cm^2	ng/L	ng/L	ng/L	ng/L	ng/L	mg/L	%
20-7-2006 GCWW		0	68*	47*	50*	15	21	10.2	87.29
		300	6	< 2 (1.2)	3	2	3	10.3	
		600	< 2	< 2	< 2	< 2	< 1		
	Dunea	0	74*	46*	54*	13	23	10.9	79.80
		300	3	< 2 (1.1)	3	< 2 (1.2)	1	10.2	
		600	< 2	< 2	< 2	< 2	< 1		

* These values are inductive because they are obtained by extrapolation of the calibration curve

Table XIII.4 Results obtained with triazines in a MP-UV/H_2O_2 process

Date	Description	Dose	Triazine					H_2O_2	T_{254nm}
			atrazine	cyanazine	desethyl atrazine	desisopropyl atrazine	simazine		
		mJ/cm^2	µg/L	µg/L	µg/L	µg/L	µg/L	mg/L	%
26-7-2006	GCWW	0	1.6	1.6	2.0	1.2	1.3	9.9	87.29
		300	0.51	0.79	1.3	0.76	0.39	9.8	
		600	0.22	0.39	0.8	0.49	0.18		
	Dunea	0	1.4	1.7	1.8	1.2	1.4	10.0	79.80
		300	0.57	0.88	1.20	0.81	0.51		
		600	0.29	0.57	0.83	0.57	0.25	10.0	

Table XIII.5: Results obtained with triazines in a LP-UV/H_2O_2 process

Date	Description	Dose	Triazine					H_2O_2	T_{254nm}
			atrazine	cyanazine	desethyl atrazine	desisopropyl atrazine	simazine		
		mJ/cm^2	µg/L	µg/L	µg/L	µg/L	µg/L	mg/L	%
25-7-2006	GCWW	0	1.4	1.7	2.0	1.2	1.1	10.9	79.98
		300	0.82	1.10	1.7	1.0	0.61	10.2	
		600	0.36	0.61	1.2	0.65	0.24		
	Dunea	0	1.7	2.0	1.9	1.3	1.6	10.3	
		0**	1.7	1.9	2.0	1.4	1.6		
		300	0.96	1.4	1.6	1.1	0.89		
		600	0.60	1.00	1.3	1.0	0.54	10.2	

Table XIII.6 Results obtained with triazines in a DBD-UV/H_2O_2 process

Date	Description	Dose	Triazine					H_2O_2	T_{254nm}
			atrazine	cyanazine	desethyl atrazine	desisopropyl atrazine	simazine		
		mJ/cm^2	µg/L	µg/L	µg/L	µg/L	µg/L	mg/L	%
20-7-2006	GCWW	0	1.4	1.7	2.1	1.5	1.2	10.5	87.29
		300	0.40	0.77	1.4	1.1	0.32		
		600	0.19	0.39	1.0	0.73	0.14	10.5	
	Dunea	0	1.4	1.9	2.0	1.7	1.5	10.3	79.80
		300	0.71	1.3	1.6	1.5	0.72		
		600	0.49	0.65	1.1	1.1	0.24	10.2	

Table XIII.7 Conversion of hormones with various lamps; Dunea water

Type lamp	Dose (mJ/cm²)	17-a-estradiol (ng/L)	(%)	17-a-ethynylestradiol (ng/L)	(%)	17-b-estradiol (ng/L)	(%)	estriol (ng/L)	(%)	estrone (ng/L)	(%)
DBD	0	74	0	46	0	54	0	13	0	23	0
	300	3	96	1	98	3	94	1	92	1	96
	600	1	99	1	98	1	98	1	92	0.5	96
MP	0	72	0	63	0	71	0	17	0	24	0
	300	1	99	1	98	1	98	1	94	0.5	98
	600	1	99	1	98	1	98	1	94	0.5	98
LP	0	68	0	57	0	57	0	18	0	22	0
	300	15	78	14	75	14	75	5	72	7	68
	600	6	91	3	95	5	91	3	83	3	86

Table XIII.8 Conversion of hormones with various lamps; GCWW water

Type lamp	Dose (mJ/cm²)	17-a-estradiol (ng/L)	(%)	17-a-ethynylestradiol (ng/L)	(%)	17-b-estradiol (ng/L)	(%)	estriol (ng/L)	(%)	estrone (ng/L)	(%)
DBD	0	68	0	47	0	50	0	15	0	21	0
	300	6	91	1	98	3	94	2	87	3	86
	600	1	99	1	98	1	98	1	93	0.5	98
MP	0	76	0	63	0	65	0	21	0	21	0
	300	2	97	1	98	1	98	1	98	0.5	98
	600	15	80	1	98	1	98	1	95	0.5	98
LP	0	69	0	50	0	57	0	17	0	20	0
	300	13	81	8	84	11	81	6	65	6	70
	600	2	97	2	96	2	96	2	88	1	95

Table XIII.9 Conversion of triazines with various lamps; Dunea water

Type lamp	Dose (mJ/cm²)	atrazine (ug/L)	(%)	cyanazine (ug/L)	(%)	desethylatrazine (ug/L)	(%)	desisopropylatrazine (ug/L)	(%)	simazine (ug/L)	(%)
DBD	0	1.4	0	1.9	0	2.0	0	1.7	0	1.5	0
	300	0.71	49	1.30	32	1.6	20	1.5	12	0.72	52
	600	0.49	65	0.65	66	1.1	45	1.1	35	0.24	84
MP	0	1.4	0	1.7	0	1.8	0	1.2	0	1.4	0
	300	0.57	59	0.88	48	1.2	33	0.81	33	0.51	64
	600	0.29	79	0.57	66	0.83	54	0.57	53	0.25	82
LP	0	1.7	0	2	0	1.9	0	1.4	0	1.6	0
	300	0.96	44	1.4	30	1.6	16	1.1	21	0.89	44
	600	0.60	65	1.0	50	1.3	32	0.97	31	0.54	66

Table XIII.10 Conversion of triazines with various lamps; GCWW water

Type lamp	Dose (mJ/cm²)	atrazine (ug/L)	(%)	cyanazine (ug/L)	(%)	desethylatrazine (ug/L)	(%)	desisopropylatrazine (ug/L)	(%)	simazine (ug/L)	(%)
DBD	0	1.4	0	1.7	0	2.1	0	1.5	0	1.2	0
	300	0.40	71	0.77	55	1.4	33	1.1	27	0.32	73
	600	0.19	86	0.39	77	1.0	52	0.73	51	0.14	88
MP	0	1.6	0	1.6	0	2.0	0	1.2	0	1.3	0
	300	0.51	68	0.79	51	1.3	35	0.76	37	0.39	70
	600	0.22	86	0.39	76	0.80	60	0.49	59	0.18	86
LP	0	1.4	0	1.7	0	2.0	0	1.2	0	1.1	0
	300	0.82	41	1.1	35	1.7	15	1.0	17	0.61	45
	600	0.36	74	0.61	64	1.2	40	0.65	46	0.24	78

XIV Process conditions of UV-pilot experiments at KWR (WP1)

MP-lamp

Date	Time	Experimental time	Capacity [%]	Sensor* [W/m²]	Flow (L/h)	Voltage (V)	Amperage (A)	Temperature Effluent (ºC)	Temperature Air relief (ºC)	Temperature Air (ºC)	Dosage H₂O₂ [L/h]	Remarks			
21-11-2006	11:44:00		100	2217	4000		2.3					Drinking water	4000 L/h	188 sec	3 min 8 sec
	11:45:00		10	817	4000		0.1	13.0	13.6	19.0		No air bubbles near sight glass	1000 L/h	384 sec	6 min 24 sec
	11:55:00		10	831	4000		0.1	13.0	13.3	19.9			200 L/h	1502 sec	25 min 2 sec
	12:00:30	00:00	10	516	4000		0.0		12.8	20.7		Switch to Dunea water			
	12:03:45	03:15										Sample taking 4000 L/h			
	12:04:20	03:50	10	551	1000		0.1		18.4	19.7					
	12:10:50	10:20										End experiment, pump shut down. Switch system to drinking water			
	12:18:00	00:00			1000		0.1		17.8	21.8		Switch to Dunea water			
	12:25:00	07:00		571	1000		0.0			22.7					
	12:26:00	08:00										Sample taking 1000 L/h			
	12:27:00	26:30			200										
	12:30:00	29:30		745	200		0.0		27.7	25.5		Higher lamp intensity due to a air bubble?			
	12:35:00	34:30		904					38.8			200 L/h			
	12:36:00	35:30										Lamps off			
	14:08:00		100		1300							Start recirculation			
	14:10:00	02:00	100	2217	1300		2.3		16.8	19.3					
	14:15:00	07:00	30	1500					38.8						
	14:20:00	12:00	10	749	1300		0.1		42.8						
	14:25:00	17:00	10	694	1200		0.1		40.4	26.3					
	14:30:00	22:00										End recirculation			
5-12-2006	9:13:00		100	800	2000						19.6	Lamps on using drinking water			
	9:18:00		100	2217	2000			13.6	14	19.0		No air bubbles near sight glass			
	9:20:00		10	922	2000			13.6	28.4	23.9					
	9:28:00		10	861	2900			13.0	13.3	23.1	5.6	start dosing H₂O₂			
	9:35:20	00:00										switch to Dunea water + MS2 phages			
	9:36:00	00:40	10	743	1390		0.1	13.9	17.3	24.8	5.6				
	9:42:00	06:40	10	640	1390			14.1	22.3	20.4	5.6				
	9:46:00	10:40	10	650	1390				23	23		Sample taking effluent (3x)			
	9:46:45	11:25										Sample taking influent H₂O₂			
	9:47:30	12:10		571	1000		0.0			22.7		Switch to drinking water, shut down lamps and stop dosing H₂O₂		4x reactor volume	2x reactor volume
6-12-2006	12:09:00		100		2800							Lamps on using drinking water			
	12:13:00		100	2217	2800								2,13 m³/h	283	142
	12:14:15		10	830	2800								1.37	439	219
	12:20:30	0:00:00										switch to Dunea water + micropollutants			
	12:24:00	0:03:30	10	461	2100			12.6				Sample taking influent		1	283
	12:25:30	0:05:00										Sample taking effluent	5.48	2	219
	12:27:00	0:00:00										Flow 1370 L/h		3	439
	12:28:00	0:01:00		467	1350			15.9		22.4		Sample taking influent		4	142
	12:31:00	0:04:00		469	1350			16.8				Sample taking effluent			
	12:33:00	0:00:00										dose H₂O₂ 5.5 L/h			
	12:36:00	0:03:00		563	1360			17.1		20.1	5.3	Sample taking influent H₂O₂			
	12:41:00	0:08:00		571	1340			18.1		26.1	5.5	Sample taking effluent			
	12:44:00	0:00:00										Flow 2130 L/h and H₂O₂ 8,5 L/h			
	12:45:00	0:01:00		522	2120			17.4			8.7	Sample taking influent H₂O₂			
	12:47:00	0:03:00		512	2110			12.6		25.1	8.8	Sample taking effluent; drop cap AOC flask, cleaned and put on the flask			
	12:50:00	0:06:00										Switch to drinking water			
	12:52:00			794	2400										
	12:53:00											shut down lamps			

* Spectral range = 215 - 365 nm

LP-lamp

Date	Time	Experimental time	Capacity [%]	Sensor* [W/m²]	Flow (L/h)	Voltage (V)	Amperage (A)	Temperature Effluent (°C)	Temperature Air relief (°C)	Temperature Air (°C)	Dosage H₂O₂ [L/h]	Remarks			
22-11-2006	10:20:00											Lamps on; Drinking water	4000 L/h	188 sec	3 min 8 sec
	10:25:00		100	112	2400	3.6	3.1	12.8	14			No air bubbles near sight glass	1000 IL/h	384 sec	6 min 24 sec
	10:38:20	00:00		54	4000	3.8	3.4		14.1	34.4		Switch to Dunea water	200 L/h	1502 sec	25 min 2 sec
	10:41:40	03:20										Sample taking 4000 L/h			
	10:42:15	03:55										Flow 1000 L/h			
	10:44:00	05:40		55	1000	3.9	3.3		13.8	34.3		Upper lamp seems to be more pink (less blue)			
	10:48:50	10:30										Sample taking 1000 L/h			
	10:50:00	11:40			200							Flow 200 L/h			
	11:00:00	21:40		73		200 Can not be measured?!!!			19.5	36.3						
	11:05:00	26:40		91					20						
	11:15:30	37:10		108					23.3			Sample taking 200 L/h			
	11:16:30	38:10										Lamps switch off			
	11:23:00	44:40										Sample taking influent at sample point effluent			
	12:45:00	00:00			1200							Start recirculation			
	12:53:00	08:00		64	1200	3.6	3.3		16.3	28.9					
	13:00:00	15:00		64	1200	3.5	3.1		16.5	31.7					
	13:05:00	20:00		65	1200	3.4	3		16.7	35.1					
	13:15:00	30:00		66	1200	3.4	3		17.1	39					
	13:26:00	41:00		66		3.2	3.2		17.1	39.2		End recirculation			
				Bad lamp		2.8	2.6								
						Can not be measured?!!!									
						5.4	4.6								
						3.7	3.5								
5-12-2006	11:20:00		100		2000					19.6		Lamps on; Drinking water			
	11:27:00		100	114	2000			12.6	12.9	25.2		start dosing H₂O₂		8.64 L/h H₂O₂ dosing	
	11:30:00		100	119	2200	3.8	3.4		13.0	29.3	8.6				
	11:40:30	00:00	100									switch to Dunea water + MS2 phages			
	11:42:00	01:30	100	58	2160			13.4	13.5	31.5	8.5	Sample taking effluent (3x)			
	11:48:00	07:30	100	54	2100				13.8		8.4	Sample taking influent H₂O₂			
	11:49:00	08:30										Switch to drinking water, shut down lamps and stop dosing H₂O₂			
												Sample taking influent phages from tank (3x)			
6-12-2006	8:49:00											Lamps on using drinking water			
	8:57:00		100	112	2300				13	29.3				11.96 L/h H₂O₂ dosing	
	9:06:00		100	122	2200				12.8	38.7					
	9:17:00		100	126	2200				12.9						
	9:22:20	00:00										switch to Dunea water + micropollutants			
	9:23:00	00:40		53	2900					45		Sample taking influent			
	9:25:55	03:35		53	3020							Sample taking effluent			
	9:27:00	00:00										Flow 2160 L/h			
	9:28:00	01:00		53					13.7						
	9:29:15	02:15		53					13.7			Sample taking effluent			
	9:31:00	00:00		56	2100						9	start dosing H₂O₂			
	9:36:00	05:00		55	2100				13.8		9.3	Sample taking effluent			
	9:36:45	00:00			3000						12	Higher flow and higher flow H₂O₂ dosing			
	9:39:30	02:45		48	3000				13.7	43	12	Sample taking effluent and influent H₂O₂			
	9:42:00	05:15										Switch to drinking water and stop dosing H2O2			
												Lights all blue, no more a pink glow at upper lamp			
	9:49:00				1200							Start recirculation			
	9:55:00			61								Open drain during UV treatment			
	10:05:00			59						46					
	10:15:00			59					15.4						
	10:20:00											End drain micropollutants solution			

* Spectral range = 215 - 365 nm

DBD-lamp

Date	Time	Experimental time	Sensor* [W/m²]	Flow (L/h)	Left ballast Voltage (V)	Amperage (A)	Power (W)	Right ballast Voltage (V)	Amperage (A)	Power (W)	Temperature Effluent (°C)	Temperature Air relief (°C)	Temperature Air (°C)	Dosage H₂O₂ [L/h]	Remarks
24-11-2006	11:35:00														Lamps on; Drinking water
	11:42:00		50	1000	301	2.3	692	301	1.8	542	12.7	14.8	14.3		No air bubbles near sight glass
	11:50:00		50	1000	301	2.4	722	302	1.8	544	12.8	14.5	14.2		
	11:54:40	00:00	20	4000	302	2.4	725	301	1.8	542		14	14		Switch to Dunea water
	11:58:00	03:20					0			0					Sample taking 4000 L/h
	11:58:50	04:10													Flow 1000 L/h
	12:00:00	05:20	20	1000	302	2.45	740	301	1.9	572		15.2	14.2		A view air bubbles near sight glass
	12:05:30	10:50		1000			0			0					Sample taking 1000 L/h
	12:06:50	12:10		200			0			0					Flow 200 L/h
	12:10:00	15:20	26	200	303	2.4	727	301	1.9	572		18.3	14.3		
	12:20:00	25:20	41	200	300	2.4	720	301	1.8	542		23.8	14.3		
	12:32:00	37:20	53	200	302	2.4	725	302	1.8	544		27.8			Sample taking 200 L/h
	12:33:00	38:20		1000			0			0					Lamps switch off
	12:39:00	44:20		1000			0			0					Sample taking influent at sample point effluent
	13:45:00	00:00		1200			0			0					Start recirculation
	13:50:00	05:00	21	1200	302	2.4	725	303	1.9	576		16	14.3		
	13:55:00	10:00	21	1200	301	2.4	722	303	1.9	576		16	14.4		
	14:10:00	25:00	21	1200	302	2.4	725	303	1.9	576		16.6	14.2		
	14:15:00	30:00	21	1200	302	2.3	695	303	1.9	576		16.1	14.2		
	14:25:00	40:00					0			0					End recirculation

4000 L/h	188 sec	3 min 8 sec
1000 L/h	384 sec	6 min 24 sec
200 L/h	1502 sec	25 min 2 sec

fluctuations Amperage between 2,3-2,5 (left ballast) and 1,8-2,0 (right ballast)

900 L/h	835 sec	13 min 55 sec
1960 L/h	237 sec	3 min 57 sec

Date	Time	Experimental time	Sensor* [W/m²]	Flow (L/h)	Left ballast Voltage (V)	Amperage (A)	Power (W)	Right ballast Voltage (V)	Amperage (A)	Power (W)	Temperature Effluent (°C)	Temperature Air relief (°C)	Temperature Air (°C)	Dosage H₂O₂ [L/h]	Remarks
4-12-2006	10:35:00														Lamps on; Drinking water
	10:37:00		47	850	301	2.4	722	301	1.8	542	12.9	14	13.8		No air bubbles in sight glass
	10:45:00		56	840	301	2.4	722	301	1.8	542	13.1	15.1	14.4		
	10:47:30	00:00												3.6	switch to Dunea water + MS2 phages
	10:50:00	02:30	28	900	301	2.4	722	301	1.8	542	10.8	15	14.1	3.3	
	10:57:00	09:30	21	890	302	2.4	725	301	1.8	542	10.9	13.1	14.1	3.8	
	11:01:30	14:00													Sample taking effluent (3x)
	11:02:30	15:00													stop dosing H₂O₂
	11:05:30	18:00	21				0			0					Sample taking influent from tank (3x)
	12:00:00		50		302	2.4	725	301	1.8	542	13.4	15	14.2		Lamps on; Drinking water
	12:06:00														switch to Dunea water + micropollutants
	12:11:00	05:00	21	890	301	2.3	692	301	1.8	542		15	14.4	3.5	Sample taking influent
	12:18:30	12:30					0			0					Sample taking 900 L/h
	12:21:00	15:00	18	1910			0			0		12.3		7.3	Flow 1960 L/h
	12:23:00	17:00					0			0					Sample taking influent
	12:25:00	19:00	17				0			0					Sample taking 1960 L/h
	12:27:20	21:20					0			0				0	stop dosing H₂O₂
	12:30:00	24:00	17		301	2.4	722	301	1.8	542		11.2			
	12:32:00	26:00	17				0			0					Sample taking 1960 L/h
	12:33:00	27:00					0			0					Flow 900 L/h
	12:34:00	28:00	18	880	301	2.3	692	301	1.8	542		12.4		0	Sample taking influent
	12:40:00	34:00					0			0					Sample taking 900 L/h
	12:41:00	35:00					0			0					Drinking water

* Spectral range = 215 - 365 nm

XV Water quality data for UV pilot experiments (WP1)
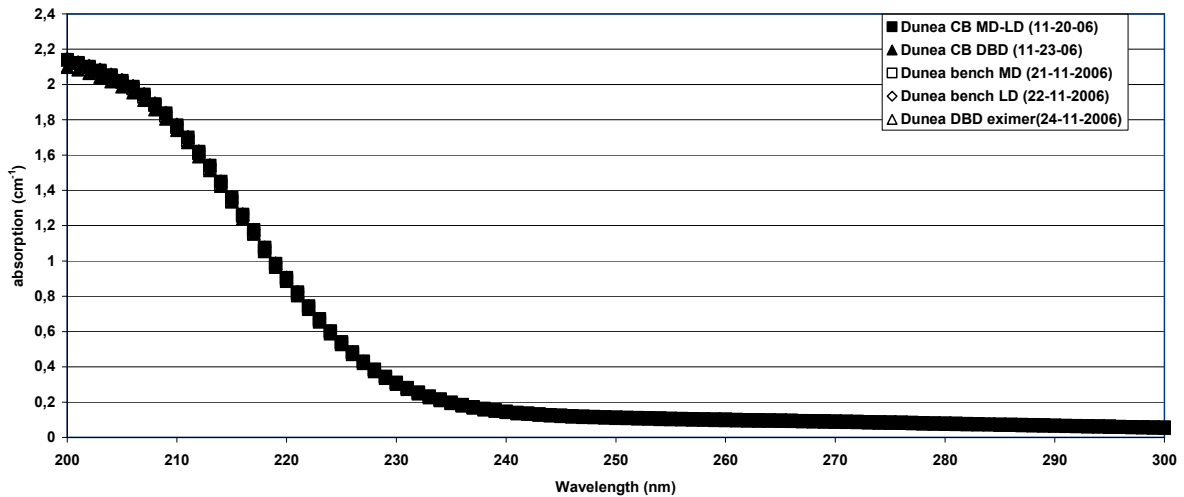
Figure XIV.1 Absorption scans of irradiated water for collimated beam and validation of the UV pilot reactor

Table XV.1 Water quality data of Dunea water after rapid sand filtration during pilot experiments

date	Nitrate	nitrate	pH	HCO$_3$-	NPOC	conductivity
	mg N /L	mg NO$_3$/L		mg HCO$_3$ /L	mg C/L	µS/cm
12-04-2006	2.7	12.0	7.83	185	4	547
12-06-2006	2.8	12.4	7.96	190	3.9	552
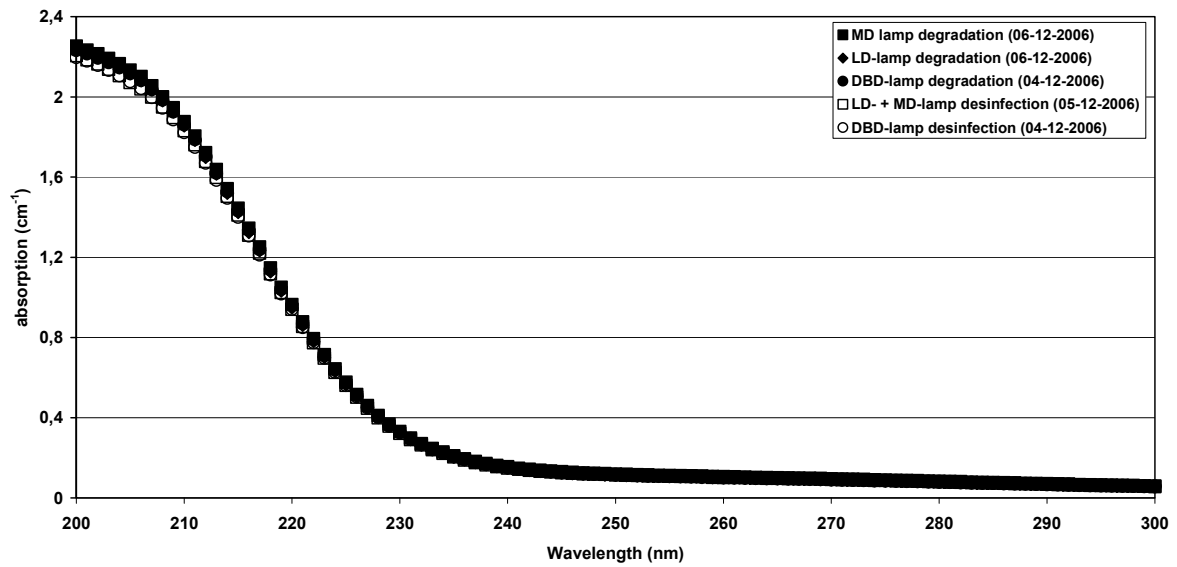
Figure XV.2 Absorption scans of water irradiated during UV pilot experiments
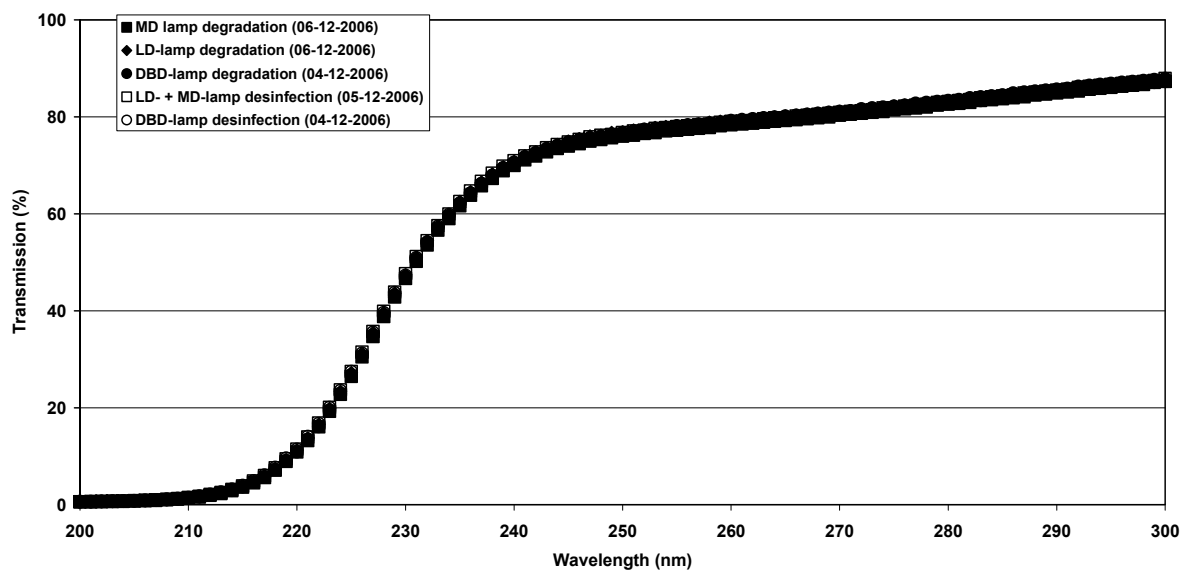
Figure XV.3: UV transmission scans of irradiated water during UV pilot experiments

XVI Results of conversion of organic micropollutants by means of the UV pilot reactor (WP1)

Table XVI.1 Results and calculations for the conversion of priority compounds by means of MP-UV/H_2O_2 process

					Pesticides				
Dose	Calculated flow	Measured flow	MTBE	alachlor	atrazine	cyanazine	metazachlor	H_2O_2	
mJ/cm^2	m^3/h	m^3/h	µg/L	µg/L	µg/L	µg/L	µg/L	mg/L	
0	0	0	3.00	1.60	1.60	1.40	1.50	< 0.06	
300	2.12	2.10	2.90	0.84	0.91	0.86	0.70		
450	1.37	1.35	2.00	0.79	0.77	0.82	0.59		
0*	0	0							
300	2.12	2.11	1.40	0.41	0.67	0.66	0.28	9.2	
450	1.37	1.34	1.40	0.23	0.44	0.55	0.14	10.8	

* MTBE, pesticiden dose 0 are only analysed for dose 0 without H_2O_2 (not quenched with Na_2SO_3)

						Pharmaceuticals							
Dose	erythro-mycine	anhydro** erythro-mycine A	anhydro** erythro-mycine B	bezafibrate	carbamazepine	diclofenac	iboprofen ***	linco-mycin	meto-prolol	phenazone	sotalol	sulfa-methoxazole	
mJ/cm^2	µg/L	µg/L	µg/L	µg/L	µg/L	µg/L	µg/L	µg/L	µg/L	µg/L	µg/L	µg/L	
0	3.10	1.80	0.90	2.50	1.90	3.10	24.10	1.70	1.70	1.70	3.00	1.20	
300	2.70	1.60	0.61	1.80	1.40	0.03	26.50	0.92	1.30	0.55	0.46	0.21	
450	2.60	1.60	0.81	1.40	1.40	0.02	23.70	0.78	1.20	0.42	0.30	0.14	
0*													
300	1.00	0.59	0.85	0.44	0.55	0.02	6.30	0.25	0.51	0.36	0.22	0.06	
450	0.79	0.65	1.50	0.29	0.32	0.02	2.30	0.10	0.29	0.21	0.08	0.09	

* samples after half hour neutralized with Na_2SO_3
** formed out of erithromycine after dilution in water
*** results calculated by extrapolating the calibration curve (0.1 - 5 µg/l)

Table XVI.2: Results and calculations for the conversion of priority compounds by means of MP-UV/H_2O_2 process

	Conversion (%)			
	300 mJ/cm²/ 0 mg H_2O_2/L	450 mJ/cm²/ 0 mg H_2O_2/L	300 mJ/cm²/ 10 mg H_2O_2/L	450 mJ/cm²/ 10 mg H_2O_2/L
MTBE	3	33	53	53
Alachlor	48	51	74	86
Atrazine	43	52	58	73
Cyanazine	39	41	53	61
Metazachlor	53	61	81	91
Erythromycine	13	16	68	75
Bezafibrate	28	44	82	88
Carbamazepine	26	26	71	83
Diclofenac	99	99	99	99
Ibuprofen	0	2	74	90
Lincomycine	46	54	85	94
Metropolol	24	29	70	83
Phenazone	68	75	79	88
Sotalol	85	90	93	97
Sulfamethoxazole	83	88	95	93

Table XVI.3 Results of byproduct formation during the MP-UV/H₂O₂ process

										AOC				
Dose	**Nitrite**			P17						NOX			Total	
		1	**2**	**avg**	**RSD**	**RSD**	**1**	**2**	**avg**	**RSD**	**RSD**	**AOC**	**RSD**	**RSD**
mJ/cm²	**µg NO₂/L**	**µg C/L**	**µg C/L**	**µg C/L**	**µg C/L**	**%**	**µg C/L**	**µg C/L**	**µg C/L**	**µg C/L**	**%**	**µg C/L**	**µg C/L**	**%**
0	5.9													
300	463	40	39	39	1	2	52	61	56	6	11	96	6	7
450	568	57	51	54	1	1	87	73	80	10	12	130	24	19

Table XVI.4 Results and calculations for the conversion of priority compounds by means of LP-UV/H₂O₂ process

					Pesticides			
Dose	**Calculated flow**	**Measured flow**	**MTBE**	**alachlor**	**atrazine**	**cyanazine**	**metazachlor**	**H₂O₂**
mJ/cm²	**m³/h**	**m³/h**	**µg/L**	**µg/L**	**µg/L**	**µg/L**	**µg/L**	**mg/L**
0	0	0	1.60	1.50	1.40	1.30	1.30	< 0.06
300	2.99	3.02	1.70	1.30	1.20	1.20	1.10	
450	2.16	2.10	1.80	1.20	1.10	1.10	1.00	
0*	0	0						
300	2.99	3.00	1.40	0.78	0.99	0.93	0.64	9.4
450	2.16	2.10	1.60	0.56	0.80	0.84	0.47	10.0

* MTBE, pesticiden dose 0 are only analysed for dose 0 without H₂O₂ (not quenched with Na₂SO₃)

			Pharmaceuticals									
Dose	**erythro-mycine**	**anhydro** erythro-mycine A	**anhydro** erythro-mycine B	**bezafibrate**	**carbamazepine**	**diclofenac**	**ibuprofen** ***	**linco-mycin**	**meto-prolol**	**phenazone**	**sotalol**	**sulfa-methoxazole**
mJ/cm²	**µg/L**	**µg/L**	**µg/L**	**µg/L**	**µg/L**	**µg/L**	**µg/L**	**µg/L**	**µg/L**	**µg/L**	**µg/L**	**µg/L**
0	3.40	1.80	1.10	2.30	1.70	3.00	23.10	1.80	1.70	1.60	3.00	1.30
300	2.80	1.50	1.30	2.40	1.70	0.63	24.70	1.50	1.70	0.87	1.30	0.66
450	3.00	1.70	0.75	2.30	1.80	0.36	24.20	1.80	1.70	0.74	1.10	0.53
0*												
300	1.60	0.90	0.77	0.69	1.10	0.16	9.70	0.70	1.10	0.77	0.95	0.27
450	1.50	1.10	0.63	0.60	0.71	0.08	7.90	0.43	0.76	0.51	0.52	0.10

* samples after half hour neutralized with Na₂SO₃
** formed out of erythromycine after dilution in water
*** results calculated by extrapolating the calibration curve (0.1 - 5 µg/l)

Table XVI.5 Results and calculations for the conversion of priority compounds by means of LP-UV/H₂O₂ process

	Conversion (%)			
	300 mJ/cm²/ 0 mg H₂O₂/L	450 mJ/cm²/ 0 mg H₂O₂/L	300 mJ/cm²/ 10 mg H₂O₂/L	450 mJ/cm²/ 10 mg H₂O₂/L
MTBE	0	0	13	0
Alachlor	13	20	48	63
Atrazine	14	21	29	43
Cyanazine	8	15	28	35
Metazachlor	15	23	51	64
Erythromycine	18	12	53	56
Bezafibrate	0	0	70	74
Carbamazepine	0	0	35	58
Diclofenac	79	88	95	97
Ibuprofen	0	0	58	66
Lincomycine	17	0	61	76
Metropolol	0	0	35	55
Phenazone	46	54	52	68
Sotalol	57	63	68	83
Sulfamethoxazole	49	59	79	92

Table XVI.6 Results of byproduct formation during the LP-UV/H₂O₂ process

Dose	Nitrite	AOC P17 1	2	avg	RSD	RSD	NOX 1	2	avg	RSD	RSD	AOC	Total RSD	RSD
mJ/cm²	µg NO₂/L	µg C/L	µg C/L	µg C/L	µg C/L	%	µg C/L	µg C/L	µg C/L	µg C/L	%	µg C/L	µg C/L	%
0	6.1													
300	7	19	17	18	1	8	33	34	34	1	2	52	9	17
450	21	43	20	32	16	51	61	44	53	12	23	84	17	20

Table XVI.7 Results and calculations for the conversion of priority compounds by means of DBD-UV/H₂O₂ process

Dose	Calculated flow	Measured flow	MTBE	Pesticides alachlor	atrazine	cyanazine	metazachlor	H₂O₂
mJ/cm²	m³/h	m³/h	µg/L	µg/L	µg/L	µg/L	µg/L	mg/L
0	0	0	1.80	1.60	1.50	1.30	1.40	1.6
300	1.96	1.91	1.70	1.20	1.10	1.20	0.98	
450	0.90	0.88	1.70	1.00	0.90	0.88	0.79	
0*	0	0	1.80	1.50	1.60	1.50	1.30	
300	1.96	1.91	1.40	0.76	1.00	1.00	0.90	9.1
450	0.90	0.89	1.10	0.37	0.63	0.71	0.26	11.3

* MTBE, pesticiden dose 0 are only analysed for dose 0 without H₂O₂ (not quenched with Na₂SO₃)

** samples were in contact with air before analysis. This had no influence on the analysed samples

Dose	erythro-mycine	anhydro** erythro-mycine A	anhydro** erythro-mycine B	bezafibrate	Pharmaceuticals carbamazepine	diclofenac	iboprofen ***	linco-mycin	meto-prolol	phenazone	sotalol	sulfa-methoxazole
mJ/cm²	µg/L	µg/L	µg/L	µg/L	µg/L	µg/L	µg/L	µg/L	µg/L	µg/L	µg/L	µg/L
0	3.30	2.10	0.75	2.80	2.00	3.10	25.10	1.90	1.90	1.80	3.30	1.80
300	2.70	1.90	0.76	2.60	1.50	0.57	26.90	1.20	1.60	1.10	1.00	0.73
450	2.40	1.70	1.30	1.70	1.50	0.16	22.10	0.95	1.50	0.69	0.42	0.54
0*	2.40	1.50	0.71	1.20	1.60	1.70	10.60	1.60	1.70	1.70	3.20	1.00
300	1.70	0.92	1.10	0.88	0.90	0.28	8.20	0.69	1.00	0.85	0.88	0.23
450	0.96	0.54	1.20	0.47	0.37	0.02	2.70	0.19	0.45	0.37	0.20	0.11

* samples after half hour neutralized with Na₂SO₃

** formed out of erithromycine after dilution in water

*** results calculated by extrapolating the calibration curve (0.1 - 5 µg/l)

Table XVI.8 Results and calculations for the conversion of organic micropollutants by means of DBD-UV/H$_2$O$_2$ process

	Conversion (%)			
	300 mJ/cm²/ 0 mg H$_2$O$_2$/L	450 mJ/cm²/ 0 mg H$_2$O$_2$/L	300 mJ/cm²/ 10 mg H$_2$O$_2$/L	450 mJ/cm²/ 10 mg H$_2$O$_2$/L
MTBE	6	6	22	39
Alachlor	25	38	49	75
Atrazine	27	40	38	61
Cyanazine	8	32	33	53
Metazachlor	30	44	31	80
Erythromycine	18	27	29	60
Bezafibrate	7	39	27	61
Carbamazepine	25	25	44	77
Diclofenac	82	95	84	99
Ibuprofen	0	12	23	75
Lincomycine	37	50	57	88
Metropolol	16	21	41	74
Phenazone	39	62	50	78
Sotalol	70	87	73	94
Sulfamethoxazole	59	70	77	89

Table XVI.8 Results of byproduct formation during the DBD-UV/H$_2$O$_2$ process

Dose	Nitrite	AOC												
		P17					NOX					Total		
mJ/cm²	µg NO$_2$/L	1 µg C/L	2 µg C/L	avg µg C/L	RSD µg C/L	RSD %	1 µg C/L	2 µg C/L	avg µg C/L	RSD µg C/L	RSD %	AOC µg C/L	RSD µg C/L	RSD %
0	6.6	11	10	11	1	6	16	15	15	1	5	26	3	11
300	86	35	14	25	15	59	44	52	48	6	12	73	16	22
450	119	140	57	98	59	60	120	71	96	35	36	190	39	21

XVII Results and calculations of disinfection capacity (WP1)

Table XVII.1 Results and calculations of the disinfection capacity of the MP-UV/H_2O_2 process

MD-lamp 05-12-2006

| Dose | Calculated flow | Measured flow | Sample number | phages | | | H_2O_2 | |
| | | | | influent | effluent | log reduction | influent without H_2O_2 | influent with H_2O_2 |
mJ/cm^2	m^3/h	m^3/h		pve/mL	pve/mL		mg/L	mg/L
450	1.37	1.39	1	5.9E+07	< 0.1	> 8.77	0.25	9.6
			2	6.2E+07	< 0.1	> 8.79		
			3	5.4E+07	< 0.1	> 8.73		
			average	5.8E+07	< 0.1	8.76		

Table XVII.2 Results and calculations of the disinfection capacity of the LP-UV/H_2O_2 process

LD-lamp 05-12-2006

| Dose | Calculated flow | Measured flow | Sample number | phages | | | H_2O_2 | |
| | | | | influent | effluent | log reduction | influent without H_2O_2 | influent with H_2O_2 |
mJ/cm^2	m^3/h	m^3/h		pve/mL	pve/mL		mg/L	mg/L
450	2.16	2.10	1	6.0E+07	< 0.1	> 8.77	0.25	9.3
			2	5.8E+07	< 0.1	> 8.76		
			3	6.1E+07	< 0.1	> 8.78		
			average	6.0E+07	< 0.1	8.77		

Table XVII.3 Results and calculations of the disinfection capacity of the DBD-UV/H_2O_2 process

DBD-lamp 04-12-2006

| Dose | Calculated flow | Measured flow | Sample number | phages | | | H_2O_2 | |
| | | | | influent | effluent | log reduction | influent without H_2O_2 | influent with H_2O_2 |
mJ/cm^2	m^3/h	m^3/h		pve/mL	pve/mL		mg/L	mg/L
450	0.90	0.89	1	7.8E+07	< 0.1	> 8.89	0.25	11.1
			2	6.8E+07	100	5.83		
			3	8.7E+07	< 0.1	> 8.94		
			average	7.8E+07		7.89		

XVIII EEO Calculations for the pilot reactor at KWR (WP1)

Table XVIII.1 Calculated E_{EO} at a dose of 450 mJ/cm^2 in the presence of 10 mg H_2O_2/L ; MP-lamp:

	ci (ug/l)	ci (mol/l)	cf (ug/l)	cf (mol/l)	EEO (450/10)			
						P =	0.804	[kW]
						F =	1.35	[m3/h]
MTBE	3	1.39E-08	1.4	6.49E-09	1.80			
Alachlor	1.6	5.93E-09	0.23	8.52E-10	0.71			
Atrazine	1.6	7.42E-09	0.44	2.04E-09	1.06			
Cyanazine	1.4	5.82E-09	0.55	2.29E-09	1.47			
Metazachlor	1.5	5.40E-09	0.14	5.04E-10	0.58			
Erythromycine	3.1		0.8		1.00			
Bezafibrate	2.5		0.3		0.64			
Carbamazepine	1.9	7.89E-09	0.32	1.33E-09	0.77			
Diclofenac	3.1	1.29E-08	0.02	8.31E-11	0.27			
Ibuprofen	24.1	1.17E-07	2.3	1.12E-08	0.58			
Lincomycine	1.7		0.1		0.48			
Metropolol	1.7	7.88E-09	0.29	1.34E-09	0.78			
Phenazone	1.7		0.2		0.66			
Sotalol	3.0		0.1		0.38			
Sulfamethoxazole	1.2		0.1		0.53			

Table XVIII.2: Calculated E_{EO} at a dose of 450 mJ/cm^2 in the presence of 10 mg H_2O_2/L ; LP-lamp

	ci (ug/l)	ci (mol/l)	cf (ug/l)	cf (mol/l)	EEO (450/10)			
						P =	0.317	[kW]
						F =	2.10	[m3/h]
MTBE	1.6	7.42E-09	1.59	7.37E-09	55.44			
Alachlor	1.5	5.56E-09	0.56	2.08E-09	0.35			
Atrazine	1.4	6.49E-09	0.8	3.71E-09	0.62			
Cyanazine	1.3	6.03E-09	0.84	3.89E-09	0.80			
Metazachlor	1.3		0.5		0.34			
Erythromycine	3.4		1.5		0.42			
Bezafibrate	2.3		0.6		0.26			
Carbamazepine	1.7	7.20E-09	0.71	3.01E-09	0.40			
Diclofenac	3	1.27E-08	0.08	3.39E-10	0.10			
Ibuprofen	23.1	1.12E-07	7.9	3.83E-08	0.32			
Lincomycine	1.8		0.4		0.24			
Metropolol	1.7	7.88E-09	0.76	3.52E-09	0.43			
Phenazone	1.6		0.5		0.30			
Sotalol	3.0		0.5		0.20			
Sulfamethoxazole	1.3		0.1		0.14			

Table XVIII.3: Calculated E_{EO} at a dose of 450 mJ/cm^2 in the presence of 10 mg H$_2$O$_2$/L ; DBD-lamp

| | c_i (ug/l) | c_i (mol/l) | c_f (ug/l) | c_f (mol/l) | EEO (450/10) (P=0,2 kW) | P = | 0.214 | [kW] |
						F =	0.89	[m3/h]
MTBE	1.8	2.05E-08	1.1	1.25E-08	1.12			
Alachlor	1.5	5.56E-09	0.37	1.37E-09	0.40			
Atrazine	1.6	7.42E-09	0.63	2.92E-09	0.59			
Cyanazine	1.5	6.23E-09	0.71	2.95E-09	0.74			
Metazachlor	1.3	4.68E-09	0.26	9.36E-10	0.34			
Erythromycine	2.4		0.96		0.60			
Bezafibrate	1.2		0.47		0.59			
Carbamazepine	1.6	6.78E-09	0.37	1.57E-09	0.38			
Diclofenac	1.7	5.34E-09	0.02	6.29E-11	0.12			
Ibuprofen	10.6	5.15E-08	2.70	1.31E-08	0.40			
Lincomycine	1.6		0.19		0.26			
Metropolol	1.7	7.88E-09	0.45	2.09E-09	0.42			
Phenazone	1.7		0.37		0.36			
Sotalol	3.2		0.2		0.20			
Sulfamethoxazole	1		0.2		0.34			

XIX Calculation of radical formation of various types of lamps (WP1)

Table XIX.1 Radical formation for MP UV-lamps

[H$_2$O$_2$] (ppm) =	15	0.0004412	M
Weglengte (cm) =	15	15	cm

MD-UV

λ (nm)	ε (H$_2$O$_2$) (M^{-1}cm^{-1})	A (H$_2$O$_2$)	A (water)	Lamp photonflow	Total photon flow absorbed	Total photon flow absorbed by H$_2$O$_2$	% of photon flow absorbed by H$_2$O$_2$
200 - 204	179.21	1.186	5.8	1.081	1.081	0.184	0.4
205 - 209	155.84	1.031	4.6	1.571	1.571	0.288	0.6
210 - 214	132.23	0.875	3.8	1.812	1.812	0.339	0.7
215 - 219	110.12	0.729	2.38	1.964	1.962	0.460	0.9
220 - 224	89.97	0.595	1.96	1.986	1.981	0.462	0.9
225 - 229	72.07	0.477	1.54	1.876	1.858	0.439	0.9
230 - 234	55.83	0.369	1.12	1.922	1.860	0.461	0.9
235 - 239	43.28	0.286	0.84	2.394	2.215	0.563	1.1
240 - 244	33.45	0.221	0.56	1.471	1.228	0.348	0.7
245 - 249	25.31	0.167	0.28	3.452	2.220	0.831	1.6
250 - 254	**19.02**	**0.126**	**0.14**	**5.927**	**2.713**	**1.285**	**2.5**
255 - 259	14.13	0.094	0.12	5.579	2.167	0.949	1.9
260 - 264	10.47	0.069	0.12	2.079	0.735	0.269	0.5
265 - 269	7.68	0.051	0.11	5.753	1.781	0.563	1.1
270 - 274	5.57	0.037	0.1	1.429	0.386	0.104	0.2
275 - 279	3.99	0.026	0.1	1.138	0.287	0.060	0.1
280 - 284	2.83	0.019	0.09	3.288	0.728	0.125	0.2
285 - 289	1.94	0.013	0.09	1.102	0.232	0.029	0.1
290 - 294	1.32	0.009	0.08	1.000	0.185	0.018	0.0
295 - 299	0.88	0.006	0.08	3.583	0.643	0.044	0.1
TOTAL				50.407	27.644	7.820	15.5

% absorbed from total photonflow	54.8
% absorbed by H$_2$O$_2$ from total photonflow	15.5
% absorbed by background	39.3
Efficiency H$_2$O$_2$-absorption	28.3

Table XIX.2Radical formation for LP UV-lamps

LD-UV

λ (nm)	ε (H₂O₂) (M⁻¹cm⁻¹)	A (H₂O₂)	A (water)	Lamp photonflow	Total photon flow absorbed	Total photon flow absorbed by H₂O₂	% of photon flow absorbed by H₂O₂
200 - 204	179.21	1.186	5.8	4.54E-06	4.54E-06	7.70E-07	0.0
205 - 209	155.84	1.031	4.6	2.59E-06	2.59E-06	4.74E-07	0.0
210 - 214	132.23	0.875	3.8	2.12E-06	2.12E-06	3.97E-07	0.0
215 - 219	110.12	0.729	2.38	1.87E-06	1.87E-06	4.37E-07	0.0
220 - 224	89.97	0.595	1.96	9.83E-07	9.80E-07	2.28E-07	0.0
225 - 229	72.07	0.477	1.54	2.03E-06	2.01E-06	4.75E-07	0.0
230 - 234	55.83	0.369	1.12	1.35E-06	1.31E-06	3.24E-07	0.0
235 - 239	43.28	0.286	0.84	3.42E-06	3.16E-06	8.04E-07	0.0
240 - 244	33.45	0.221	0.56	7.40E-07	6.18E-07	1.75E-07	0.0
245 - 249	25.31	0.167	0.28	1.63E-05	1.05E-05	3.92E-06	0.0
250 - 254	**19.02**	**0.126**	**0.14**	**4.34E-02**	**1.99E-02**	**9.41E-03**	**21.2**
255 - 259	14.13	0.094	0.12	2.15E-04	8.33E-05	3.65E-05	0.1
260 - 264	10.47	0.069	0.12	1.14E-06	4.03E-07	1.48E-07	0.0
265 - 269	7.68	0.051	0.11	1.06E-04	3.27E-05	1.03E-05	0.0
270 - 274	5.57	0.037	0.1	4.22E-06	1.14E-06	3.08E-07	0.0
275 - 279	3.99	0.026	0.1	2.88E-05	7.28E-06	1.52E-06	0.0
280 - 284	2.83	0.019	0.09	2.05E-05	4.55E-06	7.83E-07	0.0
285 - 289	1.94	0.013	0.09	8.16E-06	1.72E-06	2.15E-07	0.0
290 - 294	1.32	0.009	0.08	6.93E-05	1.28E-05	1.26E-06	0.0
295 - 299	0.88	0.006	0.08	3.99E-04	7.16E-05	4.86E-06	0.0
TOTAL				4.43E-02	2.01E-02	9.48E-03	21.4

% absorbed from total photonflow	45.4
% absorbed by H₂O₂ from total photonflow	21.4
% absorbed by background	24.0
Efficiency H₂O₂-absorption	47.1

Table XIX.3Radical formation for DBD UV-lamps

DBD-UV

λ (nm)	ε (H₂O₂) (M⁻¹cm⁻¹)	A (H₂O₂)	A (water)	Lamp photonflow	Total photon flow absorbed	Total photon flow absorbed by H₂O₂	% of photon flow absorbed by H₂O₂
200 - 204	179.21	1.186	5.8	6.90E-03	6.90E-03	1.17E-03	0.0
205 - 209	155.84	1.031	4.6	5.08E-03	5.08E-03	9.30E-04	0.0
210 - 214	132.23	0.875	3.8	4.14E-03	4.14E-03	7.76E-04	0.0
215 - 219	110.12	0.729	2.38	3.41E-03	3.40E-03	7.98E-04	0.0
220 - 224	89.97	0.595	1.96	2.84E-03	2.83E-03	6.60E-04	0.0
225 - 229	72.07	0.477	1.54	3.49E-03	3.46E-03	8.18E-04	0.0
230 - 234	55.83	0.369	1.12	4.97E-02	4.81E-02	1.19E-02	0.4
235 - 239	43.28	0.286	0.84	5.83E-01	5.39E-01	1.37E-01	5.0
240 - 244	33.45	0.221	0.56	9.42E-01	7.86E-01	2.23E-01	8.1
245 - 249	25.31	0.167	0.28	6.08E-01	3.91E-01	1.46E-01	5.3
250 - 254	**19.02**	**0.126**	**0.14**	**2.89E-01**	**1.32E-01**	**6.26E-02**	**2.3**
255 - 259	14.13	0.094	0.12	1.22E-01	4.74E-02	2.08E-02	0.8
260 - 264	10.47	0.069	0.12	4.98E-02	1.76E-02	6.44E-03	0.2
265 - 269	7.68	0.051	0.11	2.41E-02	7.47E-03	2.36E-03	0.1
270 - 274	5.57	0.037	0.1	1.36E-02	3.67E-03	9.90E-04	0.0
275 - 279	3.99	0.026	0.1	1.13E-02	2.86E-03	5.98E-04	0.0
280 - 284	2.83	0.019	0.09	1.15E-02	2.54E-03	4.38E-04	0.0
285 - 289	1.94	0.013	0.09	1.14E-02	2.40E-03	3.00E-04	0.0
290 - 294	1.32	0.009	0.08	1.13E-02	2.10E-03	2.06E-04	0.0
295 - 299	0.88	0.006	0.08	1.33E-02	2.38E-03	1.62E-04	0.0
TOTAL				2.77E+00	2.01E+00	6.18E-01	22.4

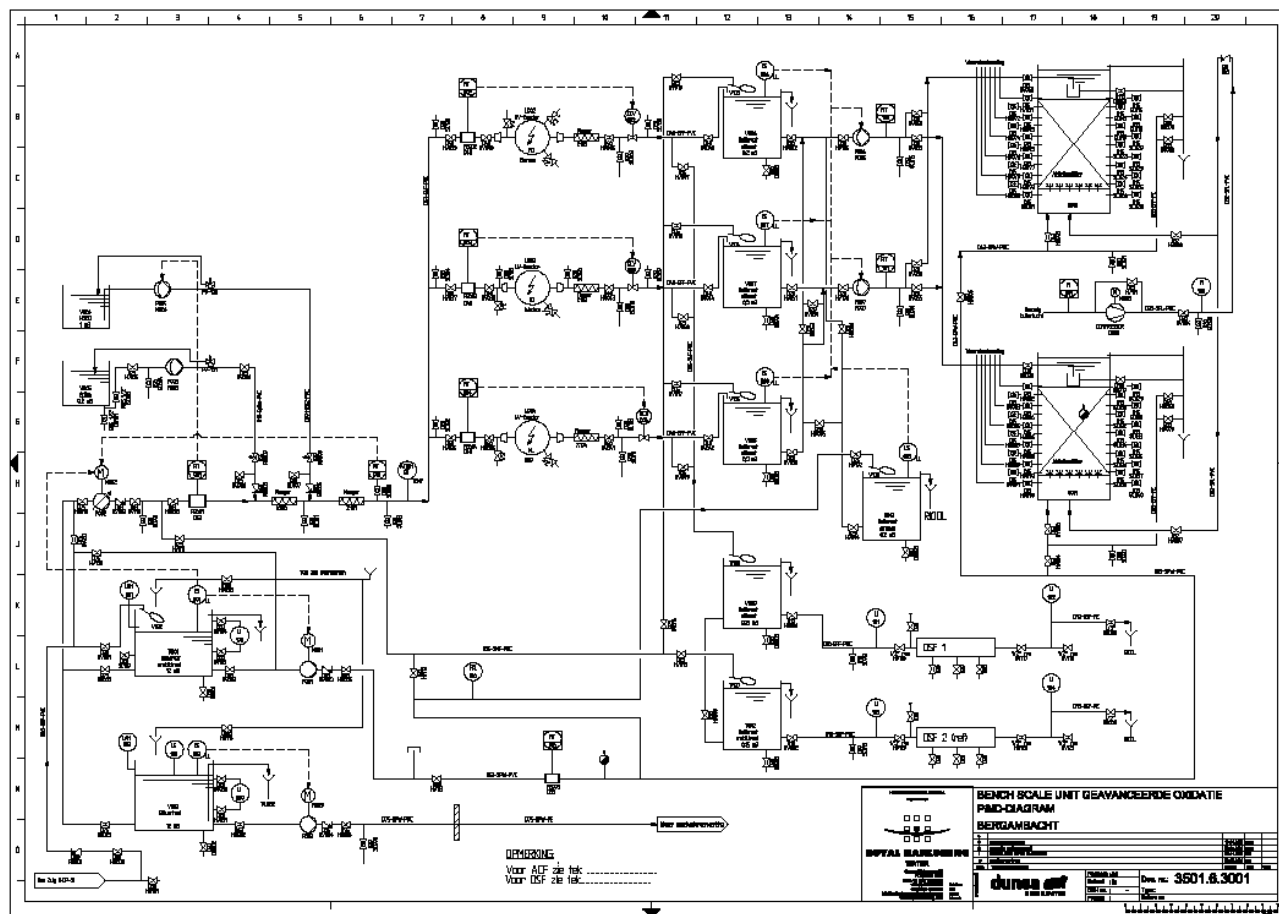|	
% absorbed from total photonflow	72.7
% absorbed by H₂O₂ from total photonflow	22.4
% absorbed by background	50.4
Efficiency H₂O₂-absorption	30.7

XX Dunea pilot plant (WP8)

Figure XX-1 Process and instrumentation diagram pilot scale unit at Dunea

XXI Details on material and methods genotoxicity studies (KWR; WP9)

Materials

All chemicals were of analytical grade.

For the Meuse water study, H_2O_2 (30%) and sodium sulfite (Na_2SO_3) were both purchased from J.T Baker (Phillipsburg, NJ, USA.). The H_2O_2 was diluted with MilliQ water prior to addition. Atrazine was obtained from Dr. Ehrendorfer GmbH (Augsburg, Germany; 99.5%). Virgin activated carbon, type Chemviron F400, was purchased from Chemviron Carbon (Feluy, Belgium).

In the Ohio river study, all spiked chemicals were diluted or dissolved with water from reverse osmosis treatment prior to addition. Atrazine and methyl tert-butyl ether (MTBE) were obtained from Supelco, Inc. (Bellfonte , PA, USA). Hydrogen peroxide, Oxypure 35% (certified by NSF for drinking water treatment), was acquired from FMC, Inc. (Philadelphia, PA, USA). Na_2SO_3 was purchased from Fisher Scientific (Pittsburgh, PA, USA). Virgin activated carbon, Calgon F400, was purchased from Calgon Carbon (Pittsburgh, PA, USA) and was used in production at the Greater Cincinnati Water Works (GCWW). The Granular activated carbon (GAC) was reactivated in GCWW furnaces before use in the pilot facility.

For the IJssel Lake study, Na_2SO_3 was purchased from J.T Baker. H_2O_2 (30%) was purchased from Kemira Chemicals (Rotterdam, the Netherlands) and diluted with water from rapid sand filtration before dosing to the main stream. The GAC was reactivated Norit ROW 0.8 SUPRA (Norit; Amersfoort, the Netherlands), which had been running for two years at the time of the study.

For the sample preparation, distilled acetone, distilled petroleum ether, ethylacetate, methanol, and acetonitril were purchased from Mallinckrodt Baker B.V. (Deventer, the Netherlands). Hydrochloric acid (Suprapur®, 30%) was obtained from Merck (Darmstadt, Germany). The SPE columns (200 mg OASIS® HLB 5cc LP glass cartridges) came from Waters Corporation (Milford, USA). Filtration columns (empty 8 mL glass column with frit), air cleaning columns (8 mL octadecyl glass column) and sea sand (washed and ignited) were all purchased from Mallinckrodt Baker B.V. (Deventer, The Netherlands).

For the Ames II assays, 4-Nitroquinoline oxide (4-NQO) and 2-aminoanthracene (2-AA)were purchased from Sigma Aldrich (St. Louis, USA). Dimethylsulfoxide (DMSO) was purchased from Acros Organics (Geel, Belgium). S9-liver enzyme fraction of Spraque-Dawley rats exposed to 1254 Aroclor was purchased from MP Biomedicals Europe (Illkirch, France) and

For the neutral red uptake and Comet assay, benzo[a]pyrene (BaP), methyl methane sulfonate (MMS), DMSO, neutral red, triton X-100 and ethidium bromide were purchased from Sigma Aldrich (St. Louis, USA). Hank's balanced salt solution (HBSS) was obtained from Invitrogen (Paisley, UK). Dulbecco's modified Eagle's medium (DMEM), Hank's balanced salt solution (HBSS) pencillin/streptomycin and 0.5% trypsin-EDTA solution were was obtained from Invitrogen, Paisley UK. Foetal calf serum (FCS) was obtained from BioWhitaker, Walkersville, USA. Normal melting agarose was obtained from Biozym, Valkenswaard, the Netherlands. Low melting agarose was obtained from Cambrex, Rockland, USA. S9 was prepared according to Ames *et al*. (1975) and Maron and Ames (1983).

Treatment of Meuse water

Pretreated water was collected from the treatment station at the river Meuse at Bergambacht, the Netherlands, in October 2007. This water was pretreated by coagulation with iron sulfate, sedimentation, micro sieves and rapid sand filtration.

The UV/H_2O_2 treatments of water from the river Meuse were performed with a KWR-designed and -built pilot UV reactor (max 5 m^3/h) equipped with four UV lamps. This reactor was used for comparative research and was not optimally configured for any specific lamp type. The lamps applied were HOK 20/100 2 kW medium-pressure (MP) lamps from Philips Lighting (Roosendaal, the Netherlands). By means of chemidosimetry (based on collimated beam experiments; IJpelaar *et al*., 2006) it was determined that with a UV dose of 550 mJ/cm^2 and a peroxide concentration of 10 mg/L

about 80% of atrazine would be converted in the KWR pilot reactor. These conditions were applied for the genotoxicity study.

After flow through of the reactor with at least three times its volume of test water (1.07 m³/h), samples were taken from the reactor effluent and influent. The samples with H_2O_2 were immediately quenched with 300 mg/L Na_2SO_3 to neutralize residual H_2O_2.

Directly after the UV/H_2O_2 treatment at the lowest flow, part of the collected effluent (about 4 liters) was filtered through GAC. The virgin activated carbon was used in a Perspex column (height 40 cm, diameter 9 cm). Before use, the activated carbon was flushed with ultra pure water (Milli-Q, resistance > 18 M-ohm/cm, TOC < 5 ppb) until the oxygen consumption of the virgin activated carbon was less than 5%. The empty bed contact time used was 30 min, with a flow of 5 L/h with a peristaltic pump. Samples of the GAC effluent were taken for genotoxicity analysis. Prior to the next run, the column was flushed with four bedvolumes of ultra pure water.

Treatment of Ohio river water

The water applied for this experiment was pretreated surface water from the Ohio River, directly upstream of the Cincinnati, OH metropolitan area, collected after coagulation with aluminium sulphate and cationic polymer (poly-diallyldimethylammonium chloride, or polyDADMAC), sedimentation, pH correction with calcium oxide and rapid sand filtration.

The UV/H_2O_2 advanced oxidation tests were performed utilizing a commercially available pilot UV reactor (max 9.1 m³/h), optimized for the lamp type applied. The lamp was one 3.5 kW Super TOC medium-pressure (MP) lamp from Aquionics (Erlanger, KY, USA). The UV dose applied was recorded using the manufacturer's instrumentation and was approximately 400 mJ/L. It had been determined that this dose, in combination with 10 mg H_2O_2 per liter, resulted in 60-65% MTBE conversion in this reactor. The reactor had been operating in a continuous mode for several months, and flow was set to 5.9 m³/h in order to achieve the aforementioned dose. Samples were taken from the reactor influent and effluent and immediately quenched with 500 mg/L Na_2SO_3 to neutralize residual H_2O_2.

The reactor effluent served as influent to a 0.10 m diameter pressurized GAC column filled with 1.73 m of GAC. The GAC used was reactivated bituminous coal (particle diameter range: 0.425 – 1.70 mm; effective size 0.55-0.75 mm) (UC<2.0) with 325 days service in the pilot unit. A flow of 0.057 m³/h (1L/min) was delivered to the head of the column by progressing cavity pumps (max. capacity 0.11 m³/h), achieving an empty bed contact time (EBCT) of 15 minutes. Samples (five replicates of 750 mL) were taken from the GAC effluent stream and 500 mg/L Na_2SO_3 was added. All samples were frozen and shipped to KWR, the Netherlands.

Three studies were performed: one in October 2007 with pretreated Meuse water from Bergambacht (the Netherlands) in a pilot reactor at KWR with MP or LP lamps, one in September 2008 with pretreated Ohio River water from Cincinnati (OH, USA) in two pilot reactors simultaneously with different lamps (MP and LP), and one in February 2010 with the same pretreated Meuse water in three pilot reactors simultaneously with three different lamps (MP, LP and DBD) at Dunea for comparison.

Sample extraction and concentration

To prevent any contamination during the extraction procedure, only glass, Teflon and stainless steel equipment was used. All materials were extensively washed and then rinsed with distilled acetone and distilled petroleum ether before use, except for Teflon tubes, which were rinsed with ethylacetate. Within 24 hours after collection, three replicates of one litre of every sample were extracted by SPE with the OASIS® HLB cartridges. Before extraction, the samples were brought to pH 2.3 with a 15% ultrapure HCl-solution in Evian mineral water. Glass filtration columns were prepared with sea sand. Filtration and SPE columns were rinsed twice with full column volumes of 20% methanol in acetonitril, dried and rinsed twice with full column volumes of Evian mineral water brought to pH 2.3. The columns were subsequently filled with fresh Evian mineral water of pH 2.3 and the filtration columns were mounted on the SPE columns. The air cleaning columns were conditioned with one volume of ethylacetate and mounted on the sample bottles.
One litre of a sample was passed through each column setup at around 10 mL/min under low vacuum. Then, the filtration columns were removed and the SPE columns rinsed by 2 column volumes of Evian water of pH 2.3 and dried for one hour. Elution was performed with 3 serial additions of 2.5 mL of 20% methanol in acetonitril (1 min incubation). The 7.5-mL eluates were collected in glass test tubes and stored at -18°C until further processing.
All extracts were evaporated under a gentle stream of nitrogen at 56°C to a volume of 0.5 mL and transferred to a pre-weighted glass conical vial. The test tubes were rinsed with 0.5 mL of acetonitril, which was added to the extract. The acetonitril was further evaporated to approximately 50 µL under a nitrogen stream at 56°C. Then 50 µL of DMSO was added as a keeper and final solvent, and the remaining methanol:acetonitril was evaporated under a nitrogen stream of 65°C in another 10 minutes. Co-evaporated DMSO was replenished to 50 µL by weight, yielding 20,000-fold concentrated extracts. All extracts were stored at -18°C until analysis.

Ames II assay
In brief, bacterial stock culture was thawed and grown overnight at 37 °C and 250 rpm in a mixture of 10 mL Growth Medium, 10 µL of 50 mg/mL ampicillin-solution and 10 µL stock culture. Growth was checked after 14-17 h by optical density (OD) measurement at 600 nm, and had to be at least 2.0 (or 0.2 for a 10-fold dilution) for continuation of the test. S9-liver enzyme fraction was freshly thawed and mixed as: 33 µL 1 M KCl, 32 µL 0,25 M $MgCl_2 \cdot 6H_2O$, 25 µL 0,2 M Glucose-6-phophate, 100 µL 0,04 M NADP, 500 µL 0,2 M NaH_2PO_4 buffer, 10 µL milliQ water, and 300 µL S9-fraction.[1]
The water extracts were diluted to 100 µL (1:1) with DMSO to obtain a sufficient amount of sample for all tests. Then, per well of a 24-well plate (Greiner Bio One), the following was added: 6 µL of diluted test sample in 100% DMSO, 30 µL overnight culture, 10 µL of S9-mix if applicable and 264 or 254 µL of Exposure Medium, respectively. Water extracts were tested in triplicate, as well as a triplicate negative control (DMSO only), a triplicate positive control for genotoxicity (table XIX.1), and a triplicate positive control for cytotoxicity (1 mg/mL 4-NQO in DMSO). After an incubation of 90 minutes at 37 °C and 250 rpm, 10 µL from each exposure mixture was transferred to a well of a 96-well plate (Greiner Bio One) for a cytotoxicity measurement. To each well of the 96-well plate, 90 µL of Exposure Medium (containing histidine) was added and this was then left to incubate for another 3 hours at 37

---

[1] The Ames II assay is performed both with and without S9 liver enzyme extract, in order to detect both direct genotoxic compounds, and indirect genotoxic compounds that need to be converted to a genotoxic metabolite by liver enzymes first.

°C and 250 rpm. Then, the OD at 595 nm of the 96-well plate was measured with an Opsys MR platereader (Clindia; Leusden, the Netherlands).

Table XIX.1. Positive controls for the different strains and S9-conditions

Strain and S9-condition	Positive control (in DMSO)
TA98 –S9	10 (Meuse) or 20 (Ohio and comparison study) µg/mL 4-NQO
TA98 +S9	5 µg/mL 2-AA
TAMix –S9	5 (Meuse) or 10 (Ohio and comparison study) µg/mL 4-NQO
TAMix +S9	100 µg/mL 2-AA

To the remaining exposure mixture in the 24-well plate, 2.61 mL of purple Indicator Medium (not containing histidine) was added. The total 2.9 mL was subsequently divided over 48 wells (50 µL per well) of a 384 well plate and left to incubate for 48 hours at 37 °C. Then, the number of yellow wells per 48 wells of one sample were counted manually.

As Ames test responses are not normally distributed, but follow a binomial distribution (Piegorsch *et al.*, 2000), no standard statistical tests could be performed on the data. As an alternative, a water extract was determined to be genotoxic if the number of yellow wells exceeded the detection limit of the test. In the past, using the classical Ames test, such a detection limit was defined as twice the average response of the negative control (e.g. Veenendaal and van Genderen, 1999). As there is no statistical basis for this definition, a different approach was used. The detection limit (*DL*) was defined as the value that will only be exceeded by values of the negative control with a very low probability (1%). From statistical theory it may be assumed that the total number of yellow wells from the three replicates follows a binomial distribution. Therefore the detection limit of the total number of yellow wells from the three replicates (X) can be approached as the smallest integer *k* that satisfies the following equation (based upon the formula for the cumulative binomial distribution, equation S1):

$$P[X \leq k] = \sum_{i=0}^{k} \binom{n}{i} p^i (1-p)^{n-i} \geq 99\% \qquad \text{equation S1}$$

With *n* the total number of wells (*n* = 144), and *p* the probability of a yellow well in testing three replicates of a negative control sample. *p* is estimated as the total number of yellow wells (*y*) from the three replicates of a negative control sample, divided by the total number of wells involved (144), so *p* = *y*/144.

Comet assay

The human HepG2 hepatoma cell line was obtained from Dr. B. Knowles of The Wistar Institute of Anatomy and Biology in Philadelphia (Knowles *et al.*, 1980). The cells were grown in a monolayer culture in DMEM supplemented with 10% FCS, 100 U/mL penicillin and 100 µg/mL streptomycin. HepG2 cells were seeded at a density of ± 2 × 10^6 cells in 75 cm^2 tissue culture flasks and cultured in a humidified incubator (Sanyo, Bensenville, USA) at 37°C and 5% CO$_2$. Near confluence, HepG2 cells were harvested by trypsination, suspended in culture medium, and split twice a week to prepare subcultures.

An S9 mix was prepared, consisting of a liver homogenate fraction (S9) and cofactors as described by Ames *et al.* (1975) and by Maron and Ames (1983). The liver homogenate fraction (S9) was prepared from male rats induced with Aroclor 1254 (500 mg/kg bodyweight) and its protein and cytochrome P-450 content was determined. The S9 was stored at <-60°C and was used within 1 year of preparation. The final concentrations of the various ingredients in the S9 mix were: 8 mM MgCl$_2$, 33 mM KCl, 5 mM glucose-6-phosphate, 4 mM NADP, 40% (v/v) RPMI 1640 medium and S9 in a concentration of 200 µL/mL mix.

For the neutral red assay for cytotoxicity, HepG2 cells were seeded at a density of ca. 5 × 10^4 cells per well in 96-well culture plates and cultured for two days. The medium was removed and cells were treated with HBSS containing aliquots of the water extracts at a concentration of 0.25%, 0.5% or 1% (v/v) in quadruplicate. Triton X-100 at a concentration of 1% in HBSS (v/v) was used as positive control substance. The samples from the Meuse water experiment were dosed for 3 h without S9. The Ohio and IJsselmeer water samples were dosed both in presence of S9 (3 h exposure) and in absence of

S9 (24 h exposure). After the 3-h or 24-h treatment in a humidified incubator, cells were washed twice with HBSS, followed by exposure to 50 µg/mL neutral red solution in HBSS for 1 h in a humidified incubator. After washing, the incorporated neutral red was then extracted by incubation in 0.02% acetic acid in 50% aqueous ethanol (v/v) for ca. 20 min. Absorbance of the extracted neutral red was measured at 540 nm by means of a spectrophotometer (Biorad, Hercules, USA) and the mean optical density for quadruplicate cultures was calculated and expressed as the percentage of neutral red uptake (viability) compared to the negative control substance DMSO. The water extracts were considered not cytotoxic if viability was greater than 90%, slightly cytotoxic if viability was between 70% and 90%, and cytotoxic if viability was less than 70%. The concentration of the water extracts to be used in the comet assay should demonstrate viability greater than 70%.

For the Comet assay, HepG2 cells were seeded at a density of ca. 2.5×10^5 cells per well in 24-well culture plates and cultured for two days. The medium was removed and cells were treated with HBSS containing aliquots of water extract at a concentration of 1% (v/v) in duplicate (exposure to a 200-fold concentration of the water samples). The samples from the Meuse water experiment were dosed for 3 h in absence of S9. 25 µg/mL MMS in DMSO was used as positive control for genotoxicity. The Comet assays with the Ohio water samples were performed both in presence of S9 (3 h exposure) and in absence of S9 (24 h exposure). The positive control was then 50 µg/mL BaP.

After the treatment in a humidified incubator, cells were washed twice with HBSS. Cells were harvested with 0.05 % trypsin-EDTA solution and suspended in 200 µL HBSS to obtain single cells in suspension. Microscopic slides were prepared by mixing 20 µL of the cell suspension with 90 µL 0.5% low-melting agarose solution in PBS. Subsequently, 95 µL of this mixture was loaded on a glass slide, which was precoated with 1.5% normal melting agarose solution, and mounted with a cover slip. The slides were stored on a cold plate until the agarose had coagulated, followed by removal of the cover slip and incubation in lysisbuffer (2.5 M NaCl, 0.1 M Na2EDTA, 0.01 M Tris,1% Triton X-100, pH 10) at ± 4ºC for overnight lysis. Slides were then transferred to an electrophoresis box (Biozym, Valkenswaard, The Netherlands) containing ice-cold electrophoresis buffer (0.3 M NaOH, 0.001 M Na2EDTA, pH > 13) and incubated for 30 min to allow DNA unwinding. Electrophoresis was performed for 30 min at 25V and 300 mA at ± 4ºC. After electrophoresis, slides were rinsed with neutralization buffer (0.4 M Tris, pH 7.5) and dehydrated with ethanol at room temperature. Slides were stained with 20 µg/mL ethidium bromide solution, which was directly pipetted on the slide and covered with a cover slip just before analysis. Slides were coded by a qualified person not involved in analysing the slides to enable blind scoring. A fluorescent microscope (Zeiss, Göttingen, Germany) equipped with a filter (BP 546 nm, FT 580 nm and LP 590 nm) was used for the analysis of the slides. Two slides per culture and fifty randomly selected cells per slide were measured using Comet Assay IV software (Perceptive Instruments, Suffolk, UK). The DNA damage was evaluated by calculation of the mean %tail DNA for a total of two-hundred cells per sample. The water extracts were considered positive when a three fold increase in tail intensity was observed. 'Hedgehog' or 'ghost' cells were excluded from measurement, but their presence was counted to provide and indication of cytotoxicity. Hedgehog cells have the appearance of a small head with a large tail, and have been associated with cells undergoing apoptosis (Meintières *et al.*, 2003).